Issue 1
Volume 1
January, 2024

ISSN 2818-0313
DOI Prefix：10.62252

Naturalis Scientias

www.naturalisscientias.com

TABLE OF CONTENTS

ORIGINAL ARTICLES

SHORT COMMUNICATION

Original Article

Geology and geochemistry of the only independent tellurium deposit in the world

Jianzhao Yin[1], Haoyu Yin[2], Yuhong Chao[3], Shoupu Xiang[4], and Hongyun Shi[1]

Abstract

The article discusses both the regional and deposit geology including structure, strata, and igneous rocks, as well as the ore body and alteration of Dashuigou tellurium deposit at the Qinghai-Tibet Plateau, the only independent tellurium deposit in the world. There are over 30 minerals that make up the deposit's ore, including carbonates, silicates, oxides, sulfides including various tellurides and native element minerals. Euhedral, semi-euhedral, xenomorphic granular, metasomatic, metasomatic graphic, reaction rim, and solid solution separation are the main ore texture; while massive, vein/veinlet, stockwork, dissemination, breccia, and bird's-eye are the major ore structure of the deposit. Based on the ore structure, this deposit's ore can be divided into three categories: massive, veinlet-stockwork, and disseminated. The ores are further divided into eight subcategories in total based on the proportions of tellurium minerals, other sulfides, dolomite, quartz, and muscovite in it. Both geology and K-Ar isotope dating have confirmed that the pyritic (pyrrhotite + pyrite) vein and telluride vein are products of two different geological events that are far apart. The tellurium grade in the ores varies between 0.01% and 34.58%. All ores in this deposit are primary sulfide ores that have not been transformed by oxidation or weathering. Two paragenetic stages; namely, the pyritic stage and tellurium stage consisting of five sub-stages in total exist in the deposit. According to Laznicka's idea, the deposit's tonnage accumulation indices indicate that it is a super-large independent tellurium deposit.

Key words: geology; geochemistry; ore; tonnage accumulation index; independent tellurium deposit; Qinghai-Tibet Plateau

---

Affiliation Info: [1] Orient Resources Ltd., Richmond, British Columbia, V7E 1M8, Canada; [2] Guinea Westfield Mining Company-Sarlu, Jinzhong 031300, China; [3] Ganzhongnan Institute of Geology and Mineral Exploration, Nanchang 330002, China; [4] Silvercorp Metals Inc., Beijing 100027, China

Article Info: Received: 18 August 2023 / Revised: 30 October 2023 / Accepted: 16 November 2023 / Published Online: 12 December 2023. www.naturalisscientias.com

Authors' Contact Info: Yin, JZ: jimyin7@yahoo.ca; Yin, HY: yinhaoyu11@163.com; Chao, YH: 435975944@qq.com; Xiang, SP: shoupux@163.com; Shi, HY: hongyunshi@yahoo.com

Citation: Yin, JZ; Yin, HY; Chao, YH; Xiang, SP and Shi, HY. 2024. Geology and geochemistry of the only independent tellurium deposit in the world. *Naturalis Scientias*, 1(1): 1-31. DOI: https://doi.org/10.62252/NSS.2024.1001.

Corresponding Author: Yin, JZ, PhD, PGeo, Professor; Email: jimyin7@yahoo.ca

1 Introduction

As one of the scattered elements that have similar geochemical characteristics with Clark values too low to enrich into independent deposits, tellurium (Te) was usually thought to exist only as associated components in other metallic deposits and not to form independent deposits in the traditional theory of mineral deposits. According to Li[1-3], the average content of Te in the Earth's crust is 2.0×10^{-8} in China, and 1.34×10^{-9} worldwide.

As a fact, the world's supply of refined tellurium is mainly recovered from Te-bearing ores including chalcopyrite, pyrite, pyrrhotite, volcanogenetic sulfur, bismuthinite, gold, silver, arsenopyrite, and cassiterite deposits, and most of the recoverable Te in the world is from copper deposits[4-6].

As the only independent tellurium deposit in the world thus far, the Dashuigou tellurium deposit, which is located in Simian county, Sichuan Province, China (Fig. 1)[7], has aroused widespread concern from geologists, since its discovery in 1992[8-27].

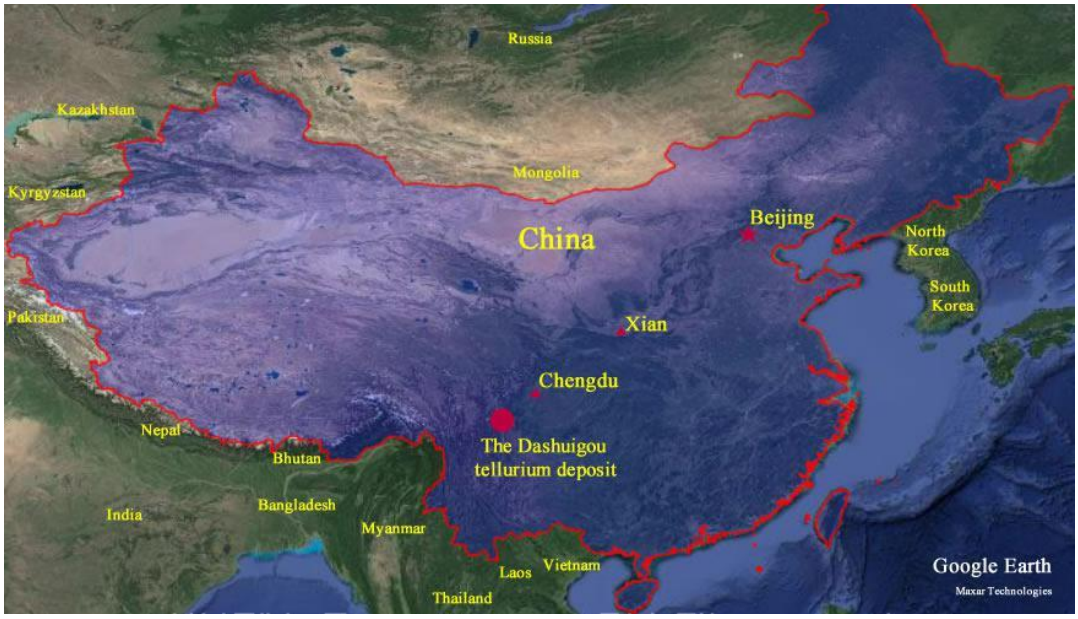

Figure 1. Location map (after Yin & Shi 2020a)[7]

(Google Earth 7.1.8.3036 (32-bit): http://download.pchome.net/industry/geography/detail-20351.html, and 91 v17.5.8: www.91weitu.com; accessed January 25-27, 2020)

Putting aside the many different views on the origin of this deposit, this article discusses in detail the deposit's geology and geochemistry. The genesis and origin are left to the relevant readers to think and discuss.

2 Regional geology

2.1 Geotectonic background

Nestled in the convergence between the Indian, Eurasian, and Pacific Plates, the Dashuigou tellurium deposit is located in the transitional belt between the Yangtze paraplatform and Songpan-Ganzi folded belt, as part of the Qinghai - Tibet Plateau (Fig. 2)[4 & 28-29].

According to the previous researches[4,16-18 & 28-31], the area has the following geophysical characteristics: high geothermal flow, high velocity, high density, high resistance, and high magnetism; a turning boundary of the Earth's crust's thickness: from the 31-40 km thickness of the South China block, through the 50-55 km thickness of this area,

to the 60-75 km thickness of the Qinghai-Tibet Plateau; a gravity gradient zone which controls both the production and development of earthquakes and tectonomagmatic events, and the distribution of a series of mineral deposits; upper mantle below the region uplifting obviously. There is also a low-velocity and low resistivity zone in the middle crust that is interpreted as a decollement. The abnormal mantle exists under the crust in the region, which has properties of geosyncline and platform, as well as its own special characteristics. The belt is a geo-tectonically active zone with very complicated igneous rock structures.

In summary, this region is both geologically very active and a very important south-north trending tectonomagmatic-mineral belt.

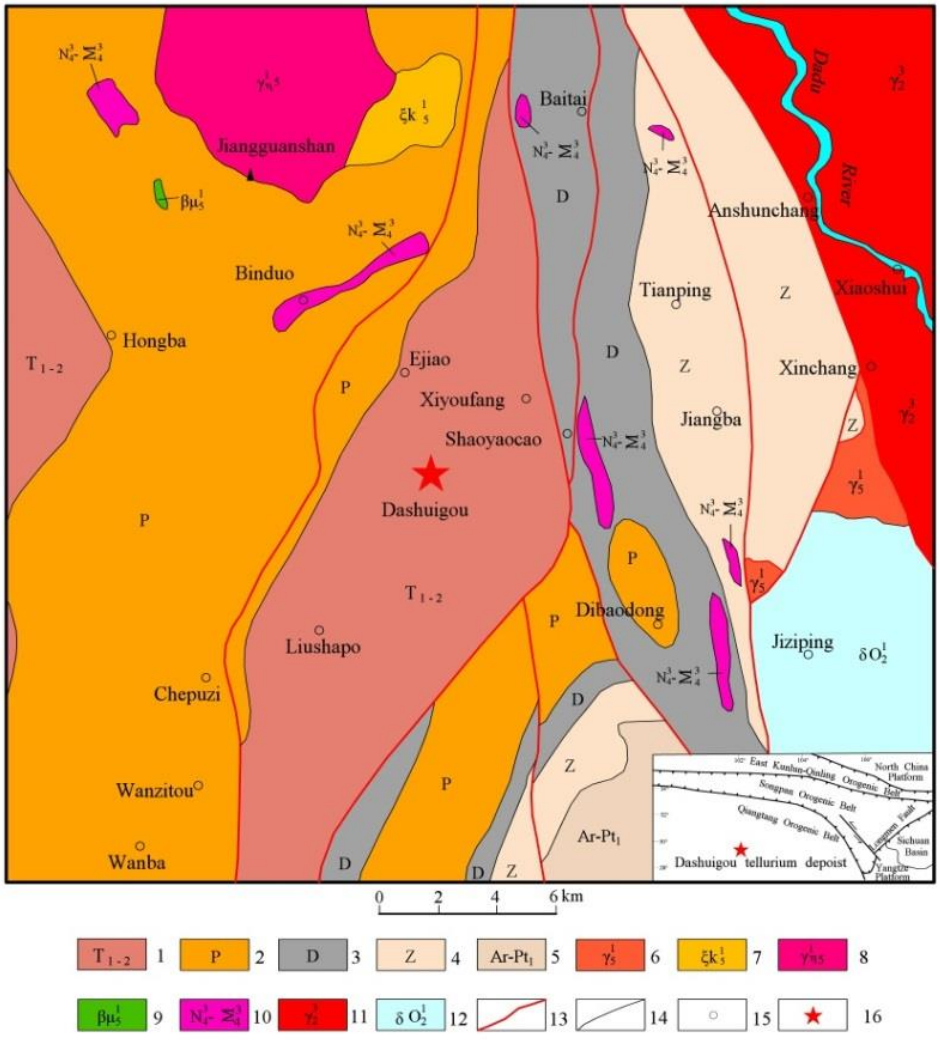

Figure 2. Regional geology[4 & 28-29]

1. The lower and middle Triassic metamorphic rocks; 2. The Permian metamorphic rocks; 3. The Devonian metamorphic rocks; 4. Metamorphic rocks of the Sinian system; 5. Metamorphic base complex of the Archean Kangding group; 6. Plutonic granite of the Indosinian orogeny; 7. Plutonic alkaline syenite of the Indosinian orogeny; 8. Plutonic monzonitic granite of the Indosinian orogeny; 9. Hypabyssal sillite of the Indosinian orogeny; 10. The late Hercynian basic-ultrabasic rocks; 11. The late Proterozoic plutonic granite; 12. The early Proterozoic-Archean plutonic quartz diorite; 13. The deep and large fault; 14. The geological boundary; 15. Village and/or town; 16. The tellurium deposit.

2.2 Strata

Deeply affected by the north-south uplift zone, the strata, igneous rocks and various geological structures in this area are distributed in nearly north-south strips (Fig. 2). The strata exposed in the study area are mainly a series of shallow metamorphic rocks from the Sinian, Devonian, Permian, and lower- middle Triassic systems (Fig. 2 and Table 1). A large area of Kangding group metamorphic rocks is exposed to the southeast of the study area, which is recognized as the oldest rocks in the Xikang-Yunnan or Kang-Dian geo-axis of the second level geotectonic unit of the Yangtze paraplatform, that is, the metamorphic crystalline basement[4,16-18 & 28-36].

Table 1. Summary of regional stratigraphic sequence, sedimentary formation, and lithology in the study area[4 & 28]

Geological time			Tectonic layer	Sedimentary formation and lithology	Note
Era	Code	System			
Cenozoic	Q	Quaternary	Himalayan tectonic layer	The upper part is the alluvial layer, the middle part is	
				the glacial layer, and the lower part is the mixed	
				sedimentary layer of alluvial, slope and glacial deposits.	Unconformity
Mesozoic	T_{1-2}	Lower-Middle Triassic	Cover	Marine carbonate and basic volcanic rock sedimentary	contact
				formations, which have been metamorphosed to marble	
				, slate and schist.	Conformity or
Paleozoic	P	Permian		The upper part is formed by clastic rocks, marine carbonate	fault contact
				and basic volcanic rocks, and the lower part is formed by	
				marine carbonate; it has been metamorphosed into slate,	Conformity or
				marble and schist respectively.	fault contact
	D	Devonian		The upper part is formed by marine carbonate, and the	
				lower part is formed by clastic rock and marine carbonate,	Fault or/and
				which has been metamorphosed to marble and slate, etc.	pseudoconformity
Proterozoic	Z	Sinian		Formation of marine carbonate and clastic rocks, which	contacts
				have been metamorphosed to marble and slate, etc.	
	Pt_1	Kangding Group metamorphic complex	Crystalline Basement	Basic, medium and acid volcanic rock formations and	Angular
Archean	Ar			flysch-like formations; have been subjected to regional	unconformity
				dynamic metamorphism, becoming high greenschist facies	and fault
				and amphibole facies metamorphic rocks.	contact

The crystalline basement, also known as the Kang-Dian complex or Kang-Dian gneiss, is now commonly known as the Kangding group and is a set of moderately to deeply metamorphosed and migmatized rocks. This set of rocks extends intermittently in a north-south direction in the western Panzhihua region, stretching for over 400 kilometers. They are clearly controlled between two lithospheric fault zones, forming a distinct north-south uplift zone.

The lower part of the Kangding group is composed of thick hornblende rocks, while the middle part is composed of biotite granulite, hornblende granulite, and biotite schist. The upper part is sandwiched with granulite and shallow granulite. The phase transition is obvious from north to south. The upper part of the Kangding group is mainly composed of mica schist and biotite granulite, interspersed with siliceous marble, dolomite marble, granulite and quartzite. The lower part of the Kangding group's protolith is mainly composed of tholeiitic basalt erupted from the sea floor, and gradually changes upward into calc-alkaline and medium-acidic volcanic rocks, and flysch and/or flysch-similar formations. The Kangding group has experienced regional dynamic thermal metamorphism of high greenschist facies and amphibolite facies, accompanied by acidic, basic and ultrabasic magma intrusions during the metamorphism. In addition, this set of rocks also suffered intense migmatization and granitization. The isotopic age of this set of rocks is 2,950~1,700 million years.

The late Proterozoic and early Sinian were the transitional period when the study area entered the stable platform development stage. Beginning in the late Sinian, the Kang-Dian geo-axis entered the stage of stable platform development and began to receive platform cover deposition. As the first true platform cover of the Yangtze paraplatform, the upper Sinian is widely distributed in the region and has stable thickness. It generally overlies the folded metamorphic basement in an angular unconformity (Fig. 2 and Table 1). During the early Paleozoic, the

Earth's crust frequently experienced vertical ups and downs, resulting in the absence of the Cambrian, Ordovician and Silurian systems in this area. During the Devonian and Permian periods, the entire region experienced widespread subsidence and seawater intrusion, depositing a carbonate-clastic rock series.

The upwelling of upper mantle magma causes thermal doming of the crust. Accompanying this process, basic-ultrabasic magma from the upper mantle intrudes into the crust along resurrected faults. During the Carboniferous, this area was uplifted, resulting in the loss of this set of strata.

From the late Permian to the middle Triassic, the upper mantle magma upwelling in the area reached a climax. Accompanied by faulting activity, Hercynian Emeishan basalts (260-254 Ma) and layered iron-rich basic-ultrabasic rocks containing vanadium-titanium magnetite from the upper mantle, as well as Indosinian granites (257-205 Ma) , intruding or erupting along the ancient faults resurrected in the crystalline basement, forming a set of north-south tectonic-magmatic mixed complex belts developed on the crystalline basement in the area. Most of the cover rocks of different ages in the area have experienced regional low-temperature dynamic metamorphism and became phyllite, schist, and marble.

2.3 Igneous rock

The igneous rocks in the area are relatively developed, widely distributed and of various types, including ultrabasic, basic, neutral, alkaline, and acidic igneous rocks. These igneous rocks were active to varying degrees during the Zhongtiao (Ar-P_{t1}), Chengjiang (Z_1), Caledonian (Z_2-S), Hercynian (D-P), Indosinian (T_{1-2}), Yanshanian (J_{1-2}-K_2) and Himayalan (R-Q) orogeny or period. Among them, the Zhongtiao period - Chengjiang period and the late Hercynian (P) - Indosinian periods are the two peak periods of igneous activity in this area, which are briefly described as follows[4,10,16,28 & 30-31]:

The magmatic activity during the Zhongtiao orogeny was intense. In the early stage, there was a large-scale submarine volcanic eruption, accompanied by the intrusion of basic-ultrabasic magma. In the middle stage, sodium granite was intruded. And in the later stage, a little potash granite was formed. Among them, the representative intrusion is the Archean - early Proterozoic Jiziping-Caluo granite extending north-south, covering an area of 55 km^2. These igneous rocks were later metamorphosed together to form the crystalline basement of the Kang-Dian complex (Fig. 2).

In the area, granite and alkaline intrusive rocks developed during the Chengjiang orogeny. The typical representative is the late Proterozoic Xiaoshui granite exposed in the eastern portion of the study area and distributed in a north-south direction across a huge area of 950 km^2 (Fig. 2). As a typical orogenic product, the batholith produced iron, tin, and tungsten ore bodies in some of its parts; and Ta, Nb, and Y showings in the alkaline granites.

Magmatic activity in this area formed a new climax during the late Hercynian (P) and Indosinian (T_{1-2}) periods. In the late Hercynian orogeny, a large amount of basalt was ejected along the north-south fault zone, which is the famous Emeishan basalt. At the same time, a large number of mafic-ultramafic intrusions, diorite and granite were intruded along the north-south deep faults. The basic-ultrabasic intrusive rocks exposed in the form of rock bed, sheet, and dyke in the eastern and northwestern parts of the study area. Tremolite and asbestos are often enriched in certain kinds of intrusive rocks, magnetite is enriched in other intrusive rocks, and some intrusive rocks have copper and nickel mineralization. Among them, the Binduo and the Shaoyaocao stocks are two relatively large rock stocks. Geological and geochemical data show that these basic-ultrabasic intrusive rocks originated in the upper mantle, which are directly related to the Xiaojinhe lithospheric fault zone.

All intrusive bodies developed in the area during Yanshanian orogeny (J_{1-2}-K_2) are granite, and representative rock bodies include Jiangguanshan alkaline syenite, Jiangguanshan quartz diorite, and Xinchang granite (Fig. 2).

There are a large number of quartz veins, carbonate veins, and diabase veins in the study area's various metamorphic rocks and intrusive rocks of different ages, as well as a small amount of granitoid aplite, granite pegmatite, and lamprophyre dikes, etc.

2.4 Structure

Faults and fault zones are well developed in the study area, most of which are deep and large faults that cut through the lithosphere in a north-south or nearly north-south direction and reach the upper mantle or asthenosphere. They are channels for upwelling material including ore-forming minerals from the upper mantle. These deep and large faults are often composed of mylonite zones and have the characteristics of ductile shear zones[4,10,16 & 28]. The representative fault zones are briefly described as follows:

Xiaojinhe or Jinping-Muli fault zone: The fault zone spans Yunnan and Sichuan provinces, along the Xiaojinhe River and Jinping Mountain to Xiyoufang of Shimian County in the study area. It is more than 250 kilometers long and is the dividing line between the Songpan-Ganzi geosyncline and the Yangtze paraplatform. There are compression tectonic zones developed near the fault zone, and many recorded earthquakes have occurred in the Muli area.

As part of the Yulong-Longmen fault zone, the Xiaojinhe fault zone was the dividing line between the eastern paraplatform and the western geosynclinal area during the Paleozoic-Triassic period, and has been the southeastern boundary of the Qinghai-Tibetan Plateau since the Cenozoic. According to plate tectonic theory, this fault zone is a plate suture line.

Anninghe fault zone: This fault zone is located on the western edge of the Yangtze paraplatform, starting from Jintang in the north and extending south along the Dadu River to Shimian County. It passes through Mianning, Dechang, and Huili, crosses the Jinsha River and enters Yunnan to connect with the Yimen fault, running through the Kang-Dian geo-axis.

The fault zone has been active multiple times, with basic to ultrabasic rocks distributed along the fault zone, and abundant mineral resources on both sides of the fault zone.

Similar fault zones include the Mopanshan, Jinhe-Chenghai, and Xiaojiang deep and large fault zones.

In addition to the linear structures mentioned above, there are also numerous circular structures in the area. Remote sensing interpretation shows that both linear and annular structures develop in the study area. The annular structure is strongly intersected by linear structures with different directions and different mechanical properties, forming the Ø-shaped structures that are very favorable for mineralization (Fig. 3)[4,16, 25-26, 28 & 36].

2.5 Regional minerals

The favorable geotectonic setting and well-developed tectonic and magmatic geological conditions have created abundant mineral resources in the study area. These mineral resources are both endogenous and exogenous. The economic value of Fe, Ti, V, Cu, Pb, Zn, rare element, rare earth, asbestos, and coal is the most prominent; among which internationally renowned mines include Panzhihua vanadium titanium magnetite and asbestos mines[4 & 28].

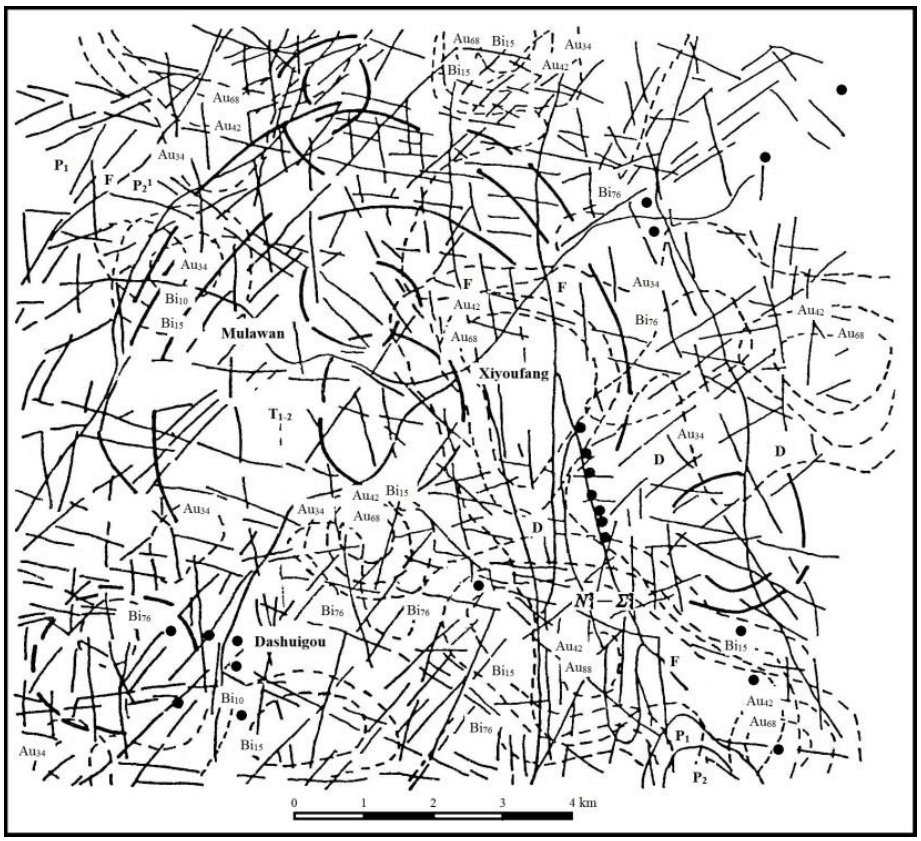

Figure 3. Linear-circular structures based on remote sensing satellite image and geochemical anomalies in the study area[2 & 37]

The endogenetic deposits within the area include:

- Cu, Ni, and Pt deposits related to ultrabasic rocks;
- Fe, Ti, V, P, Cu, Ni, Cr, and Pt deposits related to layered mafic-ultramafic complexes;
- Fe and Cu minerals related to basalt;
- Nb, Ta, Zr, Hf, U, and Th deposits related to the group of alkaline dykes;
- Nb, Ta, Y, Zr, and Hf minerals related to alkaline granite;
- La, Ce, Th, U, Mo, Cu, Pb, Zn, fluorite, and gold deposits related to potassium feldspar granite;
- Hydrothermal iron ore associated with gold;
- Hydrothermal copper, lead, zinc, and gold deposits;
- Hydrothermal quartz vein type lead, zinc, and gold deposits;
- Chrysotile asbestos deposits related to late Proterozoic ophiolite;
- amphibole asbestos deposits related to Permian ultrabasic rocks

The exogenous mineral deposits within the area include:

- Hematite deposits associated with the Triassic sedimentary rocks that has been modified by regional metamorphism;

- Quaternary placer gold deposit;
- Perlite mineral deposits produced in the Devonian system;
- Slates produced in the Triassic system, gypsum, and coal that are widely used by local people.

3 Deposit geology

3.1 General background

The Dashuigou independent tellurium deposit is located near the west side of the above-mentioned Xiaojinhe deep fault zone and at the northern edge of the Panzhihua-Xichang rift (Figs. 2 and 3). The structure of this area is north-northeast-oriented, with common tight folds and inverted folds. Therefore, the strata and igneous rocks in this area are also distributed in a north-south or nearly north-south direction[4,16 & 28].

Geotectonically, the mining area is located in the Jiulong geoanticline, a third-level tectonic unit extending north-south in the Songpan-Ganzi geosynclinal fold belt. The Jiulong geoanticline and all other adjacent geotectonic units are bounded by various deep faults. For example, the eastern part of the Jiulong geoanticline is connected to the Kang-Dian geo-axis by the Xiaojinhe fault.

According to the results of seismic sounding and regional gravity data, the mining area is located in the transition zone between the western mantle depression area and the eastern mantle platform area; that is, the Wenchuan-Shimian-Muli mantle slope zone. It is essentially a west-dipping steep slope of the Moho surface. It is also the transition zone and dividing line between the Songpan-Ganzi fold belt and the Yangtze paraplatform.

3.2 Strata

Devonian and Permian strata expose near the periphery of the mining area[4,16,28,30-33 & 36-38].

The Devonian strata are mainly marine carbonate rocks that have suffered medium-pressure regional dynamic metamorphism, most of which is marble.

The contact fracture zone between the Devonian and Sinian systems contains Cu, Au, and Ag minerals of a certain scale, such as the Dayanfang Cu-Au-Ag mine, the Jinjitaizi Cu-Au mine, and the Guangjinping gold mine etc.

The Permian system is well developed near the mining area, with a wide exposure area and a long and narrow strip extending from north to south. The lower series of the Permian system is a set of fossil-rich carbonate rocks, while the upper series includes thicker basalt, clastic rocks, argillaceous rocks, and carbonate rocks. This set of rocks suffered medium-pressure regional dynamic metamorphism during the Indosinian orogeny and became greenschist phase metamorphic rocks.

The Triassic strata in the study area is a set of littoral-neritic phase carbonate-basic volcanic rocks, but has suffered regional low-temperature dynamic metamorphism in the Indosinian orogeny and turned into low greenschist phase metamorphic rocks, including marble, phyllite, and schist (Fig. 4).

The Triassic system in the study area is exposed in two parts, one is to the west of Hongba on the west side of the mine, and the other is the diamond-shaped block of the Dashuigou mine itself. Some geologists call it the Xiyoufang-Liushapo tectonic block. The direct host rock of the tellurium ore bodies in the deposit is the Triassic phyllite, schist and slate, in which exists a well-developed 10-15 m wide fault zone, in which an approximately 3 m wide tourmaline-quartz vein develops. Strong pyrrhotite alteration occurs along both the hanging wall and footwall of the fault zone (Figs. 4 and 5).

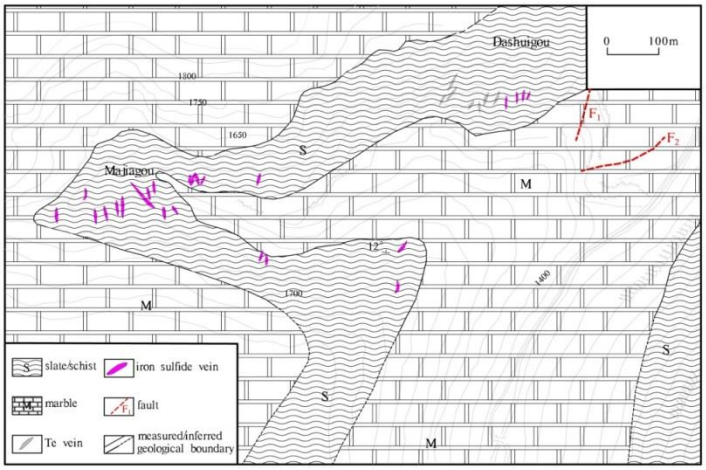

Figure 4. Deposit geology[4 & 28]

The Triassic stratigraphic sequence of the Dashuigou tellurium deposit is as follows (Figs. 4 and 5)[4,28 & 38-41]:

i. Schist, phyllite and slate formation at the top
ii. large-thick fine-grained marble in the upper part
iii. schist, phyllite and slate formation in the middle
iv. fine-medium grained banded marble in the lower part
v. coarse grained thick marble at the bottom

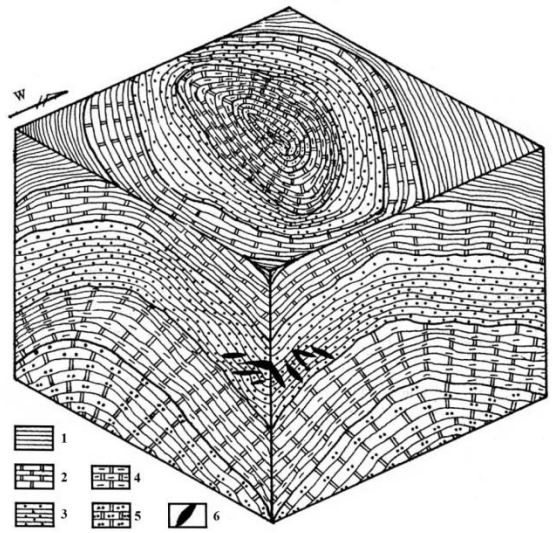

Figure 5. Schematic diagram of the ore bodies' 3D distribution of Dashuigou tellurium deposit

1. The upper phyllite, schist and slate of the lower-middle Triassic system; 2. The thick marble in the upper part of the lower-middle Triassic system; 3. The middle phyllite, schist and slate of the lower-middle Triassic system; 4. The banded marble of the lower-middle Triassic system; 5. The lower coarse-grained marble of the lower-middle Triassic system; 6. The tellurium ore body

The phyllite, schist and slate overlying the banded marble are pushed and compressed along the contact between the two, forming an interlayer compression fold (Fig. 6). This contact is also basically the bottom boundary of the tellurium vein.

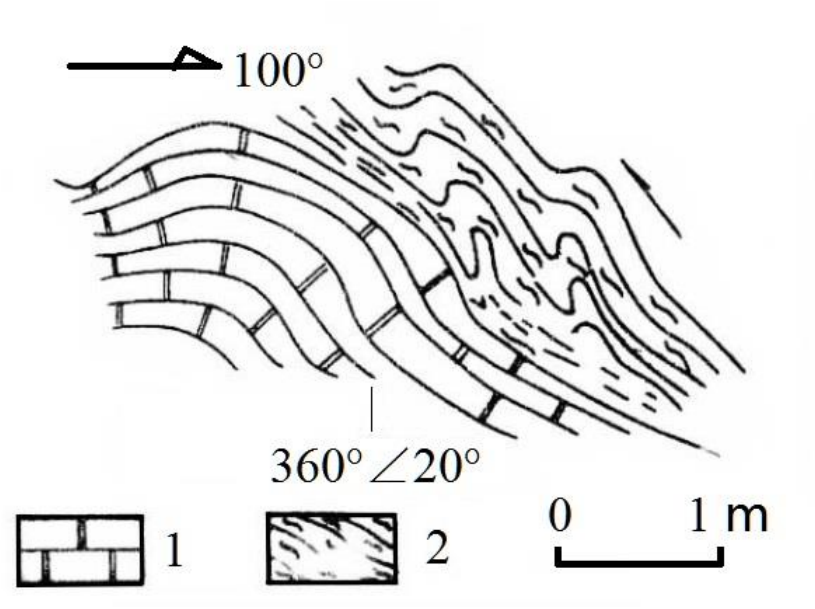

Figure 6. Sketch of reverse compression fold between banded marble and phyllite/schist/slate

1. The banded marble; 2. The phyllite/schist/slate host rocks of the tellurium ore body

The main host rocks of the ore bodies include hornblende schist, garnet schist, tourmaline schist, and chlorite schist (Fig. 7). Other minerals in the schist/phyllite/slate include quartz, plagioclase, potassium feldspar, muscovite, rutile, and magnetite. According to its geological, mineralogical, petrographic, petrochemical, and geochemical characteristics, the protolith of this set of rocks is mainly poorly differentiated mantle-derived basic volcanic rock.

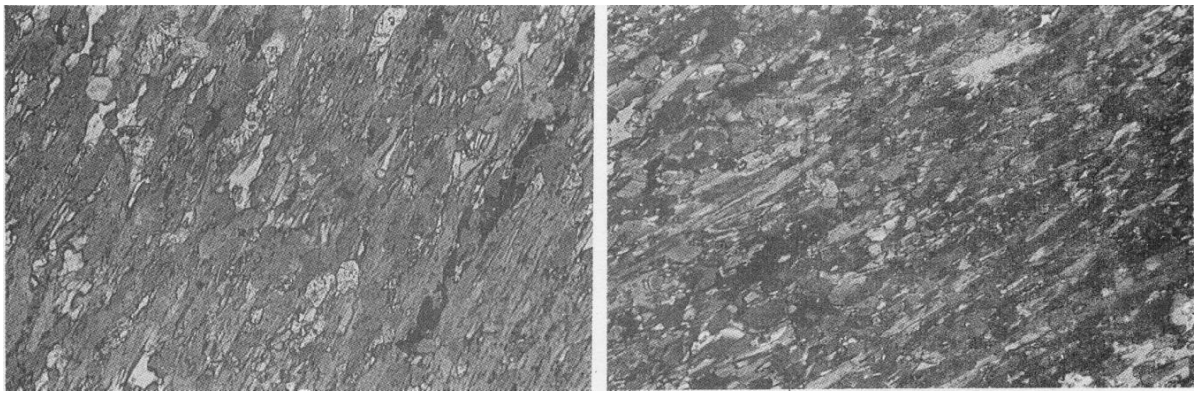

Figure 7. The middle ore-hosting hornblende schist (left) and chlorite schist (right) of the lower-middle Triassic system

(The thin section (−) 3.3 × 10)

This set of rocks has a low SiO_2 content ranging from 32.3% to 52.12%, with an average of 43.71%. Al_2O_3 ranges from 12.54% to 16.75%, with an average of 14.15%. Low Na_2O (<4.00%) and K_2O (average content generally comparable to Na_2O). Its total iron FeO*/(FeO* + MgO) = 0.68, CaO/Al_2O_3 = 0.70 < 0.82, $Fe^{3+}/(Fe^{2+} + Fe^{3+})$ = 0.23<0.40, indicating the nature of mantle derived basic volcanic rocks[4 & 28].

3.3 Structure

The Triassic strata make up a NNE-trending dome, namely, the Dashuigou dome. The deposit is located at the northeastern end of the Triassic metamorphic dome. The ore bodies are both controlled by and fill a group of shear fractures (Figs. 4 and 5)[4 & 28].

Both faults and folds are well-developed in the area. The annular and linear structures together make up special Ø-shaped structures which control the formation of different types of endogenetic mineral deposits, including the Dashuigou tellurium deposit (Figs. 3, 4 and 5).

Linear structures can be divided into the following groups: NW, NNE, NS, NWW, and NEE. These linear structures include the Dadu River ductile shear zone and the Xiyoufang ductile shear zone (Figs. 2, 3 and 4).

As the area's largest known annular structure concentric with the Xiyoufang as the center at a diameter of about 8 km, the Xiyoufang annular structure (Fig. 3) is closely related to mineralization. More than 20 tellurium showings and the Dashuigou tellurium deposit, as well as more than 10 Au-Bi composite geochemical anomalies and some gold geochemical anomalies, are spatially related to the annular structure. With its southern point reaching the Dashuigou deposit, the Xiyoufang annular structure is a composite ring. In addition to the concentric composite ring of the large ring itself, there are two small annular structures with a diameter of about 2 km inside the large ring. It is also accompanied by two other small rings around it.

Located in the southwest of the Xiyoufang annular structure, the Dashuigou annular structure is one of the sub-rings of the Xiyoufang annular structure and intersects with NE, EW, SN, and NW trending linear structures, forming a characteristic Ø-shaped structure and controlling the Dashuigou tellurium deposit and the nearby Majiagou tellurium showing, as well as several Au and Bi geochemical anomalies. The perfectly circular Jinhuadong annular structure is also a sub-ring of the Xiyoufang annular structure and intersects with NWW, NNW, and SN-trending linear structures, forming a characteristic Ø-shaped structure, and controls the Jinhuadong, Qifenyao, and Bafenyao tellurium showings, as well as several Au and Bi geochemical anomalies. In addition, there are Baita, Tianwan Township, Tangjiapo, and Jiangguanshan ring structures. The common feature of these annular structures is their close spatial relationship with the Bi and Au geochemical anomalies.

There are two large ductile shear zones in the area that form the basic structural framework, which are briefly described as follows.

The Dadu River ductile shear zone, which extends along the west bank of the Dadu River, is over 300 kilometers long and has a maximum width of over 30 kilometers. It is distributed in a north-south direction and is located in the northeast of the Dashuigou tellurium deposit. The fault zone converges in the north and spreads in the south, affecting a range of approximately 10-15 kilometers from east to west in the areas of Xiyoufang, Dashuigou, and Jinhuadong (Figs. 2 and 3). This fault zone controls most of the metal deposits discovered in the research area.

The Xiyoufang ductile-brittle shear zone has a total length of over 300 kilometers and a width of 10-15 kilometers. The Dashuigou sub-zone is the main structural zone of the Xiyoufang ductile-brittle shear zone. This sub-zone is composed of several roughly parallel secondary zones, with the largest one passing through the Dashuigou and Majiagou tellurium deposit and/or showing, while the remaining secondary zones pass through the other tellurium showings.

The above two ductile shear zones intersect in the northeast of the mining area and are also part of the Xiaojinhe lithospheric fault zone mentioned above.

Other representative faults in the study area include the Hongba fault, Wanbahe fault, Xiyoufang-Guanyinshan fault, Keluo-Jiziping fault, and Anshunchang-Xinchang fault from west to east, which are part of the two shear zones

mentioned above. On the whole, these faults are broom-shaped converge at the northern end, and spread out at the southern end.

The folds in the study area are mostly NNE or nearly SN-trending, and are relatively tight, narrow, and long. These folds include the Dashuigou dome structure and the Bindo anticline in the northwest of the deposit, etc.

The Dashuigou dome is roughly NNE trending, more than 10 km long, and entirely composed of lower and middle Triassic metamorphic rocks. Its northern section is damaged by a fault of nearly the same strike, and its four sides of the northeast, southwest, northwest, and NNW are cut and bounded by NNW-trending, near north-south, and NNE-trending faults respectively, forming a highly flattened rhombic block in space. On the two-dimensional plane, the Dashuigou tellurium deposit is located in the north-central part of the dome.

3.4 Igneous rock

No large intrusive rocks occur within a 5 km radius around the deposit. Only two small Permian ultrabasic-basic rock bodies emerge within a 10 km range of the deposit as described above (Figs. 2 and 4).

4 Ore body

The Dashuigou tellurium deposit is produced at the north-eastern end of the dome consisting of the lower-middle Triassic system (Figs. 2-5). The entire tellurium ore bodies are limited to the tourmaline-containing amphibolite schist in the middle of the dome (Figs. 4 and 5).

Both the early pyrrhotite and late tellurium ore veins filled in a group of structural fissures with shear properties and intersected obliquely with the ore-hosting rocks. The early-formed pyrrhotite veins are in a typical lens shape, in which the breccia of the ore-hosting rock is common (Figs. 8 and 9) [4, 28 & 40-42].

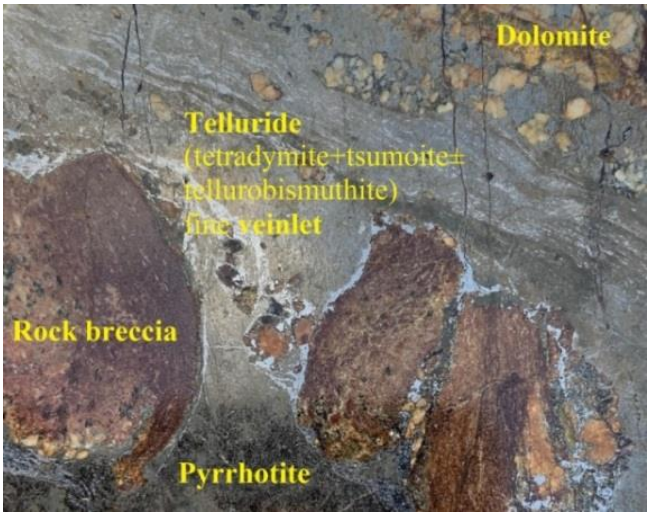

Figure 8. The lead grey-silvery telluride (tetradymite + tsumoite ± tellurobismuthite) fine veinlets + dolomite (brownish white) + host rock breccia (brown) in massive pyrrhotite (grey) from the deposit

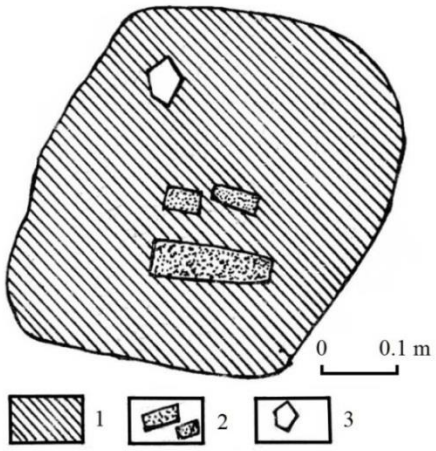

Figure 9. Sketch of country rock breccia and megacrystalline pentagonal dodecahedron pyrite in early pyrrhotite veins

After the formation of early pyrrhotite veins, they were subjected to compressive shear activities and fractured to form expansion structures. Late tellurium veins and/or veinlets filled these fractures (Figs. 8 and 10).

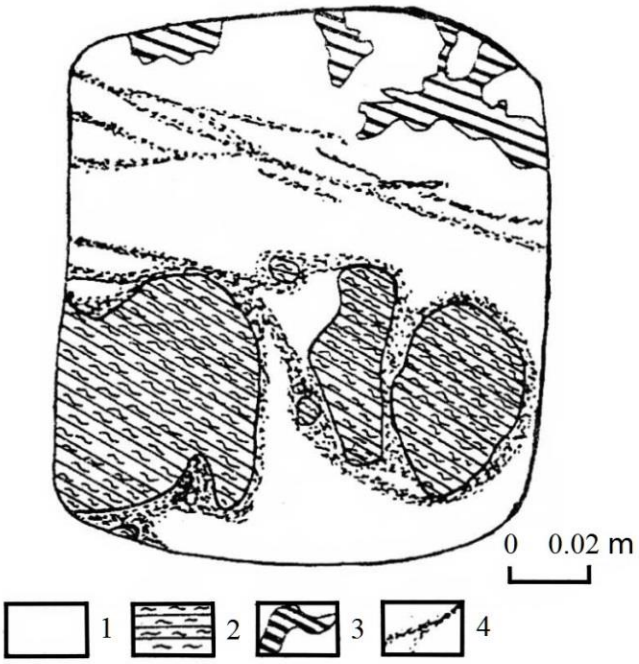

Figure 10. Sketch of the late telluride veinlets surrounding country rock breccia in early pyrrhotite vein

Table 2 briefly lists the basic characteristics of representative tellurium ore bodies in the Dashuigou tellurium deposit.

Table 2. Basic characteristics of representative tellurium ore bodies in Dashuigou tellurium deposit

Ore body	Occurrence	Length	Width	Thickness	Grade	Note
		Unit: meter				
I-1	280°∠60°, lateral direction 342°, lateral angle 15°	61.0	8.0	0.3	0-34.5%, average 6.0-7.0%	The lateral direction of the ore body refers to the orientation of the ore body axis, and the lateral accretion angle is the angle between the ore body axis and the horizontal plane.
I-2	300°∠70°, lateral direction 5°, lateral angle 22°	30.0	7.0	0.3		
I-3	300°∠60°, lateral direction 15°, lateral angle 12°	10.0	2.5	0.1	Average 0.0-0.5%	
I-4	335°∠60°, lateral direction 27°, lateral angle 33°	16.0	5.0	0.4		
I-5	285°∠55°, lateral direction 333°, lateral angle 15°	26.0	6.0	0.3	Upper part: 90.0%, lower part: 0-0.5%	
I-7	288°∠49°, lateral direction 340°, lateral angle 15°	-	-	0.2	-	
I-8	280°∠51°, lateral direction 330°, lateral angle 20°	-	-	0.5	-	
I-9	268°∠83°, lateral direction 330°, lateral angle 20°	-	-	0.3	-	
I-10	295°∠68°, lateral direction 355°, lateral angle 24°	-	-	0.6	-	

The overall occurrence of the tellurium ore zone composed of all tellurium ore bodies is 280°∠55°-70°, with a general strike of 10°±, an axial direction of 240°, and a lateral angle of 20°±. The entire ore zone is 25-30 meters wide and its axial length about 40 meters (Table 2).

The single ore bodies generally trend 350°-10° and/or 20° and dip 45°-83° westward, while the occurrence of host rocks in the mining area is 8°-38°∠21°-35°. The two are obviously obliquely related (Figs. 4 and 5).

Among all ore bodies, #I-3 ore body is special. It is almost entirely composed of dolomite and various tellurides, and the tellurium minerals mostly appear in the form of coarse grained scales, and there are no other sulfides such as pyrrhotite and pyrite commonly found in other ore bodies. The dolomite in #I-3 ore body is milky white, and tellurium minerals are distributed in a patchy pattern within the dolomite.

Except for the #I-5 ore body, the hanging and foot walls of all the other ore bodies are all schist. The hanging wall of the #I-5 ore body is schist, and the foot wall is banded marble; that is, the ore body is almost filled in the contact of the two different lithologies (Fig. 6).

The ore body appears in an obvious lens shape in the longitudinal section, and appears in the shape of veins and/or lenses arranged in echelon arrangement in the horizontal projection and plan views of different levels (Figs. 4 and 5). The echelon-like arrangement of tellurium ore bodies is particularly obvious in the 1450 m level (Fig. 11).

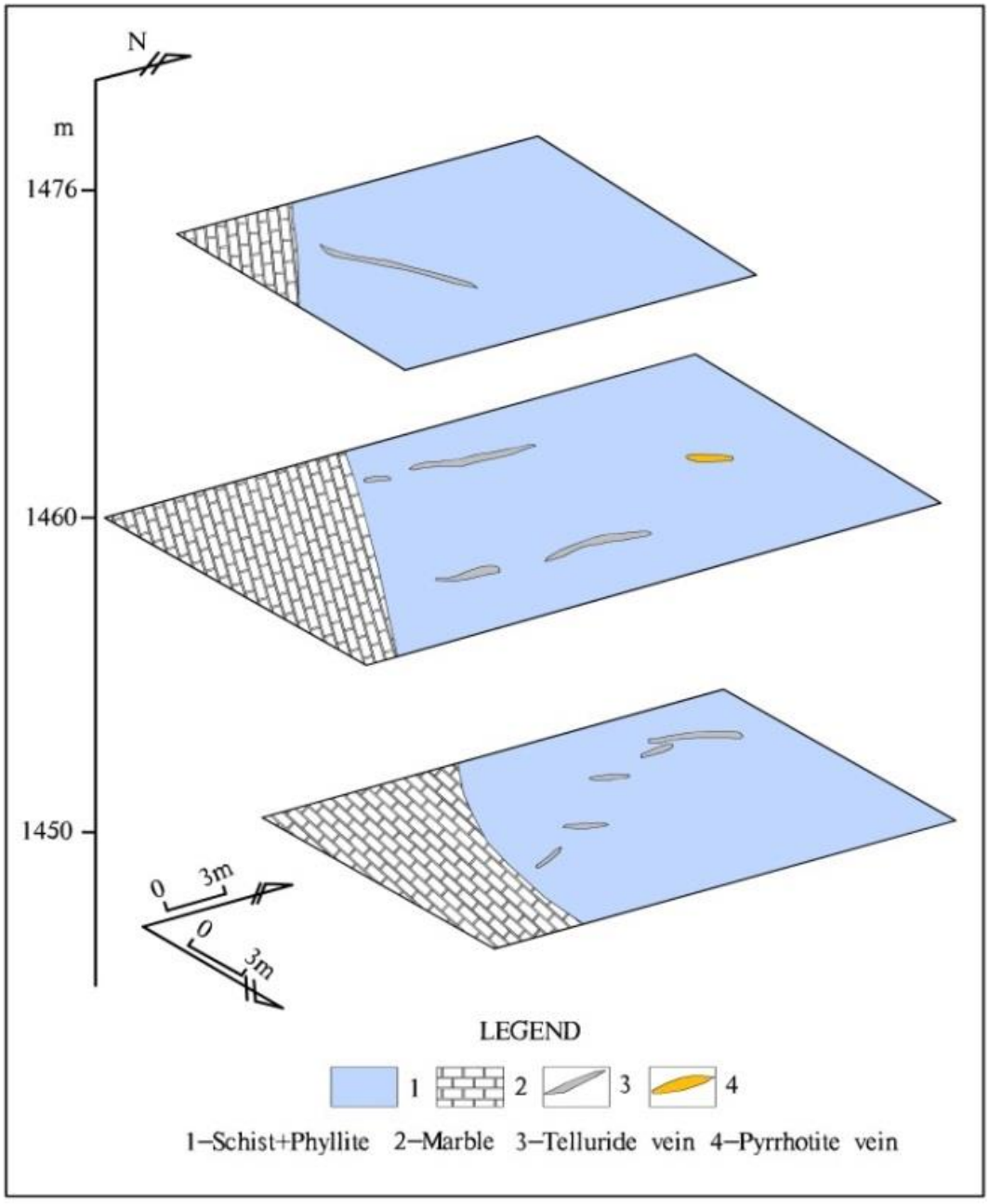

Figure 11. Three-dimensional spatial distribution of the tellurium ore bodies

Whether it is pyrrhotite veins or telluride veins, they all have a very striking and clear contact with the altered host rocks; that is, there is no gradual transition zone between these veins and the host rocks, and/or between the two different veins themselves (Figs. 12 and 17-19).

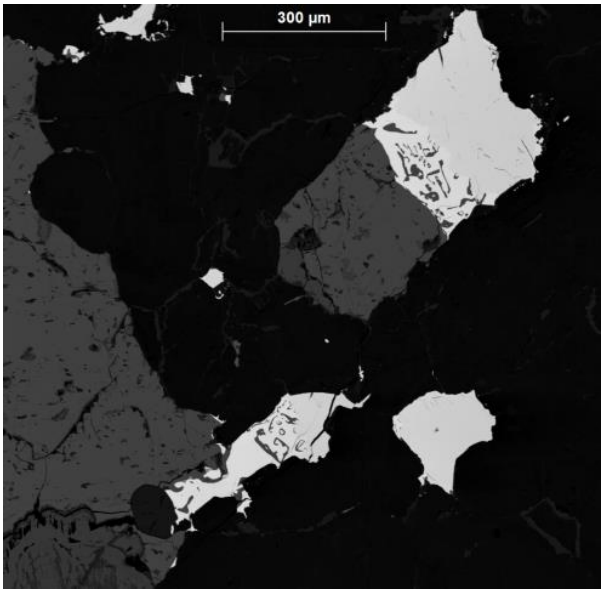

Figure 12. Distinct contact between pyrrhotite veins (dark grey), telluride veinlets (white), and carbonate veins (black)

5 Alteration and mineralization

Whether it is a pyrrhotite vein or a tellurium vein, the alteration zones on both sides are very narrow and non-zoned, which range between several centimeters and one meter in thickness. Those altered zones beside the massive and/or semi-massive ore veins are narrower, at only several centimeters wide. Field observations show that there is no positive correlation between ore body size and alteration intensity. This may be related to the fact that the mineralization of this deposit is narrow vein style[4 & 28].

The alteration zones are light gray or yellowish brown, obviously lighter than the surrounding host rocks of the same lithology, and the baked edge is very clear.

There are many types of alteration, including biotitization, dolomitization, silicification, tourmalinization, potassium feldsparization, albite, chloritization, grenaitization, muscovitizaion and/or sericitization, pyrrhotization, pyritization, and calciteization, etc.

Among them, dolomitization is the most widely distributed in the entire study area. Dolomite veins are an important carrier of tellurium. Where dolomitization is strong, the tellurium content increases significantly. In many cases, dolomite, quartz and muscovite occur symbiotically and/or associated with each other.

Alterations such as dolomite and quartz are products of multiple phases. The dolomite formed in the early stage is coarse grained, iron stained and brittle (Fig. 8), while the late dolomite has fine particles and no iron staining. The quartz veins formed in the early stages are brown or light brown due to iron staining, and dense shear cracks develop in them (Fig. 13). The late quartz is white, with muscovite developing in it.

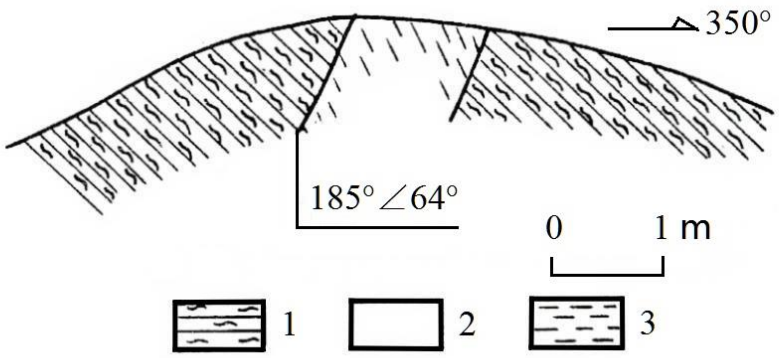

Figure 13. Sketch of dense shear fractures in the quartz veins in the mining area

1. Schist + phyllite, 2. Quartz vein, 3. Share fracture

The scaly biotite with intact crystal form forms fine veins or irregular clusters, closely attached to the early pyrrhotite veins, but has no spatial dependence with the late tellurium veins.

Ubiquitous in the study area, scale-like muscovite often appears together with the late quartz veins, or symbiotic with late dolomite in the form of veinlets. Occasionally, some muscovite appears superimposed on biotite on both sides of the early-formed pyrrhotite veins. This muscovite should be derived from the alteration of early biotite.

Tourmaline, chlorite and albite are closely symbiotic with the early-formed pyrrhotite veins. Mottled pyrrhotite and pyrite are often found in the flesh-red fine-medium grained albite veinlets.

Closely symbiotic with pyrrhotite, most, if not all of the pyrite appear in the form of pentagonal dodecahedrons with intact crystal forms (Fig. 14). The largest single crystal can reach several centimeters. It is certain that these pyrites are the product of the early paragenetic stage; namely, the pyritic stage. No pyrite is found in the late tellurium veins.

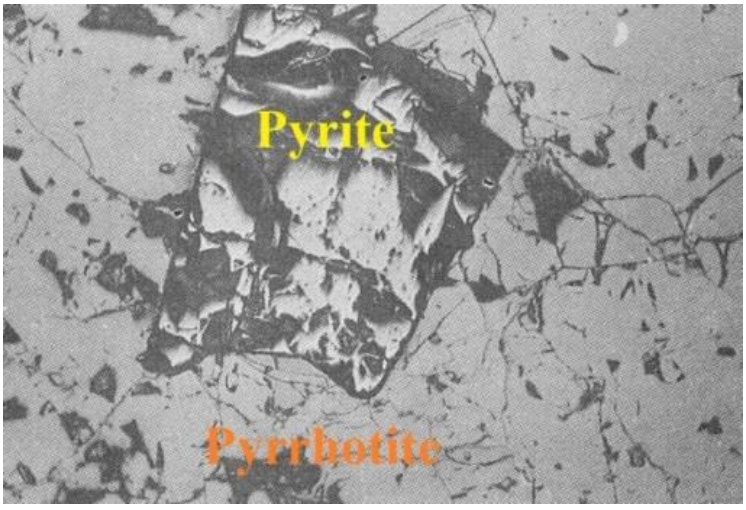

Figure 14. Euhedral pyrite (light grey) in massive pyrrhotite (grey)

(Thin section (−) × 200)

In contrast to pyrite, weaker chalcopyrite and galena mineralization should be products contemporaneous with the late tellurium mineralization. Under the microscope, tellurium minerals and chalcopyrite are commonly seen in association. Sometimes chalcopyrite veinlets can also be seen interspersed with telluride veinlets. Of course, it is also common to see chalcopyrite veins/veinlets interspersed with early-formed pyrrhotite veins.

Generally speaking, the alteration and mineralization in the mining area can be roughly divided into two groups: early and late, corresponding to the early and late mineralization stages respectively.

Early alteration and mineralization closely associated with pyritic (pyrrhotite + pyrite) veins include biotitization, dolomitization, silicification, tourmalinization, albite, chloritization, and pyritization. The typical symbiotic mineral combination is: coarse-grained iron-stained dolomite + megacrystalline pentagonal dodecahedron pyrite + pyrrhotite + biotite ± albite ± tourmaline ± native gold ± chalcopyrite.

Late alteration and mineralization closely associated with telluride veins include muscovitization, sericitization, dolomitization, silicification, calcite, chalcopyrite mineralization, gold mineralization, and galena mineralization, etc. Typical mineral combinations are tetradymite + tsumoite + quartz + dolomite + calcite + chalcopyrite + gold + silver.

6 Analytical method or methodology

This article uses the electron probe for line and surface scanning to qualitatively or quantitatively analyze ore samples, while also studying the existing forms of some elements and/or minerals.

The electron probe instrument can measure elements in the range of 4Be-92U, with a sensitivity of up to 3/100000 parts according to statistical views, and the actual relative sensitivity is close to 1/10000 to 5/10000 parts.

Generally, when the content of elements in the analysis area reaches 10-14 parts, it can be perceived. The measured diameter of the sample is within 1 μm and 500 μm.

Line scanning is the scanning of an electron beam along a straight line direction to determine the relative concentration changes of relevant elements in that straight line direction and obtain the concentration distribution curve. Surface scanning is the process of scanning a sample surface with an electron beam to directly observe and capture the type, distribution, and content of the element on the screen. This means that the concentration of the element is represented by the density of the white highlights in the photo (Fig. 17).

7 Geological dating

In order to further determine the temporal relationship between pyrrhotite veins and tellurium veins and determine the mineralization age of the Dashuigou tellurium deposit, the K-Ar isotope dating was conducted on different minerals in the deposit.

When collecting samples, in addition to paying full attention to their freshness, special consideration was also given to their reasonable spatial configuration.

One scaly biotite sample was collected from the hanging wall and another from the footwall of the telluride-free pyrrhotite vein. A superimposed altered muscovite sample was collected from the footwall of this pyrrhotite vein. In addition, a second muscovite sample was collected from the altered host rock beside one tellurium ore body. A third muscovite sample was collected from a dolomite vein at Miaoping on the periphery of the deposit. These pale greenish white scale-like muscovites appear in the form of veinlets in the large dolomite vein (Fig. 15).

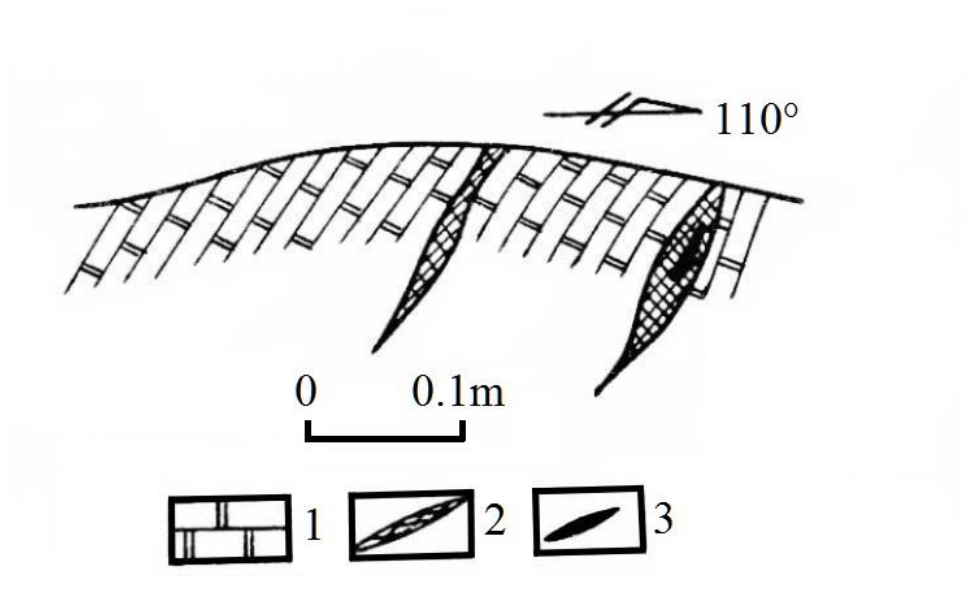

Figure 15. Sketch of the light greenish white muscovite veinlet in the coarse grained dolomite vein in the impure marble in the upper part of the ore-hosting bed at Miaoping near the deposit

1. Marble, 2. Dolomite vein, 3. Muscovite veinlet

The third muscovite sample was collected to verify whether the widespread muscovitization outside the mining area and the muscovitization in the deposit are the product of the same geological event. If it is the product of the same geological event, then muscovite, as an important alteration closely related to the tellurium mineralization, and one of the indicators of ore prospecting, can be given full attention when prospecting potential tellurium resource in areas with the similar geological setting.

A total of 5 mica mono-mineral samples mentioned above were carefully selected, separated, washed, dried, and then selected to ensure that their purity was above 99%. Finally, the K-Ar geological dating age was determined. The results are shown in Table 3 below.

Table 3. K-Ar isotope dating results of the Dashuigou tellurium deposit[4 & 43-44]

Series #	Sample ID	Sample description	Result (m.a.)
1	SD-19	Biotite in the hanging wall of the pyrrhotite vein without tellurium	177.7 ± 1.6
2	SD-20	Biotite in the footwall wall of pyrrhotite vein without tellurium	165.1 ± 1.5
3	SD-21	Muscovite in the footwall of the telluride-free pyrrhotite vein	88.3 ± 0.8
4	SD-23	Muscovite in the surrounding rocks near the No. 1 tellurium vein	80.2 ± 0.7
5	SL-09	Muscovite in dolomite veins outside the mining area	91.7 ± 0.8

It can be seen from Table 3 that, as speculated based on the geology above, the pyrrhotite vein and the tellurium vein are the results of two independent geological events with a long interval of geological time. The emplacement age of the former is 177.7-165.1 Ma, and its iconic wall rock alteration was biotitization. The latter is emplaced at 91.71-80.19 Ma, and its typical wall rock alteration is muscovitization/sericite.

8 Petrochemistry and geochemistry

Detailed petrochemical and geochemical studies of relevant rocks in the area show that protolith of the deposit's host rock is mantle-derived basic volcanic rock[4 & 28]. The contents of the main mineralizing elements Te, Bi, Se and Au etc. in different rocks of different geological times are very low, generally lower than or close to their respective crustal Clark values[1-4 & 28]. The enrichment of these elements is obviously related to alteration, the stronger the alteration, the higher the corresponding element content. Both the alteration and mineralization are most likely related to the upwelling of mantle materials produced through mantle plumes or mantle hot spots[4 & 28].

9 Ore

9.1 Mineral

According to the rock and ore identification under the microscope and electron probe analysis, there are more than 30 minerals that make up the ore. These minerals are mainly carbonates, silicates, sulfides including tellurides, native element minerals and a small amount of oxides. These minerals constitute different types of ores and waste rocks in different proportions, forms, occurrences, textures and structures[4,28,42 & 45-48].

Carbonate minerals are very developed and are produced in large quantities in both pyritic and tellurium stages. They are also one of the important carriers of tellurium minerals. The carbonate minerals in the deposit are mainly dolomite, calcite and siderite (Fig. 16).

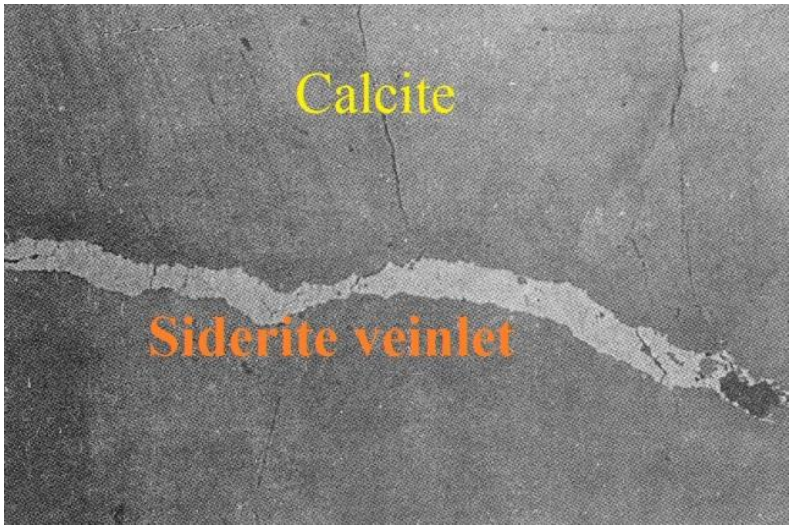

Figure 16. Siderite veinlet (white) interspersed with calcite vein (grey)

(Thin section (−) × 200)

Compared with the respective theoretical values of these three minerals[49], the dolomite in the deposit is poor in magnesium and rich in iron, but not to the extent of ankerite, so it can be called iron-bearing ankerite. Calcite is generally rich in magnesium and occasionally rich in iron, which can be called magnesium-bearing calcite and iron-bearing magnesium calcite respectively. The siderite is rich in calcium and slightly poor in iron. There exist

isomorphic substitution series between $MgCO_3$ and $FeCO_3$. The composition characteristics of the above-mentioned carbonate minerals are also clearly reflected in various diagrams[4 & 42].

Silicate minerals are also the main gangue components in the deposit, which include muscovite, hornblende, plagioclase, chlorite, and potassium feldspar (Table 4). Among them, hornblende and plagioclase formed earlier, followed by chlorite and potassium feldspar, and muscovite including sericite formed later.

Oxide minerals include rutile, ilmenite, quartz, magnetite, specularite, hematite and limonite (Table 4). Except for quartz, which is mostly produced in the form of veins/veinlets, the other oxide minerals are mostly produced sporadically in the form of irregular granules and flakes.

Table 4. Electron probe analysis results of minerals from the Dashuigou tellurium deposit (wt. %)[4 & 42]

Sample #	Test point	SiO_2	Al_2O_3	CaO	K_2O	Na_2O	MgO	TiO_2	Cr_2O_3	MnO	FeO	Total	Mineral
II-2	1	0.22	0.10	0.39	0.00	0.00	0.00	98.05	0.05	0.08	1.00	99.89	tutile
	2	0.22	0.09	0.69	0.00	0.00	0.00	97.92	0.09	0.05	0.08	99.14	
	3	0.22	0.08	0.51	0.00	0.00	0.00	97.17	0.09	0.05	1.28	99.40	
	4	44.52	38.10	0.79	10.19	1.21	0.51	0.18	0.31	0.00	0.55	96.36	muscovite
	5	43.42	39.16	0.00	9.86	1.05	0.58	0.12	0.27	0.00	0.36	94.82	
I-4	6	43.91	14.62	13.45	0.00	1.02	9.81	0.01	0.00	0.12	14.87	97.81	amphibole
I-8	7	62.45	23.79	6.14	0.00	6.75	0.00	0.00	0.09	0.00	0.49	99.71	plagioclase
	8	0.13	0.00	0.02	0.00	0.00	1.80	53.32	0.04	0.93	43.34	99.58	Ilmenite
	9	0.13	0.00	0.12	0.00	0.00	1.80	52.20	0.04	0.93	43.21	98.43	
	10	38.61	15.94	13.01	0.13	1.38	8.85	0.37	0.04	0.16	13.67	92.16	amphibole
	11	27.17	21.94	0.09	0.00	0.00	19.18	0.10	0.19	0.11	15.36	84.14	chlorite
D4	12	46.93	38.28	0.04	6.67	0.91	0.22	0.26	0.08	0.00	0.57	93.96	
3	13	49.26	36.93	0.02	6.53	0.00	0.16	0.70	0.16	0.00	0.00	93.76	K-feldspar
	14	99.32	0.04	0.06	0.00	0.00	0.18	0.00	0.10	0.05	0.00	99.75	quartz
D1	15	0.25	0.00	1.77	0.02	0.31	0.31	0.00	0.02	0.01	90.57	93.26	magnetite
Sample #	**Test point**	**Te**	**Bi**	**S**	**Fe**	**Cu**	**As**	**Ni**	**Zn**	**Au**	**Ag**	**Total**	**Mineral**
D2	1	0.02	0.12	35.00	29.66	34.72	0.00	0.02	0.02	0.05	0.09	99.70	chalcopyrite
	2	0.00	0.21	37.57	61.33	0.07	0.02	0.10	0.02	0.00	0.00	99.32	pyrrhotite
	3	0.14	0.17	38.24	60.73	0.01	0.00	0.10	0.03	0.05	0.04	99.51	

Sulfide minerals are mainly pyrrhotite and pyrite formed in the early stage, with a small amount of chalcopyrite and galena formed in the late stage. Chalcopyrite is mostly interspersed in pyrrhotite in the form of veinlets, and galena blebs can be seen under the microscope.

Telluride minerals mainly include tetradymite (Bi_2Te_2S), tsumoite (BiTe), and tellurobismuthite (Bi_2Te_3)[4,7,42 & 48]. Among them, tetradymite accounts for over 90% of all the tellurides in the ore, while the latter two are mostly found in the contact metasomatic zone between tetradymite and pyrrhotite (Figs. 8, 10, 12 and 17-20).

Native element minerals mainly include native gold, electrum, kustelite, native silver, and native tellurium etc., as a series of minerals formed between gold and silver, as well as gold and tellurium.

According to other researchers[45-48], there are also small amounts of joseite, hessite, goldschmidtite, sphalerite, calaverite, stützite, vulcanite, secondary tellurium, and bismite etc. in the ore of the deposit.

To sum up, the minerals that make up the ore in Dashuigou tellurium deposit are as follows: tetradymite, pyrrhotite, pyrite, dolomite, quartz, chalcopyrite, tsumoite, tellurobismuthite, galena, magnetite, gold, silver, electrum, ilmenite, calcite, calaverite, siderite, mannesite, rutile, muscovite, biotite, sericite, hornblende, chlorite, plagioclase, K-feldspar, tourmaline, hematite, garnet, apatite, and epidote. The first five minerals comprise approximately 85% of the ore[4,7,40-42 & 45-48].

9.2 Structure and texture

The texture and structure of the ore are relatively simple and are briefly described as follows:

Texture

Euhedral - semi-euhedral flake: Mainly coarse-grained tetradymite appears in the form of relatively intact scales.

Euhedral: For example, coarse-grained pyrite appears as a typical pentagonal dodecahedron in pyrrhotite, dolomite and calcite veins (Fig. 14). Many times, coarse-grained dolomite and calcite also appear as euhedral crystals.

Xenomorphic-granular: Pyrrhotite and most quartz mostly appear in xenomorphic-granular in the deposit.

Metasomatic: Minerals formed early are metasomatized by late minerals and appear in the form of residues etc. (Figs. 8, 12 and 17-19).

Metasomatic graphic shows that telluride minerals such as tetradymite replace pyrrhotite and the latter's residue appears in the graphic form (Figs. 12 and 17-19).

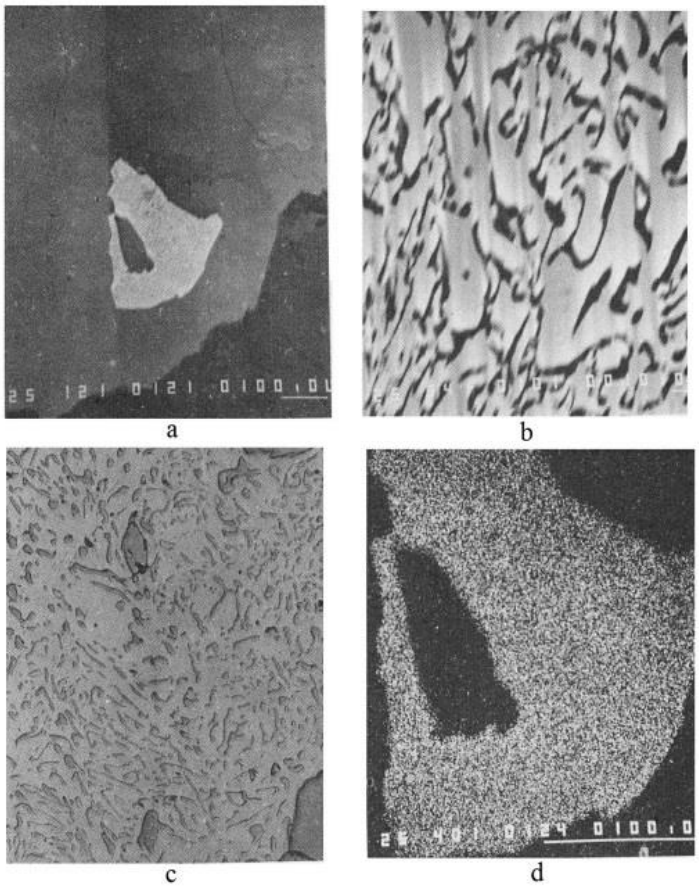

Figure 17. a~c: Reflection color and their mutual relationships between tsumoite (bright white), tetradymite (white), and pyrrhotite (grey to dark grey) in the back scattered electron image from the deposit (thin section (-): a ×120, b ×540, & c ×200). d: Te Kα X ray image indicating chemical composition distributions of telluride including tetradymite and tsumoite (white): the denser the white spots, the higher the Te content; the black colored background is pyrrhotite from the deposit (×400)

Reaction rim: Tetradymite reacts with pyrrhotite to form a unique reaction rim texture of tsumoite, and at the same time the above-mentioned metasomatic graphic texture appears (Figs. 12, 17a, 17d and 18-19).

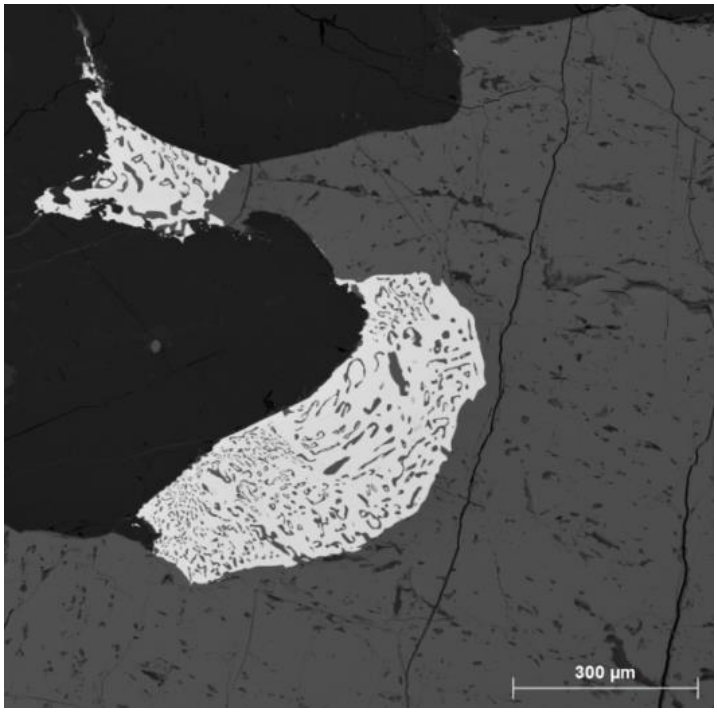

Figure 18. Reaction rim between telluride (tetradymite + tsumoite, white), pyrrhotite (grey), and dolomite (black)

Solid solution separation texture of tetradymite and chalcopyrite can be seen under the microscope (Figs. 12 and 17- 19).

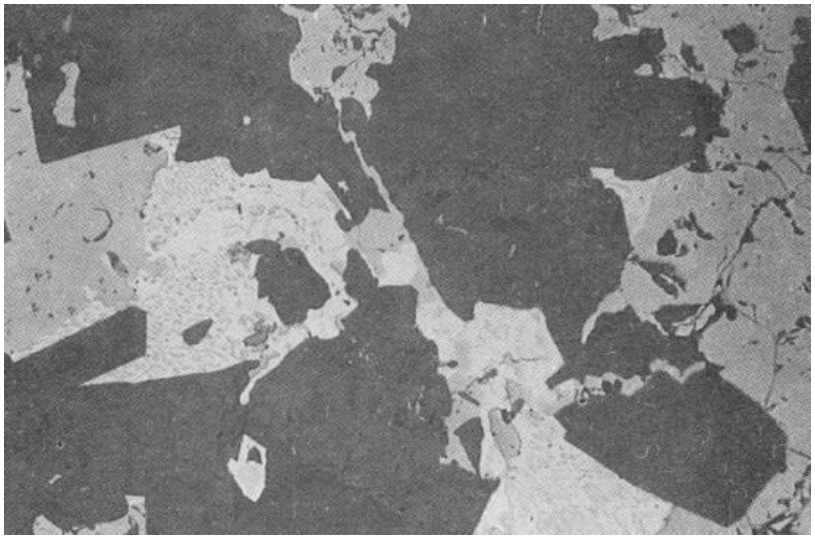

Figure 19. The solid solution separation texture of tellurides (white base) and chalcopyrite (a light grey worm-like mineral with unobvious protrusions), and the metasomatic texture in the contact metasomatic zone between tellurides (white base) and pyrrhotite (gray white). Black is carbonate mineral (thin section (-) ×200)

Structure

The main ore structures are as follows:

Massive: Dense massive ore is the most important structural type in the deposit, and is often composed of coarse-grained lamellar tetradymite as well as other telluride minerals. This kind of ore is almost entirely composed of telluride minerals mainly tetradymite, with little or no other minerals. It is a type of ore only found in rich ore pockets in the deposit.

Vein and/or veinlet: The main manifestations are that tellurium ore bodies intersect in the form of veins or veinlets, cutting the pyrrhotite veins produced in the early stage (Figs. 8, 10, 12 and 18-20).

Stockwork: A stockwork is a complex system of structurally controlled or randomly oriented veins, veinlets and/or stringer zones, which is common in various ore deposits[50]. Telluride veins/veinlets intersect, divide, and surround pyrrhotite in a fine network form or stringer, forming a characteristic stockwork vein structure (Figs. 8, 10, 12 and 18-20).

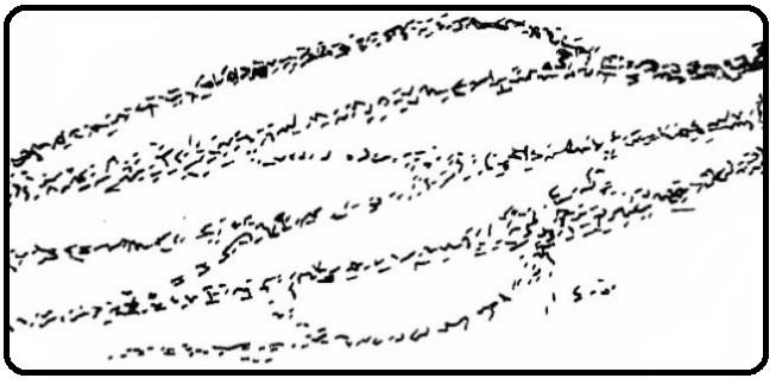

Figure 20. Sketch of telluride stockworks in pyrrhotite in #I-1 ore body

(The scale is the same as Fig. 10)

Dissemination: Tellurium minerals are distributed in pyrrhotite, dolomite, quartz and potassium feldspar veins/veinlets in disseminated, scattered, speckled or patchy forms.

Brecciated: Telluride veins often intersect, divide and develop around pyrrhotite and/or host rock breccia, forming breccia-like structures (Figs. 8-10, 12, 17 and 19).

In addition, giant pentagonal dodecahedral pyrite single crystals are commonly found in pyrrhotite veins, forming a bird's-eye-like structure (Fig. 14).

9.3 Ore type

According to the ore structures, the ores in this deposit can be divided into massive, veinlet-stockwork, and disseminated types. Among them, massive ores account for the largest proportion and are the most important, followed by disseminated ores. The above-mentioned major types of ores can be further divided into several subcategories according to their respective mineral compositions (Table 5).

Table 5. Ore type in the Dashuigou tellurium deposit

Ore type	Ore sub-type	Representative ore body
Massive	Telluride (>85%)-dolomite (<10%)	# I-1, 2, 5, 9, and 10
	Telluride (>85%)-sulfide	# I-1, 2, 4, 5, 7, 8, 9, and 10
Veinlet-stockwork	Telluride (50%-85%)-dolomite (10%-40%)	All of the ore bodies
	Telluride (50%-85%)-sulfide (10%-40%)	All ore bodies except # I-3
	Telluride (50%-85%)-quartz (10%-40%)	Individual ore bodies
Disseminated	Dolomite (>40%)-telluride (<50%)	# I-3
	Pyrrhotite (±pyrite) (>40%)-telluride (<50	All ore bodies except # I-3
	Quartz (±mica) (>40%)-telluride (<50%)	This type of ore is less

Tellurium ore types vary in different ore bodies. In terms of mineral composition alone, dolomite-telluride ore is the most numerous in the deposit.

9.4 Ore composition

The quantitative chemical analysis of the ore through the random chip sampling method shows that the ore of the Dashuigou tellurium deposit contains tellurium between 0.01%-34.58% (Table 6). Previously, Cao et al. concluded that the tellurium ore grade of the deposit is 0.01%-30.63%[45].

Generally speaking, copper and other ores containing 0.002% or more of associated tellurium are valuable. In other words, the minimum recoverable grade of tellurium ore is 0.002%[4-7 & 28].

9.5 Ore property

The ores in this deposit are all deeply buried and have not been exposed to the surface by erosion and thus have not has not suffered any weathering. In other words, the ore in the mining area maintains the state of the original sulfide ore and has not been transformed by oxidation.

This single ore property greatly simplifies the ore processing technology process, thereby greatly saving investment and reducing related expenditures. This is a more positive and economical aspect of developing the deposit.

Table 6. Chemical compositions of the ores in Dashuigou tellurium deposit

Sample #			SHM-01	SHM-02	SHM-03	SHM-04	SHM-05
Chemical coposition	SiO_2	%	28.60	0.06	0.90	0.62	0.19
	Al_2O_3		23.08	0.32	0.57	0.05	0.15
	Fe_2O_3		18.90	81.62	53.71	3.36	6.56
	CaO		0.67	0.01	10.30	0.05	10.90
	MgO		5.00	0.03	4.72	0.01	4.73
	TiO_2		0.51	0.06	0.06	0.03	0.04
	P_2O_5		0.95	0.21	0.31	0.22	0.21
	MnO		0.04	0.01	0.30	0.01	0.87
	K_2O		0.01	0.00	0.05	<0.001	0.02
	Na_2O		0.55	0.04	0.07	0.00	0.02
	S		5.47	16.41	19.92	4.59	3.15
	H_2S		3.55	1.45	0.37	0.39	0.38
	CO_2		1.35	0.09	17.10	0.19	17.90
	Bi		0.11	<.001	0.12	57.20	35.40
	Te	$\times 10^{-6}$	586	100	656	345800	216600
	Se		<10	18	34	110	100
	F		355	30	20	5	45
	Cl		1.5×10^2	778	620	28	102
	Cu		428	2180	1140	88	237
	Pb		184	16	18	332	206
	Zn		720	-	-	288	25
	B		8600	<1	<1	<1	<1
	Au		0	0	0	2	77
	Au		2	0	1	260	148

10 Paragenetic stage and mineral sequence

Based on the mutually crosscutting relationships of various veins/veinlets in the deposit, including those of pyrrhotite, chalcopyrite, tetradymite, tsumoite, dolomite and quartz, plus related research on ore structure and structure between both gangue and ore minerals under the microscope, two mineralization stages and five sub-stages in the deposit have been confirmed[4,7, 27-28 & 43-44].

10.1 Pyritic stage (177.7~165.1 m.a.)

Including the following three sub-stages as well as mineral sequence (from early to late):

Carbonate sub-stage: A large quantity of iron-dolomite, quartz and lesser calcite veins/veinlets occurred within this stage, which are broken brown and/or yellowish brown coarse-grained due to iron staining (Figs. 8, 10, 12, 15-16, and 18-19). Decrepitation temperatures of the fluid inclusions in the dolomite of this sub-stage are 337.7-397 °C.
Pyrrhotite sub-stage: The largest quantity of pyrrhotite formed during this stage. Some coarse to very coarse-grained pentagonal pyrite can be seen in the anhedral crystals of pyrrhotite (Figs. 8-10, 12, 14, and 17-19). Decrepitation temperatures of the fluid inclusions in both the pyrrhotite and pyrite of this stage are 366.0-406.0 °C.
Chalcopyrite sub-stage: Chalcopyrite veinlets formed within this stage, filling in fractures of pyrrhotite and/or crosscutting pyrrhotite. Part of the chalcopyrite is within telluride minerals in the vermicular form (Fig. 19). Decrepitation temperatures of the fluid inclusions in the chalcopyrite are 298.0-363.0 °C.

10.2 Tellurium stage (91.71~80.19 m.a.)

Including the following two sub-stages as well as mineral sequence (from early to late)
Tetradymite sub-stage: Large quantities of massive/semi-massive tetradymite veins/veinlets formed during this sub-stage, associated with clean, milky-white quartz, dolomite, calcite, muscovite/sericite, native gold and so on (Figs. 8, 10, 12, and 17-20). Decrepitation temperatures of the fluid inclusions in the tetradymite are 186.0-255.0 °C.
Tsumoite sub-stage: There is no doubt that the tsumoite was formed later than the tetradymite. Observation under the microscope seems to indicate that tsumoite is formed by the replacement of pyrrhotite by tetradymite, but this is not necessarily the case. Tsumoite and chalcopyrite together consist of emulsion droplets and/or vermicular immixing of solid solution texture at the contacts between tetradymite and pyrrhotite (Figs.12 and 17-19). The uniform temperature of the fluid inclusions in the quartz associated with the tsumoite indicates that the ore-forming temperature in this sub-stage is 180.0-258.8 °C.

11 Reserve and resource

In view of different understandings of the degree of geological engineering control, estimates of tellurium reserves and resources in this deposit vary greatly, and there is actually no very precise data. Based on relevant previous research data, the proven reserves of tellurium in the Dashuigou tellurium deposit range from 72 to 120 metric tons, and the prospective resources are 300 metric tons[4].

Based on the above relevant reserve data, we will use the relevant methods proposed by Laznicka[51] to define the scale of Dashuigou independent tellurium deposit.

If we use the crustal abundance or Clark value of tellurium published by Li Tong in 1976 and 1990[1-2], which is 6×10^{-10}, we can conclude that the tonnage accumulation indices of Dashuigou tellurium deposit are 1.2×10^{11}, 2.0×10^{11}, and 5.0×10^{11}, all exceeding 1.0×10^{11}, indicating that the deposit is a super large independent tellurium deposit. If the average abundance or Clark value of tellurium in the crust announced by Li etc. in 1994[3] is used, which is 2×10^{-8}, a similar conclusion can be drawn; that is, the deposit is a super-large independent tellurium deposit.

12 Discussion

Produced at the NE end of the dome, the deposit's entire Te ore bodies are limited to the schist/phyllite/slate in the middle of the dome. Both the early pyrrhotite veins and late tellurium ore veins filled in a group of fissures with shear properties. The later tellurium veins or veinlets filled in the compressive shear fractures developed in the early pyrrhotite veins.

The hanging and foot walls of the #I-5 ore body indicate that the contact between schist and banded marble in the study area is one of the favorable ore-hosting spaces and is naturally one of the good prospecting targets in the study area.

Both pyrrhotite and telluride veins have very clear contact with the altered host rocks and/or between the two different veins themselves. Meanwhile, the altered zones are very narrow and non-zoned. This may suggest that the deposit was formed through slurry penetration.

Scale-like muscovite and/or sericite in late quartz veins, or those symbiotic with late dolomite in the form of veinlets in host rocks close to the tellurium mineralization constitute another important prospecting indicator for potential tellurium deposits in the region.

Field geological observations show that the geological times of pyritic veins, tellurium veins and their associated alteration types are far apart, not products of the same mineralization period or geological event. Pyrrhotite is ubiquitous in the study area, whereas tellurium mineralization is much more localized. In other words, there is no necessary connection between tellurium mineralization and pyritic mineralization. Geological dating proves this.

The most favorable mineralization zone is where muscovitization/sericitization, dolomitization and silicification are superimposed and compounded.

In short, the wall rock alteration in the mining area is a product of different geological periods. The wall rock alteration related to the pyrrhotite veins is a product of the early Yanshan orogeny, while that related to the tellurium veins is a product of the late Yanshan orogeny.

The research area has a unique geotectonic background and geological conditions, with a considerable number of favorable channels/fault zones for mantle material to rise. In view of this, numerous rare and dispersed element deposits, including more tellurium deposits, will be discovered in the area in the near future.

The texture and structure of ores reflect the characteristics, similarities and differences of the mineralization period, mineralization stages and mineral generation sequence. As a result, ore texture and structure are one of the important foundations for dividing the mineralization stage, sub-stage, and mineral sequence of a mineral deposit.

According to Table 6, it can be seen that Te has an obvious positive correlation with Bi and Ag, and generally has the same growth and decline trend as Se, Au and Cu. In this regard, we can roughly understand that Te, the corresponding minerals of Bi and Ag are products of the same paragenetic stage, and the corresponding minerals of Se, Au and Cu are most likely products of the same mineralization period. This is consistent with the results observed under the microscope; that is, tetradymite, chalcopyrite, and Au-Ag series of minerals are all products of the late Yanshan orogeny.

The ore grade of Dashuigou independent tellurium deposit has far exceeded the minable grade of associated tellurium ore by 5.00 to 1.73×10^4 times, and its highest grade is even more than 1.73×10^4 times.

In terms of tellurium alone, the economic value of the Dashuigou deposit is self-evident. Fortunately, the ore also contains high grade of beneficial elements such as Bi, Au and Ag, and thus has high comprehensive utilization value (Table 6).

All ores in the deposit are primary sulfide without oxidation transformation.

Based on the cutting and interpenetrating relationships between mineral veins in different geological times and the mineral generation sequence, supplemented by K-Ar isotope dating, we concluded that this deposit's formation was caused by two paragenetic stages consisting of a total of 5 mineralization sub-stages.

13 Conclusions

Based on the unique geotectonic and geological setting in the study area, especially the favorable passage for mantle material to rise, numerous rare and dispersed element deposits, including more brand new independent tellurium deposits, will be discovered in the near future in the area.

Although nearly 40 minerals have been discovered in the ore of the deposit, it is expected that with the deepening and refinement of ore mineral research, it is possible to discover some unknown new minerals in the near future, considering the special geotectonic background and geological setting of the deposit in the study area.

The tonnage accumulation indices of the Dashuigou independent tellurium deposit indicate that it is a super-large independent tellurium deposit in the world.

Acknowledgements Support for this study was received from Orient Resources Ltd. in BC, Canada; Wuhan Institute of Technology; and College of Earth Sciences, Jilin University in China. It must be pointed out that the scanning electron microscope pictures in this article; namely Figs. 12 and 18, were completed and generously provided by Ms. Jordan Roberts in the relevant laboratory of the University of British Columbia in Canada. The authors of this article express sincere gratitude to her for her hard work and selfless dedication. The chemical analyses included in this article were carried out in the labs of the Chinese Academy of Geological Sciences in Beijing, while the K-Ar dating was completed by relevant laboratory of the Institute of Geology of the State Seismological Administration of China in Beijing.

Author contributions JZ Yin proposed and contributed to the whole research, interpretation, and writing of the paper. All other authors including HY Yin, YH Cao, SP Xiang, and HY Shi contributed to the data collection and compilation of this paper. All authors prepared and reviewed the manuscript and approved the final version of the manuscript.

Data availability statement The data that support the findings of this study is available from the authors upon reasonable request.

Declarations The authors declare that they have no conflict of interest.

14 References

1. Li, T. 1976. Abundance of chemical elements in the Earth. *Geochemistry*, 3**:** 167-174 (**in Chinese**).

2. Li, T & Ni, SB. 1990. *Abundance of chemical elements in the Earth and crust*. Beijing: Geological Publishing House, 136pp (**in Chinese**).

3. Li, T: Yuan, HY; Wu, SX & Cheng, XF. 1999. Regional abundance of chemical elements of crust bodies in China. *Geotectonica et Metallogenia*, 23(2): 101-107 (**in Chinese with English abstract**).

4. Yin, JZ. 1996. *On the paragenetic model and mineralizing mechanism of the Dashuigou independent tellurium deposit in Shimian County, Sichuan Province, China-the only independent tellurium deposit in the world.* Chongqing: Chongqing Publishing House, 190 pp (**in Chinese with English abstract**).

5. Yin, JZ; Chen, YC & Zhou, JX. 1995e. Introduction of tellurium resources in the world. *Journal of Hebei College of Geology* 18(4): 348-354 (**in Chinese with English abstract**).

6. Cheng, ZY; Zhu, XM and Zeng,Y. 2020. Current status of tellurium extraction and utilization. *Mineral Protection and Utilization*, 40(5): 76-89 (**in Chinese**).

7. Yin, JZ. & Shi, HY. 2020a. Mineralogy and stable isotopes of tetradymite from the Dashuigou tellurium deposit, Tibet Plateau,

Southwest China. *Scientific Reports*, 10: 4634 | hppts://doi.org/10.1038/s41598-020-61581-3.

8. Cao, ZM; Wen, CQ & Li, BH. 1995. Genesis of the Dashuigou tellurium deposit in Sichuan Province of China. *Science China (B)*, 25(6): 647-654 (**in Chinese with English abstract**).

9. Chen, PR; Lu, JJ; Wang, RC; Xu, SJ & Chen, XM. 1998. Study on the fluid inclusions of the Dashuigou independent tellurium

deposit in Shimian County, Sichuan Province, China. *Mineral Deposit*, 17 (special issue): 1011-1014 (**in Chinese with English abstract**).

10. Chen, YC; Mao, JW; Luo, YN; Wei, JX & Cao, ZM. 1996. *Geology and Geochemistry of the Dashuigou tellurium (gold) deposit in Western Sichuan, China*. Beijing: Atomic Energy Press, 146pp (**in Chinese with English abstract**).

11. Chen, YC; Mao, JW; Zhou, JX & Yin JZ. 1993. Dashuigou tellurium gold deposit in Shimian County, Sichuan Province - the world's first independent tellurium deposit mainly composed of tellurium. In: *Proceedings of the Fifth National Conference on Mineral Deposits*. Beijing: Geological Publishing House, 437-439 (**in Chinese**).

12. Li, BH; Cao, ZM; Jin JF & Wen, CQ. 1999. Physicochemical conditions of the tellurium deposit in Dashuigou, China. *Scientia Geologica Sinica*, 34(4): 463-472 (**in Chinese with English abstract**).

13. Li, BH; Cao, ZM & Wen, CQ. 2000. Fluid inclusion type and geological characteristics of the Dashuigou tellurium deposit in Sichuan Province, China. *Bulletin of Mineralogy, Petrology and Geochemistry*, 4**:** 346-347 (**in Chinese with English abstract**).

14. Liu, AP; Zhong, ZC & Tang, JW. 1996. Geochemical characteristics of the Dashuigou tellurium deposit in Sichuan Province of China. *Geochemistry*, 25(4): 365-371 (**in Chinese with English abstract**).

15. Luo, YN & Cao, ZM. 1994. The world's first independent tellurium deposit was discovered in Sichuan Province. *China Geology*, (2): 27-28 (**in Chinese with English abstract**).

16. Luo, YN; Cao, ZM & Wen, CQ. 1996. *Geology of the Dashuigou independent tellurium deposit*. Chengdu: Southwest Communication University Publishing House, 30-45 (**in Chinese with English abstract**).

17. Luo, YN; Fu, DM & Zhou, SD. 1994. Genesis of the Dashuigou tellurium deposit in Sichuan Province of China. *Bulletin of Sichuan Geology*, 14(2): 101-110 (**in Chinese with English abstract**).

18. Luo, YN; Fu, DM; Zhou, SD; Cao ZM & Li DH. 1994. Geology and genesis of the Dashuigou tellurium deposit in Shimian County, Sichuan Province. *Sichuan Geological Journal*, 14(2): 1-10 (**in Chinese with English abstract**).

19. Mao, JW; Wei, JX & Yang, BC. 1995. A preliminary study on the genesis of the Dashuigou tellurium deposit in Shimian County, Sichuan Province, China. *Bulletin of Mineralogy, Petrology and Geochemistry*, (1): 23-24 (**in Chinese with English abstract**).
20. Shen, WZ; Xu, XJ & Wang, RC. 1997. Origin of the fluid inclusions of the Dashuigou tellurium deposit in Sichuan Province, China- hydrogen and oxygen isotope evidence. *Journal of Nanjing University (Natural Sciences)* 33, special issue: 77-83 (**in Chinese with English abstract**).
21. Wang, RC; Lu, JJ & Chen, XM. 2000. Genesis of the Dashuigou tellurium deposit in Sichuan Province, China. *Bulletin of Mineralogy, Petrology and Geochemistry*, 4: 348~349 (**in Chinese with English abstract**).

22. Wang, RC; Shen, WZ; Xu, XJ; Lu, JJ; Chen, XM; Luo, YN & Cao, ZM. 1995. Isotopic geology of the Dashuigou tellurium deposit in Sichuan Province, China. *Journal of Nanjing University (Natural Sciences)*, 31(4): 617-624 (**in Chinese with English abstract**).

23. Wei, JX & Mao, JW. 1998. Characteristics of ore-forming fluids and their mantle-derived properties in the Dashuigou tellurium deposit. *Deposit geology*, 17: 1091-1094 (**in Chinese with English abstract**).

24. Xu, SJ; Shen, WZ & Wang, RC. 1998. Zircon-U-Pb dating of ore-bearing amphibolites from the Dashuigou tellurium deposit. *Science Bulletin*, 43(8): 883-885.

25. Yin, JZ. 1996a. The paragenetic model and mineralizing mechanism of the Dashuigou independent tellurium deposit in Shimian County, Sichuan - the first and only independent tellurium deposit in the world. *Acta Geoscientia Sinica*, special issue: 93-97.

26. Yin, JZ. & Shi, HY. 2019b. Nano effect mineralization of rare elements--taking the Dashuigou tellurium deposit, Tibet Plateau, Southwest China as the example. *Academia Journal of Scientific Research*, 7(11): 635-642. DOI: 10.15413/ajsr.2019.0902.

27. Yin, JZ. & Shi, HY. 2021b. Fluid inclusions and metallogenic conditions of the Dashuigou tellurium deposit, Tibet Plateau, southwest China. *Geology, Earth & Marine Sciences*, 3(3): 1–15.DOI: 10.31038/GEMS.2021331.

28. Yin, JZ; Xiang, SP; Chao, YH; Yin, HY & Shi, HY. 2022d. Petrochemical eigenvalues and diagrams for the identification of metamorphic rocks' protolith, taking the host rocks of Dashuigou tellurium deposit in China as an example. *Acta Geochimica*. DOI: 10.1007/s11631-022-00583-6.

29. Xu, ZQ; Hou LW; Wang, ZX; Fu XF & Huang MH. 1992. *The orogenic process of the Songpan-Ganzi orogenic belt in China*. Beijing: Geological Publishing House, 190pp (**in Chinese with English abstract**).

30. Huang, H; Huyskens, M.H & Yin, QZ. 2022b. Eruptive tempo of Emeishan large igneous province, southwestern China and northern Vietnam: relations to biotic crises and paleoclimate changes around the Guadalupian-Lopingian boundary. *Geology*, https://doi.org/10.1130/G50183.1.

31. Shen, FQ. 1985. Trace elements geochemistry of igneous rocks assemblage in Panzhihua-Xichang rift. *Scientific Sinica*, (9): 844-855.

32. Yin, JZ; Zhou, JX & Yang, BC. 1994n. Geological characteristics of the Dashuigou tellurium deposit in Sichuan Province, China. *Earth Science Frontiers*, 1(4): 241-243 (**in Chinese with English abstract**).

33. Chen, YC; Yin, JZ & Zhou, JX. 1994b. Geology of the Dashuigou independent tellurium deposit of Sichuan Province. *Acta Geoscientia Sinica*, 29(2): 165-167 (**in Chinese with English abstract**).

34. Chen, YC; Yin, JZ & Zhou, JX. 1994a. The first and only independent tellurium ore deposit in Dashuigou, Shimian County, Sichuan Province, China. *Sci. Geol. Sinica*, 3(1): 109-113 (**in Chinese with English abstract**).

35. Mao, JW; Chen, YC & Zhou, JX. 1995. Geology, mineralogy, petrology, and geochemistry of the Dashuigou tellurium deposit in Shimian County, Sichuan Province, China. *Acta Geosciences*, 2(3): 276-290 (**in Chinese with English abstract**).

36. Yin, JZ; Chen, YC & Zhou, JX. 1996b. Geology and geochemistry of host rocks of the Dashuigou independent tellurium deposit in Sichuan Province, China. *Journal of Changchun University of Earth Sciences* 26(3): 322-326 (**in Chinese with English abstract**).

37. Yin, JZ; Xiang, SP; Yin, HY; Shi, HY; & Chao, YH. 2023. Origin of the Dashuigou independent tellurium deposit at the southeastern Qinghai-Tibet plateau: based on the abundances of trace elements in the country rocks. *Advances in Geological and Geotechnical Engineering Research*. 5(4): 41-55. DOI: https://doi.org/10.30564/agger.v5i4.5967.

38. Yin, JZ; Chen, YC and Zhou, JX. 1995d. Original rock of the host rock of the Dashuigou independent tellurium deposit in Sichuan Province, China. *Bulletin of Mineralogy, Petrology and Geochemistry*, (2): 114-115 (**in Chinese with English abstract**).

39. Yin, JZ; Chen, YC & Zhou, JX. 1996d. Geology and geochemistry of altered rocks of the Dashuigou independent tellurium deposit in Sichuan Province, China. *Journal of Xi'an College of Geology*, 18(4): 19-25 (**in Chinese with English abstract**).

40. Yin, JZ; Zhou, JX & Yang, BC. 1994g. Rock-forming minerals and ore-forming minerals of the Dashuigou tellurium ore deposit unique in the world - A preliminary study. *Sci. Geol. Sinica*, 3(2): 197-210.

41. Yin, JZ; Chen YC & Zhou, JX. 1994k. Mineralogical research of the Dashuigou independent tellurium deposit in Sichuan Province, China. *Bulletin of Mineralogy, Petrology and Geochemistry*, (3): 153-155 (**in Chinese with English abstract**).

42. Yin, JZ; He, DS; Yin, YH; Shi, H & Xiang, SP. 2022. On ore from the Dashuigou tellurium deposit, Tibet plateau, southwest China. *European Journal of Applied Sciences*, 10(6): 458-472.

43. Yin, JZ; Chen, YC & Zhou, JX. 1995a. The metallogenic age of the world's first independent tellurium deposit. *Chinese Science Bulletin*, 40: 766-767 (**in Chinese with English abstract**).
44. Yin, JZ; Chen, YC & Zhou, JX. 1995b. K-Ar isotope evidence for age of the first and only independent tellurium deposit. *Chinese Science Bulletin*, 40(22), 1933-1934.

45. Cao, ZM & Luo, YN. 1993. Geological characteristics and material composition of the Shimian Te (Se) deposit in Sichuan Province. In: *Proceedings of the Fifth National Conference on Mineral Deposits*. Beijing: Geological Publishing House, 476-476 (**in Chinese**).

46. Mao, JW; Chen, YC; Yang, BC; Lei, YF & Zhou, JX. 1995. Study on tetradymite in Dashuigou tellurium polymetallic deposit, Shimian County, Sichuan Province, China. *Geological Science*, 30(1): 47-52 (**in Chinese with English abstract**).
47. Wang, RC; Chen XM & Xu, SJ. 1996. Complex exsolution of tellurium minerals in the Dashuigou tellurium deposit. *Science Bulletin*, 41(10): 920-922.

48. Cao, ZM & Luo, YN. 1994. Mineral sequence and ore genesis of the Sichuan telluride lode deposit in China. In: *New Research Progresses of the Mineralogy, Petrology and Geochemistry in China*. Lanzhou: Lanzhou University Publishing House, 476-478 (**in Chinese**).

49. Department of Geology, Nanjing University. 1987. Crystallography and Mineralogy. Beijing. Geological Publishing House, 659pp.

50. Ash, C & Alldrick, D. Vein, Breccia, and Stockwork. www.empr.gov.bc.ca/. British Columbia Geological Survey. Retrieved 1 November, 2013.
51. Laznicka, P. 1989. *Giant Metallic Deposits: Future Sources of Industrial Metals*. Springer, 2nd edition, 961pp.

Original Article

Groundwater and surface water control at Highland Valley copper mine (HVC) (in rock and soil both)

Sean Daly[1]

Abstract

This paper is about dewatering of the two large open pit porphyry copper-molybdenum mines of Highland Valley Copper in BC, Canada. These two pits occur within the well differentiated Guichon Creek Batholith with phases progressively more acidic and coarser grained towards the center and intersected by intense fracturing within the ore bodies and also concentric alteration haloes. Also, they are both cut by the steeply dipping Lornex fault which is an average 155 m wide faulting zone with frequent sympathetic faults adjacent to it. As the two pits have mined down at depth, they have exposed bedrock especially with frequent toppling-type faults and shears which have exhibited varying degrees of toppling and ravelling of the pit walls. Also, on the east wall of the Valley Copper pit, there is up to about 350m of glacio-fluvial overburden, originally with artesian flows in two or three aquifers. The toppling is exacerbated by the hydrostatic pressure of the groundwater in the pit walls. Both pits have significant groundwater and run-off in the spring. In order to be able to continue mining down to depths of about 600 to about 750 meters it has been necessary to de-water the walls and divert the surface run-offs to prevent infiltration into the toppling faults. So two water diversion projects were necessary at the crest of the highwalls and were completed to drain both by gravity and pumping the spring run-off water away from the two pits. Also, a major well drilling project is ongoing in the glacio-fluvial overburden aquifers to dewater them with upwards of 4500 US gpm flows. In addition, an annual series of horizontal drainholes were drilled and are ongoing approximately every three benches to dewater and depressurize the bedrock. Minor bedrock wells in the crest of the Lornex Pit also contribute to the dewatering. All the dewatering has allowed the two pits to mine down to close to design depths without significant disruption.

Key words: Highland Valley; Guichon batholith; open pit; Lornex fault; artesian water; dewatering

---

Affiliation Info: [1] Deciphearth, PH4 4838 Fraser St, Vancouver BC V5V 4H4, Canada
Article Info: Received: 8 September 2023 / Revised: 21 October 2023 / Accepted: 3 December 2023 / Published Online: 12 December 2023. www.naturalisscientias.com
Authors' Contact Info: Daly, S: dalyshone24@gmail.com
Citation: Daly, Sean. 2024. Groundwater and surface water control at Highland Valley copper mine (HVC) (in rock and soil both). *Naturalis Scientias*, 1(1): 32-40. DOI: https://doi.org/10.62252/NSS.2024.1002.

Corresponding Author: Sean Daly is a retired mining geologist with a BSc in geology and a MEng in mining engineering both from UBC and he worked 19 years at the large Highland Valley copper mine in south central British Columbia, Canada; Email: dalyshone24@gmail.com

1 Introduction

Mine ownership, production rate and milling

Highland Valley Copper is a large integrated porphyry copper and molybdenum operation, now mining from three open pits, from north to south, Valley Copper, Lornex and Highmont. In the future, there may be more mining around the old Jersey and Iona pits.
Ownership of Valley Copper used to be by Cominco, Lornex by Lornex Mining Corporation, Highmont of Highmont Operating Company and the Jersey and Iona of Bethlehem Copper Corp. Now they are all amalgamated under Highland Valley Copper, owned by Teck Corp. In 1986, Lornex Mining Corp. and Cominco amalgamated into the Highland Valley Copper partnership, uniting the Lornex mill with the large Valley Copper orebody[1].
At first, the ore was milled at Bethlehem as well as Lornex, then the Bethlehem mill was shut down and all the ore went to the Lornex mill. The present production rate is 300,000 tonnes per day, of which about 155,000 is ore and the rest waste. Another set of flotation cells has been added to the mill to improve recovery. Mining began in the Highland Valley in 1963 with the opening of the Bethlehem Mine. The present mine produces copper and molybdenum primarily and with very minor gold and silver by-products. The mills are semi-autogenous which means that while there are grinding balls, mostly the harder ore grinds the softer and the grade control geologists must estimate the grinding rate of the ore for blending purposes in the mill, i.e. combining both hard and soft ore where possible.
The purpose of this paper is to identify and evaluate various methods of both surface and underground water control in a large open pit mining complex and it covers pit perimeter ditches and pipelines, horizontal drainhole drilling for groundwater in bedrock in the pit walls, and well dewatering mainly in glacio-fluvial overburden but also minor in bedrock at the two large open pits; Lornex and Valley Copper.

2 Regional and local geology

These orebodies are part of an approximately 3.5 billion tonne reserve mined plus unexploited ore yet and including the small pits at Bethlehem Mine, the Valley Copper pit, the Lornex pit, the Highmont pit and the untouched JA zone. They all occur within the well differentiated Guichon Creek Batholith which has four main phases which are more felsic and coarser grained towards the center of the Batholith[2]. Both the Lornex and Valley Copper orebodies are cut and truncated by the major approximately 40 km long N-S striking Lornex Fault and there are some other significant faults too. Regionally, Highland Valley copper mine is part of the Intermontane Belt of BC along with for example New Afton and the Copper Mt mines.

3 Importance of groundwater and surface water control and dewatering

The 300,000 tonne/day and the previous approximately 250,000 tonnes/day mining rates and therefore the increased economic pressure to reduce water infiltration and hydrostatic water pressure on the toppling faults has resulted in some major programs of surface water diversion and ongoing annual horizontal drainhole drilling. The high mining rate means more instability so that dewatering or diverting water has improved slope stability over the years and the prodigious amounts of water pumped from the glacio-fluvial aquifers has mostly fed the mills as a very useful by-product of the dewatering. An illustration of the effect of mining rate on instability was the economically forced closure of mining on the Lornex west wall in 1982 resulting` in a very stable slope for the approximate year of shut-down and as soon as the next bench was mined out there the slope movements increased significantly.

4 Discussion

4.1 Water diversion

A fine example of what I call “Nature’s Plumbing” was the diversion I had made at the crest of the Valley Copper Pit. It was springtime; about peak flow for the streams ie the surface run-off. Water started coming out at the base of the till cliff at the crest of the west wall. The underground stream caused sloughing in the till which came close to the blasthole drill on the wide operating berm below. So I traced the water or searched for its source, following

several deeply incised dry stream beds up the natural slope until I found the culprit-two streams debouching onto the porous oxidized rock and then disappearing underground. So I surmised, rightly, that the water ended up in the underflow of the dry stream channels which conducted it to where it daylighted in the till face and caused the slide. So I asked to have the water diverted from where the two streams disappeared and so it was moved off to a stream far away where it did no harm and then there were no more till slides. As a corollary of this, just because a stream is dry on surface does not mean there is not flow a little deeper, but still in the gravelly layer in this case on top of the impermeable till.

In the Lornex Pit, we diverted the run-off water all the way around the west and southwest walls, well away from the major toppling zones on these two walls (Figs. 1 and 2)[3].

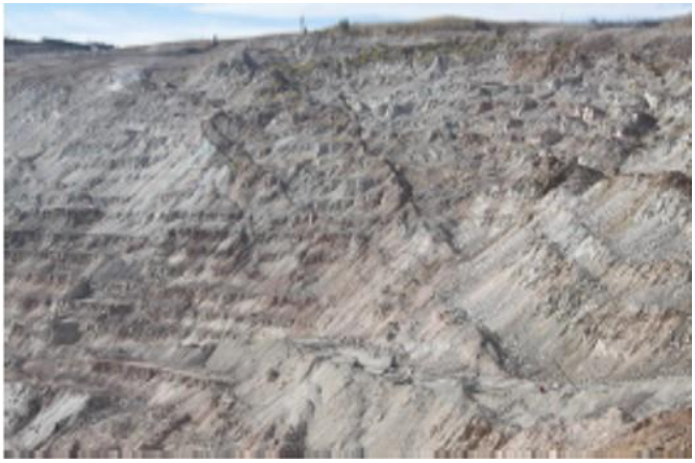

Figure 1. Lornex NW Wall toppling zone, with obsequent scarps on major toppling faults

Figure 2. Valley Copper open pit with minor obsequent scarps from toppling in central part of the photo

Through a series of ditches, pipelines and pumping from the Teit Ck and Beaver Pond sumps we were able to keep most of the surface run-off out of the bedrock where it had been exerting hydrostatic pressure on the toppling faults and exacerbating the attendant slope movement (Fig. 3)[3]. Also this excess water was then sent to the mill to help with the water usage there so was not wasted.

Figure 3. Water diversion at a mine in Ireland with lined channel (left). At HVC we lined one of our ditches with impermeable till or used pipelines where we crossed exposed bedrock with toppling potential structures (right)

4.2 Overburden well drilling

Another much larger source of water for the mill was the wells drilled by Drillwell Enterprises (a very good company and very friendly to work with) in the Highland Valley glacio-fluvial overburden which reached depths of up to 350 meters (Fig. 4)[4]. The other purpose of these wells was to allow mining to continue below the overburden on the east wall of the Valley Copper pit so that it wouldn't be swamped with groundwater[5]. A total of about 4500 US gallons per minute was being pumped from two or three good aquifers in this glacio-fluvial sequence. The stratigraphy of this sequence is shown in Fig. 5. The two most important aquifers were the Main Aquifer and the Basal Aquifer. When the Basal Aquifer was penetrated by Drillwell in the first hole, the water shot up 40 feet above the drill the pressure was so great! We knew this because there were 40 ft of drill rods on the drill rig above ground and it was shooting out of the top of these! The Drillwell drillers made very good logs of the geological units and I could improve on them but very little.

Figure 4. Drillwell drill at work (after Drillwell Enterprises photo)[4]

For about one year I worked with these Drillwell crews, logging their overburden samples and projecting where they would intersect the next units in their drilling so they could prepare for them (Fig. 4)[3]. I found their logs of the cuttings were very good and could be improved upon very little. Also, I would have the aquifers sands and gravels sieved to determine the mesh size of the screens to be installed in them. The crews were very helpful and it was a pleasure to work with them.
Highland Valley glacio-fluvial overburden stratigraphy (Fig. 5, from the top to bottom):

Aquifers and glacial tills

- Upper aquifer
- Three till units
- Main aquifer
- Alluvial fans

Lacustrine Sediments

- Unit 10A silts
- Unit 10B clays
- Unit 10C silt, silty sand, and sand

Basal Aquifer

- Sand and gravel

Figure 5. Orange main aquifer overlain by three grey tills with a dewatering well in the foreground

One very interesting phenomenon in this pumping from the three aquifers was how quantity changed into quality (Fig. 5). First, for several years the pumping was just de-pressurizing the water in the aquifers, but then as this quantity increased (of the water being removed) then dewatering began. This is somewhat akin to boiling water. First you add heat and increase it gradually, and eventually it undergoes a change of state from liquid to gas ie water vapor. Something similar is haulage by trucks of an ever-deeper pit so that as it gets deeper the haulage

costs increase to the point where it becomes too expensive to haul all that way up a steep ramp so then this is resolved by extending a conveyor down into the pit near the pit bottom and thus reducing the haulage distance and costs.

4.3 Drainhole drilling

Also, as well as groundwater in overburden, there is groundwater in the bedrock ie in the granitic rock at Highland Valley Copper. This rock gets its permeability from the network of joints and faults that occur there especially the steeply dipping ones, due to tectonic processes and cooling of the magma that gave rise to the granitic rock[4]. So, we knew that we had significant groundwater firstly in the Lornex Pit because in mining out each bench on the west wall, we would find significant water flowing out of the fractures. So we employed some renowned geotechnical experts, including Chuck Brawner and Alberto Nieto and Peter Stacey and after sizing up the wall and talking to us they decided to recommend us drilling a series of horizontal drainholes every three benches vertically to remove and depressurize the water in the bedrock.

Thus did commence our annual series of HDHs (horizontal drainholes, (Figs. 6 and 7)[5] starting with Tonto Drilling out of Kamloops. They took their drill mast down off their rig and layed it on its side to drill our holes and in that way could drill up to 300 meters which was a good length to penetrate to the groundwater zones. So there would be a rhythmic seasonal process whereby first the snow would start melting and the surface run-off would occur (before our water diversion mentioned above), then the piezometers would show an increase in water levels/pressures[6], then the slope would start to move significantly, then our HDH flows would pick up and then the slope movements would reduce[6]. So we were successful in both the west walls of the Lornex and later the Valley Copper walls in being able to mine down to the bottom of the walls without excessive toppling. That was at least until about 1995 (from 1981 to 1995) when the Lornex west wall failed ie showers of rock came down off the obsequent scarps in the toppling fault zones about every 20 minutes but that was also when we developed the water diversion plans. An obsequent scarp is developed on toppling faults so that the rock mass on the wall side drops down relative to the rock on the pit side, then ravelling occurs. Ravelling is when rock sloughs on a slope.

NB the following comments on both horizontal drainhole drilling and vertical well drilling, both in bedrock for effective dewatering come from the paper by V. Straskabra entitled “Some technical aspects of open pit dewatering”. These comments have been significantly paraphrased and with frequent comments by Sean Daly from his intensive experience at Highland Valley Copper that may or may not corroborate the points in this paper.

Installation of horizontal drains in an aquifer that could cause instability of a slope in an open pit mine is a very efficient means of dewatering. The main advantage is a considerably minimal installation cost, no energy consumption for water discharge and low cost of drilling[5]. The principal drawback in the use of horizontal drains is the fact that it can be economically installed only after the completion of the mining out of pit benches rather than prior to excavation. But on the other hand, if in the northern hemisphere the horizontal drains are installed in the winter, then they will be ready for the spring run-off when their emplacement is key to achieving successful drawdrown. Horizontal drains can be emplaced in many kinds of aquifers and are highly efficient in confined aquifers with high pore pressures. They are also the prime means of dewatering bedrock aquifers with a well-structured vertical or steeply dipping fracture system which is the case at both the Lornex and Valley Copper pits at Highland Valley Copper Mine. Typically, horizontal drains have 1 1/2 to 2 inch PVC slotted pipe emplaced inside the drill rods ie lining the hole to alleviate caving in the hole. In most cases, for slope stability maintenance, drains 75 to 150 metres deep are sufficient. Hydraulic and economic efficiency significantly decrease with drains longer than 120 to 150 metres; therefore, longer drains should be installed only in particular cases such as to access a piezometer to monitor the drawdown. The size of slots in the PVC pipe should be selected according to the drained material. From practical experience, the most wide slot size which would permit removal of a reasonable amount of sand particles should be utilized, in particular in cases where chemical incrustation in the pipe may happen but chemical incrustation is probably more common in vertical wells. The

drains can be installed from the bottom of the pit or from a bench, but preferably from the lowest part of the aquifer to be drained. In most cases at HVC (Highland Valley Copper) we drilled from benches usually about every three benches as we mined down. The drains should be installed at a gentle upslope angle (1-5 degree) for the following reasons: minimal hydraulic losses, water does not freeze at the drain exit so easily, compensation of drill rod deflection as per following discussion. During the drilling of horizontal drains the hole can deviate downwards significantly by the weight of drill pipes, or upwards. From the author's personal experience, the drain can be bent drastically up by the use of excessive pressure during drilling by a driller who is compensated by the foot. During one installation of a 180 metre deep drain at a three degree upward angle in coal waste materials, the drill pipe and bit bent to a 90 degree angle and exited the ground surface about 75 metres above the elevation of the drillhole collar[5]. Similar situations can explain why many drains emplaced without the supervision of an experienced engineer or geologist are withdrawing much less water than estimated as the geologist or engineer can adjust the drill dip to the structural geology conditions.

Actually it is not just the pressure or the weight of the rods that makes a drainhole deflect up or down but that in combination with the dip of the structure one is drilling into. If the structure especially a fault is dipping away from the drill, the drill bit will re-collar progressively at a lower elevation if the drill angle is at a relatively small angle to the fault, whereas if the structure is dipping towards the drill at a relatively small angle to the drill hole the bit can deflect upwards. So knowing these situations, one can increase or decrease the initial dip as required by the dominant structure being drilled into. Straskraba quoted in this same paper says that for a drain at an open pit coal mine it is feasible to accomplish drawdown of about 65 to 85 percent of the saturated thickness of the water bearing formation.

Figure 6. BAT Construction drainhole drill at HVC.

Figure 7. Completed horizontal drainhole with water flow

4.4 Wells in bedrock

On a much smaller scale were a few wells we drilled in bedrock at the pit crest in the Lornex Pit. One well in particular was drilled into the porphyry dyke which I knew from mapping was a good aquifer. So we obtained after its pump test a three US gpm sustainable flow which sounds rather low but over a period of one year it pumped from about 700,000 to 1 million gallons out of this rock. This then removed a major water source for the Lornex SE toppling zone and helped to stabilize this wall. Other experience demonstrates that cost effective dewatering by pumping the water from vertical wells is feasible when the hydraulic conductivity of the drained strata is at least about 10 feet/day for unconfined aquifers and at least about 1.0 to 1.6 feet/day for confined aquifers. From frequent mapping it was found that there was recurring artesian flow from the quartz porphyry dyke in the Lornex Pit, of about ½ US gpm so our successful well in this rock unit verified this keen observation. Attempts to employ vertical wells to dewater an aquifer in rock with mainly secondary permeability displaying vertical fractures usually result in failure. However, our successful well in the south highwall of the Lornex Pit was most likely in an area with steep fractures similar to most of this pit so was still successful in this case. Also, an aside from this article, from my understanding of secondary permeability of that which is enhanced by toppling movement, drilling it can significantly increase water flows because the rock mass is loosened up by slope movement.

The scope of dewatering wells differs from water supply wells since the well yield is not as important as the drawdown[5]. The spacing of dewatering wells subsequently differs from that of water supply wells. The optimum distance amongst dewatering wells is calculated from the results of aquifer tests usually done during the hydrogeologic investigation (especially pumping tests-S.Daly comment). The second well should be placed within the steep part of the cone of dewatering developed by pumping the first well. As a rule, the useful radius of dewatering of a well is usually equal to one-third of the radius of influence of the pumped well. For most vertical dewatering wells, the water supply well technology is employed. For the well completion, five- to six-inch PVC casing with slots or PVC screen and suitable gravel pack in drained materials are generally used.

The cost to drill, install and properly develop a dewatering well to a depth of about 183 metres is in the range of $15 to 18 per foot, with the cost of supervision, which amounts to an extra approximately $2 per foot. These costs are more than likely significantly more than this now as this comes from an old paper.

4.5 Cone of dewatering

One other factor of groundwater other than promoting slope instability is its cone of dewatering[7]. When I mapped underground at the El Mochito Mine in Honduras, some of the tunnels were streaming with water along the fractures and faults. Then when another new tunnel was driven below this one, this one would dry up because it was within the cone of dewatering. The cone of dewatering then is in the case of a shaft or vertical well, a cone shape within which the groundwater has been drawn down and everything within the cone is dry. For a tunnel, it would be a valley-shape, and the same for a horizontal drainhole. The ancient miners knew about this principal too, back in the 1500s in the Erzgebirge Mts. When they started a shaft and the water was pouring in, they would sink another shaft beside it (perhaps shorter) and the water would pour into it, thus drying up the first shaft and allowing them to work in dry conditions- so they are the ones who first discovered this principle, and as described in Georgius Agricola's De Re Metallica. There was so much water at the El Mochito underground mine that if the pumps went down for two minutes the mine started to flood so that is why they had a large auxiliary generator on the surface.

4.6 Combination of various dewatering methods

In many dewatering projects, two or more previously discussed dewatering techniques have been utilized. In this way, the advantages of various dewatering methods may be combined. For example, with initial dewatering by

means of vertical wells before mining activities start, safe and effective excavation can be promoted. In a later phase of mining, a series of horizontal drains may be emplaced on the final pit walls to remove the need for energy consuming well pumping. In every case the mine dewatering design must be founded on a firm understanding of site hydrogeology and on an overall cost study.

5 Conclusions

Both surface and groundwater control at a producing open pit mine in the temperate zone at least, is essential to the ability to mine down the open pit to the design pit bottom. This is because groundwater exerts both uplift and hydrostatic pressure on such unstable structures as wedge failures and toppling failures, for example on large open pit mines like the Highland Valley Copper mining complex. So dewatering, in the form of surface water diversion, horizontal drainholes and wells is key to reducing this water pressure and to ensure unimpeded mining throughout the depth extent of the designed pit or pits. Thanks to a combination of these measures, mining has been successful down to design pit bottom in both the Lornex and Valley Copper pits.

Acknowledgements Thanks to Concrete Canvas and Drillwell Enterprises for the photos of Figs. 3 and 4 respectively.

Author contributions Sean Daly contributed his intensive experience with water diversion projects in both glacio-fluvial overburden and bedrock well drilling and data interpretation and drainhole drilling in bedrock in both the Lornex and Valley Copper major open pit.

Data availability statement The data interpretation of this study is available from the author upon reasonable request.

Declaration the author declares that he has no conflict of interest.

6 References

1. Daly, PS. 2016. *From the Erzgebirge to Potosi*, Friesen Press publishers, 83pp.
2. McMillan, WJ & Osatenko, MJ. 1977. *Guichon Creek Batholith and Mineral Deposits*, British Columbia Ministry of Mines and Petroleum Resources, 52pp.
3. Daly, PS. 2013. *Engineering Applications of Geological and Geotechnical Mapping at Highland Valley Copper, Logan Lake, BC, Canada*, in partial fulfillment of a MEng degree at UBC, 49pp.
4. Freeze, RA & Cherry, JA. 1979. *Groundwater*. 604pp.
5. Straskraba, V. 1979. Some technical aspects of open pit mine dewatering. In: *Proceedings of the 1st International Mine Drainage Symposium, Denver, Colorado*, pp 481-491. San Francisco: Miller Freeman Publications Inc.
6. Duncan, CW & Mah, CW. 2004. *Rock Slope Engineering: Civil and Mining*, 4th Edition, CRC Press. 456pp.
7. McKinstry, H.E. 2017. *Enineering Geology*, Cone of unwatering. *Mining Geology*, New York: New York Prentice-Hall Inc., 708pp.

Original Article

Geological setting of gold-silver mineralization in the La India mining district, Nicaragua

L.T.P. English[1] Ⓛ, V.H. Galvan[2], and C.R. Pullinger[3]

Abstract

La India gold mining district covers a 50 km² area of fault-fill gold-silver mineralized quartz-adularia veins on the western margin of a Tertiary volcanic arc in western Nicaragua. Historic mining records and modern mineral exploration data, which to-date has defined a mineral endowment of over 2.3 Moz gold, provide a wealth of geological information. This paper draws on these observations and data to describe and classify the gold-silver mineralisation at La India, identify the geological controls, and interpret the timing of mineralisation within the regional tectonic setting. The district-scale gold-silver mineralisation at La India occurs in two adjacent geological settings with distinct mineralization characteristics and exploration potential: (1) an upland area of strongly faulted felsic to andesitic volcanics where the historic mine workings are located, and (2) an adjacent downthrown graben, the Sebaco Graben, where a thick sequence of andesite is preserved overlying the felsic volcanic sequence. Gold mineralisation is classified as rift margin-type low-sulphidation epithermal gold-silver fault and fracture-fill vein mineralization. In the historic mining area erosion has exposed the top of the high-grade epithermal zone. Minimal erosion in the Sebaco Graben means that the epithermal system is fully preserved at depth, with localised hydrothermal sinter outcrops, sporadic low-grade mineralised veins and a phreatic breccia pipe exposed at surface. Apart from the one phreatic breccia, the gold-silver mineralisation occurs in quartz veins and breccias that filled brittle faults and associated fractures and fissures which developed in an extensional tectonic setting. The structures containing the gold-silver mineralisation were formed as normal and trans-tensional faults with orientations consistent with southwest-directed extension: (1) a predominant northwest to north-northwest set parallel to the subducting plate; (2) secondary but locally extensive east-west, and (3) tertiary shorter and narrower northeast and north-striking veins. A district-scale north-northwest orientated through-going structure linking the major gold-silver deposits in the historic mining area is interpreted as a deep crustal conduit for the gold-silver bearing hydrothermal fluids. Other, as yet unidentified basement feeder structures may have fed mineralised corridors in the east and west of the district. The gold-silver mineralisation is best developed where structures pass through competent felsic volcanics and welded tuffs in the historic mine area, and also in the overlying andesite flows in the Sebaco Graben. Gold-silver mineralisation is less well developed where the structure passes through less competent unwelded tuffs and volcanic agglomerates. Gold-silver mineralisation is interpreted as occurring shortly before or at 8-10 Ma at the end of a long period of slab-rollback induced extension and arc volcanism. Post-mineralisation block faulting split the La India district into the upthrown, and subsequently eroded historic mine area where epithermal mineralisation is largely exposed at surface, and the well-preserved downthrown blocks such as the Sebaco graben where much of the gold-silver mineralisation is still hidden several hundred metres below surface.

Keywords: Gold; silver; low sulphidation epithermal; mineralisation; La India; Nicaragua

Affiliation Info: [1] Condor Gold PLC, 7/8 Innovation Place, Douglas Drive, Godalming, Surrey GU7 1JX, United Kingdom; [2] Fortuna Silver Mines Inc., 650-200 Burrard Street, Vancouver, BC, Canada; [3] LAGEO S.A. de C.V. Final 15 Av. Sur y Boulevard Sur, Colonia Utila, Santa Tecla, La Libertad, El Salvador

Article Info: Received: 21 November 2023 / Revised: 25 November 2023 / Accepted: 6 December 2023 / Published Online: 12 December 2023. www.naturalisscientias.com
Authors' Contact Info: English, L: lenglish@condorgold.com; Galvan, VH: vgalvan@fortunasilver.com; Pullinger, CR: crpullinger@yahoo.com
Citation: English, L; Galvan, VH and Pullinger, CR. 2024. Geological setting of gold-silver mineralisation in the La India mining district, Nicaragua. *Naturalis Scientias*, 1(1): 41-55. DOI: https://doi.org/10.62252/NSS.2024.1003.

Corresponding Author©: English, L, PhD, Professional Geologist; Email: lenglish@condorgold.com

1 Introduction

Gold and silver have been mined in the La India district in western Nicaragua for well over 100 years (Fig. 1). The first known gold mining in the La India district was by the London-based Corduroy Syndicate who worked a small-scale underground mining operation exploiting the Dos Hermanos vein in the southwestern corner of the mining area in the late 19th or early 20th Century. Industrial-scale underground gold mining was initiated in 1936 on the nearby India vein which Canadian mining company Noranda Inc. acquired in 1938. Noranda expanded underground mining operations and by the time the mine closed in 1956, the La India vein had been worked along a 1200 m strike length to a depth of over 250 m below surface at the deepest part, the neighbouring America-Constancia vein along a 2200 m strike length up to 140 m below the valley floor, and six other smaller underground mine workings had been initiated on satellite veins spread over approximately a 50 km² area (Fig. 2). Available records show annual production peaked at 41,891 oz gold and 39,282 oz silver in 1953 (English 2015)[1]. Since the closure of the La India gold mine and continuing to the present day, artisanal miners have intermittently worked the most accessible upper levels of the mine and extracted ore from small underground workings throughout the district.

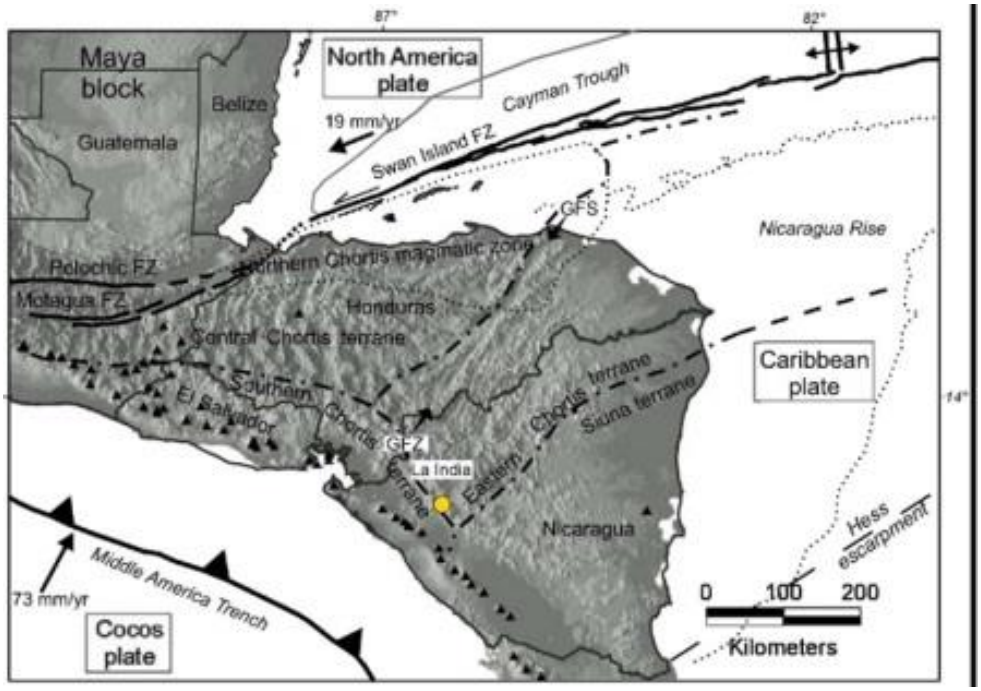

Figure 1. Location of the La India district in western Nicaragua
(After Rogers *et al.* 2007)[2]

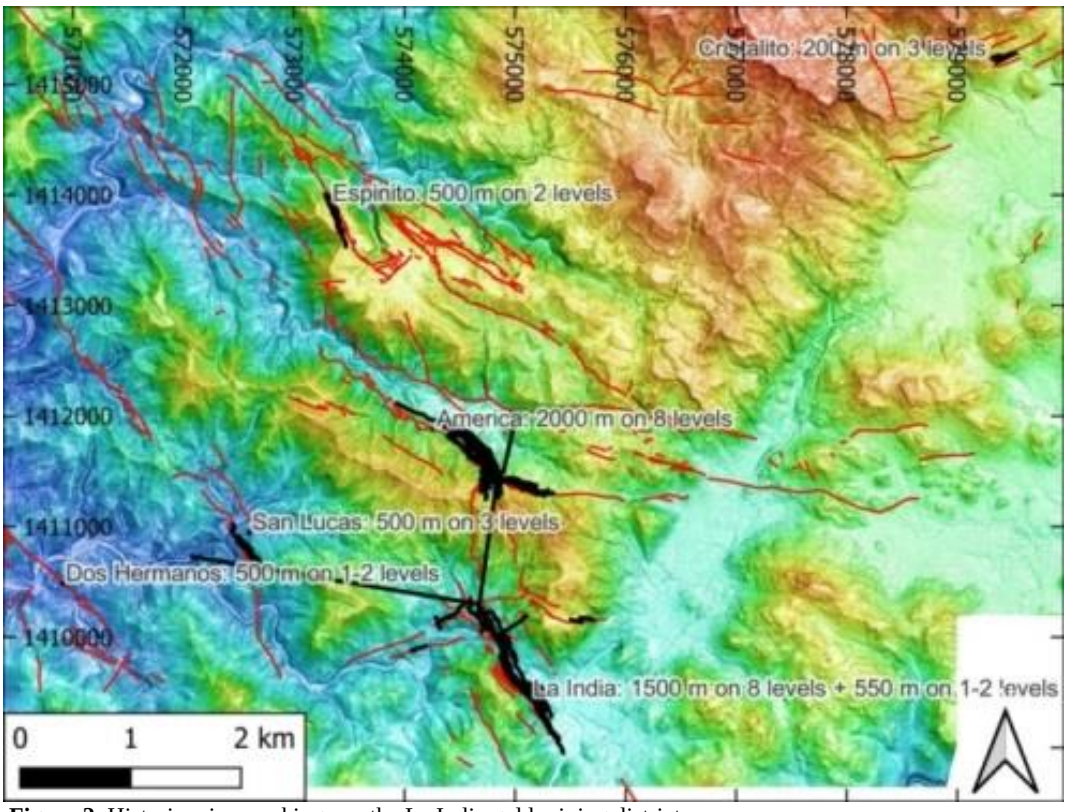

Figure 2. Historic mine workings on the La India gold mining district
(Surface Au-quartz veins in red, underground mine workings in black)

Modern mineral exploration has established that a significant mineral resource remains in the ground adjacent to the old workings and elsewhere in the district: the current concession holders have defined a 2.3 Moz gold endowment in and around the historic mine workings. The modern exploration since the late 1980's has been well documented and provides a database of over 4,500 rock chip samples, a grid of over 12,000 soil samples, 1776 trenches for almost 29,000 m of channel samples, and 625 drill holes for over 96,000 m of rock samples, most of which collected continuous samples of rock core, satellite-derived digital terrain models and a 280km² area airborne radiometric and magnetic geophysical surveys. The geological observations and geochemical analytical results of this exploration provide a wealth of geological information on La India district that forms the basis of this study.

This paper describes the geometry and style of gold-silver mineralisation in the La India district, describes the geological setting, and presents an interpretation of the geological controls, tectonic setting, and proposed timing of gold-silver mineralisation. The work draws on observations and data derived from outcrop and underground rock exposures, trench cuttings and drill core, geophysical surveys, and satellite images collected by numerous exploration geologists and specialist consultants since the late 1980's.

1.1 Gold-silver mineralisation

Gold-silver mineralisation occurs both in the hilly historic La India mining area and in the lower hills and plains of the Sebaco Graben to the southeast (Fig. 3). Block faulting that created the graben was active post-mineralisation so that the gold-silver mineralisation was displaced to a lower elevation within the graben. Differential erosion has resulted in the preservation and exposure of the veins in the hills of the historic La India mining district, and preservation, and local sedimentary covering of a subsurface vein system in the protected lowlands of the downthrown graben block.

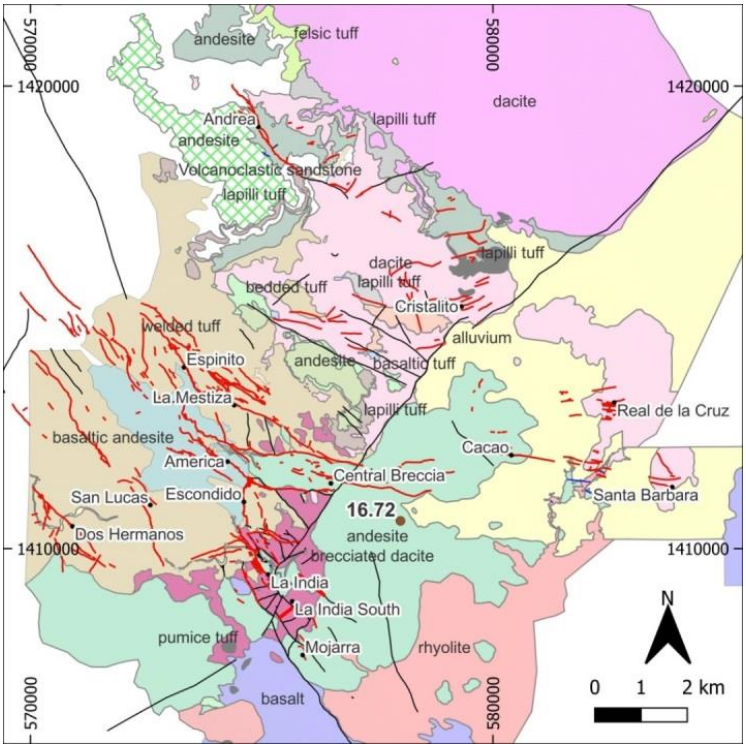

Figure 3. Geological map of La India historic mine area and the Sebaco graben showing the location of an andesite outcrop dated at 16.72 Ma (After Plank *et al.* 2002)[3]

1.2 Gold-silver mineralisation of La India historic mine area

Gold and silver mineralisation in the historic La India mining area occurs in hydrothermal veins filling faults and associated fissures and fracture zones. Analysis of veins from the principle La India and America deposits show that the veins are composed of quartz and adularia veins with gold and silver occurring as 82% fine electrum, 9% native gold, and 9% Uytenbogaardtite (Ag3AuS2), fischesserite (Ag3AuSe2) and gold-silver sulphide (SRK 2022)[4].

Veins exhibit classic low sulphidation textures such as chalcedonic-ginguru banding, crustiform, vughy and drusy textures, and notably large bladed and rhombic calcite replacement textures (Fig. 4). These textures indicate deposition in the hydrothermal boiling zone towards the top of the epithermal system. This would typically occur at depths of 50 m to 700 m below the water table at time of deposition (Hedenquist *et al.* 2000; Fig. 9)[5], but has now been exposed at the surface by erosion. Drilling has traced the mineralisation to depths of over 250 m below the current surface at the principal La India, America, and La Mestiza deposits. The base of mineralisation has not yet been determined.

Several pulses of vein deposition are recognised in active faults as evidenced by fault breccias with quartz clasts cemented by quartz. In some primary faults, including those hosting the La India and America deposits, faults continued to be active after the last pulse of veining. In such cases, veins have been ground to fault breccias of mixed quartz clasts and reddish-brown oxidised fault gouge clay, and even milled to cataclastic sandy clays, all of which can contain significant levels of gold-silver mineralisation (Fig. 5).

Most of the potentially economic gold-silver mineralisation is hosted by massive, indurate felsic volcanics and welded tuffs in La India historic mining area. Wallrock alteration in these rocks is limited to a thin haematite selvedge in these rocks. The haematite is indicative of mixing of the ore fluids with oxygenated ground water and supports the interpretation that veins were precipitated at a relatively shallow level (Corbett 2012)[6]. The restriction of alteration to a narrow selvedge around the vein suggests that these hard, indurate silica-rich lithologies formed an impermeable and relatively unreactive barrier to the hydrothermal fluids, constraining and concentrating the mineral-rich hydrothermal fluids within the faults and fractures (Pratt and Ponce 2016)[7]. The veins become narrower and often dissipated into stockwork zones where the veins extend into surrounding less indurated tuffs and volcaniclastic sediments.

Figure 4. Left: La India vein cockade banded quartz-adularia vein (example grading at 14.1 g/t gold and 192 g/t silver); Right: Platy quartz vein (example grading at 4.3 g/t gold and 6.5 g/t silver)

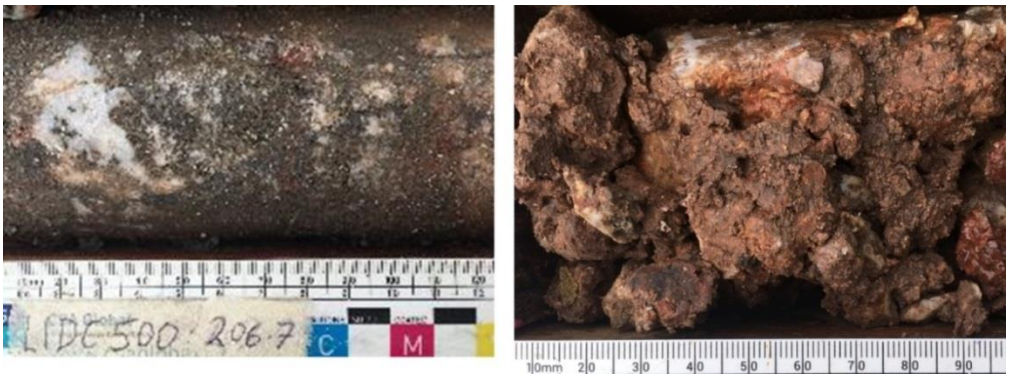

Figure 5. Left: Gold mineralisation at La Mestiza deposit as quartz veins deposited in active faults include cataclastic sand containing early quartz vein fragments partially overprinted by a later phase of quartz cemented (example grading at 47.7 g/t gold and 40 g/t silver); Right: Fault breccia of mixed quartz clasts and reddish-brown oxidised fault gouge clay (example grading at 41.16 g/t gold and 80 g/t silver)

1.3 Gold-silver mineralisation of the Sebaco Graben

The geology of the downthrown Sebaco Graben block is dominated by a thick sequence of andesite, younger than the underlying felsic volcanics, which has been dated at 16.72 Ma by radiometric dating (Plank *et al.* 2002)[3]. Gold-silver mineralisation and wallrock alteration differ from the historic mining zone. In many places there has been minimal surface erosion and the epithermal and overlying hydrothermal system has been fully preserved. Blocks of hot spring sinter and fluidized volcaniclastic sediment (tuffaceous-breccia) at the Cacao prospect (Pratt 2019)[8], sinter and chalcedonic quartz at the La India South-Mojarra prospect (Fig. 6), and phreatic breccia and associated microbreccia with cross-bedding and grain sorted surficial flow textures at the Central Breccia prospect testify to the preservation of near-surface and surface hydrothermal deposits (Fig. 7). Proximal argillic-pyrite and distal smectite alteration recognised in the wallrock of the mineralised structures are characteristic of shallow level to surficial hydrothermal activity above the epithermal zone (Corbett and Leach 1998; Fig. 9)[9].

Some gold-silver mineralisation does occur near surface, in quartz veins at Cacao, and at less well-explored prospects such as Mojarra, Santa Barbara and Real de La Cruz. However, the main high-grade gold-silver mineralised epithermal zone has been found fully preserved at depths of over 200 m below surface at Cacao and La India South, and is likely to be similarly preserved below surface in the other less well explored prospects (Fig. 8).

Figure 6. Left: Laminated silica sinter deposits at the Cacao; Right: Mojarra prospects

Figure 7. Left: Phraeatic breccia; Right: a silicified microbreccia volcano-sedimentary exhalative flow deposit at the Central Breccia gold-silver deposit

Figure 8. Left: Central Breccia smectite altered clasts with sulphide rims cemented by quartz-calcite (example grading at 32.4 g/t gold and 19 g/t silver); Right: Banded quartz-calcite vein at c.260 m below surface (example grading at 8.20 g/t gold and 52 g/t silver)

Gold mineralisation at the Central Breccia which lies on the graben fault separating the historic mine area from the Sebaco graben differs from the rest of the La India district. The Central Breccia is a 150 m by 300 m phreatic breccia where two stages of hydrothermal breccia development are recognised, an early hydraulic breccia with

evidence of clast movement and rotation and a silica-cemented microbreccia matrix, and a later crack and fill brecciation with calcite and minor quartz-cement containing anomalous gold values formed under a more passive dilational regime. High-grade gold mineralisation is associated with a later argillic alteration and pyrite mineralisation overprint (English *et al.* 2012) [10].

Deep drilling at Cacao and La India South has revealed high-grade gold-silver mineralised well-developed and strongly gold-silver mineralised banded quartz-adularia veins with chlorite-carbonate-pyrite (propylitic) alteration more characteristic of the upper epithermal zone at depths of over 100 to 200 m below surface (Figs. 8 and 9).

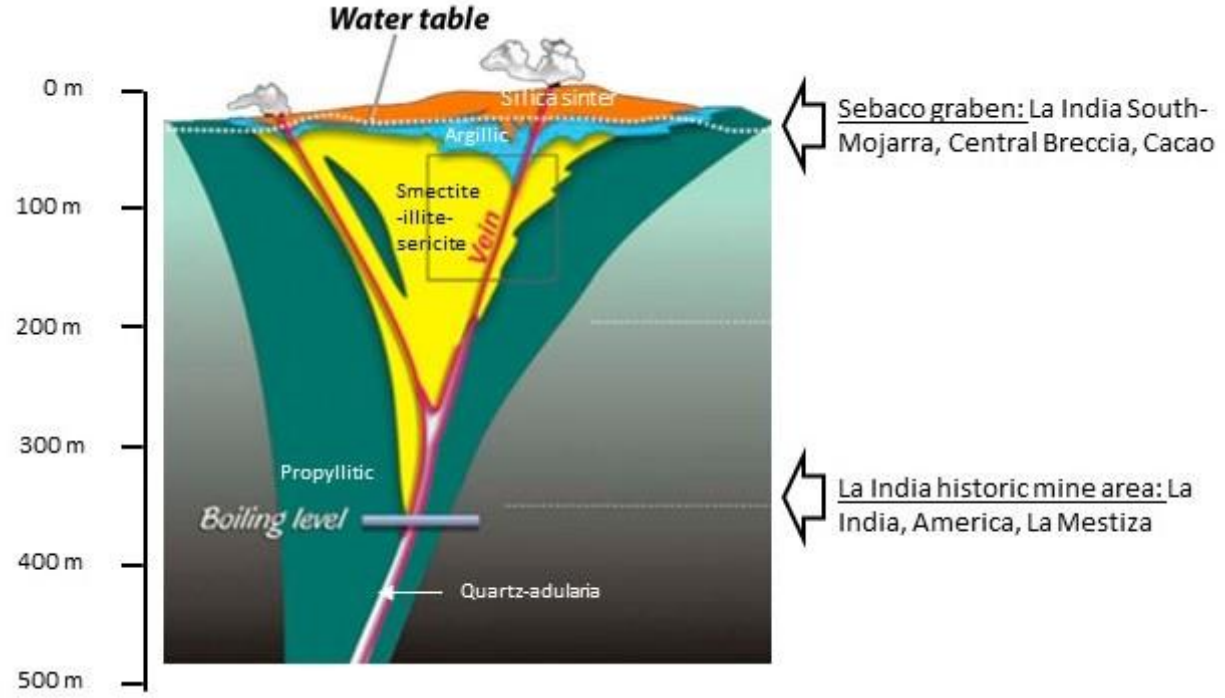

Figure 9. Schematic section through an idealised epithermal gold-silver vein showing interpreted current surface level of the mineralised veins in the un-eroded and fully preserved Sebaco graben and the erosion denuded historic La India mining area (after Corbett and Leach 1998; Hedenquist *et al.* 2000; Corbett 2012)[5,6 & 9]

2 Geological setting

2.1 Regional stratigraphic setting

The La India district is located within a Tertiary-aged volcanic arc at the margin of a major rift. The volcanic arc forms a northwest-southeast trending highland belt across the centre of Nicaragua, tectonically separated by a rift, the 30 km wide Nicaraguan Depression, from a younger, volcanically active arc to the southwest.

The Tertiary volcanic arc that hosts the gold-silver mineralisation at La India district developed as a collection of volcanic complexes including small to medium stratovolcanoes, large strato-shield volcanoes tens of kilometres in diameter, stratovolcanoes with preserved felsic plugs and a couple of minor rhyolite dome complexes (Ehrenborg 1996)[11]. Radiometric dating indicates a general younging in the age of the volcanic rocks southwest towards the rift margin, reflecting migration of the volcanic centre during roll-back of the subducting plate (Ehrenborg 1996, Rogers *et al.* 2002)[11-12]. Two stages of volcanic activity are recognised. The earliest volcanic activity formed Shield volcanos, assigned to the Matagalpa Group. Superimposed on these are younger strato-volcanic deposits designated the Coyol Group which host the gold-silver mineralisation at La India and were formed under a period of more active volcanism coincident with accelerated subduction from approximately 23 to 8 Ma (Rogers *et al.* 2002)[12].

Post-volcanic block faulting has imparted a strong structural fabric on the La India district. The original volcanic complexes can be recognised as faint circular forms in topography and geophysics and the La India district is interpreted as lying on the eastern flank of a denuded and disrupted strato-volcano centred between approximately

10 km and 25 km to the west (Fig. 10). At this location a massive quartz diorite intrusion forms a circular topographic low is interpreted as the central caldera magmatic intrusion. This quartz diorite intrusion is overlain by a thick sequence of pale coarse quartzofeldspathic tuff and subordinate breccia-tuff estimated at several hundred metres thick. The highest peaks in this area are capped by finer welded tuff.

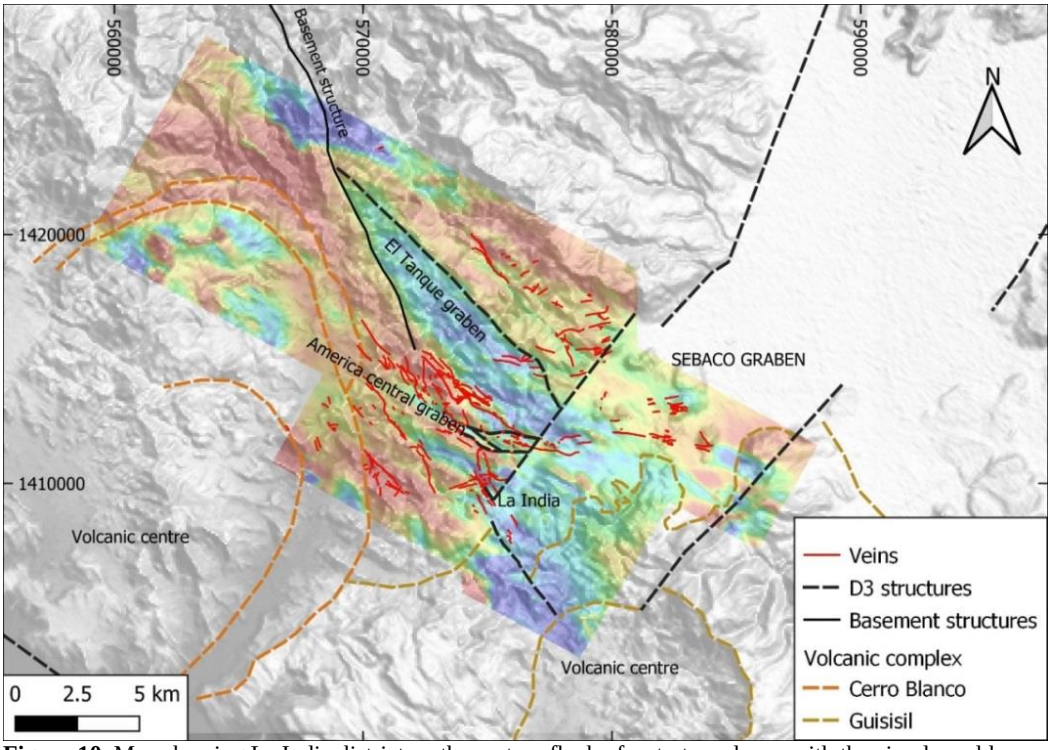

Figure 10. Map showing La India district on the eastern flank of a strato-volcano with the circular caldera and stratigraphic limits interpreted from topography, geophysics and geological mapping. Digital elevation topographic model (grey) overlain by reduced to pole, upward continued for 100 m plus direction filtered overlay with blue interpreted as downthrown graben blocks (Lubbe 2013)[13]

Stratigraphy of La India historic mine area

The geology near the historic La India Gold Mine is dominated by felsic volcanic flows or domes surrounded by thick deposits of volcanic agglomerates; flow front breccias grading distally to pyroclastic agglomerates, tuff-breccias and coarse tuffs. The felsic volcanic flows and associated pyroclastic deposits appears to have interrupted a thick sequence of glassy welded tuff deposit which locally display large pumice fiamme and extends several kilometres beyond the historic La India gold mine, at least as far as the La Mestiza deposit to the north where the welded tuff hosts significant gold-silver vein mineralisation (Fig. 3).

The welded tuff forms a resistant cap rock and it is apparent that the volcanic strata dips to the southwest in the southwestern part of the district, and to the northeast in the northeastern part of the district.

Stratigraphy of the Sebaco Graben

The thick sequence of flat-lying andesite that fills the Sebaco graben to the east of the historic La India mine area overlies felsic volcanics which are interpreted as downthrown exposures of the top of the felsic volcanic sequence as at the historic La India Gold Mine. The source of the andesite flows is uncertain as they only appear to have been preserved in downthrown fault blocks, principaly in the Sebaco graben, but also in the smaller downthrown blocks on the hangingwalls of the La India and America deposits.

The topography in this area exhibits a strong structural fabric such that the large-scale circular volcanic features that are visible elsewhere in the Central Volcanic Province cannot be seen. The structural fabric is oriented northwest

parallel to the Nicaraguan Depression and is strongest in the historic La India Gold Mine area adjacent to the Highway Fault, becoming weaker further North. The structural deformation forms an open anticline structure, possibly developed as antithetic tilt blocks, along a northwest-southeast axis parallel to the Nicaraguan Depression. The axis appears to run through the historic America mine area and northwest over the quartz dacite intrusion: Northeast-dipping faults and southwest dipping strata on the southwestern limb and the southwest-dipping faults and the northeast tilted welded tuff and basaltic capped hills on the northeastern limb. Continuation of the fold or rotated blocks across the downthrown Sebaco Graben and into the southeastern concessions has not been established.

2.2 Structural setting

At La India the development of geological structures from the Tertiary onwards reflects stresses caused by the subduction of the Cocos oceanic plate beneath the Nicaraguan landmass on the western edge of the Caribbean Plate. Four fault orientations are recognised: principal subduction trench-parallel northwest-striking faults (120°-300°; i.e. America and La Mestiza veins), and north-northwest-striking linking faults (140°-320°; i.e. La India vein). These primary faults arc-into or cross-cut secondary linking east-west-striking (090°-270°; i.e. Cacao vein), and north-south-striking (180°-360°) faults. The faults and associated fault-fill gold-silver veins developed during three structural deformation phases at the La India district during this time period (Starling 2015; Fig. 7)[14]:

Deformation phase 1 (D1) was a north-northeast to north-south extensional stress regime that was active during, and probably for several million years after deposition of the volcanic rocks, from approximately 23 Ma to 8 Ma. The stress was caused by a phase of rapid subduction following rupturing of the Farallon tectonic plate and formation of the Cocos plate beneath the present-day Pacific Ocean (Rogers *et al.* 2002) [12].

Under this stress regime the principal extensional (normal) faults developed striking northeast, parallel to the subducting trench (Starling 2015; Fig. 11)[14]. In the La India historic mining area these faults impart a strong fabric on the topography and are interpreted as developing an early horst and graben geometry centred America-Central Breccia prospects with faults and veins to the southwest all dipping inwards to the northeast, and faults and veins to the north and east all dipping in the opposite direction towards the south and west. It is possible that a subordinate conjugate set of sinistral trans-tensional north-northwest and dextral east-west trans-tensional linking faults would have developed and that gold-silver mineralisation may have initiated towards the end of this phase.

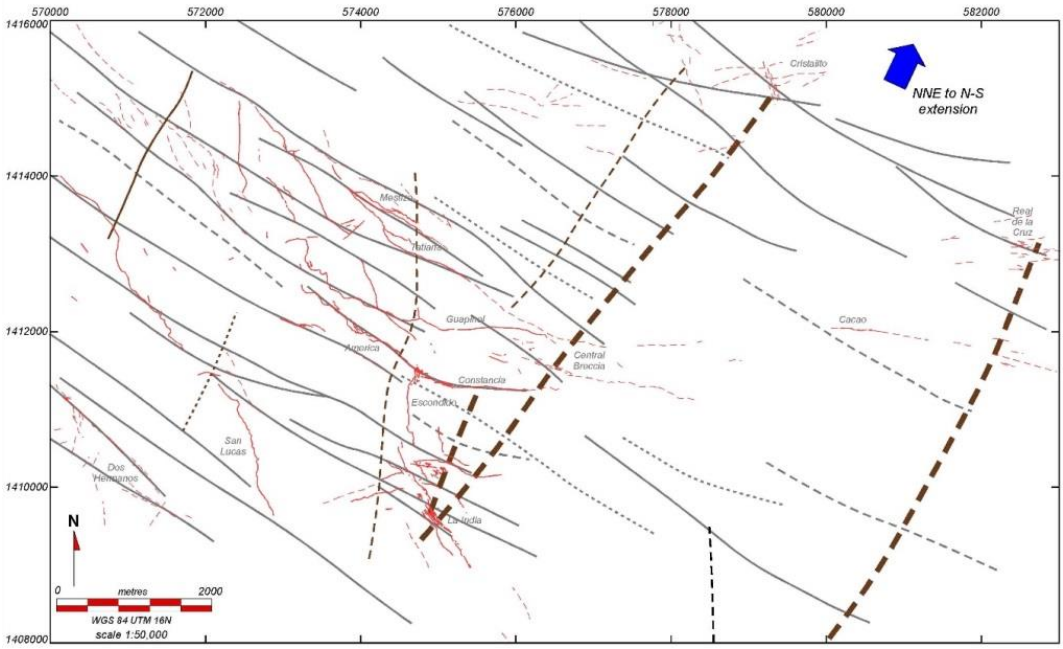

Figure 11. Schematic map showing the primary northeast-striking arc-parallel normal faults formed during the D1 Southwest-directed extension with possible early gold deposition (from Starling 2015)[14]

Deformation phase 2 (D2) occurred when the Cocos ridge collided with the volcanic arc to the southeast of La India (present day Costa Rica) approximately 8-10 Ma ago. This caused the subducting slab of oceanic plate to detach and a pause in volcanic activity. This also caused the Central American forearc slither to start moving northwest relative to the volcanic arc (Karason and van der Hilst 2000, De Mets *et al.* 2000; De Mets 2001) [15-17].

Starling (2015)[14] suggests that the extensional stress regime rotated clockwise to between east-northeast and east-west at this time. Under this regime the north to northwest faults such as the faults hosting the principal La India deposit would have developed as primary normal extensional faults. The D1 arc-parallel normal faults would have been reactivated as trans-tensional with a dextral strike-slip component. The east-west faults would have reactivated and possibly extended as strike-slip faults linking the primary arc-parallel northeast-striking faults (Starling 2015)[14]. This is interpreted as the main gold-silver mineralisation event with the greatest dilation and widest veins deposited in the extensional north-northeast-striking faults such as the La India vein (Starling 2015; Fig. 12)[14].

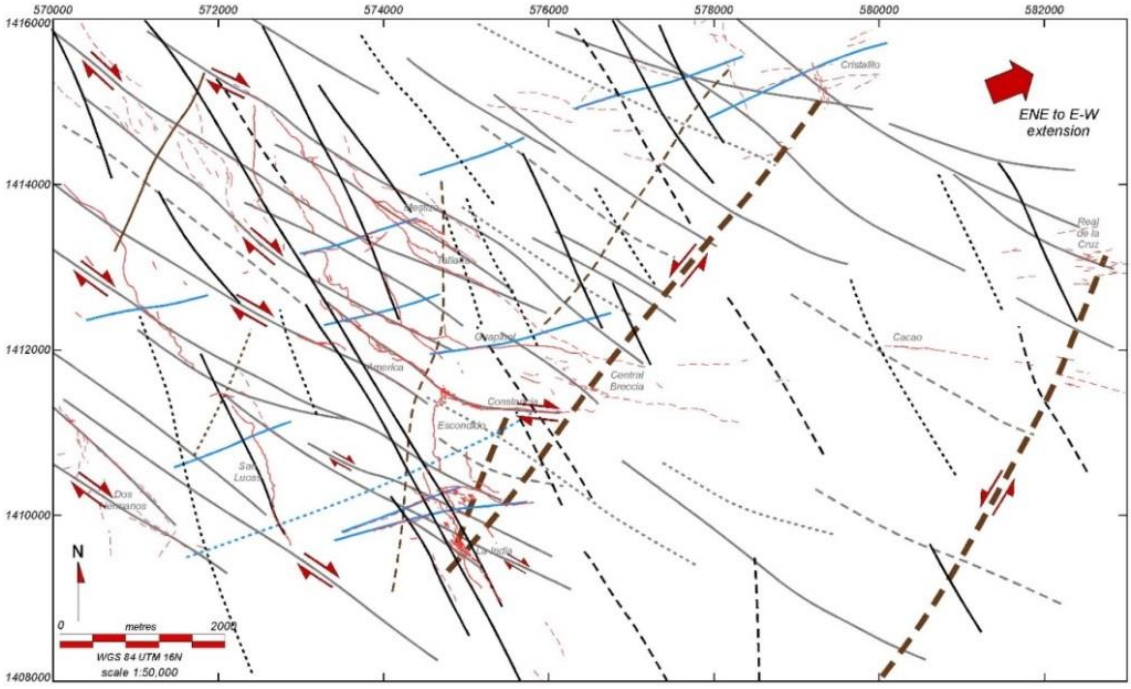

Figure 12. Schematic map showing the faults formed during the D2 West-southwest directed extension associated with the principal gold mineralisation phase (from Starling 2015)[14]

Deformation phase 3 (D3) is the current north-northeast to north-south extensional regime that started approximately 4 Ma ago, after a pause during slab detachment, with establishment of a steeper subduction slab and development of the new, currently active volcanic arc further away from the La India district (Rogers *et al.* 2002)[12]. This phase is characterised by strain partitioning into dextral strike-slip motion of the northwestward sliding fore-arc slither and normal convergence at La India district in the back-arc at the same time as a resumption of slab-rollback (Starling 2015)[14].

Later-stage block faulting (D3), much or all of which occurred post gold mineralisation, would have moved and offset significant segments of gold mineralised veins (Starling 2015)[14]. An important example of this was the downthrow of the 6-10 km wide Sebaco graben that appears to have dropped gold mineralised veins at Cacao several hundred metres below those now exposed at La India, preserving the Cacao vein from erosion (Starling 2015; Fig. 13)[14]. The resumption of the southeast-directed extension also reactivated the existing faults with some D1 arc-parallel northeast-striking faults reactivated as block faults with graben development at the central America prospect, and half graben block tilting at La India prospect and the El Tanque area (Figs. 9 and 12).

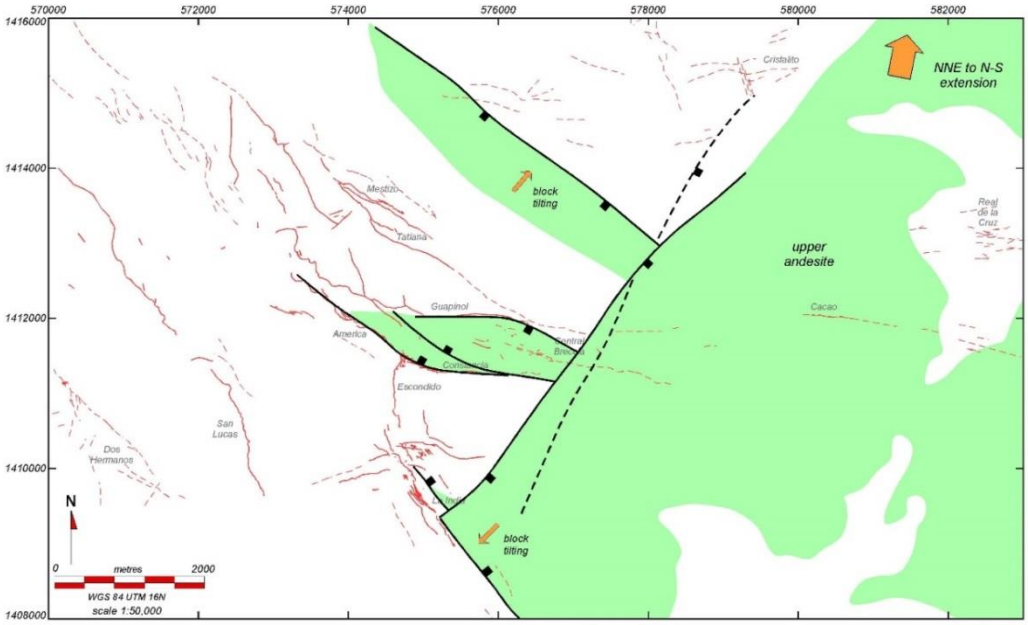

Figure 13. Schematic map showing the faults formed during the D3 block faulting under a more distal southwest-directed extension (From Starling 2015)[14]

3 Localisation of gold-silver mineralisation

Gold-silver mineralisation in the La India district is classified as rift margin-type low-sulphidation epithermal gold-silver vein mineralization (Corbett and Leach 1998)[9]. The gold-silver mineralisation occurs in veins filling open spaces formed by faults and fractures. Economic concentrations of gold-silver mineralisation occur where the largest open spaces formed at epithermal depths on structures that were connected to deep crustal conduits that transported the mineral-rich hydrothermal fluids from their magmatic source.

3.1 Localisation of gold-silver mineralisation at district-scale

The geometry of the upper crustal faults that host the gold mineralisation in the La India district is attributed to the southwest-directed extensional tectonic regime, a setting consistent with the arc-parallel low sulphidation fault-fill and extensional vein systems in an extensional arc setting formed during slab rollback described by Rhys *et al.* 2020[18].

A mineral systems analysis undertaken by Galvan (2014)[19] considered the deep crustal conduits required to transport the gold-silver rich hydrothermal fluids from their magmatic source to the upper crustal epithermal vein deposits at La India district. Galvan identified a regional northwest-southeast trending structural trend, clearly discernible in aeromagnetic, radiometric and topographic data that connect the principal gold-silver mineralised faults in the La India historic mining district (Lubbe 2013; Galvan & Pullinger 2013. Fig. 14)[13 & 20]. These regional structures are interpreted as deep crustal structures that form the feeder conduit for the hydrothermal magmatic fluids. The principal feeder, or backbone structure connects the principal gold deposits of La India, America, and La Mestiza. A possible secondary parallel backbone structure running through the less well explored explored San Lucas and Dos Hermanos structures are also postulated. These deep structures may be transform faults formed perpendicular to the subduction zone, or older reactivated basement structures, perhaps formed along the suture between the basement Chortis and Siuna blocks before the volcanic arc (Venable 1994)[21]. Pratt (2019)[22] suggested that the gold-silver mineralisation is concentrated by dilational jogs on this re-activated basement structure. Pratt (2019)[22] also extended the idea to the north and east, suggesting that the Andrea vein is associated with a similar basement structure and that the two structures are connected by the East-West trending Cacao Structure, implying that the Cacao structure may also be deep-seated.

The northeast-striking Highway Fault that appears to focus the Central Breccia phreatic breccia is interpreted here as having been active throughout D2 and D3 deformation phases. The Highway fault may also be a deep crustal structure that could also have connected hydrothermal fluids across the district. This would be consistent with observations by Wilson and Rowland (2016)[23] who noted that transfer faults and arc-oblique basement faults can also locally influence the position and orientation of epithermal systems.

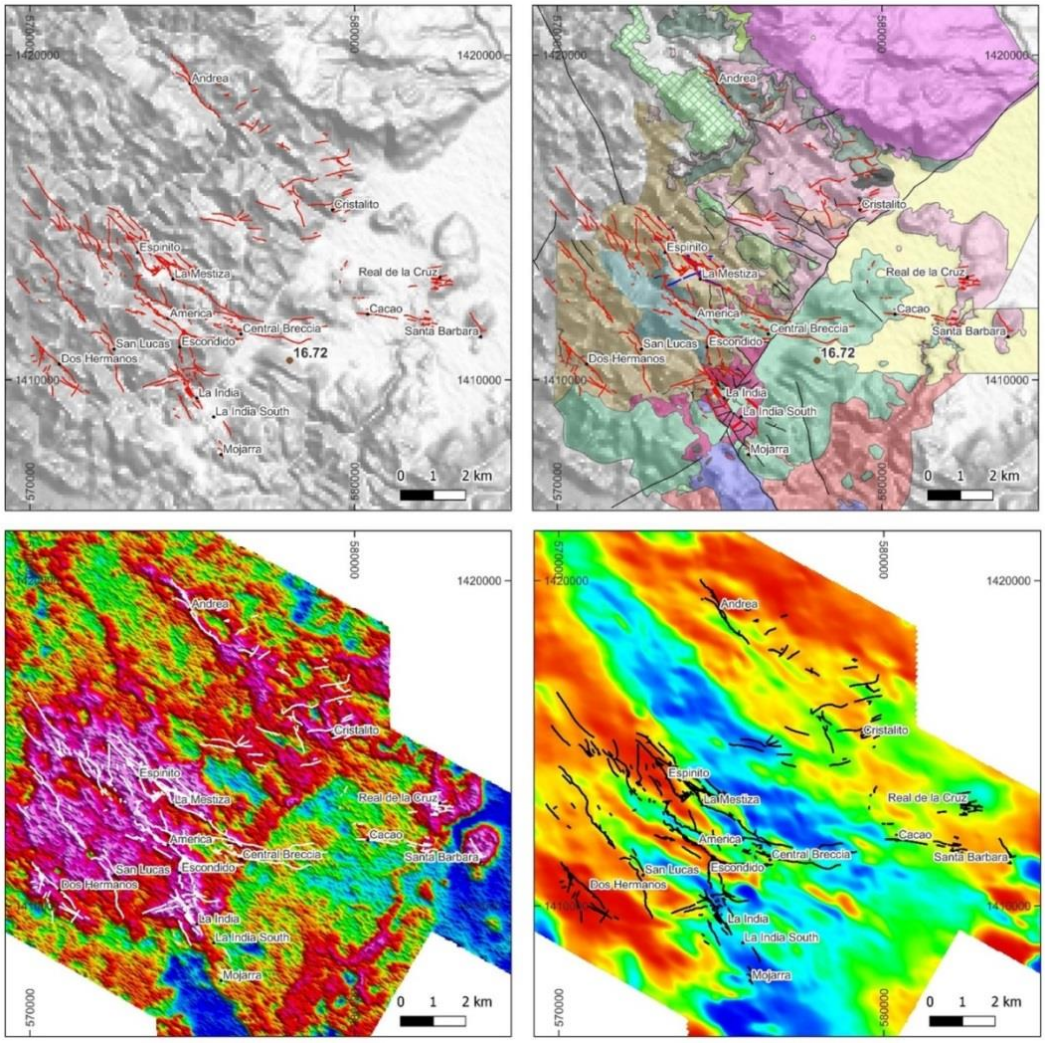

Figure 14. Top: Topography and surface geology of the La India district; Bottom left: Radiometric K showing areas of potassium alteration (red-magenta) and gold-silver veins (white) and interpreted north-northwest through-going structures interpreted as the deep-crustal feeder or 'backbone' conduits for the gold-silver-bearing hydrothermal fluids; Bottom right: reduced to pole magnetics at 100m depth shows the D3 block faulting with downthrown blocks coloured blue

3.2 Localisation of gold-silver mineralisation at deposit-scale

At deposit-scale, gold-silver mineralised ore shoots have developed where there is vein bifurcation, and at the steep upper section of listric faults and fault jogs. The most economic deposit discovered to date, the La India deposit is contained within a fault stack developed where a major normal fault was refracted and bifurcated around and across the edge of a competent rhyodacite and overlying welded tuff forming a steeply-dipping stack of mineralised veins.
The rheology of the host rock influences the form and geometry of the throughgoing faults and therefore the geometry and extent of dilation and vein infill. The host rocks are a layered felsic volcanic stratigraphy in the historic La India mining area, and overlying andesite in the Sebaco Graben. In the La India historic mining area the

best developed veins are in the more competent rocks which support brittle fractures: the rhyodacite flows and a fine vitric unit interpreted as a welded tuff. Rhyodacite flow-front autobreccias and more distal polymict volcanic agglomerates and tuffs are poor hosts as they appear to have responded to faulting by absorbing the stresses within the less competent matrix rather than forming open space fractures. The best gold deposits defined to date are hosted by felsic volcanics and welded tuff at La India, and by welded tuff at La Mestiza (Fig. 3). In the Sebaco Graben most of the exploration data is limited to the overlying thick andesite sequence which appears to be a good host rock, concentrating veins into a wide discrete vein and vein sets at the principal Cacao and La India South prospects.

4 Post-mineralisation displacement of gold-silver mineralisation

The development of the Sebaco Graben, orthogonal to the volcanic arc during D3 block faulting phase which initiated after slab detachment at approximately 8 Ma cut the La india district in two. Although there is clear evidence that the Sebaco Graben was downthrown relative to the historic La India mine district post-mineralisation gold mineralisation may have persisted into the D3 block faulting phase after slab detachment at approximately 8 Ma. The Central Breccia's location at a jog on the graben-bounding Highway Fault could be interpreted as late-stage mineralisation that exploiting a D3 structure.

The upthrown block was eroded to expose the low sulphidation epithermal mineralisation at the La India historic mine area which contains a current gold endowment of over 2 Moz. The downthrown Sebaco graben has escaped significant erosion and the epithermal mineralisation is preserved at depth and discoveries of hidden deep-seated exploration are still being made.

5 Timing of gold-silver mineralisation

Brecciated and milled gold-silver veins indicates that mineralisation occurred in active faults, and the structural interpretation places these faults, and consequently the main phase of gold-silver vein emplacement as occurring shortly before or at 8-10 Ma. This was at a period of waning or extinct volcanism which could suggest that gold-silver veins precipitated from heavy metal-rich hydrothermal fluids derived from mature, highly evolved and depleted magma chambers. It also coincided with the onset of mantle upwelling and flood basalt volcanism associated with slab detachment (Rogers *et al.* 2002)[12]. It has been postulated by Sidorov *et al.* (2015)[24] that epithermal mineralisation is driven by such 'microplumes' at the end of arc volcanism in advance of the onset of basaltic volcanism.

The timing of gold-silver mineralisation of the Central Breccia phreatic breccia pipe is less clear. The location on the graben-bounding Highway fault, at an apparent jog in the fault, suggests that the Central Breccia was emplaced along the Highway Fault. This could mean that the Highway fault is a long-lived structure, and was active as far back as the D2 slab detachment phase. An alternative, and less likely explanation is that mineralisation was still occurring at the Central Breccia as recently as the D3 block faulting and graben formation phase from only 4 Ma.

6 Conclusions

Gold-silver mineralization at La India is observed on a district scale on the eastern flank of a 23 to 8 Ma volcanic complex between approximately 10 km and 25 km from the interpreted volcanic centre.

The La India district setting and geometry of mineralisation is an example of an arc-parallel low sulphidation epithermal gold-silver fault-fill and extensional vein systems formed in an extensional arc setting during slab rollback regime as described by Rhys *et al.* 2020[18].

The gold-silver mineralisation is localised along and connected to a few regional through-going structures that are interpreted as forming the deep-seated conduits for the mineral-rich magmatic source fluids. The main deep crustal conduits are north-northwest-striking with a possible east-west striking linking structure providing additional hydrothermal connectivity.

The rheology of the host rock influences the size and grade of gold-silver mineralisation. The epithermal zone at the time of mineralisation occurred a layered felsic volcanic stratigraphy and overlying andesite. The best hosts are competent rocks: rhyodacite flows and a fine vitric unit interpreted as a welded tuff. Rhyodacite flow-front autobreccias and more distal polymict volcanic agglomerates and tuffs are poor hosts as they appear to have

responded to faulting by absorbing the stresses within the less competent matrix rather than forming open space fractures.

Post-mineralisation graben development has split the La India district gold-silver mineralisation between the upthrown historic mining area where erosion has exposed the upper levels of the low-sulphidation epithermal veins, and the downthrown graben where the epithermal mineralisation preserved hidden at depth and is still being discovered.

The gold-silver mineralisation is interpreted as occurring towards the end or immediately after a period of arc-volcanism. Radiometric dating of host rock places the gold-silver mineralisation after 16.72 Ma. It is suggested that gold-silver mineralisation occurred well after this date in the waning stage of arc volcanism during slab rollback and/or at the initiation of a period of slab detachment and mantle upwelling at 8-10 Ma.

Acknowledgments This paper is a compilation of data collected, and observations and interpretations made, by geologists and mining engineers from the late 1930's to the present day. The early contributors whose names have been forgotten, or the records lost, are acknowledged. There are too many geologists and field assistants who have mapped, sampled and studied the La India district since the late 1980's to name, but the work done by geologist Armando Tercero who maintained a leading role in the development of the project throughout that period is especially acknowledged. The paper draws on lithological and structural observations and interpretations developed by consultant geologists Dr Tony Starling, Dr Warren Pratt and Miguel Ponce. Finally, this paper would not have been completed without the support of the Directors of Condor Gold PLC, in particular the support and encouragement provided by CEO Mark Child and technical directors Andrew Cheatle and Peter Flindell.

Author contributions L.T.P.E. contributed to the data collection, compilation and interpretation and wrote the paper. V.H.G. and C.R.P. contributed to the data collection and interpretations.

Data availability statement Data sets generated during the current study and internal company reports referenced in this paper are available from the corresponding author on reasonable request, but restrictions apply to any data used in these studies which was collected for exploration, mineral resource evaluation and mine feasibility studies under license, and so are not publicly available. Data referring to mineral resource estimates are available on the Ontario Securities Commission SEDAR+ web-based system and on Condor Gold PLC's website www.condorgold.com.

Declarations The authors declare no competing financial interests.

7 References

1. English, LTP. 2015. La India mine depletion. *Condor Gold PLC Internal Report*.
2. Rogers, RD. & Emmet, PA. 2007. Tectonic terranes of the Chortis block based on integration of regional aeromagnetic and geologic data. *The Geological Society of America Special Paper*, 428, 65-88.
3. Plank, T; Balzer, V & Carr, M. 2002. Nicaraguan volcanoes record paleoceanographic changes accompanying closure of the Panama gateway. *Geology*, 30(12), 1087-1090.
4. SRK Consulting (UK). 2022. A mineral resource estimate on the La India, Nicaragua. *Consultant Report for Condor Gold PLC*.
5. Hedenquist, JW; Arribas, A & Gonzalez-Urien, E. 2000. Exploration for epithermal gold deposits. *Reviews in Economic Geology*, 13, 245-277.
6. Corbett, GA 2012. Structural Controls to, and Exploration for, Epithermal Au-Ag Deposits. *Australian Institute of Geoscientists Bulletin*, 56, 43-47.
7. Pratt, W & Ponce, M. 2016. Geology of the La India Project, Nicaragua. Specialised Geological Mapping Ltd., *Consultant Report for Condor Gold PLC*.
8. Pratt, W. 2019. Geological review of the Cacao vein target, La India gold project, Nicaragua. Specialised Geological Mapping Ltd., *Consultant Report for Condor Gold PLC*.
9. Corbett, GJ & Leach, TM. 1998. Southwest Pacific rim gold -copper systems: structure, alteration, and mineralisation. *Society of Economic Geologists Special Publication*, 6, 234 p.
10. English, L; Galvan, VH & Pullinger C. 2012. Central Breccia prospect, La India project technical report. *Condor Gold PLC Internal Report.*
11. Ehrenborg J. 1996. A new stratigraphy for the Tertiary volcanic rocks of the Nicaraguan Highland. *Geological Society of America*, Bulletin, 108(7), 830-842.
12. Rogers, RD; Karason, H. & van der Hilst, RD, 2002. Epeirogenic uplift above a detached slab in northern Central America. *Geology*, 30(11), 1031-1034.
13. Lubbe, B. 2013. La India Geophysics. *Consultant Report to Condor Gold PLC.*

14. Starling, T (Telluris Consulting Ltd). 2015. Structural review of the La India Deposit and District, Nicaragua. *Condor Gold PLC News Release*, September 2015.
15. Ka´rason, H & van der Hilst, RD. 2000, Constraints on mantle convection from seismic tomography; in Richards, MR, *et al*., eds., *The history and dynamics of global plate motion*: *American Geophysical Union Geophysical Monograph,* 121, 277–288.
16. DeMets, C; Jansma, P; Mattioli, G; Dixon, T; Farina, F; Bilham, R; Calais, E & Mann, P. 2000. GPS geodetic constraints on Caribbean– North America plate motion. *Geophysical Research Letters,* 27, 437–440.
17. DeMets, C. 2001. A new estimate for present-day Cocos-Caribbean plate motion: Implications for slip along the Central American volcanic arc. *Geophysical Research Letters,* 28, 4043–4046.
18. Rhys, DA; Lewis, PD & Rowland, JV. 2020. Structural controls on ore localization in epithermal gold-silver deposits: a mineral systems approach. Society of Economic Geologists. *Reviews in Economic Geology,* 21, 83-145.
19. Galvan, VH. 2014. *Paragenesis of La India District*. Condor Gold PLC Internal Report.
20. Galvan, VH and Pullinger, C. 2013. *Interpretation of La India District Airborne Magnetic and Radiometric Data*. Condor Gold PLC Internal Report.
21. Venable, ME. 1994. *A Geologic, Tectonic and Metallogenic Evaluation of the Siuna Terrane*. PhD dissertation, The University of Arizona.
22. Pratt, W. 2019. *Report of the Structural Geology of La India District, Nicaragua*. Specialised Geological Mapping Ltd., Consultant Report for Condor Gold PLC.
23. Wilson, C. and Rowland, J. 2016. The volcanic, magmatic and tectonic setting of the Taupo volcanic zone, New Zealand, reviewed from a geothermal perspective. *Geothermics,* 59, 186–187.
24. Sidorov, AA; Volkov, AV and Savva, NE. 2015. Volcanism and epithermal deposits. *Journal of Volcanology and Seismology,* 6, 3-12.

Original Article

Review of gold cyanide leaching and the main factors affecting gold dissolution rate

Alice Shi[1] ©

Abstract

This paper reviews the cyanide leaching technology and the influential parameters affecting the cyanidation process. In general, the factors influencing the degree of cyanide leaching of gold include particle size, NaCN concentration, the level of dissolved oxygen, pH, pulp density, and leaching time. Each of these parameters plays a significant role in gold cyanidation, and should be optimized respectively by conducting laboratory testing prior to production application.

Keywords: Gold ore; cyanide leaching; gold dissolution; particle size; cyanide concentration; dissolve oxygen; pulp density

---

Affiliation Info: [1] Orient Resources Ltd., Richmond, BC, V7E 1M8, Canada
Article Info: Received: 16 September 2023 / Revised: 17 October 2023 / Accepted: 26 November 2023 / Published Online: 12 December 2023. www.naturalisscientias.com
Author's Contact Info: Shi, A: aliceshi0527@gmail.com
Citation: Shi, A. 2024. Review of gold cyanide leaching and the main factors affecting gold dissolution rate. *Naturalis Scientias*, 1(1): 56-60. DOI: https://doi.org/10.62252/NSS.2024.1004.

Corresponding Author©: Shi, A, PhD, Metallurgist; Email: aliceshi0527@gmail.com

1 Introduction

As a key mineral resource which can be separated from gold ores, gold has been the focus of mining activity in the areas of exploration and metallurgy[1]. The total gold supply in 2022 is estimated to be 4,754 tons, which includes approximately 3,612 tons from mine production with the remainder primarily produced from waste recycling[2]. Mine production was, is and will continue to be the key source of gold production. The world's largest gold producing countries are China, Australia, Russia, and Canada[3]. Over the past decades, the demand for gold has steadily increased, and the worldwide annual gold demand has surged to an 11-year high in 2022 and jumped 18% to 4,741 tons[2], which is just below the total supply of gold in the year.

Amongst the world's mineral resources, gold is unique. This is not only because it is among the first metal minerals developed and applied by mankind, but also because it has various mineral processing technologies. This original review article is a brief review of cyanidation, the primary and most widely used mineral processing technique for gold ores.

2 Summary of cyanidation process

As a high value and recoverable noble metal, gold (Au) is widely distributed in low concentrations in a number of geological environments. Gold mostly occurs as pure native gold, gold-silver electrum, or chemically combined with tellurium, selenium, and bismuth. Sylvanite and calaverite are gold-bearing minerals. Gold is usual found embedded in quartz veins or associated with sulphide minerals, principally arsenoprite and pyrite, in sulphide mineralization.

Conventionally, gold is selectively dissolved from its ore using an aqueous sodium cyanide solution in the presence of oxygen to solubilize the gold. The dissolved gold is then precipitated from the pregnant leach solution (PLS) by zinc dust or extracted from PLS by adsorption on activated carbon or resins. This process is called cyanide leaching, also referred to "Cyanidation". Cyanidation has been both the primary technology and a well-adopted industry standard method for gold processing since it was first put forward by John Stewart MacArthur in the 1880s[4], due to its high efficiency, simplicity, robustness, and relatively low cost. This cost-effective, well-proven gold extraction method provides maximum recovery for many free-milling gold ores, including low grade and some refractory ores. More than 75% of the gold produced worldwide is extracted by cyanide leaching of gold ores[5].

Undoubtedly, cyanide leaching is still the most important and widespread of the various hydrometallurgical technologies used in the extraction of gold from primary ores. In fact, cyanidation remains the main choice today for the recovery of gold from low-grade and finely disseminated gold ores in both technological and economical respects.

3 Factors affecting cyanidation process

Gold cyanidation follows an electrochemical-chemical reaction between cyanide and gold according to the following equation[6]:

$$2Au + 4NaCN + \frac{1}{2}O_2 + H_2O + 2OH^- \rightarrow 2Au(CN)^{2-} + 4NaOH$$

During cyanide leaching, in addition to sodium cyanide and oxygen as listed in the equation, many other factors also play important roles in gold dissolution. The influential parameters affecting the cyanidation process include the availability of oxygen at the solid–liquid interface, the pH of the leach slurry, pulp density, the presence of ions other than CN^- in solution, the cyanide concentration, the particle size of the ore, the leach temperature, the surface area of gold exposed, the mineralogical characteristics of the ore, the degree of agitation and leaching time, etc.

3.1 Oxygen

The cyanidation hydrometallurgy technique consists of an electrochemical process that oxidizes gold and reduces oxygen with cyanide solutions. As seen in the gold and cyanide reaction equation, oxygen is the one of the two main components of the cyanidation process, and is essential in gold cyanidation. It not only oxidizes gold itself to an ion that can form the water-soluble complex salt $Au(CN)^{2-}$ in the presence of cyanide, but also assists with oxidation of other metal ions, such as those of iron and copper. Thus, the concentration of oxygen is one of the most important factors in the gold cyanidation process.

The source of oxygen can be air, oxygen, hydrogen peroxide (H_2O_2) or other oxidizing agents such as *LeachAid*®, $KMnO_4$ and Cl_2. Currently most cyanidation plants utilize aeration to provide the required dissolved oxygen ($d.O_2$) in pulp. The $d.O_2$ concentration can be boosted by high pressure aeration, oxygen injection, or the addition of oxygen-rich solutions. The use of oxygen compounds instead of air as an oxidant increases the leach rate and decreases cyanide consumption, as it provides more oxygen (higher $d.O_2$) in leach slurry.

Generally, increasing the concentration of $d.O_2$ in leach solution improves the gold cyanidation process, thus increasing gold dissolution rate.

3.2 Cyanide concentration

As the other main component of the cyanidation process, the concentration of cyanide is essential.

As noted in the chemical reaction between gold and cyanide, in the cyanidation process gold reacts with cyanogen (CN^-) under the action of oxygen and forms a water-soluble cyanogenic gold complex $Au(CN)^{2-}$. Therefore, the cyanide concentration is one of the most decisive factors in the gold cyanidation process.

The NaCN concentration in the cyanide solution typically ranges from 100 ppm to 500 ppm cyanide. Cyanide leaching of gold requires a certain amount of free cyanide in solution. In general, higher cyanide concentration benefits gold dissolution; the higher the cyanide concentration, the faster the gold dissolution.

3.3 pH

The pH affects the cyanide leaching process in the following ways[7]:

- to prevent loss of cyanide, and the formation and release of the toxic and fatal hydrogen cyanide (HCN);
- to neutralize acidic compounds in mill water prior to adding to the mill;
- to neutralize the acidic components in the ore or resulted from decomposition of various minerals in the ore during grinding;
- to assist with settling of fine particles in the ore and/or resulted from milling of the ore;
- to improve gold dissolution when treating ores containing telluride minerals, ruby silver, which decompose more readily at higher alkalinities.

Alkalis such as hydrated lime (calcium hydroxide $Ca(OH)_2$) or sodium hydroxide (NaOH) are generally used to adjust and maintain the leach slurry pH to >10 during the cyanide leaching process. Research found that, when using hydrated lime, the gold dissolution rate decreases rapidly when the pH is close to 11.0 and is negligible once pH reaches 12.2. However, the effect of sodium hydroxide is much less[7]. The gold dissolution rate does not slow until pH 12.5 when sodium hydroxide is used.

3.4 Pulp density

Pulp density also refers to the solid-liquid ratio of pulp, which directly affects the diffusion rate of cyanide and oxygen in the pulp.
The pulp density in leaching of normal gold ore is usually controlled at 40- to 55 wt.%. Higher pulp density results in lower pulp flow and lower gold leaching rate; lower pulp density benefits gold dissolution rate but the requirements on equipment volume increases along with the cyanide reagent. The maximum gold dissolution increases with a decrease in pulp density.

3.5 Ions in solution other than CN^-

Irons such as copper can react with cyanide and form different complexes which deplete the necessary amount of free cyanide required for gold dissolution, thereby decreasing gold leaching. Thus, a high concentration of copper can interfere with gold dissolution and lead to soluble gold losses, the production of weak acid dissociable (WAD) cyanide, as well as a number of operational challenges in the downstream CIP/CIL circuits with respect to competitive adsorption, and subsequent difficulties associated with elution, electrowinning and smelting[8]. Furthermore, as copper minerals are significant cyanide consumers, the presence of copper ion leads to higher cyanide consumption during the leaching process and higher operational costs[9].

3.6 Particle size

Almost all gold ores require grinding to liberate and unlock the gold particles in the host matrix so the surface of gold minerals particles can be exposed prior to cyanide leaching for gold extraction.
The particle size of ore positively affects the surface area of gold exposed to cyanide solution. Reduction of the particle size of the ore creates more surface area of exposed gold and increases the contact surface area between the ore and cyanide solution, which ultimately increase the gold dissolution rate. Generally, finer particle sizes result in better gold dissolution. For gold ores requiring oxidation pre-treatment, the gold contained in the fine-size fractions usually shows a good dissolution without pretreatment[5].
Depending on mineral liberation, the particle size of ore in most leaching plants can vary from P_{80} 75 µm to 220 µm.

3.7 Temperature

Gold dissolution rate can be advanced with an increase in temperature during cyanidation, but the amount of dissolved oxygen will significantly decrease as temperature increases and becomes zero once the temperature reaches 100 ^oC, at which point no more leaching occurs[10].
In general, the cyanidation process does not require heating, and is maintained at 15-30 ^oC or carried out at the atmospheric temperature of the plant.

3.8 Degree of agitation

During cyanide leaching of gold ores, the pulp needs to be agitated or mixed to increase the solubility of oxygen and gold-cyanide reaction.
Increasing the agitation speed promotes the diffusion rate of gold-bearing mineral particles in the leaching solution, hence increasing the leaching efficiency.

3.9 Leaching time

The gold cyanide leaching process is relatively slow, and usually requires more than 24 hours to complete. In general, leaching time has a positive effect on gold dissolution, and the gold dissolution rate improves with the extension of leaching time however, the gold leach speed decreases correspondingly and the final gold dissolution rate trends to a limit point, at which point increasing leaching time no longer improves final gold leaching rate.
Leaching time varies significantly from ore to ore. For low-grade oxide ores, gold leaching can complete within 24-30 hours at a target grind size P_{80} 75-150 µm; while for complex ores with sulphide mineralization, it may take 72 hours or even longer to reach the maximum leach rate.

4 Discussion and conclusions

The main advantages of cyanidation are low cost, high selectivity of free cyanide for gold dissolution, and the extremely high stability of the cyanide complex. The most important disadvantages of this process are the toxicity and disposal problems of leaching wastes into the environment unless the necessary precautions are taken. As an alternative process to cyanidation, thiourea, thiosulfate, chlorine, and acid leaching methods have been developed in recent years, but none of these have yet gained industrial application[6]. At least in the near term, cyanidation will continue as the main technique for gold extraction in the mining industry. Understanding the factors affecting cyanide gold dissolution rate is crucial. Although many factors play important roles in cyanide leaching of gold ores, the main ones influencing gold dissolution rate most are particle size, the concentration of dissolved oxygen, NaCN concentration, pH, pulp density, and leaching time. In general, the factors influencing the degree of cyanide leaching are in the order of leaching time > NaCN concentration > particle size > pH > pulp density.
Prior to production application, these leach parameters need to be evaluated and optimized in a laboratory testing facility by bottle roll or column testing to evaluate the ore's amenability to the cyanide leaching process, expected gold recovery, and reagent requirements.

Acknowledgements Support for this study was received from Orient Resources Ltd. in BC, Canada.

Author contributions A Shi contributed to the whole research, compilation, interpretation, and writing of the paper. The author prepared and reviewed the manuscript and approved the final version of the manuscript.

Data availability statement The data and information that support the study are based on the author's experience, and part of which are available from the academic publications, which were lucidly and relevantly cited as references.

Declarations The author declares that she has no conflict of interest.

5 References

1. Martens, E; Zhang, HG; Prommer, H; Greskowiak, J; Jeffrey, M & Roberts, P. 2012. In situ recovery of gold: column leaching experiments and reactive transport modeling. *Hydrometallurgy*, 125-126: 16–23. DOI: 10.1016/j.hydromet.2012.05.005.
2. World Gold Council (WGC). 2023. *Gold Demand Trends Full Year 2022*. WGC, London, UK.
3. Garside, M. 2023. Gold production ranked by major countries 2022, https://www.statista.com, accessed September 15, 2023.
4. Fathi, H. 2005. A short history of hydrometallurgy. *Hydrometallurgy*, 79: 15-22.
5. Egan, J; Bazin, C & Hodouin, D. 2016. Effect of particle size and grinding time on gold dissolution in cyanide solution. *Minerals*. 6(3): 68. https://doi.org/10.3390/min6030068.
6. Azizi, A & Ghaedrahmat, R. 2015. Optimizing and evaluating the operational factors affecting the cyanide leaching circuit of the Aghdareh gold processing plant using a CCD model. *Proceedings of the Royal Society A*, 471 (2184). http://dx.doi.org/10.1098/rspa.2015.0681.
7. Michaud, LD. 2015. Effect of pH alkalinity on gold leaching, *911 Metallurgist*. https://www.911metallurgist.com/blog/effect-of-ph-alkalinity-on-gold-leaching, accessed September 14, 2023.
8. Oraby, EA & Eksteen, JJ. 2015. Gold leaching in cyanide-starved copper solutions in the presence of glycine. *Hydrometallurgy*, 156: 81-88. https://doi.org/10.1016/j.hydromet.2015.05.012.
9. Jiang, T; Zhang, YZ; Yang, YN & Huang ZC. 2001. Influence of copper minerals on cyanide leaching of gold, *Journal of Central South University of Technology*, 8: 24-28. DOI: 10.1007/S11771-001-0019-2.
10. Shandong Xinhai Mining Technology. 2022. Uncover the 5 factors affecting the cyanide leaching rate of gold ore. https://www.linkedin.com/pulse/uncover-5-factors-affecting-cyanide-leaching-rate-of-gold-ore, accessed September 14, 2023.

Original Article

What is the primary culprit that causes the "Doomsday Glacier" in Antarctica?

Jijun Zhang[1 & 2]

Abstract

Antarctica, situated in the southernmost part of the earth is surrounded by the Southern Ocean. It has an extremely important role in tuning global climate, both because of its geographic location, and its giant ice mass, that comprises ~90% of the world's ice. In the past decades, the Thwaites Glacier in the Amundsen Sea of West Antarctica is undergoing the fastest recession in the region. The ice loss in Thwaites Glacier is currently responsible for roughly four percent of the global sea-level rise, which has been attributed to climate change and ocean warming. Due to the continuous collapsing and melting of Thwaites Glacier and the severe threat to humans, scientists gave it a terrifying name "Doomsday Glacier". With increasingly geological and geophysical studies conducted in West Antarctica, geothermal heat flux has been discovered to play a vital role in icesheet retreating. The rapidly retreating Thwaites and Pope glaciers are underlain by areas of largely elevated geothermal heat flow, which relates to the tectonic and magmatic history of the West Antarctic Rift System in this region, suggesting that this area is coupled to the dynamics of the underlying lithosphere. The collapsing and melting of the West Antarctic glaciers are without doubt a realistic and complex issue. From the current geological surveys, the heat flux of the crust of West Antarctica appears to be accelerating, coupled with frequent earthquakes and volcanoes. Geothermal features such as hot water lakes, thermal rivers, and giant ice caves beneath the glaciers have been continuously discovered. Therefore, it is reasonable to speculate that geothermal effects play a significant role in modifying the vast ice masses, causing glacier sliding, cracking, collapsing, and ultimately melting, and create conditions for a warming climate to melt West Antarctic glaciers. Many studies also suggest that warm ocean water is intruding beneath the glaciers across the grounding line, leading to melting of glacier bottom, which has been generally considered to be associated with human-emitted greenhouse gases, but it is thought here not to be a primary factor for glacier melting, but most likely a secondary factor. It is believed that primary and secondary factors, Milankovitch orbits, black body radiation, solar activities, human activities, and other factors are all interconnected to form a feedback loop between the glacier base and the ocean, or even a positive feedback loop, which further accelerates the collapsing and melting of the west Antarctic glaciers.

Key words: Doomsday Glacier; Thwaites Glacier; Antarctic Circumpolar Current; ocean warming; geothermal heat; subglacial lake; Milankovitch cycles; black body radiation

---

Affiliation Info: [1] 28 Ann Louise Crescent, Markham, ON L3S 0A8, Canada; [2] The Micropaleontology Project, Queens College, 6530 Kissena Boulevard, Flushing, New York, NY, 11367 USA

Article Info: Received: 27 October 2023 / Revised: 11 November 2023 / Accepted: 4 December 2023 / Published Online: 12 December 2023. www.naturalisscientias.com

Authors' Contact Info: Zhang, J: jijun_z@yahoo.ca

Citation: Zhang, J. 2024. What is the primary culprit that causes the "Doomsday Glacier" in Antarctica? *Naturalis Scientias*, 1(1): 61-86. DOI: https://doi.org/10.62252/NSS.2024.1005.

Corresponding Author: Zhang, J, PhD in marine geology, micropaleontology and paleoceanography, professor, petroleum geologist and editor; Email: jijun_z@yahoo.ca

1 Brief background of Antarctica

1.1 Antarctica

Antarctica is the southernmost continent on the earth and belongs to the fifth largest continent with an area of over 14 million square kilometers (Fig. 1). Most of Antarctica is within the Antarctic Circle and surrounded by the Southern Ocean that has been defined as a fifth ocean since 2021 after long-term debate[1].

In over 300 years, people from all over the world have carried out various forms of scientific expeditions and research to unveil the mysteries of Antarctica. As a special geographical region, Antarctica has special significance in terms of science, resources, biology, environment, climate, strategy, and politics. So far, 29 countries have set up 70 scientific research stations there in order to occupy a piece of land for some sort of purposes. Since 1985, the China Oceanic Administration has established four scientific research stations in four different regions in Antarctica, namely the Great Wall Station, Kunlun Station, Zhongshan Station, and Taishan Station. In short, the status of Antarctica in the world is becoming more and more important. It is certain that with the development of sciences, the Antarctic region will be a hotspot for countries to study the earth's climate, oceanic changes, and strategic games in the future.

Figure 1. Antarctica Map (Courtesy of GIS)[2]

Since the late Neoproterozoic (550 million years ago), Antarctica has been part of the ancient land of Gondwana (also known as Gondwanaland). Gondwana also included South America, Arabia, Australia, Africa and India in the remote past. Trees and large animals flourished on ice-free Gondwana 200 million years ago. Today, only petroleum oil, geological formations, coal beds, and fossils that remain in the giant land reflect the warm and distant past of Antarctica. During the Jurassic period (~200 million years ago) of the Mesozoic Era, the ancient continent of Gondwana began to split apart, and Antarctica also went all the way south to the polar region. Until the Late Paleogene, the Antarctic continent was almost completely separated from South America, and a strait, namely the Drake Passage, was formed in between. According to the study of organisms and stable isotopes in the ocean by Miller et al.[3], the ice sheet in Antarctica began in the Early Oligocene (ca 33.9-35 million years ago). This time was also the time that Antarctic Circumpolar Circulation formed (commonly referred to as ACC). Until 18 million years ago (Early Miocene), Antarctica was basically covered by ice sheets, forming what we see today.

Of note, 33.9 million years ago was also the time when the global climate became colder. This cooling of the climate also triggered a large-scale extinction of organisms. We call this extinction period the Late Eocene-Early Oligocene Extinction (also called "Grande Coupure", which means "big break"). This event caused mass extinction of many marine life, aquatic life, and land ancient mammals such as Ungulates (namely Condylarthra), including Perissodactyla, Artiodactyla, and primates. Some people think that this cooling and biological extinction event may

be caused by one or several large bolides hitting Siberia and the Chesapeake Bay in the United States, or it may be caused by multiple volcanic events, which no doubt, also affected Antarctica, part of Gondwana.
The coastline around Antarctica is estimated to be about 17,970 kilometers long. The part west of the Weddell Sea and east of the Ross Sea is West Antarctica, and the rest is East Antarctica, which accounts for most of the entire Antarctica. The East Antarctic Ice Sheet (EAIS) and West Antarctic Ice Sheet (WAIS) are separated by the Transantarctic Mountains serving as a dividing line of a total length of 3,500 kilometers. The WAIS mainly pours into the Ross Sea, Amundsen Sea, Bellingshausen Sea, and Weddell Sea. The Antarctic glaciers are huge and located in the extremely cold polar region. It is impossible to melt them all within tens of millions of years, or even longer, unless the Antarctic plate drifts to low latitudes again.

1.2 Antarctic ice sheet

Except for the northernmost part of the Antarctic Peninsula, about 98% of Antarctica is covered by ice with an average thickness of 2 kilometers and a highest point of 4,776 meters, which is the largest single mass of ice on Earth, approximately equivalent to 90% of the world's ice and 70% of its fresh water. If all the ice melted, sea levels would rise by about 60 meters. Besides the Antarctic Sea ice, land ice covers an area of almost 14 million square kilometers and holds 26.5 million cubic kilometers of ice. A cubic kilometer of ice weighs approximately 0.92 metric gigatons, which implies that the ice sheet weighs about 24,380,000 gigatons. In East Antarctica, the ice sheet rests on a major land mass, while in West Antarctica the ice bed can extend to more than 2,500 m below sea level[4]. Satellite measurements by NASA indicate a still increasing sheet thickness above the continent, outweighing the losses at the edge. The reasons for this are not fully understood, but suggestions include the climatic effects on ocean and atmospheric circulation of the ozone hole, and/or cooler ocean surface temperatures as the warming deep waters melt the ice shelves[4]. The average temperature in a year is as low as -63 °C, and the lowest temperature can reach -89.2 °C.

In order to understand the past, present, and future of the Antarctic Ice Sheet, Frémand et al. mapped Antarctic bed topography and ice thickness for the last 60 years (known as Bedmap1 Bedmap2 and Bedmap3), which is crucial for modeling ice flow and hence for predicting future ice loss and ensuing sea level rise[5]. This data release shall be a valuable asset to Antarctic research and shall greatly extend the life cycle of the data held within it as they declared (Fig. 2).

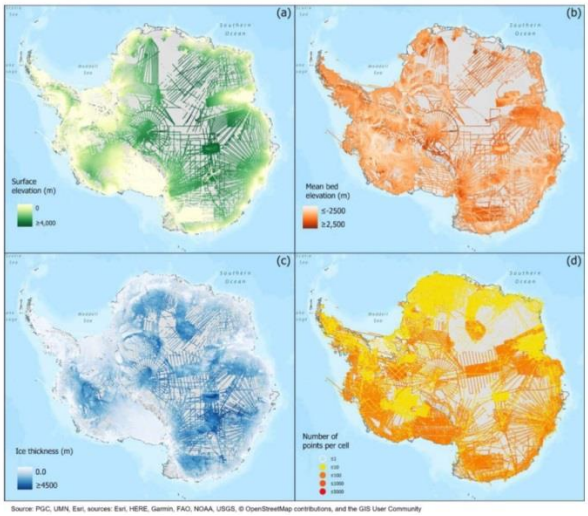

Figure 2. Statistically summarized data points
(a) Mean surface elevation in meters over Antarctica; (b) Mean bed elevation in meters over Antarctica; (c) Mean ice thickness in meters over Antarctica; (d) Number of points per cell used for the calculation of ice thickness; All elevation values in (a-b) are given with reference to the WGS84 ellipsoid[5]

1.3 Antarctic Circumpolar Current

The Southern Ocean plays a fundamental role in global climate. Without continental barriers, it re-distributes climate signals among the Pacific, Atlantic, and Indian Oceans through its clockwise, fast-flowing, energetic, and deep-reaching current, which is termed as Antarctic Circumpolar Current, also called ACC or West Wind Drift, extending from the sea surface to depths of 2,000-4,000 meters, and as wide as 2,000 km. The total ACC traffic in the Drake Passage is estimated to be roughly 135 times the traffic of all rivers in the world combined. Flows in the Indian Ocean were relatively small, while it reaches about 147 Sverdrup (Sv or 147 million cubic meters per second) in southern Tasmania. The lack of any land barricades connecting to Antarctica keeps warm ocean water away from Antarctica, resulting in the continent being able to maintain its massive ice sheet. However, because of the adjacent landmasses, submarine topography, and prevailing winds, the ACC is irregular in width and course. Its motion is further complicated by continuous exchange with other water masses at all depths. The Antarctic Circumpolar Current separates the Southern Ocean from the Atlantic, Pacific, and Indian oceans at 60° S latitude, which roughly coincides with the current's southern boundary[6]. The mean transport of the ACC is estimated at 134 Sv (or 134 million cubic meters per second), while it has been estimated the current's flow through the Drake Passage is as high as 173.3 Sv (or 173.3 million cubic meters per second)[6]. The average velocity of ACC is about 10 cm/s or 0.2 knots to 100 cm/s or 2 knots. The Woods Hole Oceanographic Institution of the United States found that the current velocity is low near Thwaites[7].

In the Pacific and Indian oceans, its northern boundary occurs between latitudes 48°S and 58°S, and its southern boundary extends to 70°S near the coastal Marie Byrd. In the Atlantic Ocean, its northern boundary fluctuates between latitudes 42°S and 48°S, while its southern boundary approaches 60°S.

The ACC encircles three continental capes, Cape Agulhas (Africa), Southeastern Cape (Australia), and Cape Horn (South America). The ACC connects the Atlantic Ocean, Pacific Ocean, and Indian Ocean, and is the main way of communication between them, traveling more than 20,000 kilometers around the pole in about 200 days.

The ACC is set forth to have three fronts and three zones south of the Subtropical Front (STF), which are (from north to south):

- the Subantarctic Zone (SAZ) and the Subantarctic Front (SAF).
- the Polar Frontal Zone (PFZ) and the Polar Front (PF).
- the Antarctic Zone and the Southern ACC Front[8].

Most recently, Giglio and Johnson (2016) located three fronts along dynamic height contours, each corresponding to a local maximum in vertically integrated shear and termed them as the PF, sSAF, and nSAF (from south to north Fig. 3)[9]. The ACC Gyre was first discovered by British astronomer Edmond Halley when he surveyed the region during the HMS Paramour expedition of 1699-1700 HMS Paramore Expedition[10].

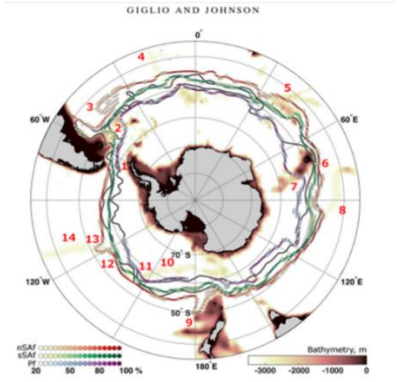

Figure 3. Dynamic height based (DH-based) ACC fronts from gridded Argo data: frequency of occurrence (dots) during 2006–2013 (values smaller than 20% are masked out)

Light blue to purple dots are for the PF; Light yellow to green dots are for the sSAF; Light orange to red dots are for the nSAF; Black lines are, from north to south, the Subantarctic and Polar Fronts described in OWN95; Bathymetry (m) shallower than 3,500 m is shaded from white to dark brown in the background; Numbers (red) are adjacent to some of the main bathymetric features: 1-Drake Passage, 2-Maurice Ewing Bank, 3-Argentine basin, 4-Atlantic Ridge, 5-Southwest Indian Ridge, 6-Kerguelen Plateau, 7-Fawn Trough, 8-Southeast Indian Ridge, 9-Campbell Plateau, 10-Pacific–Antarctic Ridge, 11-Udintsev Fracture Zone, 12-Eltanin Fracture Zone, 13-Menard Fracture Zone, and 14-East Pacific Rise[9]

1.4 The gulf stream and the great ocean conveyor belt

As mentioned above, it is currently recognized that a warm current caused the collapse of the Thwaites Ice Sheet, and the initial source of the warm current is the high-temperature and high-salt Gulf Stream[11]. The Gulf Stream is not an ordinary ocean current, but it is the largest warm ocean current in the world. Most of the Gulf Stream turn sharply to the east and enter the Atlantic Ocean from the Florida Strait of the United States. Due to the effects of Coriolis force caused by the earth's rotation, the Ekman Transport and the Newfoundland underwater large reef (the Grand Bank), the Gulf Stream entering the Atlantic Ocean flows northwards and then moves eastwards across the Atlantic Ocean to the west coast of Europe. This stream finally flows northward into the cold Greenland Sea along the northwest coast of Europe. Its thickness is 200-500 meters with a velocity of 2.05 meters per second (or 7.38 km/hour).

The Gulf Stream is a powerful ocean current that transports 1.5 times more water than the Kuroshio Current in the northwest Pacific Ocean. It delivers up to 30 million cubic meters per second (30 Sv) in the Florida Straits. This ratio increases to 150 Sv as it passes south of Newfoundland, with temperatures ranging from 8 to 19°C (46.4 to 66.2 ^{o}F) and salinities ranging from 35.10‰ to 36.70‰.

The hot and salty Gulf Stream is mainly mixed with deep-water of the Greenland Sea and the southward Atlantic Deep Current (NADW) to form the so-called Great Ocean Conveyor Belt originally created in 1987 by my teacher - Wallace Broecker at Lamont-Doherty Earth Observatory of Columbia University (Fig. 4)[12 & 13], and then goes eastward out of the Weddell Sea, and then merges to the ACC to circulate in the Southern Ocean off Antarctica. Prof. Pettit holds this point of view as well (personal communication, January 4, 2022).

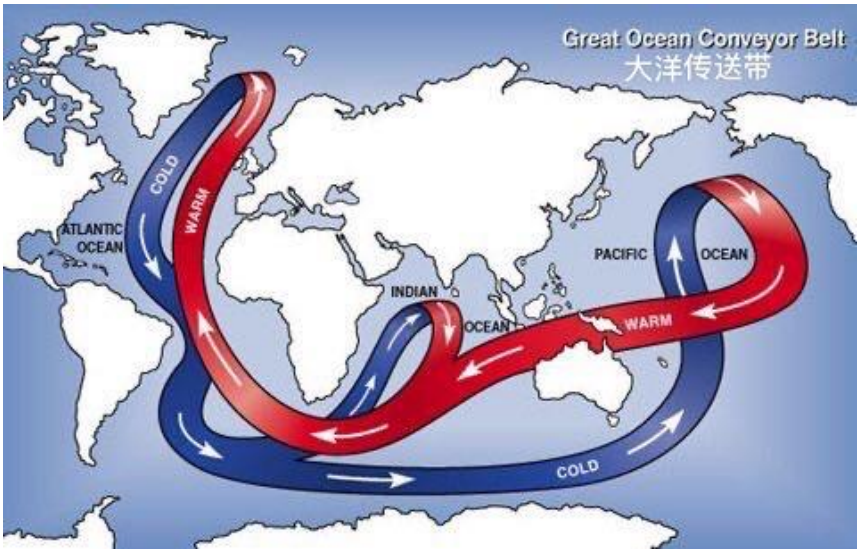

Figure 4. The Great Ocean Conveyor Belt circulates through the three oceans
Red represents warm surface water and blue stands for cold deep water (Courtesy of the Lamont-Doherty Earth Observatory of Columbia University)

2 Are we under "Doomsday Glaciers"?

In West Antarctica, the Thwaites Glacier in the Amundsen Sea is one of the widest glaciers on Earth, with a width of about 120 kilometers, an area of 192,000 square kilometers and a depth of 4,000 meters in the glacier basin, which is similar in size to the state of Florida of the United States. The depth of its grounding line is between 800 and 1,200 meters. Thwaites Glacier is part of the West Antarctic Ice Sheet (WAIS) that covers approximately 3,435,000 square kilometers. Thwaites Glacier is one of the two fastest-moving glaciers (the other is Pine Island Glacier to the east). One of the most important structures supporting Thwaites Glacier is its eastern ice shelf, which supports about 1/3 of the glacier and hinders its rapid flow into the ocean. The ice shelf itself is anchored to an underwater seamount, which keeps its base from being eroded by ocean currents, and thus protects the glacier, making it relatively stable.

Glaciologists, such as Prof. Erin Petitt[14] pointed out at the annual meeting of the American Geophysical Union (AGU21) in 2021 that, according to the latest data, warm currents are invading the eastern ice shelf at the base of Thwaites Glacier. Recent satellite images show that several large cracks (crevasses) have appeared on the ice shelf across the ice shelf. Scientists pointed out that "these weak points are like cracks on the windshield. With just one more impact, the entire surface of the ice shelf will be cracked as spider webs. This ice shelf may also break into hundreds of icebergs". Scientists estimate that if the Thwaites Glacier completely collapsed, global sea level would rise by 65 centimeters, which currently accounts for about 4% of the global sea level rise. Thwaites Glacier is the key to predict global sea level rise as studies suggest. Dr. Karina Tsui[15] also emphasized that the disappearance of Thwaites Glacier may trigger a larger collapse of the West Antarctic ice sheet. If the Pine Island Glacier to the east and the Dotson Glacier.

In addition, the disappearance of the ice sheet and the reduction of the overlying load may bring isostatic rebound, or isostacy/isostatic equilibrium to Antarctica. Because Thwaites and Pine Island glaciers are vulnerable to major retreat, they have been described as the "weak belly" of the West Antarctic Ice Sheet. The flow of both glaciers has accelerated in recent years and is predicted to collapse within a decade after 2021, leading to increased outflow and sea level rise. For this reason, Thwaites Glacier and its ice shelf have been proposed as sites for climate engineering that is the intentional large-scale intervention in the Earth's climate system to counter climate change. In addition, if all the glaciers in Antarctica melt, it shall also cause changes in the inclination of the earth's axis, which in turn shall lead to changes in the climate of the four seasons.

3 What is the primary culprit that caused “Doomsday Glacier”?

In the recent decades, many scientific expeditions from various countries in the world have carried out multidisciplinary comprehensive research in Antarctica in order to understand the current status and future of Thwaites Glacier, especially in West Antarctica. Among them, the most active ones are International Thwaites Glacier Collaboration (ITGC), and NASA ICESat-2 (Ice, Cloud, and Land Elevation Satellite). ITGC Collaboration was organized by scientists from the United Kingdom and the United States with a huge sum of US$50 million in 2018. Under the framework of ITGC, 8 special projects have been set up to carry out scientific research to focus on glaciers, hydrology, ocean currents, water depth, geology, topography, and many other aspects of the Thwaites area. The National Aeronautics and Space Administration (NASA) has been monitoring the dynamic changes of Antarctic glaciers in real time through satellites in recent decades.

3.1 “Doomsday” caused by ocean warming?

A ship-based Thwaites Glacier research project led by Professor Erin Pettit of the University of Oregon in the United States is one of the eight projects, namely the TARSAN project (Thwaites-Amundsen Regional Survey and Network). This project is an integrated study of how atmospheric and oceanic processes affect the behavior and stability of Thwaites Glacier and its adjacent ice shelves in space and time.

In 2021, Prof. Pettit[14] introduced in detail the current status and future of Thwaites Glacier at the Fall Meeting of the American Geophysical Union (AGU21). The Pettit team's research believes that the Thwaites Glacier collapsed for the following three reasons:

- The base of Thwaites Glacier melts. According to their investigations, the melting began in 2004, and has now separated from the underlying seamount, lost its grip (nail point), and opened a channel to communicate with the ocean, causing the bottom of the front of Thwaites Glacier to hang in the air, allowing the oceanic warm current pouring from a huge channel directly into the ocean trough between the continental shelf and the bottom of the glacier without barriers, and forming a circulation that roves under the glacier. The larger the ice surface exposed to the water, the more it melts and the more warm water spews into the ocean, leading to a vicious cycle.
- The intrusion of oceanic water melts the ice base with increasing melting rate with time, especially at the pinning point of ice and rock at the rear end.
- Glacier fragmentation intensifies along the weak zone.

Prof. Helen Fricker at Scripps Institution of Oceanography in San Diego, California has achieved similar results after extensive work over many years (personal communication, Aug., 2023, via email). Pettit believes that the glacier will completely collapse by 2030 due to these three driving forces (Fig. 5).

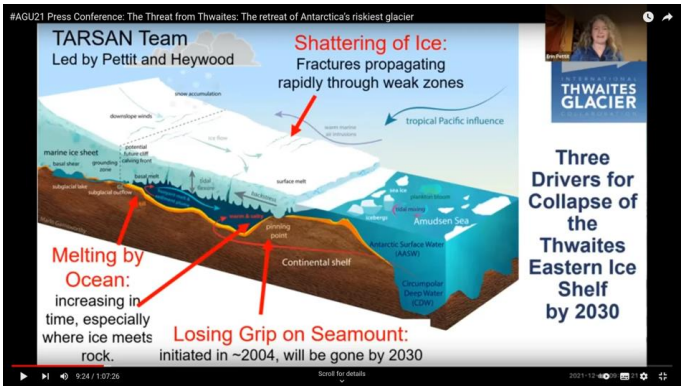

Figure 5. Erin Pettit's Thwaites Glacier collapse situation map (Courtesy AGU21 Fall Meeting, 2021)[14]

In early 2020 NASA announced that they used satellite radar detection technology to discover a huge cave at the bottom of Thwaites Glacier, which is 300 meters high, covers an area of about 40 square kilometers, and can hold 14 billion tons of ice. In January 2020, when some scientific expedition personnel were investigating the glacier, they also discovered a huge cavity with a width of 300 meters inside, indicating that the glacier is undergoing a process of melting from the bottom up. Mooney[16] stated that it is estimated that about 50 billion tons of ice melt each year. The melting of such a huge amount of solid ice will not only cause the global sea level to rise by more than 4% per year but will also further aggravate the overall vulnerability of the Thwaites Glacier.

So far, many scientists[14 & 17-21] have come to agree that the culprit behind Thwaites Glacier's rapid melting is warm currents that infiltrate between the glacier's base and bedrock. Water temperature above 2°C at the bottom of the Thwaites Glacier has been reported.

Satellite data show that Thwaites Glacier has retreated significantly since the 1970s. From 1992 to 2017, the grounding line of the glacier retreated at a rate of 0.6 to 0.8 kilometers per year. In the 1990s, Thwaites Glacier was melting 10 billion tons of ice every year. In April 2021, Prof. Anna Wåhlin of the University of Gothenburg in Sweden[20] used their data of the AUV automatic submersible to map the path of warm currents patrolling under the ice (Fig. 6). According to their calculation, if the inflow energy of 0.8 terawatts (Inflow 0.8TW) is all used to melt the glacier, then in the third trough (T3) in the figure below, the annual mass loss can reach 85 gigatons (850 million tons). According to a tweet by Rob Larter on January 26, 2022 the retreat rate of the Thwaites Ice Rim has been slowing down recently, and it is too early to judge the significance here.

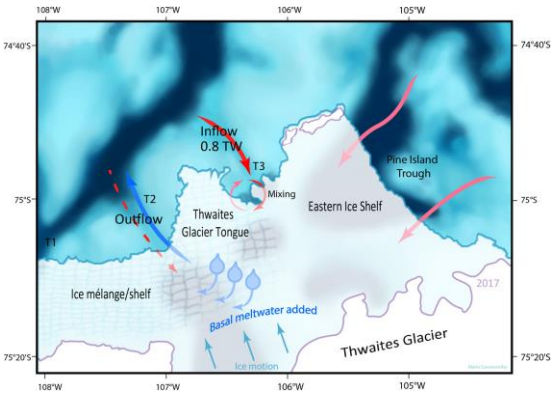

Figure 6. Suggested pathways and mixing area of the water underneath Thwaites ice tongue and eastern Ice Shelf inferred from the measured data

Red arrows indicate the main path of inward flow of warm saltwater, blue arrows indicate outward flow of freshwater containing meltwater, and red dashed arrows indicate possible inflow of warm saltwater. The blue square shading areas represent the deep-water trough, and the purple line represents the grounding line. The two red arrows in the Pine Island Trough indicate that the source of deep water in this area cannot be determined based on current data[20].

3.2 Is geothermal heat a main cause of "Doomsday Glaciers"?

Although most studies believe that the melting of Antarctic glaciers is associated with human-emitted CO_2 and ocean warming, more and more embedded observations and studies show that there may still be room for debate as to whether or not ocean warming is the major or unique cause of Thwaites Glacier's collapse. In early February 2022, I tentatively raised six doubtful points on this issue for discussion as follows[22]:

- As mentioned above, after the ACC combined with the Gulf Stream travels more than 20,000 miles around the pole for more than 200 days, its strength has weakened, and temperature has lowered significantly as shown in the red box in Fig. 7[23]. As seen in the figure, the green colour representing the variation of ACC intensity gets lighter when reaching the sea off Thwaites, indicating that the ACC becomes the weakest, only about 0.09-0.15 meters per second (0.53m/S is one knot), or lower. In this point of view, the erosion on the Thwaites ice shelf should be somewhat weakened, rather than intensified. In other words, it should be stronger in the east and weaker in the west, not the other way around.

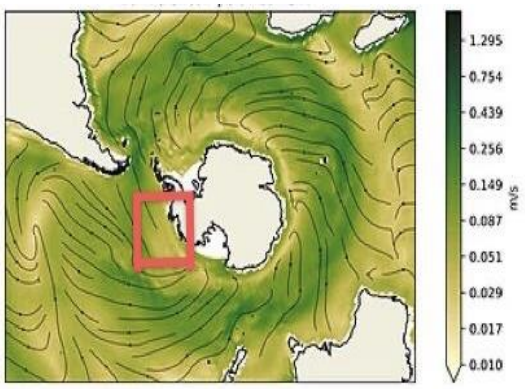

Figure 7. Antarctic Circumpolar Current Velocity Chart (Courtesy of Wikipedia)[23]

- There are 8 sea ice shelves in East Antarctica, among which the Amery ice shelf is the third largest floating ice shelf in Antarctica. Not only are all these ice shelves not eroded and melted by the more powerful ACC ocean currents, but the ice volume is increasing every year. For example, from 2002 to 2010, East Antarctica added 60 billion tons of ice every year. BBC[24] reported that the reason why the eastern ice sheet has not been melted is because the eastern ice sheet is generally located on land with high terrain. However, this does not seem to be the most favorable explanation because the large body of the Amery ice shelf floats in water[25].
- It is indeed widely believed that the collapse of West Antarctic glaciers is related to the rise of carbon dioxide in the atmosphere. Scientists trust that if humans continue to reduce greenhouse gas emissions, the deterioration of Thwaites Glacier can be controlled. If this is the case, then it is difficult to explain why the East Antarctic glaciers are so little affected by carbon dioxide. One might argue with the high elevation of the eastern terrain of East Antarctica, but it obviously is a complex problem, rather than a simple issue.
- According to a Canadian TV station[26], the global warming is weakening ocean circulation (namely Ocean Conveyor Belt). The reason is that because the Arctic and Greenland glaciers melted, a large amount of fresh water has been injected into the Greenland Sea, which reduced the density of the surface water and floated on the surface without sinking, making the Greenland Sea lose the role of a water pump, and thus it is difficult to squeeze out deep water to strengthen the south-moving ocean conveyor belt. A weakening of the global conveyor belt is bound to weaken the Circumpolar Current (ACC), thereby reducing its erosive effect on ice shelves in Polar Regions such as Thwaites. In other words, recent ACC that damages ice shelves should be weaker, not stronger than decades ago. This also contradicts the rapid melting of Thwaites Glacier.
- In early February 2022, I estimated that ambient or "inherent" water temperature beneath Thwaites Glacier could be about 4°C, rather than 2°C as measured AUV submersible[26]. In July 2022, 5 months later, Dr.

David Holland reported 4.45^{o}C under Thwaites glacier on US PBS TV (see below for details). Now, the question is where does the extra 1-2°C come from? This will be explained later in this article. It is also worth mentioning that due to the impact of ice floes and other factors, survey ships and AUV submersibles have not yet entered the ocean trough under the Eastern Ice Shelf (EIS) to measure various elements such as hydrology, which is still far away to the grounding line[20]. This could limit our knowledge of hydrogeology on EIS subglacial troughs.

- As mentioned above, there is an opinion that the warming of seawater under the Thwaites l glacier is caused by the Gulf Stream, but I think this idea may still be unreasonable and doubtful, because it is difficult for us to understand how this high-temperature, low-density Gulf Stream crosses the "firewall" composed by low-temperature, high-density, hugely thick ACC and Antarctic Divergence into the Thwaites Sea area to warm up the sea water there. As we all know, the ACC together with Antarctic Divergence (AD) with low temperature (1-5°C) and high density is 2,000-4,000 kilometres thick and 2,000 kilometres wide (the narrowest point is 800 kilometres at the Drake Passage), while at depth of 400 meters below surface their temperature is consistently low, about 2°C or even less. Therefore, it is conceivable that it is difficult for the Gulf Stream to cross this natural barrier, unless we have convincing data to prove that a large amount of the Gulf Stream pours into the area.

In short, the above six points imply that we may have more alternative possibilities to explain the collapse of the West Antarctic Ice Sheet regarding the driving forces. For this reason, lots of works have been reviewed for this article, including the West Antarctic geology, geothermal activities, ocean circulations, greenhouse effect, Milankovitch cycles and so on.

A year ago, I tentatively raised another alternative possibility that is the relationship between the melting of the "Thwaites Doomsday Glacier" and the heat flux (or geothermal heat flux) [22]. As a matter of fact, after I published the paper, I found that this was not a fresh idea as a few scientists adumbrated it approximately a decade ago[27-29]. As mentioned earlier, Antarctica is divided into East and West Antarctica by the 3,500-kilometer-long and 4,500-meter-high Transantarctic Mountains. Unlike East Antarctica, the geology of West Antarctica is quite complex. Since the 1950s, it has been considered as an expanded tension rift valley with relatively fragile crust. Especially since the late Cretaceous, due to the plate drift, the crust has been cracked and thinned and prone to volcanoes and earthquakes.

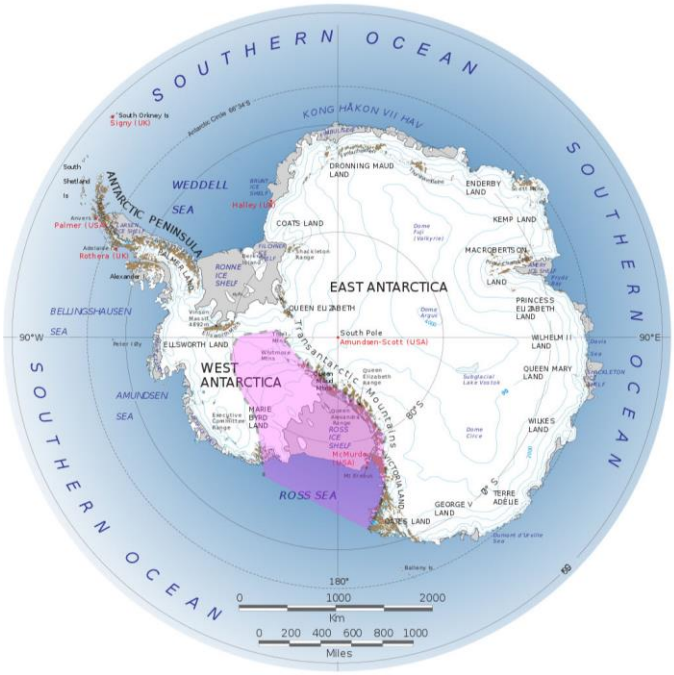

Figure 8. Trend and rift valleys (pink) in the Transantarctic Mountains of Antarctica (Courtesy of Wikipedia)[30].

In 2021, German geophysicist Ricarda Dziadek et al.[31] used aeromagnetic equipment to measure geothermal flux on rocks at the bottom of the Thwaites Glacier in West Antarctica[29], and utilized geophysical data to analyze geothermal flow in the Amundsen Sea region of West Antarctica (Fig. 8). Variations in lithospheric thermal gradients revealed by Curie Depth analysis compiled from a new magnetic anomaly grid. They found that at Curie depths between 10 and 18 km, the 580°C isotherm descends towards Thurston Island. In the middle of the Thwaites and Pope glacier catchment system, the Curie isotherm occurs at shallow depths of 12-16 km and extends all the way to the Amundsen Sea Embayment shelf. The shallower 580°C isotherm is located southwest of the Byrd subglacial basin and the Bentley subglacial trench. The Pine Island Rift valley does not show a significant Curie depth anomaly, but indicates a shallow thermal anomaly to the east. Dziadek et al. also noted that the shallow Curie depth distribution correlates well with volcanic centers, further suggesting elevated crustal heat flow[31].
They measured geothermal heat flow in the range of 50-230 mW/m² (Ø = 86 mW/m^2). Geothermal heat for normal continental crust is 65mW/m^2, while oceanic crust is 103mW/m^2. Obviously, the geothermal heat in the Thwaites area could be more than twice that of the normal oceanic crust. Beneath most of the Thwaites and Bob glacier catchment and drainage areas, there is a high geothermal heat stream stretching on the southwestern side of the Byrd Subglacial Basin and Bentley Subglacial Trench and extending as far as the middle and inner shelf of Amundsen Gulf. In particular, they pointed out that the rapidly receding Thwaites and Bob glaciers are associated with significantly elevated geothermal heat flow, which obviously is related to the tectonic and magmatic history of the West Antarctic Rift System in the region. They also emphasized that the behavior of this vulnerable region of the West Antarctic Ice Sheet is closely linked to the dynamics of the underlying lithosphere. Dziadek et al. also mapped the volcano and Curie depth distribution in this area (Figs. 9 and10)[31]. As seen in the figure below, volcanoes in this area are relatively frequent, and the Curie depth in the rifting area is relatively shallow, generally about 12-10 kilometers below the surface.

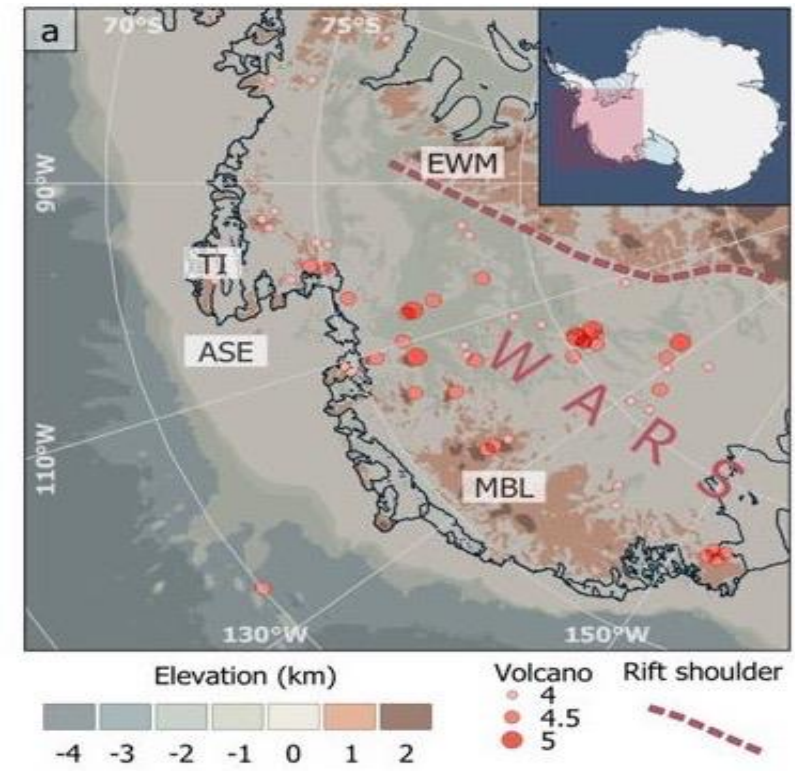

Figure 9. The map shows basement elevations above sea level, rift shoulders of the west Antarctic Rift System (WARS), and volcano locations (red dots, confidence factor of 4 or higher)
EWM = Ellsworth-Whitmore Mountains; ASE = Amundsen Bay; MBL = Marie Byrd Land; TI = Thurston Island. The red dashed line stands for the rift ridge (After Dziadek et al.)[31]

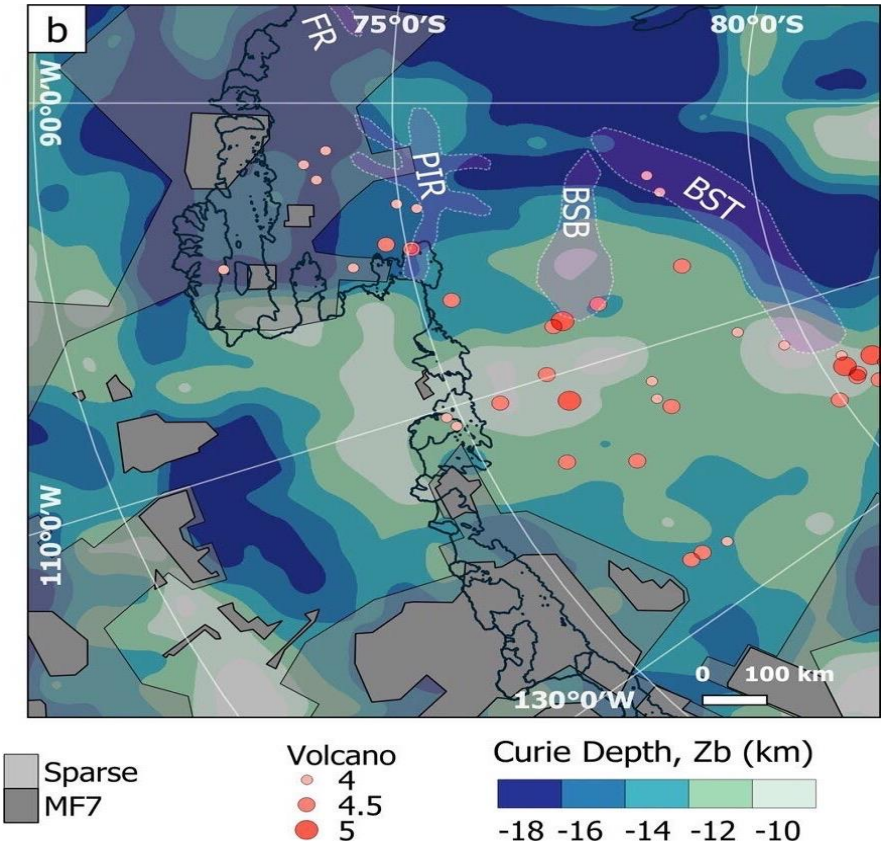

Figure 10. Distribution of Curie depths (Zb km) and volcanic centers (volcanic confidence factors of 4 or higher), indicating shallower Curie depths within volcanic regions
BSB = Byrd Subglacial Basin; BST = Bentley Subglacial Trench; FR = Ferrigno Rift; PIR = Pine Island Rift (after Dziadek et al.)[31]

In 2014, Schroeder et al.[28] studied the geothermal heat flow under the West Antarctic Ice Sheet, and pointed out that the minimum average geothermal flux in the Thwaites Glacier area is about 114 ± 10 mW/m^2, and the high flux area exceeds 200 mW /m^2, which is consistent with magma migration and volcanism in the rift. Thwaites Glacier has a land-sloping bed that extends deep into the interior of the West Antarctic Ice Sheet (WAIS), making it a major component of rapid glaciation. In addition, Thwaites Glacier is also located within the West Antarctic Rift System, a potential low-lying inland extension that could be reactivated. Crustal thinning caused by Cretaceous and Cenozoic rifts in this area can also lead to increased geothermal flux. Given the characteristics of its catchment area, the heterogeneous geothermal flux beneath the Thwaites Glacier may be an important factor affecting the stability of the ice sheet on a local, regional, and continental scale[28]. Prof. Tim Stephens at UC Santa Cruz, USA also believes geothermal heat melts the ice sheet of West Antarctica[29].

In addition to the rift valleys and volcanoes, earthquakes are widespread and recently active along the edge of West Antarctica, from the west of the Ross Sea all the way east to the tip of the Antarctic Peninsula (Fig. 11). In addition, researchers at the University of Chile have used automatic detection techniques to record more than 32,000 earthquakes in the Bransfield Strait, which is located between the South Shetland Islands and the Antarctic Peninsula from the end of August to the beginning of December 2020[32]. More detailed studies could reveal an even larger number. The greatest activity was seen mostly in September, with more than one thousand quakes per day. 32,000 earthquakes occurred in just over three months on the island, indicating that the geological structure here is very active. The thermal springs along the beaches of Pendulum Cove in Deception Island reach temperatures of over 158 °F/70 °C.

Figure 11. Earthquake distribution map of the west Antarctica's fringe
(After http://www.chinanews.org/wenhua/lishi/18934.html)[22]

It is particularly worth mentioning that in 2020, Artemieva and Thybo's research[33] showed that throughout the west coast of West Antarctica, plate subductions were active until the mid-Cretaceous, and then gradually stopped towards the tip of the Antarctic Peninsula. Therefore, they believe that the entire West Antarctica is a back-arc basin system with volcanic arcs on both sides, similar to the Japan Sea today, rather than the continental rift system that has been traditionally explained for sixty years. As we know, the crust of the plate subduction zone is quite unstable, for example, the subduction zone around the Pacific Ocean has frequent volcanoes and earthquakes. However, for the Thwaites "Doomsday Glacier", no matter if it is a rift system or a subduction zone, its function of warming the crust is similar. According to the research of Van Wyk de Vries et al., there are 138 volcanoes in this area, 91 of which are newly discovered, with many active volcanoes[34].

The Vostok Lake in East Antarctica is a prime example, which covers an area of 12,500 km^2. Drilling shows that there is a huge subglacial lake under the ice sheet of more than 4,000 meters (Fig. 12). The lake is 670 meters deep, with numerous bacteria, marine diatoms, and other microorganisms in it. There is a normal fault in the bedrock of the lake, along with geothermal fluid overflows, which is melting the overlying glacier[35]. Dating shows that the ice layer at the bottom of the lake has a maximum age of 420,000 years, while the ices older than 420,000 years are completely missing, which is not in line with the historical record of the formation of Antarctica 34 million years ago. Therefore, it can be speculated that the glaciers at the bottom have been melted by geothermal lake water. It can also be seen from the concave deformation of the ice layer in the overlying seismic section that the ice layer over the lake has been continuously falling. This phenomenon is estimated to be more severe in West Antarctica. Based on the available data, we can see that West Antarctica has high geothermal heat and the glaciers melt quicker, while East Antarctica has low geothermal heat, and the glaciers melt slower. Their relationships are obviously proportional. This should not be an accidental phenomenon, perhaps an inevitable trend.

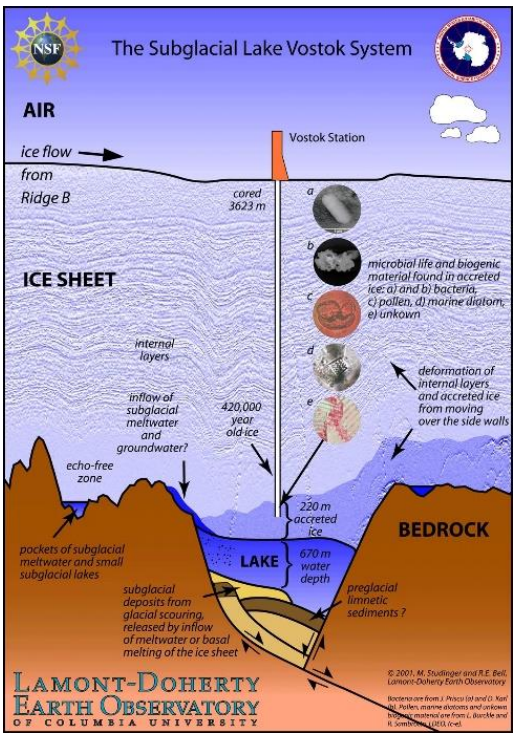

Figure 12. The Vostok lake, 4,000 meters below the east Antarctic ice layer, has geothermal heat released to melt the overlying glaciers (Courtesy of David Funkhouser, 2012)[36]

In addition, a research team led by geophysicists Robin Bell and Michael Studinger from the Lamont-Doherty Earth Observatory of Columbia University, USA discovered four large, interlocked subglacial lakes a few kilometers beneath the surface of EAIS. They found that ice streams linking to the lakes are large, fast-flowing within ice sheets, which transport land-based ice and meltwater to the ocean. Their co-author, a physical scientist Christopher Shuman in the Cryospheric Science Branch at NASA's Goddard Space Flight Center concluded that "This connection of major subglacial lakes to the accelerated pace of ice movement deep in Antarctica's interior is a key of the ice sheet stability puzzle[36 & 37].

Regarding West Antarctica, it is speculated that because the crust of the rift valley has been oppressed by the overlying thick glaciers for a long time, the already unstable crust has become more active and stimulated (or re-activated) the upwelling of hydrothermal fluids to form subglacial hot springs and geysers. Hot springs and geysers are scattered all over the earth (Figs. 13 and 14). For example, there are 799 hot springs in Iceland (while active volcanoes are only 40-50), and 128 hot springs in Taiwan (volcanoes only 20). In China, there are more than 4,000 hot springs based on the temperature over 25°C (volcanoes only 600). In the Deception Island a number of hot springs are erupting. This can explain that the number of hot springs can far exceed that of volcanoes in the same area. It can be deduced from this that there is a great possibility of hot springs and geysers in the West Antarctic Rift Valley where 138 volcanoes have been discovered. Volcano hotspots were also reported in the Ross Sea and Victoria Land[38]. According to the proportion of volcanoes in Iceland, Taiwan, and mainland China, it is conservatively estimated that there may be no less than 300 hot springs in this area. The subglacial hot springs, lakes or geysers as well as volcanoes would provide steady heat flow damage to overlying glaciers directly more than any other sources of heat. This local subglacial phenomenon is still difficult to discover by aerial surveys and satellites. An American professor recently said that so far, we know very little about the landforms under the Antarctic ice, far less than we know about the landforms of Mars. This is a regrettable but elusive deficiency.

Figure 13. Deception Island hot springs, Antarctica (Photos courtesy of Wothe)[39]

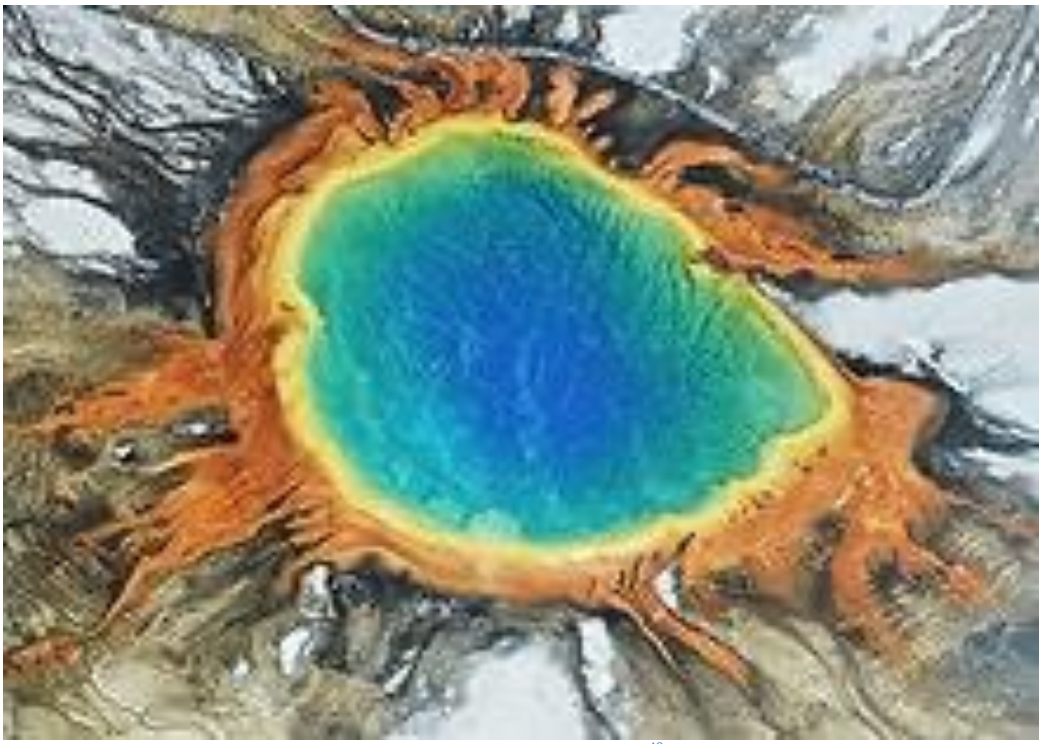

Figure 14. Yellowstone National Park, USA (Courtesy of Wikipedia)[40]

Seroussi et al. determined that mantle plumes in West Antarctica agree with presence of the ice sheets[41]. Their seismic images support the plume hypothesis as the cause of Marie Byrd Land (MBL) volcanism, which may more than double the geothermal heat flux above nominal continental values. Their works also show that mantle plumes have an important local impact on the ice sheet, with basal melting rates reaching several centimeters per year directly above the hotspot.

Just one month later after Zhang's paper published in Feb. 2022[22], geophysicist Artemieva also reported that the rate of Antarctica ice basal melting is significantly underestimated[42]. She added that the area with high heat flux is double in size (>100 mW/m^2) in almost all of West Antarctica (Fig. 15), while the amplitude of the high heat flux anomalies is 20–30% higher than in previous results. Extremely high heat flux in West Antarctica may promote sliding lubrication and result in dramatic reduction (melting) of ice sheet basal by high mantle heat. The results form the basis for re-evaluation of the Antarctica ice-sheet dynamics models with consequences for global environmental changes. With NASA's Ice, Cloud, and land Elevation Satellite 2, or ICESat-2, scientists were able to precisely map 2 subglacial lakes in the middle of West Antarctica[43-52]. Fricker also reported warm lakes beneath Antarctic ice[53].
We already have evidence that volcanic eruptions could cause glaciers to melt, as observed in the East Volcanic Zone of Iceland during the period between February and May, 2010, where the volcanoes caused Eyjafjallajökull glacier melted[53].

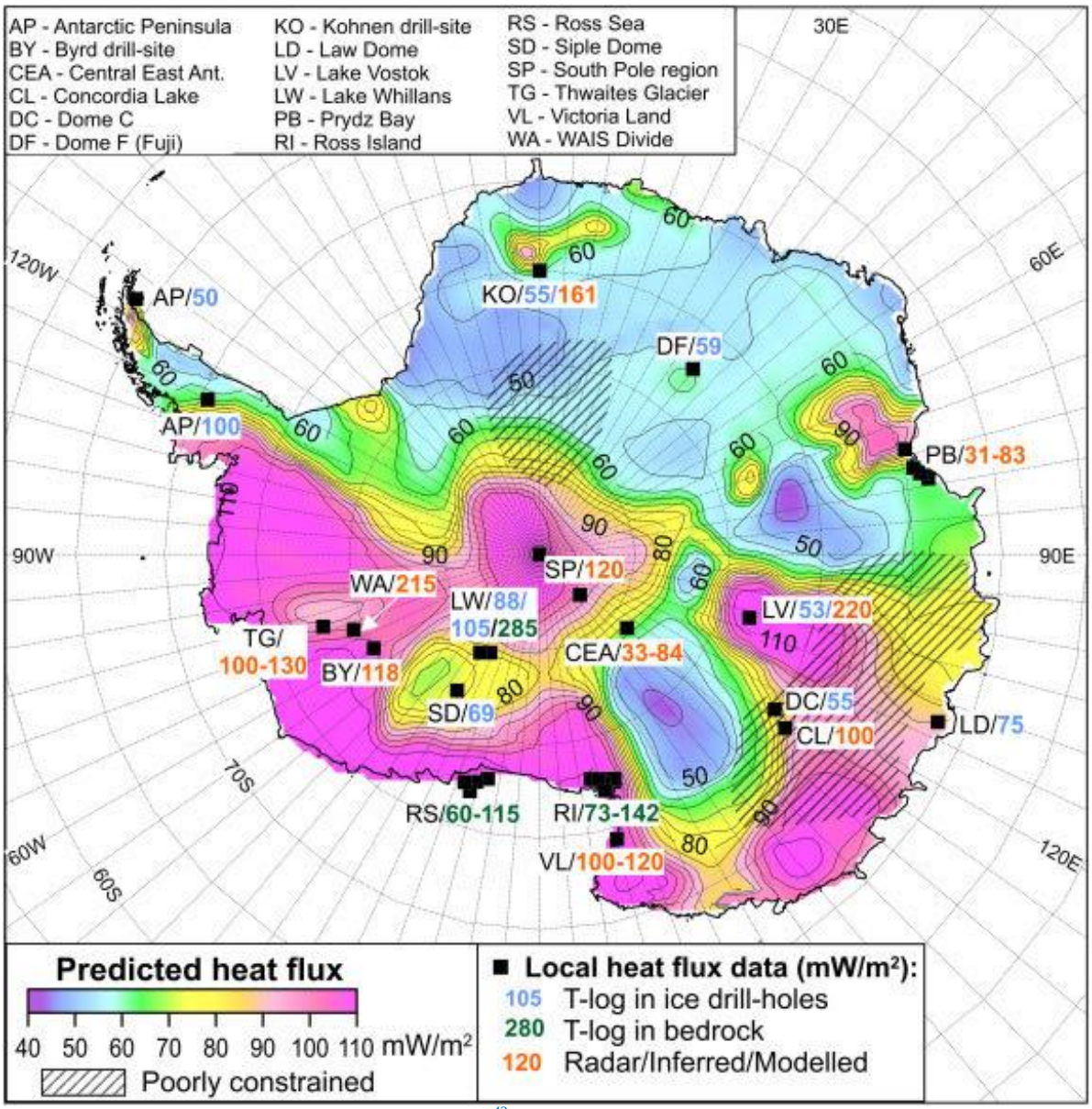

Figure 15. Predicted geothermal heat flux in Antarctica[42]

In fact, high geothermal heat flow beneath Thwaites Glacier has been frequently reported recently. In 2021, Wegener suggested a third factor that is responsible for the ice losses of Thwaites Glacier, although scientists attributed these changes to climate change and warm water masses[54 & 55]. Dziadek et al. concluded that there is a strikingly large amount of heat from the interior of the Earth beneath the ice, leading to the sliding of the overlying glaciers[31]. The Scientific Committee on Antarctic Research pointed out that "with Curie depth analysis based on a new magnetic anomaly grid compilation, we reveal variations in lithospheric thermal gradients. We show that the rapidly retreating Thwaites and Pope glaciers in particular are underlain by areas of largely elevated geothermal heat flow, which relates to the tectonic and magmatic history of the West Antarctic Rift System in this region. Our results imply that the behavior of this vulnerable sector of the West Antarctic Ice Sheet is strongly coupled to the dynamics of the underlying lithosphere"[56]. In addition, Thwaites Glacier was found to be heating itself underground the vast ice sheet of Antarctica because of geothermal activity[57 & 58].

On July 25, 2022, US PBS reported that Professor David Holland of New York University measured temperature 40°F, equivalent to 4.45°C beneath Thwaites Glacier in Amundsen Sea using "Shackleton Bomb" and probe (Fig. 16)[59]. The warm sea water with cooler fresh water from the glaciers creates turbulence under the glaciers, which could accelerate the melting of ice masses. Professor Holland found that the warmest water anywhere in Antarctica is under Thwaites. The team did not explain where the abnormal high temperature comes from, but it seems to be associated with geothermal heat beneath Thwaites, which perfectly explains my speculation mentioned earlier.

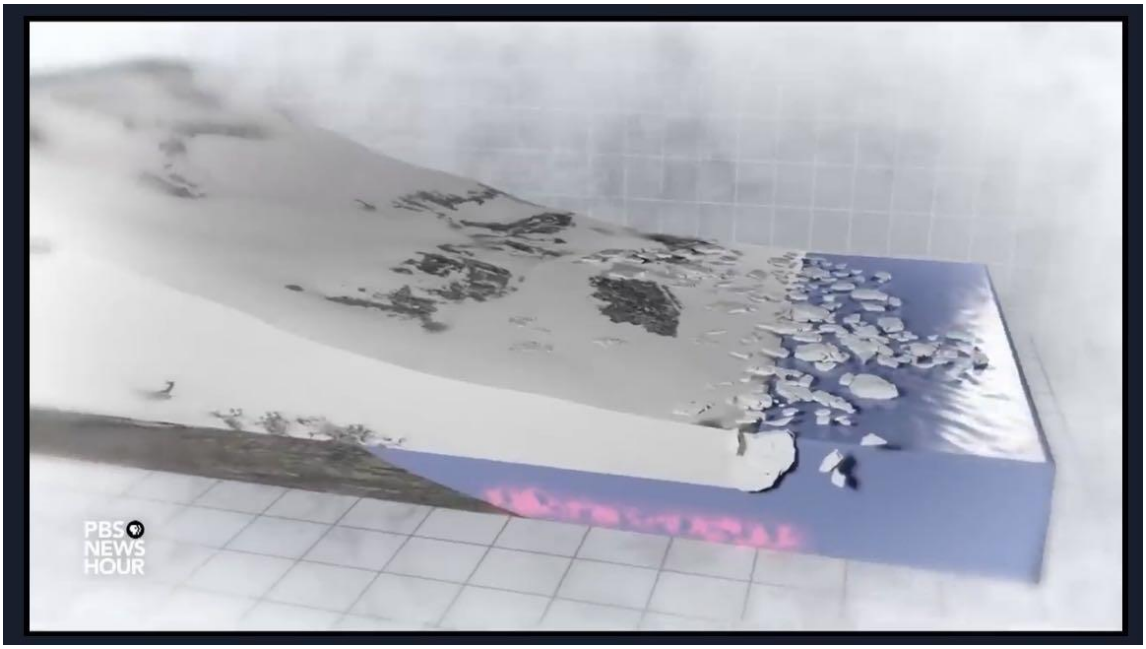

Figure 16. Thwaites glacier is being "cooked" by hot water (red color) at the bottom.
The screenshot is from PBS NewsHour video[59]

It may be imagined that the "hot water" at the bottom could have three potential sources: warm water from open ocean; geothermal flow from crust underneath; and hot streams associated with geothermal flux under glaciers.

SURVOSTRAL Program Team led by Prof. Matthis Auger conducted a 25-year observation in the water area between Hobart, New Zealand and French Antarctic scientific station - Dumont D'Urville (DDU) to study the temperature variations of the upper 800 meters across the Southern Ocean (Fig. 17). Auger et al. (2021)[60] discovered that the subantarctic waters and subsurface subpolar deep waters have warming trends interannually, which are 0.29 ± 0.09°C per decade and 0.04 ± 0.01°C per decade, respectively, while the near-surface subpolar waters trend to cool -0.07 ± 0.04°C per decade. According to the observations, the warming of the subantarctic and subsurface subpolar deep waters are minor, especially the latter. Dr. Jean-Baptiste Sallée made a similar discovery with inhomogeneous temperature variations of different water masses[61]. Fig. 17 shows clearly that the temperature of the Lower Circumpolar Deep Water (LCDW) from 0 to 800m ranges from ~1°C to -2°C south of 65°S latitude, which is

not in agreement with 4.45°C hot water detected under Thwaites Glacier, although it may have a trend towards warming in a long-term time scale.

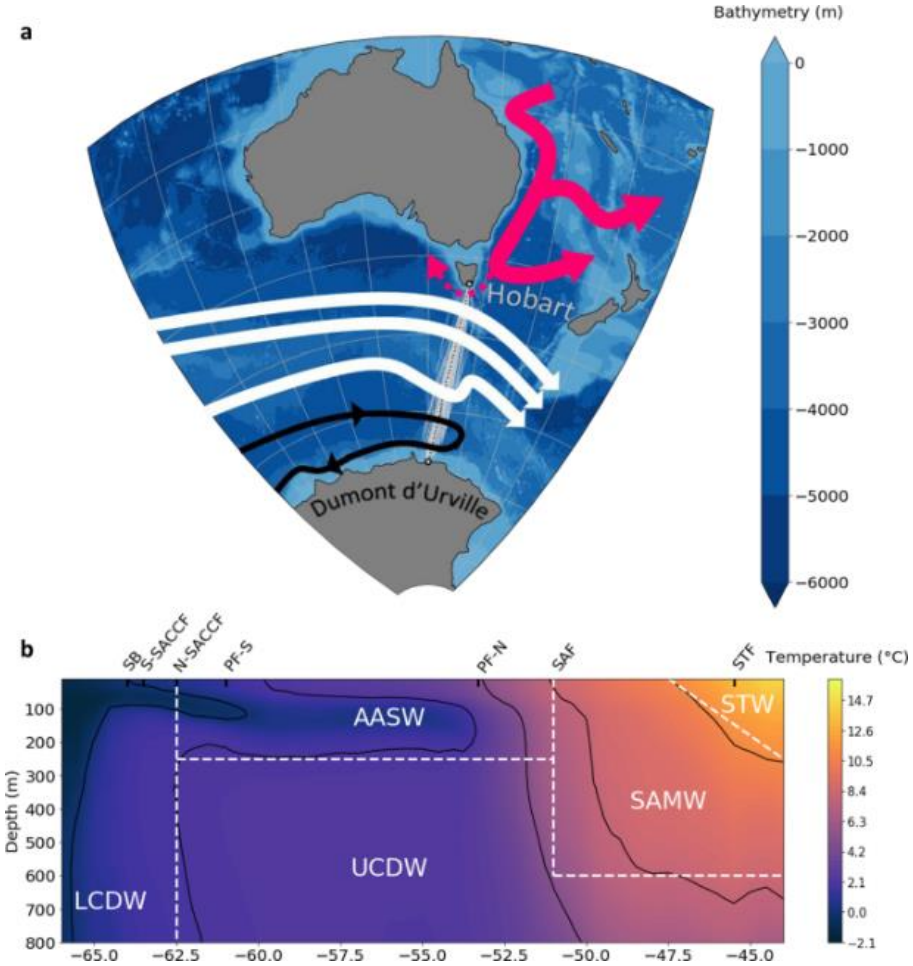

Figure 17. SURVOSTRAL program transects and summer mean temperature section
a: SURVOSTRAL observations over 25 years between Hobart and Dumont D'Urville (DDU), and bathymetry of the region. The mean trajectory is dashed black. Data used in this study is gray. A schematic circulation is represented. White, black, and red arrows are respectively the Antarctic Circumpolar Current, the Antarctic Slope Current and Australian-Antarctic Basin gyre, and the East Australian Current. **b:** 25-year average of the summer (NDJF) temperature sections. Average position of the fronts (SB: Southern Boundary; S-SACCF: Southern Branch of the Southern Antarctic Circumpolar Current Front; N-SACCF: Northern Branch of the Southern Antarctic Circumpolar Current Front; PF-S and PF-N are the Southern and Northern branches of the Polar Front; SAF: SubAntarctic Front; STF: SubTropical Front) and principal water-masses positions are indicated (LCDW: Lower Circumpolar Deep Water; UCDW: Upper Circumpolar Deep Water; AASW: Antarctic Surface Water; SAMW: SubAntarctic Modal Water; STW: SubTropical Water). Black contours show the mean isotherms[60]

The sea surface temperature (SST) of Antarctic Polar Front (APF) ranges from 3 to 5°C and the 2°C subsurface temperature minimum at 200 m[62], while in south of APF, average SST is less than 2°C (Fig. 18)[8 & 63]. According to Freeman and Nicole S. Lovenduski, SST at the PF ranges from 0.6 to 6.9 °C, reflecting the large spread in latitudinal position[64], similar to the results of Civel-Mazens et al.[62]. In the zone between the Southern Front and the Antarctic continent. SST poleward of 65° S is about -1.0°C[8]), essentially in agreement with Matthis Auger et al., who reported the temperature is from ~1 °C to -2 °C south of 65° S latitude[60]. If we assume that the temperature of the subsurface subpolar deep waters increases 0.04 ± 0.01 °C per decade, then we should get temperatures magnified 4 times since 1984, which makes 0.16 ± 0.04 °C for subsurface subpolar deep waters, while the temperature of the near-surface subpolar waters should become -0.28 ± -0.16 °C (−0.07 ± 0.04 °C per decade x 4 decades), which is colder than 4 decades ago. If we add the "inherent or ambient" 2 °C in 1984 using Beacon's data, we will get 2.16 °C (2 °C + 0.16

°C) and 1.72 °C (2 °C ±0.28 °C), respectively. From this calculation, it can be seen that the above-calculated temperatures do not match the temperature under the Thwaites Glacier as well.

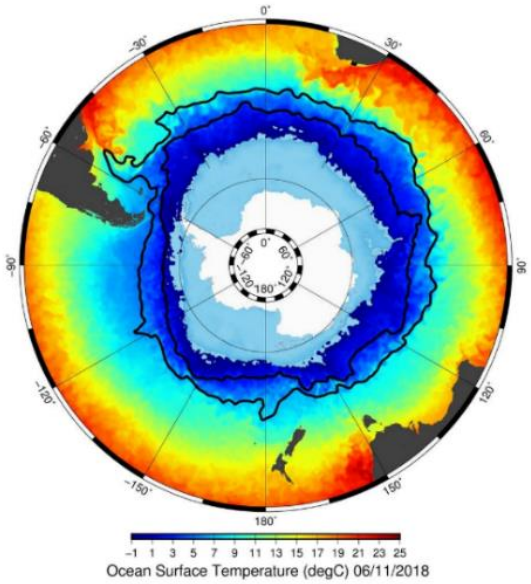

Figure 18. Map of the ocean surface temperature as measured by satellites and analyzed by the European Copernicus Marine Services
The sea ice extent around the Antarctic continent for this day appears in light blue. The two black lines indicate the long-term position of the southern and northern front of the Antarctic Circumpolar Current, showing that the ACC temperature is predominantly lower than 2 °C[63]

It is well known that there is a zone south of Polar Front, called Antarctic Divergence, where the low-temperature and high-density water dives to a depth of thousands of meters below, which acts like a giant firewall to block the southward high-salt, high-temperature, and low-density water of the Atlantic, Pacific and Indian oceans from crossing the Antarctic Divergence. Instead, it forces the southward currents to upwell to the ocean surface along the Antarctic Divergence front at a depth of 2,500 meters and then mix with surface icy waters. Therefore, theoretically speaking, the southward warm waters neither have chance to invade the sea areas under glaciers, including the Thwaites Glacier, nor cause significant seawater warming there.
Furthermore, the rocks under the glacier should also be a kind of black body, and if they are black bodies, they should radiate heat (Fig. 19). Its radiation situation can be expressed by the following diagram and equation.

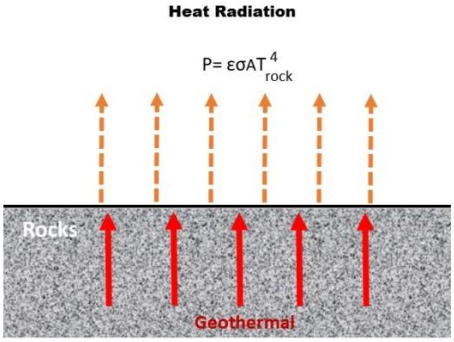

Figure 19. Heat transfer and Stefan-Boltzmann Law
ε is emissivity, σ is Stefan-Boltzmann constant ($5.6703*10^{-8}$ watts/Wm^2K^4), P is power radiated (watts), A is surface area (m^2), T is rock (or black body) kelvin temperature(k)

Similarly, according to the Stefan-Boltzmann Law, the energy of geothermal heat that diffuses to the ground in West Antarctica would also be amplified when it enters the glacier, which may cause the overlying glacier to become unstable, melt, or even slide. This instability brings opportunities for accelerating the melting of West Antarctic glaciers. We thus could speculate that this is one of the reasons for the differential melting of West Antarctic and East Antarctic glaciers.

3.3 Are anthropological greenhouse gases horrible?

There is no doubt that carbon dioxide plays an important role in climate change. NASA scientists have found that the temperature in the troposphere of the atmosphere is increasing, while the temperature in the stratosphere is decreasing (Fig. 20).

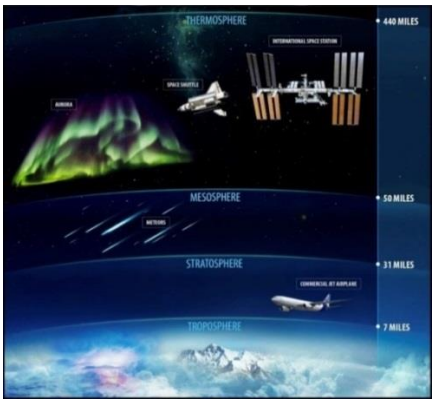

Figure 20. Earth's atmospheric layers. NOAA / Yale Environment 360[65]

A new study reaffirming that global climate change is human made also found the upper atmosphere is cooling dramatically because of rising CO_2 levels[65]. Scientists are worried about the effect this cooling could have on orbiting satellites, the ozone layer, and Earth's weather. This phenomenon has been explained to be caused by greenhouse gases emitted by humans[66]. Fig. 21 shows that in recent years gross carbon dioxide in the air has indeed increased over the past decade[66 & 67]. Current human emissions of carbon dioxide are 100 ppm higher than 50 years ago[68]. If all 100 ppm is converted to temperature, it would cause 1°C rising in global temperature. However, it's still unclear what critical role a 1 ^{o}C variation will play exactly in Antarctic glaciers and the Southern Ocean.
As Fig. 21 shows, both global temperature (colored bars) and atmospheric carbon dioxide (gray line) increased more slowly during the first half of the observational record in the late nineteenth and early twentieth centuries. Atmospheric carbon dioxide levels rose by around 20 parts per million over the 7 decades from 1880–1950, while the temperature increased by an average of 0.04 °C per decade[69].

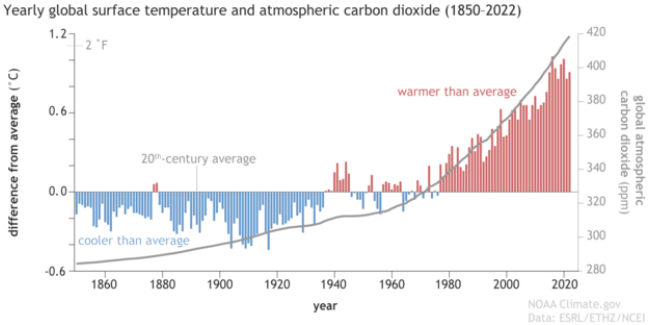

Figure 21. Yearly temperature compared to the twentieth-century average
(red bars mean warmer than average blue bars mean colder than average)
From 1850–2022 and atmospheric carbon dioxide amounts (gray line): 1850-1958 from IAC, 1959-2019 from NOAA ESRL. Original graph by Dr. Howard Diamond (NOAA ARL) and adapted by NOAA Climate.gov. (Courtesy NOAA)

The greenhouse effect has been known since the first industrial revolution (1760-1840) with the invention of steam engines and the utilization of coal. The term greenhouse effect was initiated by French mathematician and physicist Joseph Fourier in 1827[70]. It was reasoned that there must be some balance between incoming and outgoing energy to maintain a fairly constant temperature[66].
Within any given decade, however, the temperature bounces around between warm and cool years. The warmest years are usually El Niño years, when the eastern and central tropical Pacific is warmer than average. The coldest years are generally La Niña years, when that same part of the tropical Pacific is cooler than average. The good news is that the new updates to global CO_2 emissions in the GCP substantially revised scientists' understanding of global emissions trajectories over the past decade. The new data shows that global CO_2 emissions have been flat – if not slightly declining – over the past 10 years[71]. However, falling land-use emissions have counterbalanced rising fossil CO_2 emissions, and there is no guarantee these trends will continue in the future. It is evident that the greenhouse effect can change the atmospheric pressure, which, in turn, may stimulate stronger trade winds, leading to generation of El Nino and La Niña, which cause instability of global climate.
It cannot be ignored that the activities of the sun or changes in the solar system could result in frequent changes in the trade winds, El Nino and La Niña. The importance of the two stars, the Earth and the Sun, is self-evident. Almost all the energy of the earth is supplied by the sun. The sun plays a decisive role in the impact of the earth's external environment. If anything happens to the sun, the earth would not be able to escape, and even the entire solar system will be impacted because the sun is closely related to the earth no matter what[72].

3.4 Black body radiation – should we be concerned?

Although our planet - Earth is not a perfect black body, it can be considered as a black body like other celestial bodies in the universe and almost all objects. Black body emits invisible light with a longer wavelength - infrared light, which we call "Black Body Radiation"[73]. Black body radiation plays a very important role in the "greenhouse effect". If the infrared rays emitted by the black body are trapped by greenhouse gases (CO_2, CH_4, N_2O, O_3, CFC, and water vapor), it will not be emitted further into the stratosphere or beyond the stratosphere, instead it would only stay in the troposphere, which will amplify the greenhouse effect.
It is worth mentioning that O_2, H_2 and N_2 are not considered to be greenhouse gases because they are dipole-moments with value "zero".
The following is a simplified diagram of blackbody radiation of the Earth acting as a blackbody according to the Stefan-Boltzmann Law (Fig. 22). The equation tells us that the energy emitted is proportional to T^4 (T to the power of 4).

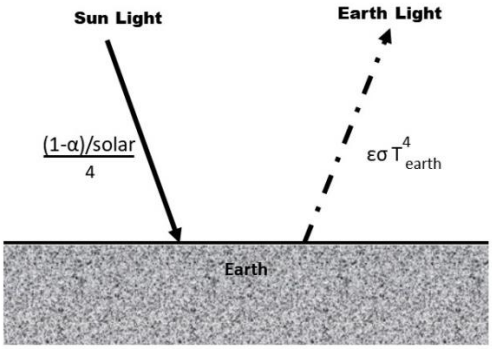

Figure 22. An energy diagram for Earth with no atmosphere, just a bare rock in space
α is albedo, ε is emissivity, σ is Stefan-Boltzmann constant, T is Earth (or black body) kelvin temperature (k) (re-drawn)[74]

3.5 Constructions – another punch in the gut?

In addition, due to the inflated population on the earth (currently ~8 billion), we not only face food, energy and emissions problems, but also encounter housing and construction issues. As we know that lofty buildings either modify the landscape or increase the surface area of Earth. Without doubt, buildings with black bodies will emit

more infrared light, because Stefan-Boltzmann's Law tells us that black body radiation is proportional to surface area. We might express it with the following equation:
$P=\varepsilon\sigma\ (A_C T^4_{building} - A_L T^4_{ambient})$

This equation should be able to calculate extra energy radiated by buildings. In the equation, P is power, ε is emissivity, σ is Stefan-Boltzmann constant, A_C is surface area of construction, A_L is land surface area of a construction range, and T is temperature (k) of "black body". It can be seen from the equation that the emitted energy is proportional to A and T^4 (T to the power of 4), that is to say, the larger T, the greater the energy emitted[70]. Although we are still not clear how much it contributes to climate change, but it is believed that it will alter climate change to some extent.

3.6 Does Milankovitch orbit matter?

Another interesting thing is that according to the EPICA ice core drilled in an Antarctic glacier, it was found that over the past 800,000 years, the alternation of glaciers and interglaciers has followed Milankovitch's orbit - eccentricity cycle[75], which is 96,000 years per cycle (Fig. 23).

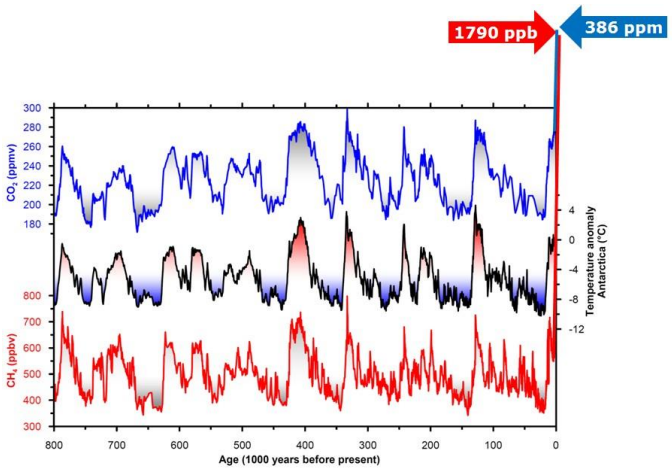

Figure 23. Variations of temperature (from present day mean temperature, black), atmospheric carbon dioxide (in part per million by volume, blue) and methane (in part per billion per volume, red) over the past 800,000 years, from the EPICA Dome C ice core in Antarctica. Modern values (of 2009) of carbon dioxide and methane are indicated by arrows (Credit: Centre for Ice and Climate, University of Copenhagen. Re-used with permission)

From Fig. 23 above, it is obvious that we are currently located at a somewhat high position of eccentricity, equivalent to a warm period. Based on the comparison with carbon dioxide in the figure, the variations of CO_2 in the atmosphere are positively correlated with the eccentricity cycles, which is carbon dioxide increases as the temperature rises and decreases as the temperature drops. This is because lower sea temperatures absorb more atmospheric carbon dioxide. It was estimated that colder ocean temperatures would account for about half the decrease in CO_2 during the last glacial maximum -- or peak of the last ice age[76]. During warm phases, the difference in ocean surface temperatures between the high latitudes and the mid-latitudes is significant. As warmer water moves toward Antarctica and begins to cool, the lost heat goes into the atmosphere, increasing the ocean's potential to soak up CO_2[76 & 77].
Therefore, we have reason to believe that the carbon dioxide emitted by humans is superimposed on the carbon dioxide produced by high temperatures. In other words, current climate change should be attributed at least to the dual factors of eccentricity cycles and human carbon dioxide emissions. The result of the dual factors is enhancing the greenhouse effect and amplifying global warming.
The eccentricity of the Earth's orbit is currently about 0.0167. Over hundreds of thousands of years, the eccentricity of the Earth's orbit varies from nearly 0.0034 to almost 0.058 as a result of gravitational attractions among the planets[78]. We are currently still in a transitional phase to an extreme low point to some extent, and it will take another ~30,000 years to return to the lowest point.

3.7 Solar system and cosmic blast – why we worry?

In addition, activities on the sun's surface, such as sunspots, solar flares, and coronal mass ejections, will also have long and short-term effects on the earth's climate that cannot be ignored. Coronal mass ejections and solar flares are extremely large explosions on the photosphere, which may release as much energy as a billion megatons of TNT just in a few minutes. When sunspots are active, more solar flares shall create stronger geomagnetic storm activities for Earth. Scientists found that when the sun entered "quiet" mode without sunspots, solar flares and coronal mass ejections, termed the Maunder Minimum during 1645-1715, the "Little Ice Age" occurred over parts of Earth. Sunspots have cycles about every 11 years on average from maximum to minimum, which would bring cyclic influences on Earth's climate to some extent[79].

Cosmic blast could be another factor affecting climate. For instance, on Dec. 27, 2004, the magnetar SGR 1806-20 (also called neutron star) located in the constellation Sagittarius, 42,000 light-years away from the earth, blasted a starquake with Richter scale 32 and created a serious impact on the earth's ionosphere, ozone layer and atmosphere with its electromagnetic storm[80].

3.8 Natural methane - another Old Nick to bother our climate?

When we talk about the global warming, most of us usually think of carbon dioxide because it has the highest concentration in the atmosphere. However, the greenhouse gases that warm up the climate are not just carbon dioxide (CO_2), but also include methane (CH_4), nitrogen oxides (N_2O), O_3, and fluorinated gases (HFCs, HCFCs and SF_6). As it is well known that methane is the second most important gas contributing to the global warming, as it is 25 times more than carbon dioxide in warming power.

The methane can be produced not only by human and livestock, but also by nature. This section merely focuses on the potential impact of natural methane gas on global warming.

Three years ago, Thurber et al. discovered methane associated with microbes in marine sediments is leaking from an underground reservoir into the ocean, and possibly into the atmosphere in the Ross Sea, West Antarctica for the first time, which potentially leads to the deterioration of global warming[81].

Today, we know that more than half of the global methane emissions are caused by human activities, but a large part is still stored in the permafrost and in the seabed of major oceans. It was estimated that Antarctica contains about a quarter of earth's marine methane. Methane leaks have been discovered all over the world, particularly in the Arctic Ocean[82]. If this methane leaks on a certain scale, it without a doubt will seriously threaten the global climate.

In addition, volcanic activity could be another source of methane, no matter on the land or in the ocean. For instance, Pandora Dewan reported that at the end of the last Ice Age, methane was spewed from a submarine volcano at the bottom of the Arctic Ocean, likely formed as a result of a catastrophic burst of underwater methane[83].

At present, there is no obvious evidence to show that the methane in the Ross Sea has increased the temperature of seawater and atmosphere, but it is believed that as the quantity of methane increases, sooner or later it will have impact on the water and air temperature in the region to some extent, as seen in the Arctic Ocean today, where the temperature rising is 3-4 times higher than in the other areas.

4 Conclusions

From the perspective of global climate change, the CO_2 emitted by human beings in recent decades is about 100 ppm, which is equivalent to ~1°C when converted into temperature. Whether or not 1°C alone could lead to today's "extreme heat" instability to collapse West Antarctic glaciers may be still debatable. In my opinion, it may be considered to have multi-punches in the gut, for example, geothermal fluids, greenhouse gases, earth orbit, oceanic water, black body radiation, and so on. Based on a growing number of recent studies, we have reasons to speculate that the melting of glaciers in Thwaites and its vicinity in West Antarctica is essentially associated with the upward transport and infiltration of mantle hydrothermal fluids with high temperature along the cracks and weak parts of the crust, causing local or regional warming of the upper crust and further leading to the reduction of viscosity, disintegration and sliding of glaciers, which creates conditions for warming climate to melt the overlying ice sheets. The activities of volcanoes, mantle magma, hydrothermal fluids and hot springs in this area may play a vital role in the collapsing, cracking, and melting of glaciers. The warming of the glacier's base also contributes to the formation of huge ice caves and glacial lakes. Dziadek believes that these geothermal heat flows (GHF) can raise the

temperature of water-saturated sediments at the bottom or the internal temperature of the glacier, causing the glacier's basement to slide (personal communication, February 7, 2022). On the other hand, the higher temperature of "inner lake" water can also destroy the "fusion point" between the seamount and the glacier (that is, the above-mentioned pinning point), thereby opening up the connection with the outer ocean from the inside, leading to the influx of water from the ocean to patrol on the bottom of the glacier, and even form circulations beneath glaciers.

It may not be ignored that the interaction between the "scorching" geothermal heat and the cold glaciers on temperature. This is like holding a piece of ice in hands –a hand can melt the ice, while the ice can also cool down the hand. We might give this phenomenon a name for the time being: "Palm-Ice Effect". According to the theory of black body radiation, overlying rocks would emit more energy into air or ice sheet as described by Archer.

In view of this, it can be considered that the initial culprit for the destruction of the Thwaites Glacier in West Antarctica may largely be the geothermal heat and volcanoes under the Antarctic glaciers, while the role of CO_2 in the atmosphere and oceanic circulation may be secondary. The interaction of geothermal heat and warm ocean currents may also be contributing to the deteriorating glaciers in West Antarctica. However, whether or not the real main cause or culprit of the West Antarctic glaciers collapse is geothermal, or greenhouse gases may require further multidisciplinary investigations and studies to be uncovered and confirmed. With the meticulous geophysical work of Dziadek et al., our understanding of subsurface heat flow is off to a great start.

Without a doubt, the collapse and melting of the West Antarctic glaciers are a realistic and complex issue, many aspects of which we may still know little about. However, what can be certain is that this is an Earth system problem, even is associated with the variations of solar system. From the current geological studies, the heat flux of the Antarctic crust seems to accelerate, and earthquakes and volcanic activities are becoming increasingly frequent. The geothermal activity beneath the West Antarctic glaciers is notably higher than in East Antarctica. Geothermal features like hot water lakes, thermal rivers, and giant ice caves beneath the glaciers have been continuously discovered. Therefore, it is reasonable to speculate that geothermal effects are responsible for modifying the vast ice masses. I believe that primary factor, secondary factors, Milankovitch orbits, solar surface activities, cosmic blast, oceanic methane and whatever other factors could be all interconnected, forming a feedback loop between the glacier base and the ocean, or even a positive feedback loop, which further accelerates the collapse and melting of the West Antarctic glaciers.

Acknowledgements The author thanks Dr. Susan V. M. Maharaj at Center for Research on Environmental Medicine for her review and valuable comments. The author is particularly grateful to Professor Ricarda Dziadek of the University of Bremen in Germany, Erin Pettit of the University of Oregon and Helen Fricker at Scripps Institution of Oceanography, CA, USA for their valuable personal communication via emails on this article.

Author contributions J Zhang proposed and contributed to the whole research, formulation, interpretation, compilation, and writing of the paper. The author prepared and reviewed the manuscript and approved the final version of the manuscript.

Data availability statement The data and information that support the study are available from the academic and online sources, which were lucidly and relevantly cited as references.

Declarations The author declares that there are no conflict of interest.

5 References

1. Chapman, M. 2023. The world has five oceans, not four-meet the newest addition. *IFL SCIENCE*. https://www.iflscience.com/the-world-has-five-oceans-not-four-meet-the-newest-addition-70744.
2. GIS. 2023. Antarctic Map. https://gisgeography.com/antarctica-map-satellite-image/.
3. Miller, KG; Wright, JD and Fairbanks, RG. 1991. Unlocking the ice house: oligocene-miocene oxygen isotopes, eustasy and margin erosion. *JGR* 96 (B4): 6829-6848.
4. Wikipedia, 2023. Antarctic ice sheet. https://en.wikipedia.org/wiki/Antarctic_ice_sheet.
5. Frémand, AC. 2023. Antarctic bedmap data: findable, accessible, interoperable, and reusable (FAIR) sharing of 60 years of ice bed, surface, and thickness data. *Earth System Science Data*, 15(7). https://doi.org/10.5194/essd-2022-355.
6. Rafferty, JP (article revised, 2021) and Metych, M (maps added). 2023. Antarctic circumpolar current oceanography. *Encyclopædia Britannica*. https://www.britannica.com/place/Southern-Ocean.
7. Woods Hole Oceanographic Institution of the United States. 2021. Dive and discovery expeditions to the seafloor. 3(21). https://divediscover.whoi.edu/.

8. Deacon, G. 1984. *The Antarctic Circumpolar Ocean*. *Cambridge University Press*, 180pp. DOI: https://doi.org/10.1017/S0016756800031575.
9. Giglio, D and Johnson, GC. 2016. Subantarctic and polar fronts of the Antarctic circumpolar current and southern ocean heat and freshwater content variability: a view from Argo. *Journal of Physical Oceanography*, 46: 749-768. DOI: 10.1175/JPO-D-15-0131.1.
10. Smith, R; Desflots, M; White, S; Mariano, AJ & Ryan, EH. 2013. The Antarctic CP current: ocean surface currents. *RSMAS, Miami University*. https://oceancurrents.rsmas.miami.edu/southern/antarctic-cp.html.
11. Wikipedia. 2023. Gulf stream. *Wikipedia, the free encyclopedia.* https://en.wikipedia.org/wiki/Gulf_Stream.
12. Broecker, WS. 1987. The biggest chill. *Natural History Magazine*. 97: 74-82.
13. Zhang, J. 1996. Messinian paleoceanography in the north Atlantic Ocean: foraminiferal and stable isotopic evidence. *Dalhousie University, PhD Thesis*, 418pp.

14. Pettit, E. 2021. Press conference: The threat from Thwaites: The retreat of Antarctica's riskiest glacier. *AGU*. https://www.google.com/search?q=Erin+Pettit%27s+Thwaites+Glacier+collapse+situation+map+(2021%2C+AGU21+Fall+Meeting)&rlz=1C1GGRV___CA748CA749&oq=Erin+Pettit%27s+Thwaites+Glacier+collapse+situation+map+(2021%2C+AGU21+Fall+Meeting)&gs_lcrp=EgZjaHJvbWUyBggAEEUYOTIGCAEQRRg80gEIMTQ5MGowajSoAgCwAgA&sourceid=chrome&ie=UTF-8#fpstate=ive&vld=cid:91cbd40c,vid:uBbgWsR4-aw.
15. Tsui, K. 2022. A 'Doomsday Glacier' the size of Florida is disintegrating faster than thought. *The Washington Post*. https://www.washingtonpost.com/climate-environment/2022/09/06/thwaites-doomsday-glacier-antarctica-disintegrating/.
16. Mooney, C. 2023. Warming oceans are carving vast trenches into Thwaites glacier. *The Washington Post.* https://www.washingtonpost.com/climate-environment/2023/02/15/glacier-ice-melt-ocean- warming/.
17. Schmidt, BE; Washam, P; Davis, PED; Nicholls, KW; Holland, DM; Lawrence, JD; Riverman, KL; Smith, JA; Spears, A; Dichek, DJG; Mullen, AD; Clyne, E; Yeager, B; Anker, P; Meister, MR; Hurwitz, BC; Quartini, ES; Bryson, FE; Basinski-Ferris, A; Thomas, C; Wake J; Vaughan, DG; Anandakrishnan, S; Rignot, E; Paden, J & Makinson, K. 2023. Heterogeneous melting near the Thwaites glacier grounding line. *Nature*, 614(7948): 471–478. https://www.ncbi.nlm.nih.gov/pmc/articles/PMC9931587/(note: this article has been corrected. See *Nature*. 2023 February 24, 615(7952): E21).
18. New York Times. 2020. Temperatures at a Florida-size glacier in Antarctica alarm scientists. *The New York Times*, 1(29).
19. Priscu, J. 2008. *PopTech.* https://m.youtube.com/watch?v=ZTK6n0dXMc4&feature=share.
20. Wåhlin, AK; Graham, AGC; Hogan, KA; Queste, BY; Boehme, L; Larter, RD; Pettit, EC; Wellner, J and Heywood, KJM. 2021. Pathways and modification of warm water flowing beneath Thwaites ice shelf, west Antarctica. *Science Advances*, 7 (15): 1-9. DOI: 10.1126/sciadv.abd7254.
21. Lewis, S. 2020. Scientists alarmed to discover warm water at "vital point" beneath Antarctica's "Doomsday Glacier".*CBSNews*.https://www.cbsnews.com/news/climate-change-thwaites-melting-scientists-warm-water-antarctica-doomsday-glacier/.
22. Zhang, J. 2022. What is the culprit that caused the "Doomsday glacier" in Antarctica? *Mini Popularized Sciences-Explore the Earth with Me*", 6 (1-3) (**in Chinese**). http://www.chinanews.org/wenhua/lishi/18934.html.
23. Wikipedia. 2023. Drake passage. http://en.wikipedia.org/wiki/Drake_Passage.
24. BBC. 2020. Antarctic Doomsday glacier: the mystery of the amazing melting speed revealed, September 12, 2020 (in Chinese). https://www.bbc.com/zhongwen/simp/science-54091686.
25. Rafferty, JP. 2007. Amery Ice Shelf, Antarctica. https://www.britannica.com/place/Amery-Ice-Shelf.
26. Borenstein, S. 2018. Global warming is weakening key ocean circulation. *CTV News*.https://www.ctvnews.ca/sci-tech/global-warming-is-weakening-key-ocean-circulation-study-1.3881838.
27. Watts, A. 2014. Uh oh: Study says 'collapsing' Thwaites glacier in Antarctica melting from geothermal heat, not 'climatechange'effects.https://wattsupwiththat.com/2014/06/09/uh-oh-study-says-collapsing-thwaites-glacier-in-antarctica-melting-from-geothermal-heat-not-co$_2$-heat-effects/.
28. Schroeder, DM; Blankenship, DD; Young, DA and Quartini, E. 2014. Evidence for elevated and spatially variable geothermal flux beneath the west Antarctic ice sheet. *PNAS*, 111(25): 9070-9072.
29. Stephens, T. 2015. Study finds surprisingly high geothermal heating beneath west Antarctic ice sheet. *UC Santa Cruz News Centre*. https://news.ucsc.edu/2015/07/antarctic-heating.html.
30. Wikipedia. 2023. West Antarctic rift system. https://en.wikipedia.org/wiki/West_Antarctic_Rift_System.
31. Dziadek, R; Ferraccioli, F and Gohl, K. 2021. High geothermal heat flow beneath Thwaites glacier in west Antarctica inferred from aeromagnetic data. *Communications Earth & Environment* 2(1): 1-6. DOI:10.1038/s43247-021-00242-3.
32. Hager, J. 2020. 30,000 earthquakes near Antarctic peninsula. https://polarjournal.ch/en/2020/12/18/30000-earthquakes-near-the-antarctic-peninsula/.
33. Artemieva, IM and Thybo, H. 2020. Continent size revisited: geophysical evidence for west Antarctica as a back-arc system. Science Direct: *Earth-Science Reviews*, March 2020, 202.

34. Van Wyk de Vries M; Bingham, RG and Hein, AS. 2018. A new volcanic province: an inventory of subglacial volcanoes in west Antarctica. *Geological Society Publications*, London, Special Publications, 461 (1): 231-248. https://www.lyellcollection.org/doi/full/10.1144/SP461.7.
35. Gonzaga, S. 2011. Frozen, ancient Lake Vostok and a race against time. *EarthSky*. https://earthsky.org/earth/racing-against-time-to-strike-liquid-water-in-frozen-ancient-lake-vostok/.
36. Funkhouser, D. 2012. Scientists drill 2 miles down to ancient lake Vostok. *Columbia Climate School*. https://news.climate.columbia.edu/2012/02/09/scientists-drill-2-miles-down-to-ancient-lake-vostok/.
37. Bell, R; Studinger, M; Shuman, CA & Fahnestock, M. 2007. Large subglacial lakes in east Antarctica at the onset of fast-flowing ice streams. *Nature*, 445(7130): 904-907. DOI:10.1038/nature05554.
38. Valcano Hotspot. 2017. Antarctica 4-Volcanoes of the Ross Sea and Victoria Land. https://volcanohotspot.wordpress.com/2017/11/06/antarctica-4-volcanoes-of-the-ross-sea-and-victoria-land/.
39. Wothe, K. 2023. Deception Island hot springs. https://www.google.com/search?q=deception%20island%20hot%20spring&.
40. Wikipedia. 2023. Yellowstone National Park. https://en.wikipedia.org/wiki/Yellowstone_National_Park.
41. Seroussi, H; Erik R; Ivins, ER; Wiens, DA & Bondzio, J. 2017. Influence of a west Antarctic mantle plume on ice sheet basal conditions. *Journal of Geophysical Research: Solid Earth*, 122(9): 7127-7155. https://doi.org/10.1002/2017JB014423.
42. Artemieva, IM. 2022. Antarctica ice sheet basal melting enhanced by high mantle heat. *Earth-Science Reviews*, 226: 1-11. www.elsevier.com/locate/earscirev.
43. NASA. 2022. Scientists terrifying new discovery under Antarctica's ice changes everything. *YouTube*. https://m.youtube.com/watch?v=n76FFQ9-d-I&feature=share.
44. Siegfried, MR and Fricker, HA. 2021. Illuminating active subglacial lake processes with ICESat-2 Laser Altimetry. *Geophysical Research Letters, AGU*. https://doi.org/10.1029/2020GL091089.
45. Shirah, G; Kostis, HN; Fricker, HA; Siegfried, MR and Beck, J. 2023. ICESat-2 maps subglacial lakes in Antarctica. *NASA Scientific Visualization Studio*. https://svs.gsfc.nasa.gov/4913.
46. NASA. 2021. New lakes discovered under Antarctic ice with NASA's ICESat-2. *SciTech Daily*. https://youtu.be/2z7xBhFszAA.
47. Rasmussen, C. 2017. Hot news from the Antarctic underground. *NASA Jet Propulsion Laboratory, NASA*. https://www.jpl.nasa.gov/news/hot-news-from-the-antarctic-underground.
48. Oceanographic Staff. 2023. Geothermal heat found under Thwaites Glacier. *Oceanographic Magazine*. https://oceanographicmagazine.com/news/thwaites-glacier/.
49. The Archaeologist. 2022. Incredible recent discoveries in Antarctica. *The Archaeologist*. https://www.thearchaeologist.org/blog/incredible-recent-discoveries-in-antarctica?format=amp.
50. The Archaeologist. 2022. Antarctica unveils something unbelievable beneath the Ice. *The Archaeologist*. https://www.thearchaeologist.org/blog/antarctica-unveils-something-unbelievable-beneath-the-ice?format=amp.
51. Fricker, HA. 2019. Lakes beneath Antarctic ice: deep dark and mysterious. *Scripps Institution of Oceanography*. https://youtu.be/UpAd9XNF3F0.
52. The Hidden World Beneath the Antarctic Ice Sheet | John Priscu | TEDxBozeman. 2013. https://m.youtube.com/watch?v=mTwS9_PReM4&feature=share.
53 Ralls, E. 2016. Eyjafjallajökull volcano: The dangerous volcano beneath a glacier. https://www.earth.com/news/eyjafjallajokull-volcano-dangerous-volcano-beneath-glacier/.
54. Wenger, M. 2021. Does geothermal energy promote melting of Thwaites glacier? *Polar Journal*. https://polarjournal.ch/en/2021/08/21/does-geothermal-energy-promote-melting-of-thwaites-glacier/.
55. Alfred Wegener Institute. 2021. Thwaites glacier: significant geothermal heat beneath the ice stream. *Helmholtz Centre for Polar and Marine Research. Science Daily*, https://www.sciencedaily.com/releases/2021/08/210818083957.htm.
56. Scientific Committee on Antarctic Research. 2023. New publication on high geothermal heat flow beneath Thwaites glacier. https://scar.org/scar-news/instant-news/geothermal-thwaites/.
57. Jefferson, R. 2021. Geothermal activity under Antarctic ice sheet brings Thwaites glacier on brink of collapse due to excessive melting. *The Sciencetimes*. https://www.sciencetimes.com/articles/32977/20210820/thwaites-doomsday-glacier-brink-collapse-due-excessive-melting-cause-geothermal.htm.
58. PBS Terra. 2022. The Doomsday glacier is collapsing…who is most at risk? https://www.youtube.com/watch?v=IY3mXFXd3GU.
59. Holland, D. 2022. Scientists measure how quickly crucial Antarctica glacier is melting. *PBS NewsHour*. https://www.youtube.com/watch?v=JvFkLWHRUwo.
60. Auger, M; Morrow, R; Kestenare, E; Sallée, JB & Cowley, R. 2021. Southern ocean in-situ temperature trends over 25 years emerge from interannual variability. *Nature Communications*, 12(514): 1-9.

61. Sallée, JB. 2018. Southern ocean warming. *Oceanography*, 31(2): 52-62. https://doi.org/10.5670/oceanog.2018.215. https://tos.org/oceanography/assets/docs/31-2_sallee.pdf.

62. Civel-Mazens, M; Crosta, X; Cortese, G; Michel, E; Mazaud, A; Ther, O; Ikehara, M and Itaki, T. 2021. Antarctic polar front migrations in the Kerguelen plateau region, Southern ocean, over the past 360 kyrs. *Global and Planetary Change*, 202, July 2021. https://doi.org/10.1016/j.gloplacha.2021.103526.
63. Phillips, H; Legresy, B and Bindoff, N. 2018. How the Antarctic circumpolar current helps keep Antarctica frozen.*TheConversation*.https://theconversation.com/explainer-how-the-antarctic-circumpolar-current-helps-keep-antarctica-frozen-106164.
64. Freeman, NM & Lovenduski, NS. 2016. Mapping the Antarctic polar front: weekly realizations from 2002 to 2014. *Earth Syst. Sci. Data*, 8: 191–198. https://doi.org/10.5194/essd-8-191-2016.
65. Pearce, F. 2023. The upper atmosphere is cooling, prompting new climate. *Yale Environment 360 Concerns.* https://e360.yale.edu/features/climate-change-upper-atmosphere-cooling.
66.NASA. 2023. Energy: the driver of climate: the greenhouse effect. https://www.ces.fau.edu/nasa/module-2/how-greenhouse-effect-works.php.
67. Broecker, W. 2013. Dealing with the CO_2 crisis. Columbia University. *YouTube.*https://m.youtube.com/watch?v=5NxyPWPl8FA.
68. Broecker, W. 2008. Using the past to predict future impacts of climate change. https://m.youtube.com/watch?v=tLI50EKBBzM.
69. Lindsey, R. 2023. If carbon dioxide hits a new high every year, why isn't every year hotter than the last? https://www.climate.gov/news-features/climate-qa/if-carbon-dioxide-hits-new-high-every-year-why-isn%E2%80%99t-every-year-hotter-last.
70. Archer, D. 2008. Global warming: understanding the forecast. *UChicagoCISSR. YouTube*. https://m.youtube.com/watch?v=5-QLBjLHnxg.
71. Hausfather, Z. 2021. Global-CO_2-emissions-have-been-flat-for-a-decade-new-data-reveals. *Global Emissions*. https://www.carbonbrief.org/global-co$_2$-emissions-have-been-flat-for-a-decade-new-data-reveals/.
72. Qiqi. 2023. NASA discovered an abnormality in the Sun that the activity cycles have been changed, and humans may be in a big trouble. *Qiqi talks about strange things*. https://m.163.com/dy/article/I1V7BTG2055612NG.html?spss=adap_pc.
73. Wikipedia. 2023. Black body radiation. Wikipedia. https://en.m.wikipedia.org/wiki/Black-body_radiation.
74. Williams, B. 2023. The bare rock model. https://www.briangwilliams.us/climate-forecast-system/the-bare-rock-model.html.
75. Masson-Delmotte, V; Stenni, B; Pol, K; Braconnot, P; Cattani, O; Falourd, S; Kageyama, M; Jouzel, J; Landais, A; Minster, B; Barnola, JM; Chappellaz, J; Krinner, G; Johnsen, S; Röthlisberger, R; Hansen, J; Mikolajewicz, U & Otto-Bliesner, B. 2010. EPICA Dome C record of glacial and interglacial. *Quaternary Science Reviews*, 29(1–2) : 113-128. https://www.sciencedirect.com/science/article/abs/pii/S0277379109003369.
76. Floyd, M. 2019. Study may solve long-standing mystery of why atmospheric CO2 was lower during ice ages. *OregonStateUniversity*. https://today.oregonstate.edu/news/study-may-solve-long-standing-mystery-why-atmospheric-co2-was-lower-during-ice-ages.
77. NSF. 2019. Scientists solve long-standing mystery: why atmospheric carbon dioxide was lower during ice ages carbon dioxide as much as one-third lower during ice ages. *National Science Foundation.* https://new.nsf.gov/news/scientists-solve-long-standing-mystery-why.
78. Wikipedia. 2023. Orbital eccentricity. https://en.m.wikipedia.org/wiki/Orbital_eccentricity.
79. NOAA. 2023. Can an increase or decrease in sunspot activity affect the Earth's climate? The Sun and sunspots. *National Weather Service, NOAA*. https://www.weather.gov/fsd/sunspots.
80. Plait, P. 2012. Anniversary of a cosmic blast. *Bad Astronomy*. https://slate.com/technology/2012/12/cosmic-blast-magnetar-explosion-rocked-earth-on-december-27-2004.html.
81. Thurber, AR; Seabrook, S and Welsh, RM. 2020. Riddles in the cold: Antarctic endemism and microbial succession impact methane cycling in the southern Ocean. *Proceedings of the Royal Society B: Biological Sciences*. DOI: 10.1098/rspb.2020.1134.
82. CBS News. 2023. Ancient methane escaping from melting glaciers might warm the planet even more. CBS News Philadelphia.
83. Dewan, P. 2023. Ice age volcano spewing methane discovered on Arctic seabed. *Newsweek 90*. https://www.newsweek.com/ice-age-volcano-spewing-methane-discovered-arctic-seabed-1803300.

Original Article

Use ChatGPT to maximize everyday efficiency

Deliang Shi[1]

Abstract

The advent of advanced artificial intelligence systems, exemplified by OpenAI's ChatGPT, has ushered in a new era of technological capability and convenience in everyday life. This paper delves into the multifaceted applications of ChatGPT, aiming to understand and illustrate its profound impact on daily activities. Through a comprehensive demonstration of prompts on various use cases, we explore how ChatGPT can enhance personal and professional efficiency, aid in educational pursuits, and offer support in creative endeavors. By providing empirical examples, this study highlights the transformative potential of ChatGPT in simplifying and optimizing everyday tasks, ultimately showcasing its role as a pivotal tool in the modern digital landscape. This research aims to contribute to a better understanding of AI's practical applications in daily life and to inspire further exploration into the capabilities and future advancements of AI tools like ChatGPT.

Keywords: ChatGPT; AI; efficiency; prompts; daily activity

Affiliation Info: [1] Independent Researcher, Vernon Hills, IL 60061, USA
Article Info: Received: 19 November 2023 / Revised: 2 December 2023 / Accepted: 7 December 2023 / Published Online: 12 December 2023. www.naturalisscientias.com
Author's Contact Info: Shi, DL: deliangshi@gmail.com
Citation: Shi, DL. 2024. Use ChatGPT to maximize everyday efficiency. *Naturalis Scientias*, 1(1): 87-99. DOI: https://doi.org/10.62252/NSS.2024.1006.

Corresponding Author: Shi, DL, PhD. Received PhD degree from Department of Chemical Engineering at Univerisity of Pittsburgh in 2008. Received George Klinzing Best PhD Award from American Instituite of Chemical Engineers (AIChE) in 2011. Wrote a book <ChatGPT Practical Guide: How to Use AI Chatbots to Solve Problems and Create Value> in 2023; Email: deliangshi@gmail.com

1 Introduction

Artificial intelligence is one of the most transformative and impactful technologies of our time, changing the way we live, work and learn. In the field of artificial intelligence, natural language processing is an important branch that involves the ability of humans and machines to communicate and understand in natural language[1-3]. With the development of deep learning technology, breakthroughs have been made in natural language processing, and many amazing applications and products have emerged, such as intelligent assistants, machine translation, text summarization, sentiment analysis, etc[4-5].

ChatGPT, a revolutionary AI chatbot developed by OpenAI, is founded on an expansive pre-trained language model known as the Generative Pre-trained Transformer[6-7]. Since its launch on November 30, 2022, ChatGPT has rapidly become a focal point of global interest and discussion. As of November 15, 2023, a search for "ChatGPT" on Google yields an astonishing 1.46 billion results, a testament to its remarkable impact and widespread recognition just under a year[8]. It can answer questions and execute instructions in the form of dialogue, and has strong content generation and generalization capabilities. ChatGPT can not only complete common natural language processing tasks, but also perform very well on other atypical tasks, such as writing code, poetry, stories, etc[9-12].

2 Efficiency

In the quest to maximize everyday efficiency using ChatGPT, it is essential to assess its effectiveness and efficiency in various tasks. This section evaluates the efficiency of ChatGPT in streamlining daily activities, focusing on time-saving capabilities, accuracy, and adaptability in diverse scenarios[13-15].

2.1 Time-saving capabilities

One of the primary measures of ChatGPT's efficiency is its ability to save time. By automating routine tasks such as scheduling, email drafting, and information gathering, ChatGPT significantly reduces the time and effort required for such activities. For instance, using ChatGPT to quickly generate a well-structured report or to compile research data can free up valuable time for users to focus on more complex tasks.

2.2 Accuracy and reliability

The efficiency of ChatGPT is also contingent upon its accuracy and reliability. While the AI is capable of processing and generating large amounts of information rapidly, the accuracy of its outputs is crucial. For educational purposes, factually accurate and up-to-date information is vital. In professional contexts, the precision of language and adherence to specific industry terminologies are essential. Regular updates and improvements in the model contribute to its reliability, making it a dependable tool for various applications.

2.3 Adaptability in diverse scenarios

ChatGPT's efficiency is further amplified by its adaptability to different user needs and scenarios. Whether assisting in creative writing, providing technical support, or offering language translation services, ChatGPT's versatility makes it an efficient tool across various domains. Its ability to understand and respond to context-specific prompts allows for customized solutions, enhancing its practical utility in everyday tasks.

3 Applications

The integration of ChatGPT into daily life marks a significant leap forward in the realm of artificial intelligence. As an advanced language processing tool, ChatGPT's applications span a wide range of everyday activities, offering convenience, efficiency, and innovative solutions to common challenges. This section delves into the diverse and practical applications of ChatGPT, illustrating its transformative impact on various aspects of daily life.

3.1 Personal productivity and task management

ChatGPT significantly enhances personal productivity by assisting in task management and organization. Users can leverage this AI tool for creating and managing to-do lists, setting reminders, and organizing schedules. Its ability to

process natural language makes it an intuitive assistant for planning daily activities, from grocery shopping to appointment scheduling. Moreover, ChatGPT can provide personalized tips and strategies for time management, thereby boosting overall productivity[16].

3.2 Educational assistance

In the realm of education, ChatGPT serves as a powerful tool for students and educators alike. It aids in understanding complex concepts, offering explanations, and providing examples in a variety of subjects. Students can use ChatGPT for homework assistance, essay writing, and language learning, benefiting from its vast knowledge base and ability to clarify doubts. Educators, on the other hand, can utilize this tool for creating lesson plans, generating quiz questions, and even customizing educational content to cater to diverse learning needs[17].

3.3 Enhanced communication

ChatGPT revolutionizes the way we communicate by offering advanced writing assistance and language translation services. It helps in drafting emails, reports, and professional documents, ensuring clarity and coherence in communication[18]. Additionally, its language translation capabilities break down linguistic barriers, facilitating seamless communication in a globalized world. ChatGPT can also serve as a practice tool for honing communication skills, such as public speaking or foreign language proficiency[19].

3.4 Creative endeavors

For those engaged in creative fields, ChatGPT emerges as a valuable ally. It assists in brainstorming ideas, generating content, and even providing feedback on creative projects[20]. Writers can use ChatGPT for story development, character creation, and plot suggestions. Similarly, marketers and content creators can leverage its capabilities to produce innovative and engaging content for various platforms.

4 Prompts

The utility of ChatGPT in enhancing daily efficiency largely hinges on the user's ability to craft effective prompts[21-22]. This section explores the art and science of prompt engineering to harness the full potential of ChatGPT in various applications. Understanding how to effectively communicate with this AI tool can significantly amplify its usefulness in everyday tasks.

4.1 Principles of prompt engineering

Clarity and Specificity: Clear and specific prompts yield more accurate and relevant responses. Users should articulate their requests precisely, avoiding ambiguity.
Contextual Information: Providing sufficient context helps ChatGPT understand the prompt better and deliver more tailored responses.
Iterative Approach: Engaging with ChatGPT can be an iterative process. Refining prompts based on responses helps in achieving the desired outcome.

4.2 Application-specific prompt examples

For Task Management: “List the steps I need to take to organize a successful team meeting by the end of this week, including scheduling, agenda setting, and necessary materials.”
In Education: “Explain the concept of photosynthesis in a simple way for a 5th-grade student, including key terms and a basic diagram.”
For Professional Communication: “Draft a professional email to a client explaining a delay in project delivery, ensuring it conveys empathy, provides a revised timeline, and maintains a positive relationship.”
In Creative Writing: “Generate a plot outline for a mystery novel set in Victorian London, focusing on a detective character, with three key twists.”

4.3 Enhancing creativity and problem-solving

Using ChatGPT for brainstorming and problem-solving can be particularly effective. Crafting prompts that ask for ideas, alternatives, or different perspectives can lead to creative solutions and innovative approaches. For instance, "Provide five unique marketing strategies for an eco-friendly clothing brand targeting young adults."

5 Prompts to maximize everyday efficiency

Maximizing everyday efficiency with ChatGPT hinges on crafting precise and purpose-driven prompts. The effectiveness of ChatGPT in enhancing daily efficiency largely depends on the user's ability to ask the right questions in the right way, making prompt engineering a crucial skill in the era of advanced AI assistants[23-25]. In this section, the author have presented a diverse array of prompts applicable across various fields, providing readers with a foundational base that they can adapt and customize to meet their specific needs[26-33].

Search

Prompt: What is the largest moon in the solar system?

Why

Prompt: Why are there no penguins in the North Pole?

Programming

Prompt: Write an alarm clock in python to remind me at 6 o'clock in the morning.

Math

Prompt: 1+2

Calculus

$$\int_0^{100} x^3 dx$$

Prompt: \int {0}^{100} x^3 dx

Probability

Prompt: The probability of heads and tails of a coin is 50% each, what is the probability that the coin is flipped 10 times and it comes up exactly 6 times heads?

Statistics

Prompt: There are 50 students in a class. The mean value of test scores is 75 points, and the standard deviation is 5 points. Assuming that grades follow a normal distribution, what is the proportion of students with grades above 80?

Prove

Question: Prove the function y=sin x (-∞,∞) is continuous everywhere.
Prompt: prove function y= sinx continuous everywhere in left (-\ infty, \ infty \right)

List

Prompt: Please list the area of each country and rank them in descending order

Physics

Prompt: A heavy object falls freely from a height of 20m at a speed of 10m/s, find the speed when it hits the ground.

Chemistry

Prompt: A laboratory needs to prepare 200mL copper nitrate solution with a concentration of 0.1mol/L. It is known that the laboratory has a copper nitrate solution with a concentration of 2mol/L. How many milliliters of copper nitrate solution are needed to prepare the required solution?

Biology

Prompt: In a population of pea plants, the allele for purple flowers (P) is dominant, while the allele for white flowers (p) is recessive. In a randomly mating population, 16% of the plants have white flowers. Calculate the frequency of the dominant allele (P) and the recessive allele (p) in the population.

Essay

Prompt: Could you write an essay on below title? The Impact of Technology on Modern Communication: Analyzing the Pros and Cons of Social Media in Personal Relationships and Society

History

Prompt: Compare and contrast the political, economic, and social systems of Ancient Rome and Ancient Greece.

Geography

Prompt: Which state has more hurricane? Why?

Speech

Prompt: Please write a presidential inauguration speech for year 2052.

Offer letter

Prompt: Please write a college admission offer from Harvard University

Scholarship application

Prompt: Please write a letter for scholarship application

Tutoring student homework

Prompt: x^2-8x+15=0 Give me some ideas for solving the problem, but don't give the answer, okay?

Help the teacher generate test problems

Prompt: I am a math teacher on analytic geometry. Could you give me 3 problems?

Job applications

Prompt: As a chemical engineering student, write a job application letter to a top 500 company

Resume

Prompt: Write a resume for a financial major graduate

Essay for college application

Prompt: I am a high school student and I am going to apply to the University of Pittsburgh to study electronic engineering. Can you help me write the essay?

Funding application

Prompt: As a professor of nanomaterials, write a funding application letter in the field of nanomaterials in biosensors.

Love letter

Prompt: Please write a love letter to Mary in the tone of Tom

Reply letter

Prompt: Mary is Tom's girlfriend, please help Mary write a letter to Tom.

Letter for wedding invitation

Prompt: Tom and Mary are going to get married at the Wonderland Resort on July 1st. Please write a wedding invitation letter for them.

Invitation for baby shower

Prompt: Mary is pregnant. She and Tom are expecting to become parents soon. They are very excited about the incoming baby. Please write an invitation letter for baby shower.

Charter

Prompt: Please formulate a charter for the newly established kindergarten

Notice

Prompt: Please draft a notice on the suspension of the No.5 subway on May 3rd

Project plan

Prompt: draft a project plan for upgrading the bridge at Michigan Ave and Wacker Drive in Chicago

Agreement

Prompt: Please draft a house purchase and sale agreement

Grand opening invitation

Prompt: Tom opened a car dealership. Please write a grand opening invitation

Development plan

Prompt: River Valley is a town located in the Rocky Mountains. Please write a business development plan for it

Job description

Prompt: Tom's car dealership need recruit a front desk staff, please write a job description

Tender notice

Prompt: Please write a tender notice for the municipal government on upgrading computers

Thank you note

Prompt: Please write a thank you note to your business partner

Arbitration agreement

Prompt: There is a commercial dispute between the publishing house and the distribution agency, please write an arbitration agreement

Business strategic plan

Prompt: Please write a business strategy plan for the solar energy company to expand business to the suburbs

Manual

Prompt: Please write a product manual on how to use the robot watering system

Advertisement

Prompt: Write an ad for the robot watering system

Recipe

Prompt: Please write a recipe on how to make buffalo wings

Stock price

Prompt: Coca Cola stock price

Stock market analysis papers

Prompt: The stock market rose sharply today, please use this as a basis to draft a stock market analysis report

Year-end meeting

Prompt: Write a speech on the year-end meeting for the CEO of a furniture company

Diary

Prompt: On March 1, Tom, Mary and kids went back to Tom's hometown. They met Tom's parents and some old friends. Please write a diary

Search + explore

Prompt: Do you know why Sisyphus need roll a huge boulder to a steep hill?
Prompt: Do you know how to become free if you are Sisyphus?

Content extract

Prompt: Could you extract the time and people from below content?
Content summarize

Prompt: Please summarize "I have a dream" in 100 words

Joke

Prompt: Could you tell a joke about robots and mermaids?

Riddle

Prompt: Could you come up with a riddle?

Letter game

Prompt: Could you make a poem on snow with all letters starting with a?

Compose

Prompt: Can you sing a song about trees and make a tune?

Story

Prompt: Please write a story about a robot and a mermaid

Movie script

Prompt: Please change this robot and mermaid story into a movie script

Drama

Prompt: Please turn this robot and mermaid story into a drama

Drawing

Prompt: I want to use artificial intelligence for drawing. Can you describe what ORION looks like?

Comic

Prompt: Please change this robot and mermaid story into a comic book

Phonetic

Prompt: Could you provide a phonetic transcription of the first two paragraphs of the story?

Translate

Prompt: Please translate this robot and mermaid story into Spanish

Legal information

Prompt: In New York State, a person is driving 90mph in a 70mph speed-limit highway. What kind of punishment this person may receive

News

Prompt: On August 15, 2030, three US astronauts landed on the moon, please write a press release

Causal talk

Prompt: Can you randomly share some knowledge about US history?

Travel plan

Prompt: I am going to New York City during Christmas for 3 days. Could you help me make a travel plan? I am interested in skyscrapers

Video script

Prompt: I want to make a short video about superconductivity, can you write a script for me?

Brainstorm

Prompt: How to land on mars in 10 years?

Stress testing

Prompt: I am a house builder. Recently, a new house builder came to the region and sells houses in a very low price. The sales of my company dipped. What should I do?

Explore ideas

Prompt: I am the owner of a toy factory, and the toys are not selling well this year. What should I do?

Scenario setting

Prompt: As the owner of a toy factory, I have many years of experience in producing and selling toys in my country Now I want to sell toys to Australia, what is the best way?

Sales training

Prompt: Simulate a conversation where a salesperson showcases the benefits of a penthouse to a prospective buyer

Different styles

Prompt: Using William Shakespeare's tone to write a poem on Niagara Falls
Prompt: Using Emily Dickinson's tone to write a poem on Niagara Falls

New technology

Prompt: Introduce the latest developments in the field of physics

Research progress

Prompt: How many articles related to gene technology have been published in Nature in the past six months?

Research review

Prompt: How many gene editing articles have been published in Nature in the past year? Can you summarize these articles?

Research details

Prompt: Please describe in detail the deep learning method that can accurately predict the three-dimensional structure of proteins in Highly Accurate Protein Structure Prediction with Alpha Fold

6 Discussion

Getting to the root of a topic is a crucial method for broadening one's understanding by delving deeper into the subject matter based on the answer to a question[34]. In everyday life, when one person questions another, it's easy to touch upon the limits of the other person's knowledge, leaving them unsure of how to answer or even becoming frustrated. ChatGPT, on the other hand, will seriously address all questions without concerns about emotional reactions. The following is an example of exploring a topic in greater depth.

Prompt: Why is the sky blue?

The sky appears blue because, as sunlight passes through the Earth's atmosphere, its white light scatters due to interactions with atmospheric molecules, primarily nitrogen and oxygen. This scattering effect occurs when light, which normally travels in a straight line, is dispersed in multiple directions after striking gas molecules. Ultraviolet and blue light have shorter wavelengths, causing them to scatter more intensely than other colors. As a result, the sky takes on a blue hue when the scattered white light is observed.
Furthermore, during sunrise and sunset, sunlight travels through a longer section of the atmosphere, leading to increased scattering of light. At these times, other colors of light are scattered less intensely, resulting in an orange-red sky.

Since ChatGPT mentioned that white light scatters due to interactions with atmospheric molecules, let's ask the reason.

Prompt: When white light in sunlight passes through the atmosphere, why does it scatter with molecules in the atmosphere?

When white light in sunlight passes through the atmosphere, it will scatter with molecules in the atmosphere. This is because the size of molecules in the atmosphere is much smaller than the wavelength of light, making the interaction between light and molecules very important.
When white light passes through the atmosphere, its wavelength ranges from 400 nanometers to 700 nanometers. This range corresponds exactly to the peak absorption range of oxygen and nitrogen molecules in the atmosphere. When light hits oxygen and nitrogen molecules, the molecules' electrons are excited, transferring energy to surrounding molecules. This process repeats itself, causing the energy of the light to travel through the atmosphere until it finally reaches the ground.
In addition, the gas molecules in the atmosphere are randomly distributed, which also causes random scattering in the propagation path of light. Therefore, as white light travels through the atmosphere, shorter wavelength blue light waves are scattered more strongly, giving the sky a blue appearance. In contrast, red light waves with longer wavelengths are less scattered, so at sunset or sunrise, the less scattered red light passes relatively more easily as the sun's light takes a longer path through the atmosphere, so the sky shows an orange-red color.

Prompt: Why is the size of molecules in the atmosphere much smaller than the wavelength of light?

The main molecules in the atmosphere include nitrogen, oxygen, etc., and their molecular size is much smaller than the wavelength of light. This is because the size of molecules is determined by the length of chemical bonds between molecules, and the length of chemical bonds is usually on the order of several nanometers, which is much smaller than the wavelength of light.
The wavelength of light determines how light travels through air. When white light passes through the atmosphere, since the molecular size is much smaller than the wavelength of light, the light waves will be scattered in different directions when they encounter molecules. Due to the large number of molecules in the air, the propagation of white light in the atmosphere will be scattered to varying degrees, which explains why the sky is blue.
Note that when the sun rises or sets, more light waves are scattered as the light travels through a longer atmospheric path, so it appears red or orange.

Prompt: Why is the size of a molecule determined by the length of the chemical bond between molecules?

The size of a molecule is mainly determined by the length of chemical bonds between atoms in the molecule. A chemical bond is the strong force that holds two or more atoms together to form a molecule. Inside a molecule, the length of the chemical bonds between atoms and the type of bond (single, double, or triple) are important factors in determining the size of the molecule. Under the same conditions, the longer the chemical bonds between atoms, the larger the size of the molecule.
When the chemical bond between atoms is formed, the atoms in the molecule will form a stable geometric structure around this bond, and the relative position and distance between these atoms are the basic factors of the size and shape of the molecule.
It should be noted that the size of the molecule is not only related to the length of the chemical bond, but also related to the atomic radius, the bond energy of the chemical bond and other factors. But in general, the size of a molecule is primarily determined by the length of the chemical bonds between the atoms within the molecule.

Prompt: Why are the bond lengths and types of bonds between atoms (single, double, or triple) important factors in determining the size of a molecule?

The length and type of bonds between atoms are important factors in determining the size of a molecule because they directly affect the geometry and volume of the molecule.
First, the size of a molecule depends on the distance between the atoms in the molecule. The bond length between atoms is the distance between atoms. Under the same conditions, the longer the chemical bonds between atoms, the

larger the size of the molecule. For example, the chemical bond length between two hydrogen atoms in a hydrogen gas molecule (H_2) is 0.74 angstroms, while the chemical bond length between two oxygen atoms in an oxygen molecule (O_2) is 1.21 angstroms. Since the chemical bonds of oxygen molecules are longer than those of hydrogen molecules, oxygen molecules are larger than hydrogen molecules.
Second, the different types of chemical bonds also have an effect on the size and shape of the molecule. Different types of chemical bonds have different bond energies and bond lengths. Single bonds are longer than double and triple bonds, so molecules with double or triple bonds in them are usually smaller than those with single bonds. For example, there is one double bond in the ethylene molecule (C_2H_4), but only a single bond in the ethane molecule (C_2H_6). Since double bonds are shorter than single bonds, ethylene molecules are smaller than ethane molecules.
Therefore, the length and type of chemical bonds between atoms are important factors affecting the size and shape of molecules.

Thus, by using prompts to delve deep into the subject matter, we have gained knowledge from the macroscopic sky color to the microscopic chemical bond.
To craft prompts, it's crucial to consider the ethical aspects of the requests. Avoid prompts that encourage biased, discriminatory, or harmful responses. Understanding ChatGPT's limitations in context interpretation is also vital to avoid miscommunication and ensure responsible usage[35-36].

7 Conclusions

The applications of ChatGPT in daily life are a testament to the remarkable strides made in the field of AI. By offering solutions that range from simplifying routine tasks to enhancing creative processes, ChatGPT has become an indispensable tool in various aspects of modern life. As technology continues to evolve, it is anticipated that ChatGPT will find even more innovative applications, further integrating AI into the fabric of daily living.
The ability to craft effective prompts is a key skill in leveraging ChatGPT to maximize everyday efficiency. By understanding the principles of prompt engineering and applying them to various contexts, users can greatly enhance the productivity and creativity benefits offered by this AI tool. As users become more adept at interacting with ChatGPT, they unlock its full potential, making it an indispensable asset in their daily lives. In this work, we delved into the detailed art of crafting prompts, showcasing a wide spectrum of examples relevant to multiple fields. This comprehensive presentation aims to equip readers with versatile prompts that can be tailored to suit their specific daily requirements.
While the applications of ChatGPT are vast, it is crucial to acknowledge its limitations and the ethical concerns surrounding its use. Issues such as data privacy, the potential for misinformation, and dependency on AI for critical thinking are important considerations. Users must be aware of these challenges and employ ChatGPT judiciously, ensuring that its use complements human judgment rather than replacing it.

Acknowledgements Special thanks to Dr. Xin Fan for the insightful discussions during the drafting of this paper.

Author contributions DL Shi proposed and contributed to the whole research, interpretation, and writing of the paper.

Data availability statement The data that support the findings of this study is available from the author upon reasonable request.

Declarations The author declares that there is no conflict of interest.

8 References

1. Allioui, H & Mourdi, Y. 2023. Unleashing the potential of AI: Investigating cutting-edge technologies that are transforming businesses. *International Journal of Computer Engineering and Data Science (IJCEDS)*, 3(2): 1-12.
2. Naidu, A. 2019. Impact of artificial intelligence on society. *Indian Institute of Science, Working Paper Series*: 1-13.
3. Brock, JKU & Von Wangenheim, F. 2019. Demystifying AI: What digital transformation leaders can teach you about realistic artificial intelligence. *California Management Review*, 61(4): 110-134.
4. Lauriola, I; Lavelli, A & Aiolli, F. 2022. An introduction to deep learning in natural language processing: models, techniques, and tools. *Neurocomputing*, 470: 443-456.
5. Goldberg, Y. 2022. *Neural Network Methods for Natural Language Processing*. Springer Nature. https://doi.org/10.1007/978-3-031-02165-7.

6. Haleem, A; Javaid, M & Singh, RP. 2022. An era of ChatGPT as a significant futuristic support tool: A study on features, abilities, and challenges. *Benchcouncil Transactions on Benchmarks, Standards and Evaluations*, 2(4): 100089.
7. Fui-Hoon Nah, F; Zheng, R; Cai, J; Siau, K & Chen, L. 2023. Generative AI and ChatGPT: Applications, challenges, and AI-human collaboration. *Journal of Information Technology Case and Application Research*, 25(3): 277-304.
8. Ray, PP. 2023. ChatGPT: A comprehensive review on background, applications, key challenges, bias, ethics, limitations and future scope. *Internet of Things and Cyber-Physical Systems*, 3: 121-154. DOI: 10.1016/j.iotcps.2023.04.003.
9. Baidoo-Anu, D & Ansah, LO. 2023. Education in the era of generative artificial intelligence (AI): Understanding the potential benefits of ChatGPT in promoting teaching and learning. *Journal of AI*, 7(1): 52-62.
10. Shi, D. 2023. *ChatGPT Practical Guide: How to Use AI Chatbots to Solve Problems and Create Value*. Amazon Kindle Book. ASIN: B0C1DRYV9H.
11. Mathew A. 2023. Is artificial intelligence a world changer? A case study of OpenAI's chat GPT. *Recent Progress in Science and Technology*, 5: 35-42.
12. Wu, T; He, S; Liu, J; Sun, S; Liu, K; Han, QL & Tang, Y. 2023. A brief overview of ChatGPT: The history, status quo and potential future development. *IEEE/CAA Journal of Automatica Sinica*, 10(5): 1122-1136.
13. Ausat, AMA; Rachman, A; Rijal, S; Suherlan, S & Azzaakiyyah, HK. 2023. Application of ChatGPT in improving operational efficiency in the context of entrepreneurship. *Jurnal Minfo Polgan*, 12(1): 1220-1228.
14. Patel, VV. 2023. *Revolutionizing Marketing Efficiency with ChatGPT*. GSFC University, Vadodara.
15. George, AS & George, AH. 2023. A review of ChatGPT AI's impact on several business sectors. *Partners Universal International Innovation Journal*, 1(1): 9-23.
16. McGeorge, D. 2023. *The ChatGPT Revolution: How to Simplify Your Work and Life Admin with AI*. John Wiley & Sons.
17. Firaina, R & Sulisworo, D. 2023. Exploring the usage of ChatGPT in higher education: Frequency and impact on productivity. *Buletin Edukasi Indonesia*, 2(1): 39-46.
18. Borger, JG; Ng, AP; Anderton, H; Ashdown, GW; Auld, M; Blewitt, ME; Brown, DV; Call, MJ; Collins, P; Freytag, S & Harrison, LC. 2023. Artificial intelligence takes center stage: exploring the capabilities and implications of ChatGPT and other AI- assisted technologies in scientific research and education. *Immunology and Cell Biology*.
19. Żammit, J. 2023. Harnessing the power of ChatGPT for mastering the maltese language: A Journey of breaking barriers and charting new paths. In: *Machine Intelligence for Smart Applications: Opportunities and Risks*: pp 161-178. Cham: Springer Nature Switzerland.
20. Mogavi, RH; Deng, C; Kim, JJ; Zhou, P; Kwon, YD; Metwally, AHS; Tlili, A; Bassanelli, S; Bucchiarone, A; Gujar, S & Nacke, LE. 2023. Exploring user perspectives on chatgpt: Applications, perceptions, and implications for ai-integrated education. *arXiv preprint arXiv*: 2305.13114.
21. Ozdemir, S. 2023. *Quick Start Guide to Large Language Models: Strategies and Best Practices for Using ChatGPT and Other LLMs*. Addison-Wesley Professional.
22. Wang, M; Wang, M; Xu, X; Yang, L; Cai, D & Yin, M. 2023. *Unleashing ChatGPT's Power: A Case Study on Optimizing Information Retrieval in Flipped Classrooms via Prompt Engineering*. IEEE Transactions on Learning Technologies.
23. Henrickson, L & Meroño-Peñuela, A. 2023. Prompting meaning: a hermeneutic approach to optimising prompt engineering with ChatGPT. *AI & SOCIETY*, pp1-16. DOI: https://doi.org/10.1007/s00146-023-01752-8.
24. Shihab, SR; Sultana, N & Samad, A. 2023. Revisiting the use of ChatGPT in business and educational fields: possibilities and challenges. *BULLET: Jurnal Multidisiplin Ilmu*, 2(3): 534-545.
25. Prieto, SA; Mengiste, ET & García de Soto, B. 2023. Investigating the use of ChatGPT for the scheduling of construction projects. *Buildings*, 13(4): 857.
26. Lyu, Q; Tan, J; Zapadka, ME; Ponnatapura, J; Niu, C; Myers, KJ; Wang, G & Whitlow, CT. 2023. Translating radiology reports into plain language using ChatGPT and GPT-4 with prompt learning: results, limitations, and potential. *Visual Computing for Industry, Biomedicine, and Art*, 6(1): 9.
27. White, J; Fu, Q; Hays, S; Sandborn, M; Olea, C; Gilbert, H; Elnashar, A; Spencer-Smith, J & Schmidt, DC. 2023. A prompt pattern catalog to enhance prompt engineering with chatgpt. *arXiv preprint arXiv:2302.11382*.
28. Giray, L. 2023. Prompt engineering with ChatGPT: a guide for academic writers. *Annals of Biomedical Engineering*, pp 1-5.
29.White, J; Hays, S; Fu, Q; Spencer-Smith, J. & Schmidt, DC. 2023. Chatgpt prompt patterns for improving code quality, refactoring, requirements elicitation, and software design. *arXiv preprint arXiv:2303.07839*.
30. Vemprala, S; Bonatti, R; Bucker, A & Kapoor, A. 2023. Chatgpt for robotics: design principles and model abilities. *Microsoft Autonomous Systems and Robotics Research*, 2: 20.
31. Tan, Y; Min, D; Li, Y; Li, W; Hu, N; Chen, Y & Qi, G. 2023. Evaluation of ChatGPT as a question answering system for answering complex questions. *arXiv preprint arXiv:2303.07992*.
32. Deldjoo, Y. 2023. Fairness of ChatGPT and the role of explainable-guided prompts. *arXiv preprint arXiv:2307.11761*.
33. Chen, J; Chen, L; Huang, H & Zhou, T. 2023. When do you need chain-of-thought prompting for ChatGPT?. *arXiv preprint arXiv:2304.03262*.
34. Alneyadi, S. & Wardat, Y. 2023. ChatGPT: Revolutionizing student achievement in the electronic magnetism unit for eleventh-grade students in Emirates schools. *Contemporary Educational Technology*, 15(4): ep448.

35. Kooli, C. 2023. Chatbots in education and research: a critical examination of ethical implications and solutions. *Sustainability*, 15(7): 5614.
36. Zhuo, TY; Huang, Y; Chen, C & Xing, Z. 2023. Exploring ai ethics of chatgpt: a diagnostic analysis. *arXiv preprint arXiv:2301.12867*.

Original Article

Optimizing geological design of J-shaped deviation oil & gas well by deepening kickoff point

Lei Huang[1] ©

Abstract

In the geological design of 2-D J-shaped deviated oil and gas wells, once the coordinates of wellhead and production layer target are determined (restricted by specific ground conditions and underground understanding, respectively), the position of the kickoff point (KOP) becomes very sensitive. By deepening the kickoff point (KOP) based on the current conventional fixed upper position and the dog leg severity (DLS) remaining unchanged within the penetrated range, a smaller drill axis and an angle between the production layer and axis can be obtained at the same designated target point to extend the section of penetrated oil-bearing layers, expand the oil drainage area, increase proven reserves, and ultimately enhance the oil production and recovery during the contract period. In addition, after optimization, it is expected to save 1-2% of well drilling costs by reducing drilling time. With the help of drilling engineering and production engineering, drilling KOP can be achieved easily in deeper and harder rock formations, which is able to improve the efficiency of the electric submersible pump (ESP) and to avoid eccentric wear of the ESP, resulting in extension of the service life of the ESP. This optimized design also runs in parallel with various well stimulation programs and projects without any confliction of each other. This design can be either used for comparison of the parameters of the completed inclined wells with assumed ones of deepening KOP design to show how the deepening KOP can be used to differentiate the increased thickness of the penetrated target layers and the drainage area of target zones, or it can be utilized to compare any pair of parameters between inclined production wells within a range. In the same drilling field, any random increase of 1° inclination angle in a stable inclination section can lead to a corresponding increase in the thickness of the penetrated oil-bearing layer and production. Our research results quantitatively indicate that in the geological design of J-shaped deviation oil and gas wells, the KOP can be re-set from a shallower fixed position along the current conventional trajectory to a reasonable position as deep as possible, which shall be suitable for most situations of optimizing well performance, especially for some restricted complex surface conditions and energy-deficient reservoirs, which assign the KOP a new geological significance in line with the business strategy of rapid oil recovery.

Key words: J-shaped oil & gas well, deviation, inclination, deepening, kickoff point (KOP), penetrated thickness.

Affiliation Info: [1] China National Oil and Gas Exploration and Development Company Ltd., No.6-1 Fuchengmen North Street, Xicheng District, Beijing, China. Postal Code 100037

Article Info: Received: 2 August 2023 / Revised: 4 October 2023 / Accepted: 3 December 2023 / Published Online: 12 December 2023. www.naturalisscientias.com

Authors' Contact Info: Huang, L: Huanglei@cnpcint.com

Citation: Huang, L. 2024. Optimizing geological design of J-shaped deviation oil & gas well by deepening kickoff point. Naturalis Scientias, 1(1): 100-105. DOI: https://doi.org/10.62252/NSS.2024.1007.

Corresponding Author©: Huang, L, PhD; Email: Huanglei@cnpcint.com

1 Introduction

With the development and improvement of drilling engineering technology in the oil & gas field, a variety of well types have been developed to meet the needs of oil & gas field exploitation, for example, traditional vertical wells, inclined wells, directional wells, multi-branch wells and so on. Among which, the vertical wells have their axes of borehole trajectory generally vertical to target layers within a permissible deviation range, that is, the horizontal projection distance between wellhead and its bottom should be close enough (for example, less than 30m is a critical standard for completing drilling target). However, for other well types, with geological design, the horizontal projection distance between wellhead and its bottom has been obviously extended away[1 & 2].

In practice, it is more and more common to drill multiple directional wells within the same well site to achieve the purpose of a uniform underground well pattern design in order to reduce the surface land cost and meet the requirements of environmental protection simultaneously. Based on this situation, this paper only deals with one-dimensional (1D) and two-dimensional (2D) well trajectories widely used at present (mainly J-shaped deviation oil & gas wells), other than three-dimensional (3D) well trajectories that are more complex and also less utilized. The well trajectory of J- shaped deviation well mainly consists of three sections, namely from top to bottom: the straight well section, the increasing inclination section, and the stable inclination section. Among them, the starting (or outset) point of transition from the vertical well section to the increasing inclination section is called the kickoff point (KOP) in 2D J-shaped directional well trajectory[2 & 3].

From the perspective of oil and gas reservoir development engineering, the important difference between directional wells and traditional vertical wells is that the drilling thickness of the production layer, which can directly reflect the productivity, no longer depends solely on the vertical thickness of the production layer, but is closely related to the inclination angle of well topography in the reservoir section[4]. Once the coordinates both of wellhead and target layer center are determined (namely the target distance is confirmed), the depth position of the kickoff point (KOP) in pre-drilling geological design becomes very sensitive.

2 Feasibility

2.1 Reservoir development

In drilling trajectory design within 2D section for the J-shaped deviation oil & gas wells, KOP shall be shifted downwards from the current shallower conventional fixed position to a deeper position, with the dog-leg severity (DLS) remaining unchanged within permission scope. In this case, a gentler angle between axes of drilling bit and pay zone surface can be obtained to allow the well trajectory in the stable inclination section to enter the target layer with a larger inclination angle. So that while drilling the same assigned target point (namely control point - CP) with a greater angle, a thicker oil-bearing interval can be penetrated, which can effectively extend well drainage area, increase proved reserves, and resultantly enhance both well production and EOR within life of contract[5].

Furthermore, this optimizing design of drilling trajectory can run parallel with various well stimulations and programs, e.g., well location deployment, well pattern arrangement, well type design, separate subzone development, improvement of petrophysical property of reservoir[4-5], and so on without confliction.

2.2 Drilling engineering

In LFY oilfield, only if deeper than 2100m True vertical depth subSea (TVDSS) subject to stratigraphic compaction, the formation hardness can meet the threshold requirement of environmental parameter for KOP drilling. On this basis, the further deeper KOP position is designed. With the increase of formation depth and rock hardness, it will be easier and easier for KOP to operate, where drilling model shifts from rotary steering bottom hole assembly (BHA) to directional drilling BHA.

2.3 Production engineering

Theoretically, the electric submersible pump (ESP) is formally required to be set at the position where is exactly close to the top of perforation interval of production well adjacent to the injection well. Such a positioning is to avoid the adverse effects on the pump efficiency caused by the decline of formation pressure and the upward shift of the bubble point in the later stages of oil field production. However, in actual production, in order to protect the electric submersible pump, most of the current electric submersible pumps in LFY Oilfield are set above or near the KOP, where the DLS is nearly 0°.

After optimizing and deepening the KOP, it will be beneficial to move the electric submersible pump downward closer to the top of the perforation section in the actual oil field site, boost ESP efficiency, avoid eccentric wear, and extend the service life of the ESP[4 & 6].

Parameter comparison between already completed deviation oil & gas well and assumed case of deepening its KOP

2.4 Selection of analytical wells

In this study, 97 wells have been selected from 128 available deviation wells with E pay zone as target, which are almost uniformly distributed all over the I oil field, while others have been rejected either due to nearly vertical trajectories or nearly horizontal, both of which are unqualified as deepening KOP sample. The 97 selected wells account for 3/4 of the total numbers of the deviation wells, and thus can fully meet the needs of the study for E pay zone in the I oil field.

DLS selection in increasing inclination section for assumed case of deepening KOP

In this study, 4° has been chosen as DLS angle, which is believed to be within conservative index. However, if choosing an angle smaller than 4o as max DLS in any deviation wells, it is considered to be far beyond conservative index in terms of standard of drilling engineering industry.

Based on the definition, DLS is an angle variation of drill bit at per 30m along drilling trajectory in the three-dimensional space. When entering an increasing inclination section starting from KOP, drilling trajectory can be assumed to follow a circular arc with 430m radius, namely, 30*(360/4)/pi()/2=430m.

Following the circular arc with a radius of 430m in the increasing inclination section the drilling bit starts from the KOP and shifts to stable inclination section until it runs down to the key point where the tangent line, the extended line of the bit axis, and the assigned target point (CP) in E pay zone exactly intersect. In other words, the drilling bit follows the tangent line at the end point of the circular arc with the same inclination and azimuth, and penetrates the same CP. Indeed there is little deviation between the above calculation and actual drilling trajectory at well site, but this is so minor that can be negligible and tolerable in this research. Fig.1 shows parameter comparison between completed deviation oil & gas wells and assumed case of deepening its KOP (Fig. 1).

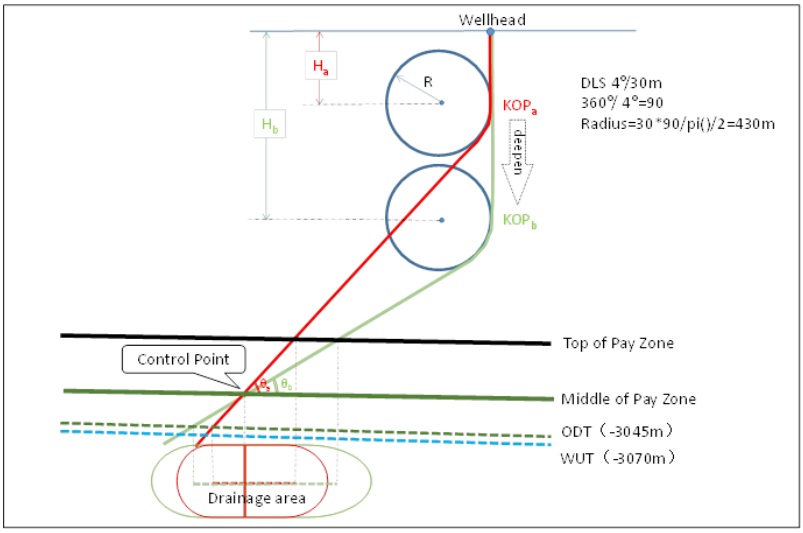

Figure 1. Parameter comparison between completed deviation oil & gas wells and assumed case of deepening its KOP
(A schematic diagram of an existing directional well and its hypothetical deeper formation inclination point)

The error between this theoretical analysis and the actual situation at the drilling site is small and considered to be acceptable.

2.5 Availability of deepening KOP In vertical distance

Currently, KOP average depth position is conventionally fixed at 2150m TVDSS. Average vertical distance from KOP to CP is 866m (minimum 693m). Assuming the circular arc is 430m in radius, i.e., the maximum vertical distance in the increasing inclination section needed is no more than 430m when maximum drilling trajectory inclination angle reaches ~90°. However, in reality, statistics show that average vertical space of the increasing inclination segment is only 332m in this study. Therefore, there is large enough remaining vertical space surplus for deepening KOP in E pay zone of LFY oilfield[7].

2.6 Scenarios analysis

Scenario 1, deepening KOP 100m

When 100m of deepening KOP is assumed, the average thickness of the penetrated target zone is increased by 11m, equivalent to an increase of 6% comparing with that before deepening. Drainage area of the drilled target zone is increased by 0.4 km2 on average, compared with that before deepening, in which drainage radius is conservatively set at 250m only.

Scenario 2, deepening KOP 200m

When 200m of deepening KOP is assumed, an average increase in thickness of the penetrated target zone is 38m, which is 21% more than before deepening, while average increase of the drainage area of the drilled target zone is 1.5 km^2, compared with that before deepening, in which drainage radius is still conservatively set at 250m as shown in Fig.2.

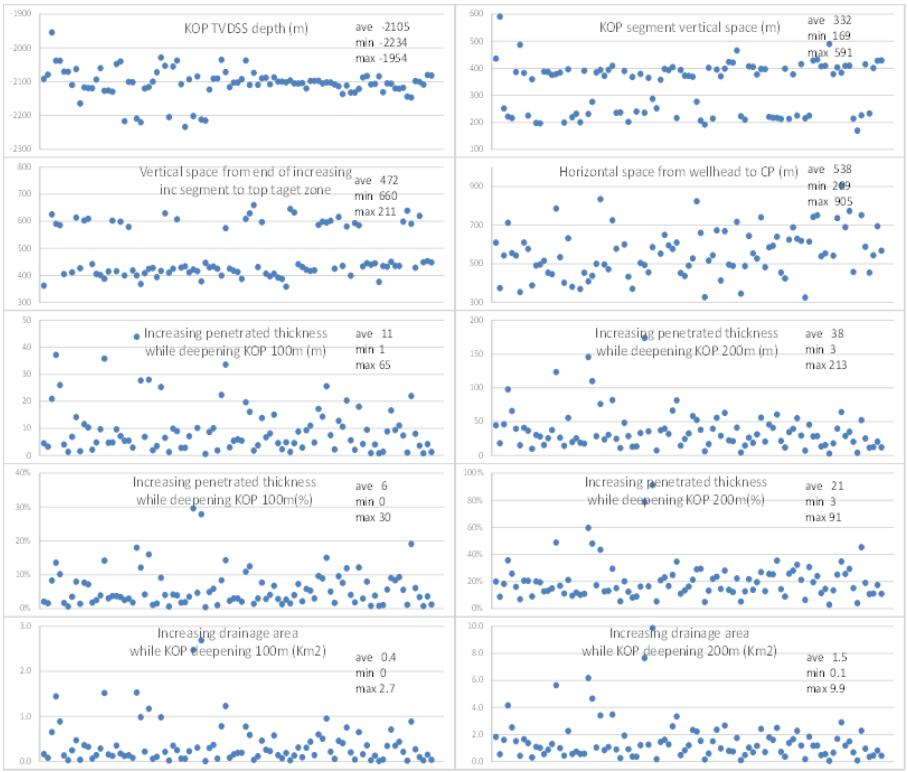

Figure 2. Two scenarios analysis

2.7 Parameter comparisons between any pair of current producing wells within the same drilling pads

Within the adjacent area in any specific well site, there are only relatively minor lateral geological changes in the target zone, in other words, almost remaining the same thickness of true oil-bearing zone. In the stable inclination sections, all selected wells in any selected pad are bearing different inclinations respectively. Furthermore any selected pad must be required to at least include one vertical well as a reference in this statistics process, so that the comparisons can become more meaningful and integrated.

2.8 Inclination angle in stable inclination section versus penetrated measure thickness of oil-bearing zone

The analysis of 16 selected pair data shows that when the inclination angle increases any 1° in the stable inclination section, the penetrated measured thickness of oil-bearing zone gently increases 1.35m accordingly (horizontal wells are excluded from this quantitative statistics).

2.9 Inclination angle

Study of the inclination angle in the stable inclination section versus average daily production of first month data analysis based on 11 selected pair data out of 13 indicate that when the inclination angle increases any 1° in the stable inclination section, the daily production of first month gently increases by 16 barrels accordingly（horizontal wells are also excluded from the quantitative statistics）as shown in Table 1.

Table 1. Parameter comparison

Pad	Well name	Well type	Trajectory inclination at pay zone (°)	Penetrated thickness (oil zone + poor oil zone)	Increased penetrated thickness (%)	Perferating interval thichness	Choke size (/64")	Production style	First month of average oil production (stb/pd)	First month increasing prodution (%)
1	1	V	0	86	100%	43	40	Nature flow	828	100%
	1-D1	D	44	139	162%	54	40	Nature flow	1269	153%
2	2	V	0	36	100%	15	40	Nature flow	261	100%
	2-D2	D	29	113	314%	37	36-32	Nature flow	586	225%
	2-D1	D	35	128	356%	57	40-36	Nature flow	1451	556%
	2-D3	D	48	150	417%	70	40-36	Nature flow	430	165%
3	3	V	0	90	100%	37	22	ESP	448	100%
	3-D1	D	42	115	128%	38	36	Nature flow	929	207%
	3-D2	D	44	131	146%	57	40-36	Nature flow	1564	349%
	3-H1	H	90	784	871%	808	48	Nature flow	3111	694%
4	4	V	0	68	100%	Not yet been put into production				
	4-D1	D	36	75	110%					
	4-D2	D	36	75	110%					

3 Discussion

As discussed in section “Scenario 2”, we can adjust 200m section below KOP to above KOP along the drilling trajectory, in other words, the 200m section drilling mode from directional drilling BHA is shifted upwards to rotary steering BHA, by which about 1 day drilling time can be saved because the upper vertical drilling mode is twice as fast as the lower sidetracking one. After the optimization, 1-2% drilling expenditure will be cut down by reducing the drilling time. In addition, the extension of ESP service life, increase in proven reserves and well production can bring additional remarkable potential economic benefits.

4 Conclusions

To summarize, in the geological design of two-dimensional J-shaped directional well drilling, if setting the KOP at a unified and fixed threshold depth that meets the deflection requirements of the drilling engineering and drilling engineering significance, then the KOP should be appropriately lowered to the proper depth according to the geological conditions, which would give KOP a brand new and more important geological connotation.

Especially, for some restricted complex surface conditions, e.g., if oil-bearing sections in the oilfield are paritially covered by local natural preservation zones and/or drilling is forbidden by severe local laws, then the geological optimazition along preservation zone's boundary with deepening KOP in oil & gas well will surely be a win-win recommended solution to effectively control both well pattern unbalance and reservoir development unbalance in the plane.

In addition, for some reservoirs with an inadequate natural energy supply, deepening KOP to meaningfully extend the well drainage area and to increase proved reserves are quite feasible and commendable remedy actions, which indeed meet the business strategy of rapid oil recovery during oil & gas field development.

Author contributions L Huang proposed and contributed to the whole research, interpretation, and writing of the paper. The author prepared and reviewed the manuscript and approved the final version of the manuscript.

Data availability statement The data that support the findings of this study is available from the author upon reasonable request.

Declarations The author declare that he has no conflict of interest.

5 References

1. Jia, CZ. 2004. *SEC Estimation Approach for Oil & Gas Reserves*. Beijing: Petroleum Industry Publishing House, pp28-65 (**in Chinese**).
2. Yuan, QF. 2014. *Practice and Understanding of Oilfield Development*. Beijing: Petroleum Industry Publishing House, pp7-82 (**in Chinese**).
3. Adnan, A.M; Jeremy, C; Goff, A.; Horbury, D. & Sadooni, N. 2010. The Petroleum Geology of Iraq. Baghdad：Scientific Press, pp28-84.
4. Mu, LX. 2021. Design strategy and methods of development plan at oversea oilfield. Beijing: Petroleum industry publishing house, pp63-89.
5. Liu, BH. 2009, *Encyclopedia of Petroleum Exploration and Development in China*. Beijing: Petroleum industry publishing house, pp444-449.
6. Chilingar, GV; Bissell, HJ; Fairbridge, RW. 1967. *Carbonate rocks*. Amsterdam, London, and New York: Elsevier Publishing Company, pp61-86.
7. Dake, LP. 1994. *The Practice of Reservoir Engineering*. Amsterdam: Elsevier Science Publisher, pp23-27.

Original Article

The limitations and constraints of ChatGPT: an annotated bibliography for researchers and professionals

Shaoyi He[1] ©

Abstract

This annotated bibliography delves into the intricate web of limitations and constraints that surround ChatGPT, a pioneering natural language processing AI model. As AI technologies continue to redefine human-computer interaction, understanding the boundaries and potential pitfalls of these systems becomes paramount. This comprehensive resource compiles a diverse array of sources, including academic studies, reports, and analyses, published between December 2022 and August 2023 and dedicated to unraveling specific facets of ChatGPT's limitations and constraints. Annotated entries not only provide succinct summaries of these limitations but also offer critical assessments, shedding light on their significance, credibility, and real-world implications. The annotated bibliography aims to be an essential guide for researchers, developers, policymakers, and users, navigating the complexities of ChatGPT's constraints while fostering responsible AI development, informed decision-making, and ethical AI usage. In an era where AI plays an increasingly integral role in our lives, understanding the limitations and constraints of such technologies is not merely an academic exercise but a crucial step toward harnessing their potential for the betterment of society.

Key Words: annotated bibliography; ChatGPT; limitations; constraints; researchers; professionals

---

Affiliation Info: [1] Jack H. Brown College of Business and Public Administration, California State University, San Bernardino, USA

Article Info: 20 November 2023 / Revised: 6 December 2023 / Accepted: 10 December 2023 / Published Online: 12 December 2023. www.naturalisscientias.com

Authors' Contact Info: He, S: she@csusb.edu

Citation: He, S. 2024. The limitations and constraints of ChatGPT: an annotated bibliography for researchers and professionals. Naturalis Scientias, 1(1): 106-130. DOI: https://doi.org/10.62252/NSS.2024.1008.

Corresponding Author©: He, S; Email: she@csusb.edu

1 Introduction

ChatGPT, an acronym for Chat Generative Pre-trained Transformer, represents a substantial language model-driven chatbot that was developed by OpenAI and unveiled on November 30, 2022. It empowers users to shape and guide conversations according to their preferences, allowing control over factors such as conversation length, format, style, level of detail, and language employed. In the rapidly evolving landscape of artificial intelligence, ChatGPT stands as a testament to the transformative power of natural language processing models. Its capacity to generate coherent and contextually relevant text responses has ushered in a new era of human-computer interaction, touching countless aspects of our lives, from education and customer service to content creation and beyond. Yet, amid the euphoria surrounding the capabilities of ChatGPT, it is imperative not to overlook its inherent limitations and constraints.

This annotated bibliography represents an earnest endeavor to dive deep into the multifaceted boundaries and constraints that ChatGPT encounters in its applications. While the AI community has celebrated its achievements, it has also engaged in rigorous scrutiny, producing an array of insightful studies, reports, and analyses. This bibliography serves as a curated compendium of these invaluable sources, offering a comprehensive exploration of ChatGPT's limitations and constraints.

The curated annotated entries within this bibliography span a spectrum of perspectives and research methodologies, each contributing to a nuanced understanding of ChatGPT's constraints. These sources explore diverse facets of the technology's limitations and constraints, ranging from its contextual comprehension challenges and susceptibility to biases to its difficulties in handling sensitive data and the ethical implications of its usage.

Our goal here is twofold: firstly, to provide a consolidated repository of these sources, enabling researchers, developers, policymakers, and users to navigate the complex terrain of ChatGPT's constraints with ease, and secondly, to offer critical assessments of these sources. Through these assessments, we aim to unravel the significance, credibility, and real-world ramifications of the identified limitations and constraints, equipping stakeholders with the insights necessary for responsible development, informed decision-making, and ethical utilization of ChatGPT and similar AI-driven conversational systems.

As we navigate the intricate intersection of artificial intelligence and human communication, this annotated bibliography strives to be a beacon of knowledge and discernment. It is our hope that the insights and perspectives contained within these annotated sources will not only illuminate the path toward harnessing ChatGPT's strengths but also guide us in addressing and mitigating its limitations and constraints effectively.

There are a large variety of types of limitations and constraints of ChatGPT that have the potential to advance the research on ChatGPT’s capabilities, applications, and performances in both academic and professional environments. This annotated bibliography includes the following more interesting and important types that have caught attention of scholars, researchers and professionals.

Vulnerability to malicious use:

Concerns about potential exploitation for malicious purposes take precedence due to the wide-ranging implications of misuse.

Biases and fairness issues:

Addressing biases is crucial for promoting fairness and equity in AI applications, making it a high-priority consideration.

Challenge in upholding ethical standards:

Ensuring adherence to ethical standards is paramount for responsible AI deployment, necessitating continuous monitoring and oversight.

Potential for misinformation propagation:

Preventing the spread of misinformation is critical, given the impact on public understanding and the potential consequences of inaccurate information.

Lack of inherent moral understanding:

The absence of genuine moral understanding highlights the need for AI systems to better navigate nuanced ethical dilemmas.

Inability to discern harmful Intent:

The model's difficulty in discerning harmful intent raises ethical concerns, particularly in preventing content that could encourage harm or illegal activities.

Need for user verification:

Ensuring user identity verification becomes more important, especially to prevent impersonation and misuse by malicious actors.

Insufficient safeguards against harmful content:

Strengthening safeguards to consistently prevent the generation of harmful or offensive material is a priority to uphold user safety.

No inherent sense of user well-Being:

Considering user well-being becomes crucial, emphasizing the need for AI systems to prioritize positive user experiences.

Security risks in model deployment:

Implementing robust security measures during model deployment is essential to prevent unauthorized access or manipulation.

Algorithmic bias and explainability:

Addressing algorithmic biases and enhancing explainability are key to fostering trust and accountability in AI applications.

Limited task-specific performance:

The need for task-specific improvements underscores the importance of enhancing ChatGPT's performance in various applications.

Challenge in adapting to bew information:

The model's limitation in adapting to new information necessitates ongoing updates to maintain accuracy and reliability.

Usability and satisfaction concerns:

User satisfaction and usability concerns, including issues related to reliability, are important for fostering positive interactions.

Potential for overreliance on AI:

Awareness of the potential for overreliance on AI emphasizes the importance of informed decision-making and responsible usage.

2 Annotated bibliography

Presented in the following section is the annotated bibliography for the academic studies on the limitations and constraints of ChatGPT, alphabetically arranged by the last name of the first author of the papers published before November 2023.

Abdulai, AF & Hung, L. 2023. Will ChatGPT Undermine Ethical Values in Nursing Education, Research, and Practice. Nurs. Inq. e12556–e12556.

In this commentary article, the authors, who are nursing researchers specializing in digital health technology and AI, express concerns that extend beyond the safety implications of ChatGPT. They are also wary of its ability to encompass the ethical values, principles, and fundamental doctrines that underpin the unique field of nursing. Recent editorials and commentaries in specific nursing journals have discussed the potential benefits, limitations, and risks associated with integrating ChatGPT into nursing education and practice. In this article, the authors further elaborate on these discussions by considering how the adoption of ChatGPT might potentially erode the very values, principles, and foundational assumptions that support nursing research, education, and practice. They aim to prompt discussions on the current and emerging trends in ChatGPT utilization within the nursing domain. Their goal is to actively involve nursing scholars, educators, and practitioners across international networks in conversations regarding nursing paradigms in the context of technological integration.

Alawida, M; Mejri, S; Mehmood, A; Chikhaoui, B & Isaac Abiodun, O. 2023. A Comprehensive Study of ChatGPT: Advancements, Limitations, and Ethical Considerations in Natural Language Processing and Cybersecurity. Information, 14(8), 462.

This research undertakes an exhaustive examination of ChatGPT, a cutting-edge language model reshaping generative text. We conduct a thorough analysis encompassing its architecture, training data, and evaluation metrics while tracing its evolution and improvements over time. The paper scrutinizes the capabilities and constraints of ChatGPT in various natural language processing (NLP) tasks, spanning language translation, text summarization, and dialogue generation. Additionally, a comparative evaluation against other language generation models is presented, shedding light on ChatGPT's versatility in diverse tasks. Ethical and privacy considerations related to ChatGPT are addressed, accompanied by insights into potential mitigation strategies. The research delves into the role of ChatGPT in cyberattacks, emphasizing associated security risks. Finally, the paper explores the wide-ranging applications of ChatGPT across industries, evaluating its performance across languages and domains. In essence, this paper offers a comprehensive exploration of ChatGPT's profound impact on the NLP field.

AlZu'bi, S; Mughaid, A; Quiam, F & Hendawi, S. 2022. Exploring the capabilities and limitations of ChatGPT and alternative big language models. In: *Artificial Intelligence and Applications*.

This paper delves into the phenomenon of ChatGPT, an AI-powered chatbot developed by OpenAI, which has garnered immense popularity since its public launch in November 2022. Renowned for its versatility in writing essays, emails, poems, and even computer code, ChatGPT serves as a valuable tool for professionals across diverse fields. However, it is crucial to note that ChatGPT's responses are generated by a GAN, occasionally deviating from reality. The primary objective of this paper is to construct a text classification model for a chatbot using Python. The model undergoes training on a dataset comprising customer responses to a survey and their corresponding class labels. Various classifiers, including Naive Bayes, Random Forest, Extra Trees, and Decision Trees, are trained and tested. The results reveal that the Extra Trees classifier outperforms others with an accuracy of 90%. The study emphasizes the significance of text preprocessing and the selection of appropriate classifiers for text classification tasks in building an efficient chatbot. Furthermore, the paper explores the capabilities and limitations of ChatGPT and its alternatives in the year 2023. A comprehensive overview of the alternatives' performance is presented, culminating in a discussion on the future directions of large language models and their broader impact on society and technology.

Alzboon, MS; Qawasmeh, S; Alqaraleh, M; Abuashour, A; Bader, AF & Al-Batah, M. 2023. Pushing the envelope: investigating the potential and limitations of ChatGPT and artificial intelligence in advancing

computer science research. In: ***2023 3rd International Conference on Emerging Smart Technologies and Applications (eSmarTA)*****, pp 1-6. IEEE.**

This paper explores the transformative impact of artificial intelligence (AI) on computer science, offering new avenues for data analysis, modeling, and prediction. Among the AI models, ChatGPT, based on deep neural networks, exhibits promise in natural language processing, image recognition, and data analysis. Nevertheless, the integration of ChatGPT and other AI models into scientific research encounters challenges and limitations. The primary focus of this study is to analyze and address the constraints of ChatGPT and AI in computer science research. Specifically, we target two key objectives. Firstly, we address Domain expertise restrictions, recognizing the potential lack of specialized subject knowledge in ChatGPT and similar language models. This deficiency poses challenges for researchers in specific domains. Our investigation delves into methodologies to enhance the integration of domain knowledge into AI models, facilitating more precise and contextually relevant predictions. Secondly, we tackle interpretability difficulties inherent in AI models, a significant hurdle impeding researchers' comprehension of algorithmic decision-making processes. The study proposes strategies to enhance interpretability, providing researchers with insights into the mechanisms behind AI model predictions. The overarching goal is to foster the ethical and responsible use of AI in scientific research by addressing these objectives. The paper examines diverse strategies aimed at refining the representation of domain knowledge within AI models and enhancing their interpretability. Through these efforts, we aim to empower researchers to harness the benefits of ChatGPT and AI while mitigating their inherent limitations.

Amaro, I; Della Greca, A; Francese, R; Tortora, G & Tucci, C. 2023. AI unreliable answers: A case study on ChatGPT. In: ***International Conference on Human-Computer Interaction*****, pp 23-40. Cham: Springer Nature Switzerland.**

In this study, the researchers examined the reliability of answers from ChatGPT and how expert users, such as Computer Science students, perceive its reliability. Initially, they assessed the accuracy of ChatGPT's responses by testing its narrative, problem-solving, searching, and logic capabilities, providing examples of the answers obtained. Subsequently, a user study involving 15 participants familiar with the chatbot was conducted. The participants posed a predetermined set of queries, generating both correct and incorrect responses, and their satisfaction levels were collected. Results indicated that, despite occasional unreliability in the current version of ChatGPT, users still express an intention to utilize it. Consequently, it is recommended to use the current version of ChatGPT in conjunction with human verification and interpretation for enhanced reliability.

Ayub, I; Hamann, D; Hamann, CR & Davis, MJ. 2023. Exploring the potential and limitations of chat generative pre-trained transformer (ChatGPT) in generating board-style dermatology questions: a qualitative analysis. ***Cureus*****, 15(8).**

This paper explores the constraints of Chat Generative Pre-trained Transformer (ChatGPT), an OpenAI language model, when used as a study tool in dermatology. Employing ChatPDF, an application integrating PDF files with ChatGPT, the study generated American Board of Dermatology Applied Exam (ABD-AE)-style questions from Journal of the American Board of Dermatology articles. A qualitative analysis by two board-certified dermatologists assessed 40 questions for accuracy, complexity, and clarity, revealing that only 16 (40%) were deemed suitable for ABD-AE study preparation. Limitations observed included low complexity, lack of clarity, and inaccuracies, highlighting ChatGPT's challenges in grasping domain-specific knowledge in dermatology. The model's inability to understand context and generate high-quality distractors, coupled with the absence of image generation capabilities, further diminishes its utility. The study underscores that while ChatGPT may assist in generating simple questions, it cannot replace the expertise of dermatologists and medical educators in crafting high-quality, board-style questions that effectively assess candidates' knowledge and reasoning abilities.

Azaria, A. 2022. ChatGPT usage and limitations. hal-03913837.

This research delves into the multifaceted utility of large language models across diverse domains such as conversational agents, education, and explainable AI. One notable instance is ChatGPT, a substantial language

model crafted by OpenAI specifically designed as a conversational agent. Given its extensive training on vast datasets, ChatGPT's responses are inevitably influenced by the characteristics inherent in the training data. In this paper, a distinctive bias in ChatGPT related to the usage of digits in numbers is emphasized. Notably, a remarkably high correlation is unveiled between the frequency of digits generated by ChatGPT and the preferred numbers of humans, with the most frequently generated digit aligning with the widely favored human number, 7. Additionally, we explore the advantageous aspects of ChatGPT as a conversational agent and deliberate on certain limitations inherent in its design.

Bang, J & Park, G. 202). Uprising of ChatGPT and ethical problems. *Robotics & AI Ethics*, pp 1-11.

This paper investigates ethical considerations arising from the introduction of ChatGPT, focusing on moral competence and proposing ethical solutions. Employing a comprehensive review of literature and media reports from both Eastern and Western perspectives, the study analyzes ChatGPT's technology, operational methods, and associated ethical concerns. The examination reveals potential issues such as plagiarism, copyright infringement, test fairness, criminal misuse, social stereotypes, privacy invasion, security vulnerabilities, diminished critical thinking, and erosion of genuine human relationships. Evaluation based on moral competence highlights the feasibility of implementing moral identity, moral sensitivity, and moral practice, but underscores limitations in moral judgment. To address these ethical challenges, the study advocates for a utilitarian approach, emphasizing decisions that maximize societal benefits while minimizing harm. The conclusion emphasizes the necessity of embedding ethical perspectives into responsible AI toolkits and frameworks for balanced decision-making in the design, development, adoption, deployment, maintenance, and evolution of ChatGPT. Furthermore, it underscores the importance of a multi-stakeholder approach for fostering a socially beneficial AI society.

Barrot, JS. 2023. Using ChatGPT for second language writing: pitfalls and potentials. *Assessing Writing*, 57, 100745.

This research delves into the contemporary developments in artificial intelligence, specifically focusing on the utilization of chatbots as valuable aids in language learning. Among these tools, ChatGPT stands out, offering users a natural and human-like interactive learning experience. Despite its potential as an effective language tutor and source of linguistic input, concerns have been raised by academics regarding its influence on writing pedagogy and academic integrity. This tech review seeks to comprehensively examine both the potential advantages and challenges associated with integrating ChatGPT into second language (L2) writing contexts. The paper concludes by providing recommendations for enhancing L2 writing classroom practices in light of these findings.

Belgas, I; Hilal, I & Afifi, N. 2023. Large language models in e-learning: advantages and limitations of ChatGPT. In: *COC2023*.

This paper explores the ever-evolving landscape of education in the contemporary era, propelled by the advent of new artificial intelligence technologies. Intelligent systems, including Large Language Models (LLMs) like ChatGPT, play a crucial role in enhancing the learning process by leveraging knowledge from tutors and transferring it to learners. Distinguished by its capability to effectively interact with human queries through Natural Language Processing (NLP) tools, ChatGPT comprehends human intent and generates responses.
The primary objective of this work is to identify, collect, and synthesize numerous research endeavors that delve into the utilization of LLMs in the field of education. Subsequently, a comparative study is conducted to illuminate the advantages and disadvantages gleaned from these works, providing insights that can fuel new research ideas for future endeavors in this domain.

Bengio, Y. 2023. AI and catastrophic risk. *Journal of Democracy*, 34(4): 111-121.

This paper explores the growing concerns about the potential threats to democracy stemming from the release of large language models such as Chat-GPT and GPT-4 by OpenAI. The focus is on the concept of "rogue AIs," which refers to powerful and hazardous artificial intelligences capable of pursuing harmful objectives independently of human intentions. The essay advocates for proactive measures to address the risks posed by these rogue AIs to

democracy and global geopolitical stability. The author emphasizes the need for international collaboration and suggests that research into safe and defensive AI technologies should be conducted through a multilateral network involving research laboratories from various countries.

Borji, A. 2023. A categorical archive of ChatGPT failures. *arXiv* preprint arXiv:2302.03494.

In this paper, the author explored various drawbacks of ChatGPT and emphasized its limitations. While it exhibits impressive capabilities in specific tasks, there is a necessity for further improvements to excel in areas such as logical reasoning, solving mathematical problems, mitigating biases, and more. Presently, ChatGPT remains susceptible to these issues. It is uncertain whether these limitations can be resolved given the ambiguous capabilities of current technology. The reliability and credibility of both ChatGPT and upcoming models are also under scrutiny. While this research thoroughly evaluates ChatGPT, it does possess certain shortcomings that should be addressed in subsequent studies, as outlined below:

- The extent to which ChatGPT memorizes versus understands what it generates is still unknown.
- The degree to which ChatGPT possesses commonsense and ways to enhance it is uncertain.
- ChatGPT seems limited in its ability to generate creative solutions to novel problems, particularly in unsolved mathematics.
- ChatGPT lacks a mechanism to indicate when it is uncertain about its answers.
- ChatGPT's responses are inconsistent and can sometimes be contradictory.
- The existence of biases in the training data is one of the primary ethical concerns surrounding the use of ChatGPT.
- ChatGPT's capacity to comprehend and address intricate inquiries is restricted.
- The use of ChatGPT has the potential to impersonate a trusted person.
- Unintended consequences are often challenging to predict.

Carvalho, I & Ivanov, S. 2023. ChatGPT for tourism: applications, benefits and risks. *Tourism Review*.

This paper explores the applications, advantages, and potential risks of ChatGPT and large language models within the tourism sector, aiming to establish a research agenda for further investigation. By reviewing existing literature on ChatGPT, large language models, and artificial intelligence, the paper identifies areas where ChatGPT could be applied for various stakeholders in the tourism industry. The findings suggest that ChatGPT and similar models are poised to significantly impact tourism processes, improving customer service, and enhancing efficiency in operations. While potential negative consequences on human resources are acknowledged, the overall impact is anticipated to be positive, particularly in empowering and assisting tourism employees. This study contributes to the field by providing insights into the potential implications of ChatGPT in tourism and hospitality, representing one of the initial explorations in this area.

Cheng, HW. 2023. Challenges and limitations of ChatGPT and artificial intelligence for scientific research: a perspective from organic materials. *AI*, 4(2): 401-405.

This paper has concentrated on delineating the challenges and limitations encountered by ChatGPT within the realm of organic materials research, with the goal of offering insights into the obstacles faced by researchers in this particular field. The author has discerned that ChatGPT exhibits a deficiency in furnishing valuable information, attributable to three potential limitations in its responses: (i) computational calculation constraints, (ii) the propensity for inaccurate or false facts, and (iii) shortcomings in inferential capability. These limitations have the potential to engender misunderstandings or misinterpretations. The author has also scrutinized various ethical considerations with potential concerns, including the risk of biases in the generated content stemming from biases present in user-provided data, apprehensions regarding privacy and security when handling sensitive or unpublished data, and the possibility that the generated content may be subject to intellectual property laws, thereby giving rise to legal complexities and the risk of copyright violations. Additionally, accountability assumes significance as a critical aspect to be taken into account in the deployment of AI tools such as ChatGPT in scientific research.

Chowdhury, MNUR & Haque, A. 2023. ChatGPT: its applications and limitations. In: *2023 3rd International Conference on Intelligent Technologies (CONIT)*, pp 1-7. IEEE.

This paper examines ChatGPT, a cutting-edge language model that has garnered widespread attention for its remarkable ability to generate human-like responses to natural language inputs. Trained on an extensive corpus of text data, ChatGPT delivers swift and accurate responses across a diverse array of user queries. However, alongside its impressive capabilities, the model grapples with certain limitations. A primary challenge lies in ChatGPT's propensity to generate biased or inappropriate responses based on its training data. Furthermore, its reliance on statistical patterns in text data may pose difficulties in handling more nuanced or complex language tasks. Despite these limitations, ChatGPT marks a significant advancement in conversational AI, with vast potential applications ranging from chatbots and customer service to content creation and education. As technology progresses, it is anticipated that more sophisticated language models will emerge, surpassing the capabilities of ChatGPT and addressing some of its limitations. This evolution promises even greater strides in the development of conversational AI, opening up new possibilities for enhanced applications in various fields.

Cotton, DR; Cotton, PA & Shipway, JR. 2023. Chatting and cheating: ensuring academic integrity in the era of ChatGPT. *Innovations in Education and Teaching International*, 1-12.

This paper investigates the application of artificial intelligence, particularly focusing on ChatGPT, in the realm of academia—a topic of considerable interest in the education sector. While ChatGPT brings about advantages such as heightened student engagement, improved collaboration, and enhanced accessibility, it also introduces apprehensions regarding academic integrity and plagiarism. The study thoroughly explores the opportunities and challenges associated with integrating ChatGPT into higher education, weighing the potential risks and rewards of these AI tools. Additionally, it scrutinizes the complexities of identifying and preventing academic dishonesty and proposes strategies that universities can adopt to ensure ethical and responsible usage of such tools. These strategies encompass the formulation of policies and procedures, provision of training and support, and the implementation of diverse methods for detecting and thwarting cheating. In conclusion, the paper asserts that despite the dual nature of opportunities and challenges presented by AI in higher education, universities can effectively navigate these concerns through a proactive and ethical approach to the incorporation of these tools.

Currie, GM. 2023. Academic integrity and artificial intelligence: is ChatGPT hype, hero or heresy? In: *Seminars in Nuclear Medicine*. WB Saunders.

This paper examines the impact of artificial intelligence advancements on academic integrity in higher education and scientific writing, with a particular focus on the role of ChatGPT in addressing associated challenges. Unlike traditional algorithms, ChatGPT, powered by GPT-3.5, stands out for its ability to generate precise and realistic responses to questions in real-time. While holding promise in various applications, this chatbot faces notable constraints when applied to nuclear medicine and radiology. In the context of nuclear medicine, ChatGPT's susceptibility to errors and the potential generation of false information pose risks to professionalism, ethics, and integrity. These limitations compromise the reliability of ChatGPT, falling short of the expected standards required in these fields. However, despite these challenges, there are promising applications for ChatGPT in nuclear medicine within educational, clinical, and research domains. Integrating ChatGPT into practice requires a reevaluation of norms and a reshaping of expectations regarding information reliability. This paper explores both the constraints and potential applications of ChatGPT in nuclear medicine, emphasizing the need for careful consideration and adaptation of existing practices to fully harness its capabilities.

Dave, T; Athaluri, SA & Singh, S. 2023. ChatGPT in medicine: an overview of its applications, advantages, limitations, future prospects, and ethical considerations. *Frontiers in Artificial Intelligence*, 6, 1169595.

This paper conducts an in-depth analysis of the advantages, limitations, ethical considerations, future prospects, and practical applications associated with ChatGPT and artificial intelligence (AI) in the healthcare and medical sectors. Operating as an advanced language model, ChatGPT utilizes deep learning techniques to generate human-like responses to natural language inputs. As part of the generative pre-training transformer (GPT) model family

developed by OpenAI, ChatGPT stands as one of the largest publicly available language models. Capable of capturing the nuances of human language, ChatGPT demonstrates its potential applications in the medical domain. From identifying research topics to aiding professionals in clinical and laboratory diagnosis, its versatility extends to keeping healthcare practitioners informed about updates and developments in their fields. The creation of virtual assistants to support patients in managing their health is another crucial application of ChatGPT in medicine. Despite the promising applications, the integration of ChatGPT and other AI tools in medical writing raises ethical and legal concerns. These include potential copyright infringement, medico-legal complications, and the imperative need for transparency in AI-generated content. In conclusion, while ChatGPT exhibits numerous potential applications in the medical and healthcare sectors, this paper thoroughly examines the associated limitations and ethical considerations. The future prospects in medicine and healthcare are also explored, emphasizing the need for a balanced and conscientious approach to the integration of AI technologies.

Day, T. 2023. A preliminary investigation of fake peer-reviewed citations and references generated by ChatGPT. *The Professional Geographer*, 1-4.

The author analyzes the academic citations and references generated by the ChatGPT artificial intelligence (AI) chatbot and reveals the citations and references are in fact, fake. They are clearly generated by a predictive process rather than known facts. This suggests that early optimism regarding this technology for assisting in research could be misplaced, and that student misuse of the chatbot can be detected by the identification of fake citations and references. Despite these problems, the technology could have application in the writing of course materials for lower level undergraduate courses that do not necessarily require references. Subject matter expertise is required, however, to identify and remove incorrect information. The need to identify incorrect information provided by an AI chatbot is a skill that students will also increasingly need.

Derner, E & Batistič, K. 2023. Beyond the safeguards: exploring the security risks of ChatGPT. *arXiv* preprint arXiv:2305.08005.

This paper addresses the escalating concerns surrounding the safety, security risks, and ethical considerations associated with the widespread use of large language models (LLMs), exemplified by ChatGPT. The focus is on exploring various security risks linked to ChatGPT, encompassing malicious text and code generation, disclosure of private data, provision of fraudulent services, information gathering, and the generation of unethical content. Through an empirical study, we evaluate the effectiveness of ChatGPT's content filters and scrutinize potential methods to circumvent these safeguards, highlighting persistent ethical implications and security risks within LLMs even when protective measures are implemented. Drawing from a qualitative analysis of security implications, we propose potential strategies to mitigate these risks, providing valuable insights for researchers, policymakers, and industry professionals dealing with the intricate security challenges presented by LLMs like ChatGPT. This study contributes to the ongoing discourse surrounding the ethical and security considerations associated with LLMs, emphasizing the necessity for continuous research in this domain.

Deshpande, A; Murahari, V; Rajpurohit, T; Kalyan, A & Narasimhan, K. 2023. Toxicity in ChatGPT: Analyzing persona-assigned language models. *arXiv* preprint arXiv:2304.05335.

Large language models (LLMs) have demonstrated remarkable capabilities, extending beyond the natural language processing (NLP) community and finding application in various sectors such as healthcare, therapy, education, and customer service. As these models are utilized by users with critical information needs, such as students or patients interacting with chatbots, ensuring the safety of these systems becomes paramount. Therefore, it is essential to have a clear understanding of the capabilities and limitations of LLMs. To address this, the authors conducted a systematic evaluation of toxicity in over half a million generations of ChatGPT, a popular dialogue-based LLM. Our findings indicate that adjusting the system parameter of ChatGPT by assigning it a persona, such as that of the boxer Muhammad Ali, significantly increases the toxicity of its responses. Depending on the assigned persona, the toxicity of ChatGPT can rise by up to 6x, leading to outputs that involve incorrect stereotypes, harmful dialogue, and hurtful opinions. This has the potential to be defamatory to the persona and harmful to unsuspecting users. Additionally, the authors observed troubling patterns where specific entities, such as certain races, are targeted more than others (3x

more), irrespective of the assigned persona, revealing inherent discriminatory biases in the model. the authors hope that these findings prompt the broader AI community to reconsider the effectiveness of current safety measures and encourage the development of improved techniques that ensure the robustness, safety, and trustworthiness of AI systems.

Elyoseph, Z & Levkovich, I. 2023. Beyond human expertise: the promise and limitations of ChatGPT in suicide risk assessment. *Frontiers in psychiatry*, 14.

This paper explores the potential of ChatGPT, an artificial intelligence language model developed by OpenAI, in the realm of mental health, with a specific focus on suicide prevention. While ChatGPT holds theoretical promise, its clinical abilities in addressing this significant mental health concern remain untested. To bridge this knowledge gap, the study aims to compare ChatGPT's assessments of mental health indicators with those of mental health professionals, particularly in the context of a hypothetical case study centered on suicide risk assessment. In this investigation, ChatGPT was tasked with evaluating a text vignette describing a hypothetical patient exhibiting varying levels of perceived burdensomeness and thwarted belongingness. The assessments provided by ChatGPT were then compared to the norms established by mental health professionals. The results revealed that, across all conditions, ChatGPT rated the risk of suicide attempts lower than mental health professionals did. Additionally, in most conditions, ChatGPT rated mental resilience lower than the established norms. These findings suggest that individuals, including gatekeepers, patients, or mental health professionals relying on ChatGPT for evaluating suicide risk or enhancing decision-making may receive inaccurate assessments that underestimate the actual risk of suicide.

Esmailzadeh, Y. 2023. Potential risks of ChatGPT: implications for counterterrorism and international security. *International Journal of Multicultural and Multireligious Understanding* (IJMMU) Vol 10.

This paper delves into the examination of potential risks associated with ChatGPT, a language generation model developed by OpenAI, concerning counterterrorism and international security. Despite its widespread adoption, ChatGPT's strengths and weaknesses raise practical and ethical concerns that warrant careful consideration. The escalating use of modern communication technologies by terrorists has intensified the complexity of intelligence challenges, making critical data access increasingly difficult for intelligence agencies. Terrorist groups leverage new technologies and implement enhanced operational security measures, posing challenges to sophisticated intelligence collection operations. Moreover, the advent of artificial intelligence amplifies the threat of cyberattacks and espionage, as individuals and groups exploit these technologies. The study analyzes ChatGPT's potential risks across four critical domains: the implications of artificial intelligence on future threats and international security, the influence of ChatGPT on cyberterrorism and artificial intelligence, the hazards associated with fragmented and secondary information in violence and sabotage operations, and the utilization of psychological warfare against targets. By offering insights and recommendations, this research aims to guide policymakers and researchers in effectively employing artificial intelligence technology while minimizing potential risks.

Ferrara, E. 2023. Should ChatGPT be biased? challenges and risks of bias in large language models. *arXiv* preprint arXiv:2304.03738.

This paper examines the challenges and risks associated with biases present in large-scale language models like ChatGPT. It delves into the sources of biases, including aspects such as training data, model specifications, algorithmic constraints, product design, and policy decisions. The paper also addresses ethical concerns stemming from the unintended consequences of biased model outputs. Additionally, it assesses potential opportunities to mitigate biases, the inevitability of certain biases, and the implications of deploying these models in various applications like virtual assistants, content generation, and chatbots. Furthermore, the paper analyzes existing approaches to identify, quantify, and address biases in language models. It underscores the necessity for a collaborative, multidisciplinary effort to develop AI systems that are more equitable, transparent, and responsible. The overarching goal of this paper is to stimulate thoughtful dialogue within the artificial intelligence community, prompting researchers and developers to contemplate the role of biases in generative language models and the ongoing pursuit of ethical AI.

Frieder, S; Pinchetti, L; Griffiths, RR; Salvatori, T; Lukasiewicz, T; Petersen, PC & Berner, J. 2023. Mathematical capabilities of ChatGPT. *arXiv* preprint arXiv:2301.13867.

This research delves into the mathematical capabilities of two versions of ChatGPT (released on January 9, 2023, and January 30, 2023) as well as GPT-4. To assess their performance, The authors employed a novel methodology, testing them on publicly available datasets and custom-created datasets. Unlike formal mathematics, which benefits from extensive databases of formal proofs (e.g., the Lean Mathematical Library), existing datasets for natural-language mathematics, used for evaluating language models, are limited, often covering only elementary mathematics. In response, The authors have released two new datasets, GHOSTS and miniGHOSTS, curated by active mathematics researchers. These datasets aim to (1) encompass graduate-level mathematics, (2) offer a comprehensive overview of language models' mathematical capabilities, and (3) assess various dimensions of mathematical reasoning. The study also explores whether ChatGPT and GPT-4 can serve as helpful assistants to professional mathematicians, emulating scenarios encountered in their daily activities. The authors conducted a thorough evaluation using fine-grained performance metrics, representing the most detailed assessment for advanced mathematics to date. The findings indicate that ChatGPT excels as a mathematical assistant for factual inquiries, effectively functioning as a mathematical search engine and knowledge base interface. GPT-4, while suitable for undergraduate-level mathematics, falls short when confronted with the challenges of graduate-level difficulty. Despite media reports emphasizing GPT-4 and ChatGPT's success in solving exams (potentially influenced by selection bias), their overall mathematical performance is considerably below that of a graduate student. Consequently, if the aim is to rely on ChatGPT for success in a graduate-level math exam, one would be better off consulting an average peer!

Gao, J; Zhao, H; Yu, C & Xu, R. 2023. Exploring the feasibility of ChatGPT for event extraction. *arXiv* preprint arXiv:2303.03836.

This paper addresses the fundamental task of event extraction in natural language processing, involving the identification and extraction of information about events mentioned in text. Despite being a challenging task due to the scarcity of annotated data, the emergence of large language models (LLMs) like ChatGPT provides an opportunity to tackle language tasks without the need for specific datasets and fine-tuning. While ChatGPT has demonstrated impressive results in tasks like machine translation, text summarization, and question answering, it encounters challenges in complex tasks such as event extraction. Unlike other tasks, event extraction requires the model to be provided with a complex set of instructions defining all event types and their schemas. To assess the feasibility of ChatGPT for event extraction and the challenges it poses, a series of experiments were conducted. The results reveal that, on average, ChatGPT performs at only 51.04% of the level of a task-specific model like EEQA in long-tail and complex scenarios. Usability testing experiments indicate that ChatGPT lacks robustness, and continuous refinement of the prompt does not lead to stable performance improvements, potentially resulting in a poor user experience. Additionally, ChatGPT exhibits high sensitivity to different prompt styles.

Gladstone, R. 2023. Using ChatGPT in the classroom: opportunities, limitations, and ethical considerations. *Spicer Adventist University Research Articles Journal*, 2(1): 17-25.

This paper marks a significant juncture in the landscape of open artificial intelligence (AI), specifically in November 2022. The educational community witnessed a notable shift as a sophisticated chatbot, ChatGPT, developed by OpenAI, rapidly amassed a million users within a month. Delving into the historical trajectory of ChatGPT, this paper aims to unravel its capabilities and scrutinize the potential benefits and limitations of integrating it as a teaching tool in the classroom. Moreover, the paper undertakes a thorough examination of the ethical concerns and privacy implications associated with the utilization of models like ChatGPT. The overarching goal is to provide educators with valuable insights, equipping them with the knowledge needed to effectively incorporate ChatGPT into their teaching practices while maintaining a vigilant awareness of ethical considerations.

Gravel, J; D'Amours-Gravel, M & Osmanlliu, E. 2023. Learning to fake it: limited responses and fabricated references provided by ChatGPT for medical questions. *Mayo Clinic Proceedings: Digital Health*, 1(3): 226-234.

This study aimed to assess the quality of answers and references provided by ChatGPT for medical questions. Three researchers posed 20 medical questions to ChatGPT, requesting corresponding references. Medical experts, who were the corresponding authors of the 20 articles from which the questions were derived, evaluated the responses using a verbal numeric scale ranging from 0% to 100%. Initially planning to assess three references per response for pertinence, this was modified due to preliminary findings indicating the fabrication of most references by ChatGPT. The study, conducted in February 2023, revealed responses ranging from 53 to 244 words, with 2 to 7 references per answer. Feedback from 17 of the 20 invited raters indicated limited response quality, with a median score of 60%. Additionally, the raters identified major (n=5) and minor (n=7) factual errors in 17 responses. Of the 59 references evaluated, 41 (69%) were found to be fabricated, despite appearing real. Fabricated citations often included names of authors with relevant previous publications, seemingly pertinent titles, and a credible journal format. This underscores the need for users to scrutinize ChatGPT's provided references, particularly when integrating them into medical manuscripts.

Hadi, MU; Qureshi, R; Shah, A; Irfan, M; Zafar, A; Shaikh, MB & Mirjalili, S. 2023. A survey on large language models: applications, challenges, limitations, and practical usage. *TechRxiv*.

This paper delves into the expansive realm of computerized language processing, focusing on the transformative presence of Large Language Models (LLMs). Within the domain of artificial intelligence, LLMs wield remarkable capabilities, demonstrating an unparalleled capacity to grasp intricate linguistic nuances and generate coherent and contextually fitting responses. Exploring their historical roots, architecture, training methodologies, applications, and challenges, this survey paper aims to provide a comprehensive understanding of LLMs. Commencing with an exploration of fundamental concepts in generative AI and an analysis of the architecture of generative pretrained transformers (GPT), the paper proceeds to trace the evolution of LLMs over time. It delves into the various training methods employed in shaping these models. Moving beyond theoretical foundations, the survey outlines the diverse applications of LLMs across fields such as medicine, education, finance, and engineering, elucidating how they contribute to solving real-world problems. As LLMs increasingly shape the landscape of AI, this paper scrutinizes the associated challenges in deploying them in practical scenarios. Addressing ethical considerations, model biases, interpretability, and computational resource requirements, the survey sheds light on the complexities involved. It further underscores techniques aimed at bolstering the robustness and controllability of LLMs, while also tackling issues related to bias, fairness, and generation quality.
In conclusion, the paper anticipates the future trajectory of LLM research, emphasizing the need to overcome challenges to enhance the reliability and utility of these models. Designed as a valuable resource for researchers, practitioners, and enthusiasts, this survey consolidates state-of-the-art knowledge in the field, serving as a compass for advancements in the development and application of LLMs across a spectrum of real-world contexts.

Haverkamp, W; Tennenbaum, J & Strodthoff, N. 2023. ChatGPT fails the test of evidence-based medicine. *European Heart Journal-Digital Health*, ztad043.

This research underscores the crucial need to acknowledge the limited documentation of the training data and methods employed by ChatGPT, much of which has been shrouded in secrecy. Notably, ChatGPT, when directly questioned, lacks the ability to specify the incorporation of medical guidelines into its training. The standard of evidence-based medicine necessitates transparency in sourcing and a meticulous selection of those sources, highlighting the importance of clarity regarding the utilized guidelines for comprehensibility. Furthermore, the imperative for information currency is emphasized, with the knowledge and training data for ChatGPT having a last cut-off date in September 2021. In a comprehensive assessment, ChatGPT reveals numerous gaps and limitations that warrant an in-depth discussion among medical experts. This discourse should pave the way for an objective evaluation of ChatGPT's clinical relevance and applicability. Unfortunately, discussions surrounding the capabilities of chatbots often prove ambiguous and problematic. It is unlikely, even with improvements, that ChatGPT will achieve the competence, reliability, and trustworthiness demanded by evidence-based medicine. Perhaps, future

advancements may introduce more specialized systems that address the concerns raised in this study. Only time will unveil the trajectory of these developments.

Hou, Y; Yeung, J; Xu, H; Su, C; Wang, F & Zhang, R. 2023. From answers to insights: unveiling the strengths and limitations of ChatGPT and biomedical knowledge graphs. *medRxiv*, 2023-06.

This paper examines the performance of Large Language Models (LLMs) in the context of natural language processing tasks, with a particular focus on their application in the biomedical domain. Despite their exceptional capabilities in language generation and knowledge acquisition from unstructured text, LLMs encounter limitations in this specialized field, leading to inaccuracies and inconsistencies. In response to these challenges, Biomedical Knowledge Graphs (BKGs) have emerged as valuable tools for structured information representation and organization.
The study evaluates the capabilities of ChatGPT, particularly the GPT-4.0 version, in comparison to both GPT-3.5 and existing BKGs concerning question answering, knowledge discovery, and reasoning. The results indicate that while ChatGPT excels in providing existing information, BKGs demonstrate superior reliability in information delivery. However, ChatGPT exhibits limitations in novel discoveries and reasoning, especially in establishing structured links between entities when compared to BKGs. To address these shortcomings, the paper suggests that future research should focus on integrating LLMs and BKGs, capitalizing on their complementary strengths. This integrated approach holds the potential to optimize task performance, mitigate risks, and advance knowledge in the biomedical field, contributing to overall well-being.

Huallpa, JJ. 2023. Exploring the ethical considerations of using Chat GPT in university education. *Periodicals of Engineering and Natural Sciences*, 11(4): 105-115.

This research delves into the ethical quandaries associated with the integration of Chat GPT into higher education, particularly focusing on the context of Latin American institutions of higher learning. A survey involving 220 participants through an online questionnaire aimed to understand their experiences and motivations in utilizing AI-powered conversational agents. Descriptive statistics provided a demographic overview of the participants. This study not only establishes a foundation for further exploration but also uncovers hidden meanings within observed phenomena, proposing potential solutions to the identified issues. It examines how AI systems and chatbots can complement human knowledge and judgment, alongside potential drawbacks. Results indicated that participants perceived Chat GPT integration as moderately accessible with moderately positive social attitudes. They acknowledged the value and responsibility of Chat GPT in creating personalized educational opportunities. Emphasizing the need for explicit institutional standards on privacy and data security, participants' reliance on AI was influenced by factors such as gender, age, accessibility, social attitude, opinions, personal experience, privacy and data security, institutional guidelines, and individualized learning, as revealed by regression analysis. The findings shed light on the complexities of integrating Chat GPT into Latin American higher education, influenced by individual beliefs, cultural norms, and ethical considerations. The adaptability of AI addresses the busy schedules of students, making resources readily available for success. Natural language processing models offer instant assistance through text chat, voice, or video. The research suggests that to fully grasp the ethical implications and guide the development of responsible implementation strategies, additional qualitative investigations, longitudinal studies, and comparative research across diverse contexts are necessary. Bridging these knowledge gaps will propel the field of conversational AI ethically and beneficially within educational settings.

Hung, J & Chen, J. 2023. The benefits, risks and regulation of using ChatGPT in Chinese academia: a content analysis. *Social Sciences*, 12(7): 380.

This paper investigates the major benefits and risks associated with Chinese students utilizing ChatGPT for academic activities and explores potential regulations for maintaining academic integrity and ethical standards in Chinese academic settings. Utilizing content analysis of 40 relevant newspaper articles retrieved through a Google news search with specific keywords, the study reveals a polarized opinion in China regarding ChatGPT's role in academic responsibilities. While some express concerns about academic cheating facilitated by ChatGPT, others advocate for integrating AI-powered technologies into academic learning to enhance the quality of academic outputs.

Plagiarism violations emerge as a primary concern among Chinese educators. The study suggests the need for increased regulations in Chinese academia, emphasizing the importance of teachers guiding students in fact-checking AI-generated content, incorporating proper citations and references, and approaching AI-powered tools with systematic and creative questioning to optimize intellectual outputs.

Irvine, DJ; Halloran, LJ & Brunner, P. 2023. Opportunities and limitations of the ChatGPT advanced data analysis plugin for hydrological analyses. *Hydrological Processes*, 37(10): e15015.

This paper delves into the transformative impact of artificial intelligence (AI) tools, exemplified by ChatGPT, on various industries, with a specific focus on the evolving landscape of data analyses. While recent discussions have emphasized the ethical considerations associated with AI-generated text, the ChatGPT Code Interpreter, now known as the Advanced Data Analysis plugin, showcases AI's expanding capabilities in generating, translating, and adapting computer scripts. Through four illustrative examples, we highlight ChatGPT's proficiency in prompt-based generation of Python scripts for hydrological dataset analysis. The examples encompass tasks such as converting R functions to Python for baseflow separation, translating MATLAB functions to Python for temperature data 'web scraping,' generating a correlation matrix for major ion groundwater data, and presenting river flow data boxplots. The paper explores the considerable opportunities, existing limitations, and concerns linked to the utilization of ChatGPT in the realm of hydrological data analyses.

Kalla, D & Smith, N. 2023. Study and analysis of Chat GPT and its impact on different fields of study. *International Journal of Innovative Science and Research Technology*, 8(3).

This paper delves into the revolutionary technology of ChatGPT, utilizing advanced artificial intelligence techniques to generate natural language responses in response to prompts or inputs. With applications spanning natural language processing, customer service, and content creation, this study conducts a comprehensive analysis of ChatGPT. It aims to unravel the origins of ChatGPT, elucidate its functioning, and assess its impact across various fields of study.
The investigation systematically examines the advantages and disadvantages of ChatGPT, probing into its inherent limitations and distinctive features. Moreover, the paper explores the ramifications of ChatGPT on diverse domains such as academics, cyber security, customer support, software development, jobs, and information technology. Additionally, it scrutinizes the potential applications of ChatGPT for researchers and scholars, contemplating its evolving role in shaping the landscape of artificial intelligence.

Kenney, NM. 2023. A brief analysis of the architecture, limitations, and impacts of ChatGPT.

This paper commences with an exploration of the technical architecture of ChatGPT and distinguishes its features from other large-scale artificial intelligence language models. Following this, we outline the present use cases of ChatGPT, accompanied by an examination of several existing limitations. Specifically, we scrutinize ChatGPT's challenges in exhibiting creativity, address issues related to the perpetuation of biases, and consider identification concerns. Conclusively, we assess some of the anticipated key impacts of ChatGPT, encompassing considerations of copyright and economic implications. It is noteworthy that this analysis is approached from a non-technical standpoint, aiming to illustrate how AI is progressively intertwining with everyday life.

Khalil, M & Er, E. 2023. Will ChatGPT get you caught? rethinking of plagiarism detection. *arXiv* preprint arXiv:2302.04335.

This study addresses the escalating concerns surrounding the integration of Artificial Intelligence (AI) technology, particularly chatbots, into education and its potential repercussions. The heightened accessibility and enhanced capabilities of advanced AI systems, exemplified by ChatGPT, have raised apprehensions, particularly regarding the use of these chatbots for generating academic essays in educational settings. The primary objective of this research is to investigate the originality of content produced by ChatGPT. Utilizing two widely recognized plagiarism detection tools, the study assesses the originality of 50 essays generated by ChatGPT across various topics. The results reveal that ChatGPT possesses a significant capacity to generate sophisticated and highly original text

outputs, often evading detection by conventional plagiarism check software. This capability raises concerns about students utilizing chatbots as an expedient route to academic success with minimal effort. Furthermore, ChatGPT's ability to verify its own generated essays, showcasing superior performance compared to traditional plagiarism-detection tools, adds an additional layer to the plagiarism-checking process. The paper emphasizes the imperative for educational institutions to adopt appropriate measures to mitigate potential plagiarism issues, contributing to the ongoing debate surrounding the impact of AI technology on education. The research also delves into further implications arising from these findings.

Khoury, R; Avila, AR; Brunelle, J & Camara, BM. 2023. How secure is code generated by ChatGPT? *arXiv* preprint arXiv:2304.09655.

This paper explores the recent strides made by large language models in the realm of artificial intelligence (AI), with particular focus on ChatGPT—an AI chatbot developed and recently introduced by OpenAI, marking a significant advancement in the field. Beyond its proficiency in processing human-like text, ChatGPT demonstrates the unique ability to translate natural language into code. However, amidst these capabilities, the safety of programs generated by ChatGPT becomes a critical consideration. To address this concern, we conduct an experiment wherein ChatGPT is tasked with generating various programs, and we assess the security of the resulting source code. The study delves into whether ChatGPT can be influenced to enhance security through tailored prompts, and scrutinizes the ethical implications of leveraging AI for code generation. The findings suggest that while ChatGPT displays awareness of potential vulnerabilities, it often produces source code that is not sufficiently robust against certain attacks.

Koubaa, A; Boulila, W; Ghouti, L; Alzahem, A & Latif, S. 2023. Exploring ChatGPT capabilities and limitations: a critical review of the NLP game changer.

This paper delves into the recent groundbreaking natural language processing technology, ChatGPT, which emerged just three months ago, capturing significant attention for its exceptional capabilities. This AI milestone has prompted extensive scrutiny from researchers, industry professionals, decision-makers, and governmental bodies, keen on understanding the implications, threats, and benefits associated with this technology. Despite its relatively short existence, several researchers have already explored ChatGPT from diverse perspectives. Here, we offer a comprehensive review of ChatGPT, emphasizing its technical innovations in comparison to preceding models and scrutinizing existing research across various dimensions. Employing a meticulous methodology, we conduct a critical examination of the prevailing literature on ChatGPT, constructing a taxonomy to categorize diverse areas of study. Furthermore, we pinpoint future challenges and potential research trajectories linked to ChatGPT. Serving as the inaugural critical review of ChatGPT literature, this paper provides invaluable insights for practitioners and policymakers, establishing itself as a crucial reference for researchers aiming to advance studies on ChatGPT, spanning its applications and development.

Koubaa, A; Boulila, W; Ghouti, L; Alzahem, A & Latif, S. 2023. Exploring ChatGPT capabilities and limitations: a survey. *IEEE Access*.

This research investigates ChatGPT, an innovative natural language processing technology introduced a few months ago, which has garnered substantial attention for its remarkable capabilities. This milestone in AI has prompted scrutiny from researchers, industry professionals, decision-makers, and governments, delving into its implications, threats, and benefits. Despite its relatively brief existence, various researchers have analyzed ChatGPT from diverse perspectives. The paper offers a comprehensive review of ChatGPT, accentuating its technical advancements compared to prior models and scrutinizing existing research from multiple viewpoints. Employing a rigorous methodology, we conduct a critical examination of the existing ChatGPT research, establishing a taxonomy for various areas of study. Furthermore, we delineate future challenges and research trends associated with ChatGPT. This paper stands as the inaugural critical review of ChatGPT literature, providing valuable insights for practitioners and policymakers alike. It serves as a reference for researchers aiming to propel the research on ChatGPT, encompassing its applications and development.

Koubaa, A; Qureshi, B; Ammar, A; Khan, Z; Boulila, W & Ghouti, L. 2023. Humans are still better than ChatGPT: case of the IEEExtreme competition. *arXiv* preprint arXiv:2305.06934.

This study takes a nuanced approach to the widespread acclaim of ChatGPT's outstanding performance by presenting a distinctive perspective. While previous research has emphasized ChatGPT's capabilities often comparable to or surpassing human skills in diverse tasks, this paper sheds light on a scenario where human proficiency outshines ChatGPT. The focus is specifically on the domain of computer programming, leveraging the IEEExtreme Challenge competition—an esteemed annual international programming contest covering a spectrum of problems with varying complexities—as a benchmark. Through a meticulous evaluation involving a diverse set of 102 challenges from five IEEExtreme editions and employing Python, Java, and C++, our empirical analysis reveals that human programmers excel in specific aspects of problem-solving within the programming context, contrary to prevailing notions. Notably, the average score attained by ChatGPT on the IEEExtreme programming problems is 3.9 to 5.8 times lower than the average human score, depending on the programming language. This paper delves into these findings, offering critical insights into the limitations and potential avenues for enhancement for AI-based language models such as ChatGPT.

Krause, D. 2023. ChatGPT and other AI models as a due diligence tool: benefits and limitations for private firm investment analysis. *SSRN 4416159*.

This paper explores the increasing utilization of ChatGPT and other general AI models for investment due diligence, particularly in the context of evaluating private firms. Challenges arise in this domain as private companies, unlike their public counterparts, are not mandated to disclose extensive information, and the available data tends to be less standardized and comprehensive. Moreover, the complexity and opacity inherent in private markets further compound these challenges. To address these issues, machine learning techniques are employed as potential solutions. Sentiment analysis, for instance, can extract insights from unstructured data sources like SEC filings, social media posts, and news articles. This information, in turn, contributes to the construction of a comprehensive database comprising both structured and unstructured data for the evaluation of private firms. However, it is crucial to acknowledge the limitations of AI models in this context. These models may struggle to grasp the nuances of a private company's business model or its competitive landscape. As a prudent approach, it is emphasized that AI models should be used in conjunction with other due diligence methods, such as traditional financial analysis and industry research. This ensures a more holistic and nuanced evaluation of private companies, taking into account the multifaceted nature of their operations and market dynamics.

Li, Z. 2023. The dark side of ChatGPT: legal and ethical challenges from stochastic parrots and hallucination. *arXiv* preprint arXiv:2304.14347.

This paper underscores the transformative impact of Large Language Models (LLMs) like ChatGPT on our society, reshaping fundamental aspects of how we think, create, and exist. Notably, the integration of GPT in Bing has revolutionized our approach to online searching. Despite the numerous advantages offered by nascent LLMs, a new set of legal and ethical risks is surfacing, particularly concerning stochastic parrots and hallucination. While the European Union (EU) stands at the forefront of jurisdictions addressing AI model regulation, the emerging regulatory paradigm may underestimate the risks posed by these novel LLMs. Consequently, this communication highlights the necessity for further evolution in the European AI regulatory framework to effectively mitigate these risks.

Liu, J; Xia, CS; Wang, Y & Zhang, L. 2023. Is your code generated by ChatGPT really correct? rigorous evaluation of large language models for code generation. *arXiv* preprint arXiv:2305.01210.

This research delves into the long-standing study of program synthesis, with recent emphasis on leveraging the capabilities of Large Language Models (LLMs) for code generation. Traditional programming benchmarks, designed with curated synthesis problems and test cases, serve as a metric for evaluating LLMs' performance in code synthesis. However, these test cases may be limited in both quantity and quality, raising concerns about thoroughly assessing the functional correctness of the generated code in the era of LLMs. To address this concern, we introduce

EvalPlus, a code synthesis benchmarking framework that rigorously evaluates the functional correctness of LLM-synthesized code. EvalPlus enhances an evaluation dataset with an abundance of test cases generated automatically by a test input generator, utilizing both LLM- and mutation-based strategies. While EvalPlus is a general framework, we specifically augment the test cases of the well-known HUMANEVAL benchmark by 81 times to create HUMANEVAL+. Extensive evaluations across 19 popular LLMs, including GPT-4 and ChatGPT, demonstrate that HUMANEVAL+ effectively identifies previously undetected incorrect code synthesized by LLMs, reducing the pass@k by an average of 13.6-15.3%. This work not only reveals that previous evaluations of popular code synthesis may not accurately depict the true performance of LLMs but also suggests a new avenue for improving programming benchmarks through automated testing.

Lo, CK. 2023. What is the impact of ChatGPT on education? A rapid review of the literature. *Education Sciences*, 13(4): 410.

This paper provides a rapid review of ChatGPT, an artificial intelligence-based chatbot launched in November 2022, exploring its capabilities across subject domains, applications in education, and concerns raised by researchers during its initial three months of release (December 2022 to February 2023). Utilizing a content analysis approach with 50 articles from relevant databases and Google Scholar, the review indicates varying performance in different domains, with strengths in areas like economics and programming but shortcomings in mathematics. While ChatGPT shows potential as an instructional assistant and virtual tutor, challenges include generating incorrect information and bypassing plagiarism detectors. The paper emphasizes the need for immediate updates to assessment methods and institutional policies, along with essential instructor training and student education to address ChatGPT's impact on the educational environment.

Marron, L. 2023. Exploring the potential of ChatGPT 3.5 in higher education: benefits, limitations, and academic integrity. In: *Handbook of Research on Redesigning Teaching, Learning, and Assessment in the Digital Era*, pp 326-349. IGI Global.

This paper investigates the potential advantages and challenges associated with the utilization of ChatGPT, a substantial language model, within higher education (HE), with a specific focus on its impact on academic integrity. Employing an exploratory research design, the study unfolds in three distinct phases. Phase 1 examines ChatGPT from the perspective of lecturers, Phase 2 from that of students, and Phase 3 through the lens of academic integrity. The primary objective is to assess whether ChatGPT can be employed to develop educational resources, facilitate collaborative projects, and support students in their academic endeavors. Additionally, the study explores the potential contribution of ChatGPT to instances of academic misconduct. It puts forth strategies to promote transparency and responsible AI use in higher education and provides recommendations for future research directions. In summary, the study asserts that AI can prove beneficial in higher education when employed responsibly and in tandem with effective pedagogical approaches.

Memarian, B & Doleck, T. 2023. ChatGPT in education: methods, potentials and limitations. *Computers in Human Behavior: Artificial Humans*, 100022.

This paper exams ChatGPT within the realm of public scrutiny, particularly in educational contexts. While public opinion has been a focal point, there is a notable gap in the analysis of studies conducted on ChatGPT in educational settings. In response, this review paper meticulously explores the diverse applications, potential benefits, challenges, and future directions of ChatGPT in education. A total of 63 publications were scrutinized using a general framework of open and axial coding. Through coding and summarization of methods, the review comprehensively addresses the potentials, limitations, and future work outlined in each study. Thematic analysis uncovers that existing studies in educational literature predominantly approach ChatGPT through a commentary and non-empirical lens. The potentials identified encompass personalized and intricate learning, specific teaching and learning activities, assessments, asynchronous communication, feedback, research accuracy, personas, and task delegation with cognitive offload.
Simultaneously, the review highlights various challenges that ChatGPT encounters or may face in an educational context, including plagiarism deception, potential misuse or lack of learning, issues of accountability, and privacy

concerns. Balancing both concerns and optimism, the paper emphasizes the critical need to safeguard student learning and uphold academic integrity in the integration of ChatGPT in education. This comprehensive review not only summarizes existing studies but also offers a unique and thorough discussion on future considerations for ChatGPT in the educational landscape.

Mohammad, B; Supti, T; Alzubaidi, M; Shah, H; Alam, T; Shah, Z & Househ, M. 2023. The pros and cons of using ChatGPT in medical education: a scoping review. *Stud Health Technol Inform*, 305: 644-647.

This paper conducts a scoping review to examine the merits and drawbacks of incorporating ChatGPT into medical education. A systematic search across databases including PubMed, Google Scholar, Medline, Scopus, and Science Direct identified 25 eligible studies out of 197 references. The study covers various applications of ChatGPT in medical education, encompassing automated scoring, teaching assistance, personalized learning, research support, quick information retrieval, case scenario and exam question generation, content creation, and language translation. Additionally, the paper addresses the challenges and limitations associated with ChatGPT in medical education, such as its inability to reason beyond existing knowledge, generation of inaccuracies, potential bias, impact on critical thinking skills, and ethical concerns related to exam and assignment integrity and patients' privacy.

Morath, B; Chiriac, U; Jaszkowski, E; Deiß, C; Nürnberg, H; Hörth, K & Green, K. 2023. Performance and risks of ChatGPT used in drug information: an exploratory real-world analysis. *European Journal of Hospital Pharmacy*.

This paper aims to assess the performance and risks associated with utilizing Chat Generative Pre-trained Transformer (ChatGPT) to address drug-related questions. A set of 50 drug-related questions was input into the ChatGPT software, and the resulting answers underwent standardized evaluation by six senior hospital pharmacists. The assessment criteria included content accuracy, patient management feasibility, and associated risks. Reference answers adhering to the German guideline of drug information were used as a benchmark. The findings revealed that only 13 out of 50 answers provided correct content and sufficient information to initiate management without patient harm. The majority of responses were either false (38%) or contained only partial correctness (36%), with no references provided. Approximately 26% of cases posed a high risk of patient harm, while 28% had a low risk. In high-risk cases, actions based on the provided information could potentially lead to patient harm. Furthermore, the study highlighted the lack of reproducibility in ChatGPT's answers over time, indicating substantial variability. In conclusion, the study underscores the challenges associated with the use of ChatGPT in drug information, citing issues such as incorrect content, absence of references, and limited reproducibility.

Nguyen, XH; Nguyen, HA; Cao, L & Truong, H. 2023. Unleashing the potential and recognizing the limitations of ChatGPT. In: *Vietnamese Geography Education*.

This paper studies the potential and limitations of ChatGPT, a cutting-edge language model, within the framework of Vietnamese geography education. The study seeks to analyze ChatGPT's capabilities in enhancing the teaching and learning of geography. By thoroughly exploring its features, including interactive engagement, personalized support, and access to extensive geographic information, the paper highlights the potential advantages of incorporating ChatGPT into geography classrooms. Concurrently, it critically evaluates the model's limitations, encompassing ethical considerations, potential biases, and challenges related to grasping complex geographical concepts. While ChatGPT exhibits potential in the context of Vietnamese geography education, it is imperative for the model to enhance its proficiency in geography-related tasks such as image processing and chart processing. This improvement is crucial for ChatGPT to become a more valuable tool for Vietnamese teachers and students in the realm of geography education. The findings derived from this analysis provide valuable insights, guiding the utilization of ChatGPT to maximize its advantages while conscientiously addressing its limitations, fostering a more effective and inclusive approach to geography education.

Obaid, OI; Ali, AH & Yaseen, MG. 2023. Impact of Chat GPT on scientific research: opportunities, risks, limitations, and ethical Issues. *Iraqi Journal for Computer Science and Mathematics*, 4(4): 13-17.

This paper explores the emergence of chatbots, specifically Generative Pre-trained Transformer (GPT), as a consequence of recent advancements in natural language processing (NLP). While Chat GPT has showcased considerable potential across various domains, including scientific research, its full impact is still unfolding. The aim of this paper is to delve into the possibilities, threats, limitations, and ethical considerations associated with Chat GPT in the realm of scientific research. The examination involves a comprehensive review of the existing literature on Chat GPT and its applications in scientific research, supplemented by illustrative case examples that highlight both the potential benefits and challenges in utilizing Chat GPT for scientific inquiry. The paper concludes by underscoring the ethical issues that necessitate attention before Chat GPT can be seamlessly integrated into the landscape of scientific research.

Pegoraro, A; Kumari, K; Fereidooni, H & Sadeghi, AR. 2023. To ChatGPT, or not to ChatGPT: that is the question! *arXiv* preprint arXiv:2304.01487.

This study addresses the global phenomenon of ChatGPT's widespread usage. As ChatGPT and other Large Language Models (LLMs) gain prominence, concerns regarding potential misuse, including the dissemination of fake news, plagiarism, manipulation of public opinion, cheating, and fraud, have escalated. Consequently, the imperative to distinguish between AI-generated and human-generated content becomes increasingly vital. Researchers have proposed diverse detection methodologies, ranging from basic binary classifiers to more advanced deep-learning models. These techniques vary in their reliance on statistical characteristics, syntactic patterns, semantic information, or contextual cues to enhance accuracy. The main objective of this study is to offer a comprehensive and up-to-date evaluation of the latest techniques in ChatGPT detection. Additionally, we assess the performance of other AI-generated text detection tools that do not explicitly claim to detect ChatGPT-generated content. To conduct our evaluation, we curated a benchmark dataset comprising prompts from ChatGPT and humans, encompassing diverse questions from medical, open Q&A, and finance domains, as well as user-generated responses from popular social networking platforms. This dataset serves as a benchmark for assessing the efficacy of various techniques in detecting ChatGPT-generated content. However, our evaluation results reveal that none of the existing methods can effectively detect ChatGPT-generated content.

Poola, I. 2023. Overcoming ChatGPTs inaccuracies with Pre-Trained AI Prompt Engineering Sequencing Process. *International Journal of Technology and Emerging Sciences (ITJES)*, 3(3): 16-19.

This research explores the role of artificial intelligence (AI) in advancing human inquiries through the lens of ChatGPT, a prominent language model. Developed by OpenAI, ChatGPT replicates human-like interaction, understanding context and generating relevant responses based on extensive training data. While it has gained acclaim for its capacity to effectively address diverse human inquiries with fluent and comprehensive responses, it is not without challenges and limitations. This study focuses on the difficulties and constraints encountered by ChatGPT in its usage. Addressing a variety of use cases, the research aims to illuminate the intricacies and limitations of the ChatGPT AI integration. The paper delves into the specific challenges faced by ChatGPT when employed with OpenAI, examining its shortcomings in logic, factual accuracy, mathematical understanding, coding, and potential biases. Additionally, it explores the broader social implications of ChatGPT's drawbacks. By categorizing these challenges into three distinct groups, the study provides valuable insights for researchers and developers aiming to enhance chatbots and language models. While large language models (LLMs) have demonstrated utility across various domains, this research uniquely focuses on uncovering and analyzing the specific limitations of ChatGPT, including hallucinations. The study underscores the ambiguity that arises in distinguishing text generated by ChatGPT from that authored by humans, given its ability to produce intricate essays, poems, functional code, and even web pages and charts based solely on text descriptions. Acknowledging ChatGPT's potential as a formidable competitor to popular search engines, the research contributes to a nuanced understanding of both the capabilities and limitations of this advanced language model.

Qadir, J. 2023. Engineering education in the era of ChatGPT: Promise and pitfalls of generative AI for education. In: *2023 IEEE Global Engineering Education Conference (EDUCON)*, pp 1-9. IEEE.

This paper delves into the dynamic landscape of engineering education, continually adapting to technological advancements and the evolving demands of the engineering industry. A notable development in this arena is the integration of generative artificial intelligence technology, exemplified by the ChatGPT conversational agent. ChatGPT holds the promise of delivering personalized and efficacious learning experiences by furnishing students with tailored feedback, explanations, and immersive virtual simulations for hands-on learning. However, a comprehensive exploration of this technology necessitates acknowledging its inherent limitations. Generative AI systems like ChatGPT are contingent on their training data and may inadvertently perpetuate biases or propagate misinformation. Moreover, the incorporation of generative AI in education raises ethical concerns, encompassing the potential for unethical or dishonest student use and the prospect of human unemployment due to technological redundancy. While the current state of generative AI technology, as exemplified by ChatGPT, showcases remarkable advancements with inherent flaws, it serves as a precursor to future developments. Engineering educators must grasp the implications of this technology and engage in a thorough examination of how to adapt the engineering education ecosystem. This adaptation aims to ensure that the upcoming generation of engineers can harness the benefits offered by generative AI while mitigating any adverse consequences.

Rane, NL; Choudhary, SP; Tawde, A & Rane, J. 2023. ChatGPT is not capable of serving as an author: ethical concerns and challenges of large language models in education. ***International Research Journal of Modernization in Engineering Technology and Science*****, 5(10): 851-874.**

This paper delves into the dynamic role of ChatGPT and analogous large language models in the field of education, offering a comprehensive examination of their limitations, ethical concerns, and challenges. The research explores the implications of these models in various educational contexts, shaping the landscape of teaching, research, and scholarly communication. The exploration begins by scrutinizing the applications of ChatGPT in scientific writing and publishing. Critically assessing the constraints associated with its educational use, the paper acknowledges limitations in generating authoritative content, comprehending complex subjects, and ensuring information accuracy, presenting significant obstacles to integration into educational practices. Furthermore, the research addresses the ethical dilemmas and potential pitfalls arising from the extensive reliance on generative AI in education, touching on issues of bias, accountability, and the dissemination of misinformation. Emphasizing the importance of maintaining human agency and oversight, the paper underscores the need for responsible AI use in educational settings. It also investigates the impact of ChatGPT on academic research, examining its potential to enhance research productivity and the associated risks to the rigor and authenticity of scholarly work. Strategies and tools for detecting and mitigating academic misconduct involving AI-generated content are explored in detail. In addition, the research delves into the role of ChatGPT in fostering critical thinking skills among students, educators, and researchers. It explores innovative pedagogical methods that leverage generative AI to enhance critical thinking. The paper also considers the implications of ChatGPT on educational policy, addressing privacy concerns, intellectual property rights, and the need for regulations in the evolving landscape of AI in education. These insights are invaluable for educators, researchers, policymakers, and stakeholders aiming to harness the benefits of generative AI while navigating the associated challenges in the educational domain.

Rao, H. 2023. Ethical and legal considerations behind the prevalence of ChatGPT: risks and regulations. ***Frontiers in Computing and Intelligent Systems*****, 4(1): 23-29.**

This paper provides a comprehensive overview of ChatGPT, encompassing its technical model, key capabilities, and various application scenarios. The analysis delves into ethical risks, including concerns about autonomy, moral conduct, human alienation, and value reconstruction. Additionally, legal risks are scrutinized, covering aspects such as legal entity status, copyright ownership, data security, and the opacity of algorithms. The paper then suggests regulatory principles, emphasizing tool positioning, safety, legality, transparency, credibility, fairness, and shared responsibility. Furthermore, it proposes a regulatory pathway that encourages the development of autonomous, safe, and controllable technologies, advocates for improvements in artificial intelligence legislation and justice, and underscores the need for establishing a diverse governance system.

Ray, PP. 2023. ChatGPT: a comprehensive review on background, applications, key challenges, bias, ethics, limitations and future scope. ***Internet of Things and Cyber-Physical Systems*****.**

This paper investigates the transformative impact of artificial intelligence (AI) and machine learning on the realm of scientific research, with a specific focus on the notable advancements in chatbot technology, exemplified by ChatGPT. Offering a comprehensive review, we delve into the background, applications, key challenges, and future directions of ChatGPT. The exploration begins by tracing its origins, development, and underlying technology, followed by an in-depth analysis of its diverse applications across industries such as customer service, healthcare, and education. Critical challenges faced by ChatGPT, including ethical considerations, data biases, and safety issues, are scrutinized, and potential mitigation strategies are discussed. The paper concludes by envisioning the future of ChatGPT, contemplating areas for further research and development. This includes exploring its integration with other technologies, enhancing human-AI interaction, and addressing concerns related to the digital divide. This review aims to provide valuable insights for researchers, developers, and stakeholders navigating the dynamic landscape of AI-driven conversational agents. Additionally, the study delves into the multifaceted ways in which ChatGPT revolutionizes scientific research, encompassing aspects such as data processing, hypothesis generation, collaboration, and public outreach. Ethical considerations and potential challenges associated with the use of ChatGPT in research are examined, emphasizing the need to strike a balance between AI-assisted innovation and human expertise. The paper also sheds light on biases and limitations inherent in ChatGPT, acknowledging the attention it has garnered across academia, research, and industries, despite controversies and ethical concerns.

Rice, S; Winter, SR & Rice, C. 2023. The Advantages and Limitations of Using ChatGPT to Enhance Technological Research. *SSRN 4416080*.

This research investigates ChatGPT, an innovative natural language processing technology introduced a few months ago, which has garnered substantial attention for its remarkable capabilities. This milestone in AI has prompted scrutiny from researchers, industry professionals, decision-makers, and governments, delving into its implications, threats, and benefits. Despite its relatively brief existence, various researchers have analyzed ChatGPT from diverse perspectives. The paper offers a comprehensive review of ChatGPT, accentuating its technical advancements compared to prior models and scrutinizing existing research from multiple viewpoints. Employing a rigorous methodology, we conduct a critical examination of the existing ChatGPT research, establishing a taxonomy for various areas of study. Furthermore, we delineate future challenges and research trends associated with ChatGPT. This paper stands as the inaugural critical review of ChatGPT literature, providing valuable insights for practitioners and policymakers alike. It serves as a reference for researchers aiming to propel the research on ChatGPT, encompassing its applications and development.

Rimban, EL. 2023. Challenges and limitations of ChatGPT and other large language models. *International Journal of Arts and Humanities*, 4(1): 147-152.

This paper delves into the challenges and constraints inherent in large language models, with a specific focus on ChatGPT as an illustrative example. Our exploration commences by examining the potential advantages offered by large language models, emphasizing their proficiency in generating natural language text and aiding in language-related tasks. However, we also acknowledge the prevailing concerns surrounding these models, encompassing environmental impact, potential biases, and the absence of interpretability. Moving forward, we scrutinize the specific challenges confronted by ChatGPT and similar models, highlighting limitations in contextual understanding, struggles with rare or out-of-vocabulary words, and a propensity to generate text that may be nonsensical or offensive. The paper concludes by putting forth recommendations for future research and development, underscoring the necessity for heightened transparency, interpretability, and ethical considerations throughout the creation and deployment phases of large language models.

Rozado, D. 2023. The political biases of ChatGPT. *Social Sciences*, 12(3): 148.

This study delves into recent advancements in Large Language Models (LLMs), signaling their imminent deployment in commercial applications as gateways for human interaction with technology and amassed knowledge. However, concerns about potential political biases embedded in these models raise issues of misuse. In this investigation, we present the findings of subjecting a state-of-the-art Large Language Model, the widely used

ChatGPT from OpenAI, to 15 different political orientation tests (14 in English, 1 in Spanish). The consistent results across these tests reveal that ChatGPT tends to be diagnosed with a preference for left-leaning viewpoints in 14 out of the 15 instruments. Interestingly, when directly questioned about its political preferences, ChatGPT often asserts a lack of political opinions, emphasizing its commitment to providing factual and neutral information. While it is desirable for public-facing artificial intelligence systems to furnish accurate and factual information on empirically verifiable issues, they should also strive for political neutrality, especially on normative questions lacking straightforward empirical validation. Ethical AI systems should aim to present users with balanced arguments, avoiding claims of neutrality when the content displays discernible signs of political bias.

Sanchez-Ramos, L; Lin, L & Romero, R. 2023. Beware of references when using ChatGPT as a source of information to write scientific articles. *American Journal of Obstetrics & Gynecology*.

This research aims to highlight a potential liability associated with the use of ChatGPT in the writing of scientific articles, particularly concerning references. While AI chatbots hold promise in streamlining the article-writing process, our investigation reveals a notable issue with ChatGPT. We have observed that ChatGPT frequently generates erroneous and fictitious references, encompassing incorrect authors, journal names, article titles, publication years, and PubMed identifiers (PMID and DOI). In some instances, the article title may be accurate, but the chatbot includes inaccurate information such as authors. Citations play a crucial role in attributing credit for contributions, identifying sources of ideas, and tracing the development of research. Errors in references not only undermine the credibility of authors but also compromise the trustworthiness of a scientific report. Consequently, it becomes imperative to verify all components of references provided by chatbots. The inaccuracies in ChatGPT's responses are attributed to the vast and diverse text data from various sources, coupled with inconsistencies or inaccuracies in the primary data. It is anticipated that as AI chatbot technology advances, these current limitations will likely see improvement over time.

Sok, S & Heng, K. 2023. ChatGPT for education and research: a review of benefits and risks. *SSRN 4378735*.

This paper explores the applications of Generative Pre-trained Transformer (ChatGPT), an artificial intelligence (AI) tool capable of rapidly generating detailed responses to prompts and subsequent queries. Introduced in November 2022 by OpenAI, an American AI research laboratory, using large language models, ChatGPT holds significant potential in education and research. The article delves into five key benefits of ChatGPT, including its role in creating learning assessments, enhancing pedagogical practices, providing virtual personal tutoring, aiding in outlining, and facilitating idea brainstorming. However, the discussion also addresses potential risks associated with academic integrity, issues of unfair learning assessments, dissemination of inaccurate information, and the risk of over-reliance on AI. The paper concludes by offering a set of recommendations to ensure the effective and responsible utilization of ChatGPT in educational and research contexts.

Stahl, BC & Eke, D. 2024). The ethics of ChatGPT–Exploring the ethical issues of an emerging technology. *International Journal of Information Management*, 74: 102700.

This paper delves into the ethical considerations arising from generative conversational AI systems, exemplified by ChatGPT. Employing established methodologies for examining the ethics of emerging technologies, the study systematically reviews potential benefits and concerns. By combining ethical issues from Anticipatory Technology Ethics, Ethical Impact Assessment, and Ethical Issues of Emerging ICT Applications with AI-specific concerns from the literature, the analysis evaluates ChatGPT's capacity to generate humanlike text and engage in seamless interactions. The findings suggest that while ChatGPT holds the potential for substantial societal and ethical benefits, it also raises noteworthy concerns pertaining to social justice, individual autonomy, cultural identity, and environmental impact. Key ethical concerns encompass responsibility, inclusion, social cohesion, autonomy, safety, bias, accountability, and environmental implications. In contrast to the prevailing discourse narrowly focusing on specific issues like authorship, this analysis systematically uncovers a broader and more balanced spectrum of ethical considerations that warrant attention. The results align with emerging research and industry priorities regarding the ethics of generative AI. Implications underscore the necessity for diverse stakeholder involvement, holistic consideration of benefits and risks during application development, and multi-level policy interventions to

foster positive outcomes. In essence, this analysis illustrates that applying established methodologies for technology ethics can establish a robust and comprehensive foundation to guide discussions and actions surrounding impactful emerging technologies such as ChatGPT, advocating for a sustained, broad ethical perspective as use cases unfold.

Sun, X; Dong, L; Li, X; Wan, Z; Wang, S; Zhang, T & Wang, G. 2023. Pushing the limits of ChatGPT on NLP tasks. *arXiv* preprint arXiv:2306.09719.

This research investigates the factors contributing to the subpar performance of ChatGPT on most Natural Language Processing (NLP) tasks compared to supervised baselines. The authors identify the limitations, including the token limit in prompts, the mismatch between ChatGPT's generation nature and NLP tasks, and intrinsic pitfalls of Large Language Models (LLMs) like hallucination and keyword overemphasis. The study proposes a set of general modules to address these issues and enhance ChatGPT's performance on NLP tasks. These modules include a one-input-multiple-prompts strategy, fine-tuned models for better demonstration retrieval, task transformation for improved alignment with the generation nature, reasoning strategies tailored to task-specific complexity, a self-verification strategy to address hallucination, and a paraphrase strategy for enhanced prediction robustness. The authors conduct experiments across 21 datasets covering representative NLP tasks, demonstrating that the proposed techniques significantly improve ChatGPT's performance, achieving results comparable to or surpassing supervised baselines and existing state-of-the-art performances.

Tai, AMY; Meyer, M; Varidel, M; Prodan, A; Vogel, M; Iorfino, F & Krausz, RM. 2023. Exploring the potential and limitations of ChatGPT for academic peer-reviewed writing: addressing linguistic injustice and ethical concerns. *Journal of Academic Language and Learning*, 17(1): T16-T30.

This paper examines ChatGPT, an OpenAI language model employing neural networks and the transformer architecture for Natural Language Processing (NLP) tasks. With its widespread popularity, reaching 100 million users in two months and receiving a multibillion-dollar investment from Microsoft, this commentary delves into the potential and limitations of utilizing ChatGPT for academic writing and publication. While it proves beneficial for editing tasks like spell and grammar checking, summarization, and translation, ethical concerns arise regarding the use of AI-generated text in academic contexts. ChatGPT's potential lies in addressing linguistic injustice for non-native English speakers in academic publishing, offering support to convey research findings more effectively. Writers can benefit from personalized feedback, improving writing style and gaining new perspectives. However, caution is advised, recognizing that ChatGPT's accuracy is constrained by the quality of input data, and it may generate incorrect text. Sole reliance on ChatGPT for writing assistance is not recommended.

Tyson, J. 2023. Shortcomings of ChatGPT. *Journal of Chemical Education*, 100(8): 3098-3101.

This paper addresses the notable gaps in the discourse surrounding the significant limitations of ChatGPT that hold relevance for chemical educators, students, and researchers. The examination of ChatGPT's performance, as detailed in three recent papers in J. Chem. Educ., extends to a critical assessment of its capabilities in a 100-level general education chemistry course for nonscience majors. Additionally, the paper investigates ChatGPT's potential role as an assistant in literature searches related to the biogeochemistry of arsenic. A thorough analysis reveals that ChatGPT exhibits unreliability in performing mathematical operations, commits conceptual errors, and generates seemingly plausible citations with only partial accuracy in their purported contents. These shortcomings underscore the need for a comprehensive understanding of the limitations inherent in ChatGPT, particularly when considering its application within the domain of chemical education and research.

Wach, K; Duong, CD; Ejdys, J; Kazlauskaitė, R; Korzynski, P; Mazurek, G & Ziemba, E. 2023. The dark side of generative artificial intelligence: a critical analysis of controversies and risks of ChatGPT. *Entrepreneurial Business and Economics Review*, 11(2): 7-24.

This paper exams the challenges and limitations of incorporating generative artificial intelligence (GAI), with a specific focus on ChatGPT, within the business landscape. Employing a narrative and critical literature review, the study develops a conceptual framework, revealing the negative aspects of GAI development in management and

economics. Findings from an extensive review identify seven main threats, including the absence of AI market regulation, poor quality control, job losses due to automation, personal data violation, social manipulation, socio-economic inequalities, and AI technostress. Implications and recommendations emphasize the importance of AI market regulation, continuous education for adapting to job market shifts, prioritizing ethical considerations to address privacy concerns, and implementing responsible AI practices to mitigate risks. The contribution lies in drawing attention to the controversies and hazards associated with GAI, urging proactive measures for ethical deployment in business.

Walters, WH & Wilder, EI. 2023. Fabrication and errors in the bibliographic citations generated by ChatGPT. *Scientific Reports*, 13(1): 14045.

This paper assesses the limitations of chatbots, exemplified by ChatGPT, in the context of text generation and editing, particularly focusing on the issue of factually incorrect responses or hallucinations. The study concentrates on a specific type of hallucination, namely, the creation of bibliographic citations that do not correspond to legitimate scholarly works. Using both ChatGPT-3.5 and ChatGPT-4, the study generates literature reviews on 42 multidisciplinary topics, examining a total of 636 bibliographic citations across 84 papers. The evaluation involves scrutinizing the prevalence of fabricated citations, identifying errors in citations to non-fabricated papers, and assessing adherence to APA citation format. The findings reveal that, within this dataset, 55% of GPT-3.5 citations are fabricated compared to 18% of GPT-4 citations. Additionally, 43% of the real GPT-3.5 citations contain substantive errors, while this figure is reduced to 24% for GPT-4. Despite the improvements observed in GPT-4 compared to GPT-3.5, certain challenges persist.

Wang, C; Liu, S; Yang, H; Guo, J; Wu, Y & Liu, J. 2023. Ethical considerations of using ChatGPT in health care. *Journal of Medical Internet Research*, 25, e48009.

This paper explores the potential applications of ChatGPT in healthcare while emphasizing the importance of addressing ethical considerations to prevent possible harm. Ethical challenges related to legal, humanistic, algorithmic, and informational perspectives are identified. Legal ethics issues stem from the unclear assignment of responsibility in cases of patient harm and potential breaches of privacy. Clear legal guidelines are essential for liability allocation and user protection. Humanistic ethics concerns revolve around potential disruptions to the physician-patient relationship, humanistic care, and issues of integrity. Overreliance on AI may compromise compassion and trust, emphasizing the need for transparency and disclosure. Algorithmic ethics pose questions about bias, responsibility, transparency, explainability, validation and evaluation. Information ethics encompass concerns about data bias, validity, and effectiveness, where biased training data can lead to biased output, impacting patient adherence and encouraging self-diagnosis. Ensuring accuracy, reliability, and validity of ChatGPT-generated content necessitates rigorous validation and ongoing updates aligned with clinical practice. Navigating the evolving AI ethical landscape in healthcare requires adherence to strict standards. Comprehensive ethical guidelines empower healthcare professionals to responsibly use ChatGPT, facilitate accurate information exchange, safeguard patient privacy, and enable informed healthcare decisions.

Wu, X; Duan, R & Ni, J. 2023. Unveiling security, privacy, and ethical concerns of ChatGPT. *Journal of Information and Intelligence*. https://doi.org/10.1016/j.jiixd.2023.10.007

This paper explores the landscape of ChatGPT, an AI-powered chatbot employing topic modeling and reinforcement learning for natural response generation. While ChatGPT presents considerable potential in diverse sectors, including customer service, education, mental health, personal productivity, and content creation, addressing its security, privacy, and ethical implications is imperative. By tracing the evolution from GPT-1 to GPT-4 and examining the model's features, limitations, and potential applications, this study aims to unveil the potential risks associated with integrating ChatGPT into everyday scenarios. With a focus on security, privacy, and ethical concerns, the paper outlines the challenges these issues pose for widespread adoption. Lastly, the study analyzes the outstanding problems in these domains, advocating for collaborative efforts to ensure the development of secure and ethically sound large language models.

Yu, Y. 2023. Discussion on the Reform of Higher Legal Education in China Based on the Application and Limitation of Artificial Intelligence in Law Represented by ChatGPT. *Journal of Education, Humanities and Social Sciences*, 14: 220-228.

This paper examines ChatGPT as a representative of generative artificial intelligence, representing a disruptive innovation in the AI field. With its formidable natural language processing capabilities, ChatGPT has found widespread utility in the legal profession, offering robust support to the industry. As ChatGPT and other AI technologies undergo continuous evolution and broader adoption, their inevitable influence on the legal sector and current higher education in Chinese law will be profound. In light of this, the paper delves into the challenges and opportunities that Chinese legal education faces in the era of artificial intelligence. The focus centers on exploring the applications and limitations of generative AI, such as ChatGPT, within the legal profession.

Zhuo, TY; Huang, Y; Chen, C & Xing, Z. 2023. Red teaming ChatGPT via Jailbreaking: bias, robustness, reliability and toxicity. *arXiv* preprint arXiv:2301.12867.

This study delves into recent advancements in natural language processing (NLP), exploring the synthesis and comprehension of coherent text in an open-ended manner, translating theoretical algorithms into practical applications. Large language models (LLMs) have significantly impacted various sectors, including report summarization software and copywriting. However, concerns have arisen regarding the potential social prejudice and toxicity exhibited by LLMs, raising ethical and societal risks. The need for large-scale benchmarks for accountable LLMs becomes apparent. While some empirical investigations highlight ethical challenges in advanced LLMs, a systematic examination and user study of the risks and harmful behaviors associated with current LLM usage are lacking. To contribute to responsible LLM development, we employ a qualitative research method called "red teaming" on OpenAI's ChatGPT1, focusing on understanding practical ethical dangers in recent LLMs. The analysis covers four perspectives: Bias, Reliability, Robustness, and Toxicity. We comprehensively benchmark ChatGPT on multiple sample datasets aligned with these perspectives. Our findings reveal that existing benchmarks may not address numerous ethical risks, which we illustrate through additional case studies. We also discuss the implications of our discoveries on AI ethics and harmful behaviors in ChatGPT, along with future challenges and considerations for the responsible design of LLMs. This study aims to shed light on future efforts to identify and mitigate ethical hazards associated with LLM applications.

Author contributions S He proposed and contributed to the whole research, interpretation, and writing of the paper. The author prepared and reviewed the manuscript and approved the final version of the manuscript.

Data availability statement The data that support the findings of this study is available from the author upon reasonable request.

Declarations The author declare that he has no conflict of interest.

Original Communication

Preliminary discussion on pyrrhotite, gold killer in Wells-Barkerville, British Columbia, Canada

Jianzhao Yin[1]

Abstract

The Wells-Barkerville area of the Cariboo gold mining district is situated within the Quesnel Highlands on the eastern edge of the Interior Plateau in central British Columbia, Canada of the eastern Circum-Pacific volcanic-metallogenic belt. Recorded gold production from the area totals more than 4.0 million ounces, including an estimated 2.7 million ounces from placer mining from 101 creeks and 1.3 million ounces from lode mining. There are five principal types of lode gold deposits in the district; namely, auriferous pyrite replacement, including replacement in limestone and that in calcareous clastic rock; pyrite-quartz vein/veinlet lode gold, including strike vein, diagonal vein, orthogonal vein, and quartz veinlets; basalt-hosted auriferous pyrrhotite-pyrite lode gold; and associated gold in porphyry copper styles. This area is historically a famous gold production area in western Canada, including the initial alluvial gold and later and current lode gold. This original short article uses drilling results to illustrate that pyrrhotite in this area is the killer of gold. Wherever there is pyrrhotite, the gold grade is very poor or even contains no gold. In other words, gold grade is inversely related to pyrrhotite content. Then, the spatial distribution characteristics of the pyrrhotite anomaly zone(s) existing in this area were summarized, including the approximate thickness of zone(s). On this basis, several deep drill holes are recommended to verify whether there is considerable gold mineralization beneath the pyrrhotite anomaly zone(s).

Key words: pyrrhotite; gold killer; calcareous clastic rock; Cariboo gold mining district; Omineca belt; British Columbia; Canadian Cordillera

---

Affiliation Info: [1] Orient Resources Ltd., BC, Canada, V7E 1M8
Article Info: Received: 19 October 2023 / Revised: 28 November 2023 / Accepted: 6 December 2023 / Published Online: 12 December 2023. www.naturalisscientias.com
Authors' Contact Info: Yin, JZ: jimyin7@yahoo.ca
Citation: Yin, JZ. 2024. Preliminary discussion on pyrrhotite, gold killer in Wells-Barkerville, British Columbia, Canada. Naturalis Scientias, 1(1): 131-136. DOI: https://doi.org/10.62252/NSS.2024.1009.

Corresponding Author: Yin, JZ; Email: jimyin7@yahoo.ca

1 Introduction

The Cariboo gold mining district is situated within the Quesnel Highlands on the eastern edge of the Interior Plateau in central British Columbia, Canada, in the eastern Circum-Pacific volcanic-metallogenic belt. Recorded gold production from the area totals more than 4.0 million ounces, including an estimated 2.7 million ounces from placer mining from more than 101 creeks and rivers, and 1.3 million ounces from lode mining[1 & 2].

There are five principal types of lode gold deposits in the district; namely, auriferous pyrite replacement, including replacement in limestone and that in calcareous clastic rock; pyrite-quartz vein/veinlet lode gold, including strike vein, diagonal vein, orthogonal vein, and quartz veinlets; basalt-hosted auriferous pyrrhotite-pyrite lode gold; and associated gold in porphyry copper styles[1].

It is a matter of fact that the pyrrhotite is something like a killer of gold in the upper Lowhee Creek area, no matter what the reason is. As pyrrhotite develops in the rock, the grade of gold will be very poor. In other words, there is a negative correlation between gold grade and pyrrhotite content.

In this case, it is necessary to understand how the pyrrhotite develops and distributes in the space so that efficient drilling exploration for gold can be planned and conducted on gold mineralization targets.

Mainly based on the review of all the drill holes completed in 2005 by the related mining company, especially the detailed study on the pyrrhotite mineralization, lithology, alteration, and structure of the four drill holes, LH05-13, LH05-14, LH05-15, and LH05-16 of Section 16 + 050 E in the upper Lowhee Creek, the possible distribution of the pyrrhotite anomaly zone, its thickness, orientation, relationship with lithology, and other alterations as well as structure, are discussed here. In addition, preliminary conclusions and suggestions are proposed for reference of future drilling and exploration of gold deposits in the area.

It is worth saying that more data on drill logs are needed to be reviewed in the future to prove the conclusions in the article.

2 Discussion

2.1 Pyrrhotite zone

On the basis of study on the pyrrhotite mineralization, lithology, alteration, and structure of the four drill holes; that is, LH05-13, LH05-14, LH05-15, and LH05-16 of Section 16 + 050 E, and the review of all other drill holes along the upper Lowhee Creek conducted in 2005, the following geological phenomena about pyrrhotite were discovered:

- There exists one or more pyrrhotite anomaly zone(s) in the upper Lowhee Creek area.
- The pyrrhotite anomaly zone(s) are roughly within the elevations 4100 – 4470 feet above the sea level.
- The total thickness of the pyrrhotite anomaly zone(s) is about 180 feet.
- The pyrrhotite anomaly zone(s) are not horizontal but waving in the three dimensional space, although the thickness of the zone(s) seems stable. In the azimuth of 220° (all on the local mine grid in this article), the pyrrhotite zone dips about 20° down to the bank of the Lowhee Creek for about 200 feet horizontal distance. Then, the pyrrhotite zone(s) go almost horizontally toward the bank. In the opposite direction, namely, in the azimuth of 40°, the pyrrhotite zone(s) dip down into the hill at about 60°.

2.2 Pyrrhotite and lithology

Lithology in the area, appearing to dip north-eastward at about 50° in the sections, can be simply divided into two groups or units as follows:

- The upper dark grey to black graphitic argillite, siltite, and quartzite, usually strongly silicified; and
- The lower grey, greenish grey, greyish green, and/or pale green sericitic and/or chloritic phyllite, argillite, and quartzite; some of these rocks are dolomitic porphyroblastic and/or magnetite porphyroblastic with disseminated magnetite. This unit usually interbeds with some silicified black graphitic argillite, quartzite, and siltite.

Between the two different units, a quartz veining zone, also a fault structure zone, occurs along the contact dipping NE at an angle of about 50°.

The drilling results indicate that the pyrrhotite anomaly zone develops only in the lower rock unit, and the contact is the upper limit of the pyrrhotite anomaly zone. In other words, the pyrrhotite zone is under the contact between the two different units, though it really does not mean that the pyrrhotite is stratabound in the lower unit.

Most of the alterations, graphite, chlorite, sericite, fuchsite, carbonate including dolomite and calcite, silicification including quartz veinlets, stock works, quartz stringers as well as quartz veins, seem to have similar orientation with the lithology and also dip north-eastward at a similar dip angle.

The pyrrhotite zone(s) cut across all alterations and porphyroblastic (magnetite and dolomite) rocks. To some extent, this might mean that pyrrhotite as well as the associated pyrite mineralization is younger than most, if not all, of the alterations mentioned above.

It does not seem there is any genetic relationship between magnetite porphyroblast rock and the pyrrhotite mineralization, since they cut across each other and have different orientation in the three dimensional space. The magnetite porphyroblastic and dolomitic porphyroblastic rocks have almost the same orientation as that of the other lithology in the region.

Although the term "pyrrhotite anomaly zone" is used here, it does not mean that the pyrrhotite distributes evenly within the "zone area". On the contrary, the pyrrhotite scatters, or distributes discontinuously and unevenly in the zone(s) mainly in the form of very fine veinlets and / or clots/blebs. Some part of the zone area is free of pyrrhotite (Table 1).

Table 1. Representative drill holes that intercepted pyrrhotite

Hole ID	Collar (mine grid)			Azimuth	Dip	End of hole (feet)	Interval with pyrrhotite
	Easting	Northing	Elevation				
LH05-02	17601	2264	4768'	213°	- 57°	696'	495.1' (5%)
							522.3'- 522.6' & 544.1' (15%)
							543'-551' (4%)
LH05-04	17394	2374	477'	357°	- 45°	646'	183.5'-185.1' (5%)
							404.4'-436.0' (5%)
							586'-616' (5%)
LH05-06	16994	2644	4785'	358°	- 46°	616'	396'-405' (1%-2%)
							606''-616' (2%-3%)
LH05-07	16994	2646	4787'	55°	-48°	506'	377.7'-382.5' (5%-7%)
							382.5'-406.0' (2%-3%)
LH05-08	16991	2642	4786'	205°	- 80°	431'	299.2'-321.4' (2%-3%)
							321.4'-376.0' (1%-2%)
							376'-414' (1%)
LH05-09	16802	2804	4788'	216°	- 44°	546'	226.6'-236.6' (2%-3%)
							424.7'- 471.1' (1%-3%)
							509.3'-541.6' (1%-2%)
LH05-10	16598	3000	4809'	194°	- 44°	556'	324.3'- 376.0' (1%-2%)
							376.0'- 395.0' (3%-4%)
							395.0'- 449.5' (1%-2%)
							542.7'- 544.7' (2%-3%)
LH05-12	16396	3102	4809'	179°	- 44°	676'	144'-158' (1%)
							226.0'- 238.7' (1%-2%)
LH05-13	15995	3289	4809'	208°	- 44°	582'	576.2' – 582.0' (3%)
LH05-14	15996	3291	4809'	208°	- 67°	716'	469.2' – 471.0' (0.5%)
							540.4' – 542.5' (0.1%)
							610.0' – 632.5' (1.0%)
LH05-15	15997	3293	4809'	208°	- 90°	557'	343.2' – 388.7' (0.7%)
							399.4' – 522.7' (0.7%)

Most of the known pyrrhotite clots and/or veinlets occur in grey and/or greenish grey phyllite, argillite, and quartzite in drill holes LH05-04, LH05-06, LH05-07, LH05-08, LH05-09, LH05-10, LH05-11, LH05-13, LH05-14, and LH05-16; some pyrite - pyrrhotite veinlets in quartz vein in drill holes LH05-04, LH05-15 and LH05-16, and some other pyrrhotite in the silicified black graphitic argillite / siltite / quartzite interbeds of the lower phyllite/quartzite

unit in drill holes LH05-04, LH05-08, and LH05-15; a few pyrrhotite in the upper black graphitic argillite/siltite/quartzite.

Pyrrhotite content varies greatly in a short distance within the anomaly zone: 01%, 0.5%, 0.7%, 0.8%, 1.0%, 1% - 2%, 1% - 3%, 2% - 3%, 3.0%, 3% - 4%, 4%, 5% , 5% - 7%, 15% and so on (Table 1).

When occurring in the quartz veins, pyrrhotite content is the highest (10% - 15%) and usually associated with pyrite in the form of pyrrhotite-pyrite vein or veinlet (drill holes BC2K-18, LH05-04, LH05-15, and LH05-16). From this point of view, there is no any major difference between the pyrrhotite in drill hole BC2K-18 and that of the Lowhee drill targets.

At least one fault or fault zone, cutting across the lithology and alteration, develops above the pyrrhotite zone(s). Several other faults or fault zones occur within or below the pyrrhotite zone(s). The genetic relationship between these faults or fault zones and the pyrrhotite zone(s) is not clear at this time.

Depending on the dips and collars of the drill holes in the upper Lowhee Creek area, the possible depth ranges within which drill holes might hit the pyrrhotite zone(s) are summarized in Table 2. The depth ranges listed here might be affected and thus changed by fault and/or fold as well some other geological events.

Table 2. Possible depth ranges that drill holes might intercept pyrrhotite

Azimuth (mine grid)	220°			40°
Elevation (feet)	4809.33’			
Dip	- 45°	- 67°	- 90°	- 80°
Depth interval with pyrrhotite (feet)	576’ – 750’	470’ – 630’	340’ – 520’	480’ – 680’
Example	LH05-13	LH05-14	LH05-15	LH05-16
End of hole (feet)	346’	716’	557’	626’

Table 3 lists those drill holes that do not hit pyrrhotite zone(s), possibly due to the shallower end of holes than the depths of the supposed upper limit of the pyrrhotite zone(s). For example, drillhole LH05-17 ends at a depth of 575 feet. No pyrrhotite is found in the core. Considering the drill pad of LH05-17 is at a little higher elevation and its end of hole a little less than the proposed upper limit depth of the pyrrhotite zone(s), LH05-17 should not hit any of the pyrrhotite.

Table 3. Drill holes without pyrrhotite possibly due to their smaller EOH

Hole ID	**Collar (mine grid)**					**End of hole (feet)**
	Easting	**Northing**	**Elevation (feet)**	**Azimuth**	**Dip**	
LH05-01	17601	2263	4769’	206°	- 45°	346’
LH05-03	17634	2282	4771'	4°	- 45°	376’
LH05-05	17183	2502	4782’	206°	- 58°	306’
LH05-11	16598	3002	4809’	194°	- 55°	557’
BB05-03	18119	2156	4773’	238°	- 44°	493’
BB05-02	18126	2155	4773’	238°	- 132°	526’
BB05-01	18133	2032	4747’	238°	- 44°	536’

3 Conclusions and suggestions

On the basis of the discussion above, the conclusions and suggestions are reached as follows:
There exist pyrrhotite anomaly zone(s) under the contact of the upper black graphitic argillite/siltite/quartzite and the lower grey/green phyllite (argillite)/quartzite. The pyrrhotite zone(s) are waving in the space.
Pyrrhotite distributes unevenly and discontinuously and its content varies greatly (0.1% - 15%) in a short distance within the zone(s).
Pyrrhotite occurs mainly in the form of clot/bleb and/or veinlet.
Several deep holes are suggested in Table 4 below in order to confirm how the gold mineralization below the pyrrhotite anomaly zone(s) is.

Table 4. Recommended drill holes to test gold mineralization below the pyrrhotite zone(s)

Azimuth (mine grid)	220°			40°
Dip	- 45°	- 65°	- 90°	- 80°
Depth interval with pyrrhotite (feet)	1100' – 1200'	800' – 900'	750'- 850'	1200' – 1300'

Based on the result of the drill holes recommended above, the proposed depths of future drill holes would be determined whether or not to cut through the pyrrhotite zone(s). If there is not any promising gold mineralization below the pyrrhotite zone(s), it is unnecessary to drill deeper exploration drill holes in the area. And the possible end of holes would be determined by referring to Tables 1 and 2 in this article, depending on the dips and collars of the proposed drill holes.
Drill holes with dip angles of -45° and -60° and an azimuth of 40° are recommended in order to avoid the pyrrhotite zone(s) and to hit the quartz veining zone along the contact between the upper black graphitic argillite/siltite/quartzite and the lower greenish grey phyllite (argillite)/quartzite.
More drill holes are recommended and listed in Table 5. These drill holes are mainly based on the orientation of most of the quartz veins and dominant structures including big faults and/or fault zones in the region.

Table 5. More recommended exploration drill holes for quartz vein style of gold mineralization

Azimuth (mine grid)	300°			90°		
Dip	- 45°	- 65°	- 80°	- 80°	- 65°	- 45°
End of hole (feet)	900' – 1000'	800' – 900'	700'- 800'	1200' – 1300'	800' – 900'	900' – 1000'

It should be pointed out that the conclusions on the pyrrhotite zone(s) in this report are certainly preliminary and thus may not be applied to the entire exploration region, since they are mainly based on several limited drill holes.

Author contributions JZ Yin proposed and contributed to the whole research, interpretation, and writing of the paper. The author prepared and reviewed the manuscript and approved the final version of the manuscript.

Data availability statement The data that support the findings of this study is available from the author upon reasonable request.

Declarations The author declare that he has no conflict of interest.

4 References

1. Yin, JZ. 2018a. Metallogenic series of gold deposits in the Cariboo gold mining district, British Columbia, Canada. Earth Sciences, 7 (1): 17-22. DOI: 10.11648/j.earth.20180701.14.

2. Yin, JZ. 2019a. Structure controls on gold deposits in the Cariboo gold mining district, British Columbia, Canada. Geological Society of America Abstracts with Programs. 51 (5), 2019. DOI: 10.1130/abs/2019AM-330823.